The Institute of Paper Chemistry

Appleton, Wisconsin

Doctor's Dissertation

Determination of the Structure
of the Black Spruce Glucomannan from the
Molecular and Hydrodynamic Properties
of its Triacetate Derivative

William S. Linnell

June, 1965

DETERMINATION OF THE STRUCTURE OF THE BLACK SPRUCE GLUCOMANNAN FROM THE MOLECULAR AND HYDRODYNAMIC PROPERTIES OF ITS TRIACETATE DERIVATIVE

A thesis submitted by

William S. Linnell

B.A. 1960, Carleton College
M.S. 1962, Lawrence College

in partial fulfillment of the requirements
of The Institute of Paper Chemistry
for the degree of Doctor of Philosophy
from Lawrence University,
Appleton, Wisconsin

June, 1965

TABLE OF CONTENTS

ERRATA

DETERMINATION OF THE STRUCTURE
OF THE BLACK SPRUCE GLUCOMANNAN FROM THE
MOLECULAR AND HYDRODYNAMIC PROPERTIES
OF ITS TRIACETATE DERIVATIVE

By

WILLIAM S. LINNELL

Page 27, third line from bottom: number or z-average.....

Page 29, Fig. 2: Cellulose Trinitrate (199); Cellulose Acetate, DS = 2.3 (188); Cellulose in Cadoxen (194); Cellulose Acetate, DS = 2.4 (201); Guaran Triacetate (21); Salep Glucomannan Triacetate (43); Branched Dextran (33)

Page 57, next to last column heading should be $\underline{n}_w^e$.

Page 58, $\underline{n}_w$ instead of $\underline{M}_w$.

Page 61, last line: three instead of five.

Page 91, 2nd paragraph, line 7: concentration instead of volume.

Page 131, left portion of flow chart:

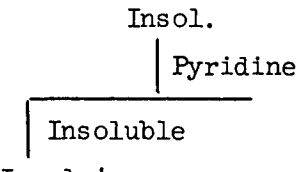

Page 133, under column heading Insol.-2, last no. in column – (1) – to be deleted.

Page 143, paragraph 1, line 3: COO^{-1}.

Page 178, 8th line from bottom of page: would be compensated.

Page 187, line 3: when $\lambda \underline{M}_z \approx 1$.

Page 188, line 3: Table XLIII.

Page 188, Table XLIII: $\underline{M}_z$ = 27,600

Page 191, Equation (37):

$$M_n = \frac{\Sigma n_i M_i}{\Sigma n_i} = \text{etc.}$$

Errata (Continued)

Page 195, equation at top of page:

$$\underline{R}_{\underline{i}} = \left(\frac{\partial \underline{n}}{\partial \underline{c}_{\underline{i}}}\right)_{\underline{T},\underline{P},\underline{c};(\underline{J}\neq 0)} = \text{etc.}$$

Page 196, last line: $\omega =$

Page 210, line 9: $\overline{\underline{v}}_{\underline{e}}$

SUMMARY

Chemical evidence is presently available in the literature for and against the existence of branches other than the unit galactose side chains in softwood glucomannans; however, chemical methods will provide no information on the length of the branches. The goal of the present study is to determine if long-chain branching occurs in the glucomannan isolated from black spruce (Picea mariana) and to elucidate the extent and nature of possible branch points.

A glucomannan was isolated from the 10% sodium hydroxide extract of a black spruce holocellulose prepared by a mild acidified sodium chlorite delignification at room temperature. The purified glucomannan was shown to be typical of coniferous glucomannans by quantitative sugar analysis, electrophoresis, and its infrared spectrum. The glucomannan was acetylated and carefully fractionated by fractional precipitation. The hydrodynamic and molecular properties of the acetylated fractions were determined by osmometry, viscometry, sedimentation equilibrium experiments, and analysis of the transient state during ultracentrifugation. Analysis of these properties according to existing polymer theories showed that the glucomannan had a relatively compact molecular configuration in comparison to linear β-1,4 linked polysaccharides and, therefore, definitely contained long-chain branches.

Lignin was found to be tenaciously associated with glucomannan fractions which had been extensively purified and the hypothesis was made that lignin may be involved in the long-chain branching. A detailed inspection of the behavior of the glucomannan fractions in relationship to the lignin content, molecular properties, solubility properties, and ease of extraction from the holocellulose and a critical review of the literature indicated that lignin was quite probably chemically linked to the glucomannan chains. The results of this investigation were consistent with a model involving the cross-linking of essentially linear

glucomannan chains through common lignin moieties. This model adequately explained the fact that degrees of polymerization found in this study were higher than previously reported in the literature for wood glucomannans and was consistent with the increase in the degree of branching with increasing degree of polymerization exhibited by the black spruce glucomannan fractions.

The above hypothesis gained support from a theoretical treatment of the viscosity-molecular weight results in order to obtain a measure of the degree of branching. This treatment showed that the results were best described by a model involving cross-linking of linear chains. Using this model the number of cross-links per molecule increased from 0.1 for an essentially linear fraction with a weight average degree of polymerization ($\underline{\underline{DP}}_{\underline{w}}$) of 82 to a value of 7.1 for a highly branched fraction with $\underline{\underline{DP}}_{\underline{w}}$ equal to 557. The calculated degree of polymerization of the linear chains which are cross-linked together was constant within a narrow range for all fractions (with an average value of 77), regardless of the degree of polymerization of the entire cross-linked molecule. This constant value is good support for the validity of the crosslinked model which was employed.

Extension of the results of this investigation to the original state of the glucomannan within the fiber indicates that the glucomannan and lignin are present in a cross-linked matrix containing at least occasional lignin-carbohydrate linkages.

Supplementary investigations carried out on other isolated glucomannans and galactoglucomannans from black spruce support the conclusions obtained from the more intensive investigation of the glucomannan isolated from the 10% sodium hydroxide extract.

INTRODUCTION

Glucomannan is the most abundant noncellulosic polysaccharide of coniferous woods (1), constituting for example approximately 20% of the carbohydrate content of black sprucewood (2). The polysaccharide consists of a linear or slightly branched chain of 1→4 linked β-D-glucopyranose and β-D-mannopyranose residues containing about 3 to 5% of 1→6 linked, terminal side chains of α-D-galactopyranose residues (3). The ratio of galactose to glucose to mannose sugar residues is generally 0.1-0.2:1:3-4 (3). The second mannose-containing polysaccharide in coniferous woods is the galactoglucomannan which has a sugar ratio of galactose to glucose to mannose residues of 0.6-1.0:1:3 (3). With the exception of the greater amount of galactose residues, this polysaccharide has a structure similar to the glucomannan and contains one or two branches per molecule (3). The galactoglucomannan is about 1% of the carbohydrate content of black sprucewood (2). The number average degree of polymerization ($\underline{DP}_n$) of isolated glucomannans from coniferous woods varies from 35 to 140 but most are in the range of 70 to 110. Isolated galactoglucomannans have been found to have a $\underline{DP}_n$ range of 45 to 100 (3). Galactoglucomannans are readily extracted from coniferous holocelluloses with dilute alkali whereas the glucomannans exhibit a greater resistance to extraction and concentrations of sodium hydroxide of 10% or greater must be employed.

In a recent review article, Timell (3) states that chemical evidence is presently available for and against the existence of branches other than the unit galactose side chains in softwood glucomannans. Branching is clearly indicated in three studies in the literature and a linear backbone in four (3). A pine glucomannan (4) and a spruce glucomannan (5) were found to contain one and three branch points per molecule, respectively. Methylation and subsequent hydrolysis, periodate oxidation, and partial hydrolysis have been employed in

determination of the glucomannan structure. These chemical methods give the number of branches per molecule and the location of the branch points but do not give any information concerning the length of the branches. With these methods it is impossible to determine if the branches are one unit side chains or chains fifty or more units long. The length of the branches will have a profound effect on the physical behavior of the glucomannan in the fiber and also in its isolated state and for this reason is an extremely important aspect of the glucomannan structure.

Long-chain branching in a polymer results in a more compact molecular configuration and a decreased hydrodynamic volume. The decreased hydrodynamic volume results in a lower hydrodynamic frictional coefficient and lower intrinsic viscosity for a branched polymer than for a linear polymer. Thus, determination of the hydrodynamic properties of an isolated glucomannan can be used to detect long-chain branching and provide a measure of the extent of the long-chain branching.

A considerable volume of evidence exists in the literature pointing to the existence of a lignin-carbohydrate linkage in coniferous woods. Strong evidence has been obtained for a lignin-glucomannan linkage in isolated glucomannan fractions (5-7). Most investigators have not analyzed isolated glucomannan fractions for lignin but the presence of only a small amount of lignin can be an extremely important factor in the branching of this polysaccharide if it is chemically linked to the glucomannan molecule. It is possible that lignin may be involved in the crosslinking of two or more glucomannan chains or simply be attached to individual chains. Although a tremendous amount of evidence supports the concept of a lignin-carbohydrate linkage, much of this evidence is indirect and a review of the literature must be made in order to appreciate the high probability for

the existence of the linkage. For this reason a literature review of the pertinent references on the lignin-carbohydrate linkage is presented in Appendix I, p. 80.

The present study was undertaken to determine if long-chain branching occurs in the glucomannan from black spruce (Picea mariana). The extent and nature of this branching is elucidated and the possible role that lignin plays therein is investigated. Conclusions are drawn from theories relating hydrodynamic properties to the molecular configuration and/or the degree of branching. Since it is impossible to isolate the entire glucomannan component of black spruce in a pure state, physicochemical measurements are made on various isolated glucomannan fractions to supplement the intensive investigation of one glucomannan fraction. In this manner the differences and similarities of the glucomannan fractions are elucidated and it is possible to extend conclusions drawn from the intensive investigation of one fraction to the entire spectrum of mannose-containing polysaccharides of black spruce. In order to prevent the possible cleavage of long-chain branches during isolation and preserve the possible presence of a lignin-glucomannan linkage, it was necessary to employ a mild isolation process.

ISOLATION OF GLUCOMANNAN POLYSACCHARIDES

HOLOCELLULOSE PREPARATION

Black spruce was chosen as the wood from which the glucomannan polymers are isolated because the chemical properties of sprucewood glucomannans have been studied extensively (2, 4, 8-16). In order to minimize degradation of the polysaccharides during delignification, a chloriting process at room temperature was employed similar to that recently described by Thompson and Kaustinen (17). In this investigation a slight modification of this process was employed in which sodium chlorite at a pH of 4 to 5 and a concentration of 200 g./l. was allowed to react with the wood chips for five days at ambient temperature. A holocellulose yield of 75.1% of the ovendry wood with a Klason lignin content of 2.30% was obtained. This holocellulose contains polysaccharide material that has been subjected to a minimum of degradation due to the low temperature of delignification and the specificity of the acidified sodium chlorite for lignin. The presence of a nonreducing carboxyl end-group which is introduced by the chlorite ion oxidation retards degradation of the polysaccharide under alkaline conditions. This is a definite advantage as subsequent isolation of the glucomannan from the holocellulose is carried out by alkaline extraction. The experimental details and a discussion of the reactions involved are presented in Appendix II, p. 88.

EXTRACTION AND PURIFICATION OF THE GLUCOMANNAN FRACTIONS

The holocellulose was extracted with a sequence of 0.1N sodium hydroxide, 10% sodium hydroxide, 18% sodium hydroxide, 18% sodium hydroxide containing 4% boric acid, and finally water. Precipitates from the crude extracts were initially isolated by precipitation with barium hydroxide and purified by extraction with sodium hydroxide solutions, fractional precipitation with barium hydroxide,

and utilization of the solubility properties at pH 4-5. Dialysis and freeze drying were then employed in the isolation of the final fractions. The details of the extraction and purification procedures are presented in Appendix III, p. 92, which also contains figures summarizing the isolation.

Sixteen hemicellulose fractions were isolated which amounted to 4.80% of the holocellulose. Although 40.2% of the ovendry holocellulose had been extracted, 4.80% recovered is a fairly good yield when it is considered that the major criterion was to isolate pure glucomannan fractions. Fractions 8 and 9 from the 10% sodium hydroxide extract which amounted to 2.20% of the ovendry holocellulose were typical glucomannan fractions with a normal sugar content for coniferous glucomannans. The major part of this investigation is concentrated on these fractions, which are referred to as the main fractions. Other fractions which are investigated are the xylose containing galactoglucomannan fractions 6 and 7 from the 10% sodium hydroxide extract, Fraction 13, the typical glucomannan (galactose:glucose:mannose = 0.1-0.2:1:3-4) from the 18% sodium hydroxide extract, the galactose-rich glucomannan Fraction 14 from the 18% sodium hydroxide containing 4% boric acid extract, the galactoglucomannan Fraction 16 from the wash solution, and a typical glucomannan, Fraction 17 from the wash solution.

CHARACTERIZATION OF HOLOCELLULOSE AND EXTRACTED RESIDUE

A chemical and physical characterization of the holocellulose showed that a minimum carbohydrate degradation occurred during delignification. The extracted residue was chemically characterized and a material balance was carried out for the extraction process. The exhaustive extraction procedure employed in this investigation removed 68% of mannose residues originally present in the holocellulose. Most of the xylose residues (86%) and only 57% of the galactose

residues originally present were extracted. The assumption is made that all the resistant galactose and mannose residues are present in the extracted residue in the form of a galactoglucomannan in which the glucose-to-mannose ratio is 1:3.8. Then it can be concluded that a galactose-rich glucomannan with galactose:glucose: mannose = 1.4:1.0:3.8 and accounting for 32% of the mannose residues in the holocellulose is extremely resistant to extraction. The material balance also showed that lignin and hemicelluloses are extracted in a relatively constant ratio, thus indicating the possibility of a close association between these components of the holocellulose. The experimental results and a detailed discussion are presented in Appendix IV, p. 105.

ACETYLATION, FRACTIONATION, AND CHEMICAL CHARACTERIZATION OF THE MAIN GLUCOMANNAN

CHEMICAL NATURE OF THE MAIN GLUCOMANNAN FRACTIONS

It was decided to carry out the major investigation on Fractions 8 and 9 (isolated from the 10% sodium hydroxide extract) which qualitative sugar analysis showed to be typical softwood glucomannans. This was corroborated by quantitative sugar analysis of the acetate derivatives of Fractions 8 and 9. The sugar ratios were (on a weight basis) galactose:glucose:mannose:xylose:arabinose = 0.20:1.00:3.27:0.12:0 and 0.24:1.00:3.47:0.12:0, respectively. The infrared spectra of Fractions 8 and 9 were typical of coniferous glucomannans and in particular were identical to an infrared spectrum of a glucomannan from Paraña pine (18). Characteristic bands were present in the spectra for β-1,4 linked mannans and glucomannans. A weak band which was attributed to lignin was also present. The infrared results are presented in Appendix XII, p. 142. Fractions 8 and 9 behaved identically when subjected to free boundary electrophoresis in a borate buffer. The electrophoretic analysis showed that at least 95% of the polymer was homogeneous. Whether the remaining material was an impurity or an artifact resulting from complexing of the borate ion is unknown. The results of the electrophoresis experiments are presented in Appendix V, p. 112. It can be concluded from the above results that the main glucomannan Fractions 8 and 9 are pure and representative glucomannans.

ACETYLATION

It appeared desirable to work with a derivative rather than the glucomannan itself because a derivative would not be expected to aggregate as readily in solution, can be fractionally precipitated more easily, and should be soluble in organic solvents which are preferable for measurements of physical properties in

dilute solution. The acetate derivative was chosen because polysaccharide acetates are very stable (19). The acetylation procedure is based on a method originally developed by Carson and Maclay (20) and recently used by Koleske (21). With high molecular weight polysaccharides, this procedure will generally give a fully acetylated polymer. However, with hemicelluloses which are relatively low molecular weight polysaccharides, it is often difficult to obtain a fully acetylated product (14, 20, 22). This acetylation difficulty is probably due to the tendency of hemicelluloses to form aggregates and thus resist dispersion in the acetylation mixture.

The method of Carson and Maclay failed to give a fully acetylated glucomannan acetate and the yield was low. Therefore, a modification of this procedure was necessary. The details of the modifications employed and the results obtained are presented in Appendix VI, p. 114. The triacetate derivatives of Fractions 8 and 9 (designated by 8-A and 9-A) had degrees of substitution of 2.97 (44.3% acetyl) and 2.98 (44.6% acetyl), respectively. Full acetylation corresponds to 44.78% acetyl.

SOLUBILITY OF THE GLUCOMANNAN TRIACETATE

A solubility study was made of the acetylated glucomannan Fraction 8-A in 172 solvents, exhibiting a wide range of solvent power. The results show that the glucomannan triacetate is most soluble in solvents which exhibit a high degree of proton-donating character and is insoluble in inert* solvents. This indicates that the factor of primary importance in dissolving the glucomannan triacetate is the solvation of the polymer in which the ester carbonyl group forms a hydrogen bond

*Solvents which exhibit little or no interaction with the polymer.

with a proton donated by the solvent. The details and results of the investigation are presented in Appendix VII, p. 118.

FRACTIONATION OF THE GLUCOMANNAN TRIACETATE

The acetylated glucomannan Fractions 8-A and 9-A were fractionally precipitated from a pyridine solution at an initial concentration of 0.5 g./100 milliliters by the gradual addition of ligroin (65-90°C.). The isolated fractions were then refractionated in a similar manner to obtain 19 glucomannan triacetate fractions fractionated with respect to molecular weight. The theory, procedure, and results of the fractional precipitation are presented in Appendix VIII, p. 125.

CHEMICAL CHARACTERIZATION OF THE ACETYLATED GLUCOMANNAN FRACTIONS OBTAINED BY FRACTIONAL PRECIPITATION

SUGAR CONTENT

Quantitative sugar analyses by the method of Saeman, et al. (23) are presented in Table I for the glucomannan triacetate fractions obtained by fractionation of the main acetylated glucomannans 8-A and 9-A. From the number average degrees of polymerization ($\overline{DP}_n$) (their determination is described in Appendix XV, p. 154), reported in Table I, it is seen that the fractions chosen for quantitative sugar analyses are widely separated with respect to molecular weight. From duplicate sugar analyses of Fraction 3(1), it appears that the analytical experimental error is greater than the variation in sugar content from fraction to fraction. The conditions employed during this fractionation were more ideal than those generally employed in the fractional precipitation of hemicelluloses due to the large ratio of solution volume to hemicellulose weight used in this study. The nonvariable sugar content of the fractions thus obtained is strong support for the chemical homogeneity of the fractions. The ratio of glucose to mannose

TABLE I

QUANTITATIVE SUGAR CONTENTS OF ACETYLATED FRACTIONS
FROM FRACTIONAL PRECIPITATION

Fraction	Number Average Degree of Polymerization	Sugar Ratio on Weight Basis[a]						Total Accounted for, %[b,c]
		Galactan:	Glucan:	Mannan:	Xylan:	Araban	Galactan: Xylan	
9-3	36.3	0.30	1.00	3.78	0.14	0	2.17	84.13[d]
3(2)	60.6	0.26	1.00	4.16	0.16	0	1.67	93.97
3(1)-1st[f]	102.5	0.21	1.00	3.63	0.10	0	2.03	90.76[d]
3(1)-2nd[f]	102.5	0.16	1.00	4.00	0.12	0	1.40	92.28[d]
2(2)-R	123	0.22	1.00	4.16	0.16	0	1.39	87.02[d]
2(1)	261	0.21	1.00	3.88	0.12	0	1.75	94.42
Insol'.	--[e]	0.24	1.00	3.76	0.21	0	1.12	100.26

[a]The ratio of sugars is calculated on the basis of their polymerized state.

[b]Sum of sugar, acetyl, ash, and nitrobenzene lignin contents when available.

[c]Used the theoretical acetyl content of 44.78%.

[d]Lignin content not included.

[e]Insoluble fraction of apparent higher $\underline{DP}_n$.

[f]Duplicate analyses.

of these fractions is within the range of 1 to 3.3 ± 0.8 that Timell (3) has reported for 24 isolated glucomannans from gymnosperms.

Galactose residues are present in amounts of 3.1 to 5.8% based on the total sugar content. Although no direct evidence exists for the presence of a chemical linkage between the galactose residues (generally present in amounts of 3 to 5%) and the mannose or glucose residues in glucomannans) much indirect evidence strongly suggests that the galactose residues are integral parts of all softwood glucomannans (3). A small and nearly constant amount of xylose residues (2.2 to 4.0% based on the total sugar content) is present in every fraction listed in Table I. Considering the extensive purification and fractionation that was carried out for these fractions, the presence of a relatively constant amount of xylose is evidence that the xylose may be chemically linked to or strongly associated with the glucomannan employed in this study. In order to test for a possible correlation between the amount of xylose and the amount of galactose, the ratio of the galactose residues to xylose residues is presented in Table I. This ratio varies from 1.1 to 2.2.

Since it was impractical to determine the quantitative sugar contents of all the fractions, qualitative sugar analyses were run on all the fractions to supplement the preceding quantitative data. Ratios of the areas of the sugar spots after chromatographic separation were calculated in order to determine if the sugar contents were constant. The details of the qualitative sugar analyses are presented in Appendix IX, p. 132. The results support the quantitative data and show that the sugar content is constant for all the fractions with the exception of a slight increase in the galactose content in the lowest molecular weight fractions. The presence of a small amount of xylose in all fractions was substantiated and no uronic acid content was detected.

LIGNIN CONTENT

The acetylated glucomannan fractions Insol'., 2(1), and 3(2) were analyzed for lignin by alkaline nitrobenzene oxidation and subsequent separation and quantitative determination of vanillin and syringaldehyde (24). The method was standardized by the determination of the nitrobenzene lignin content and the Klason lignin content of black sprucewood. Nitrobenzene oxidation was chosen as the method of lignin analysis because it is specific for lignin and can be used to determine small amounts of lignin in small samples. The results are presented in Table II.

TABLE II

LIGNIN CONTENTS

Fraction	$\overline{DP}_n$ [a]	Per Cent Lignin Based on Glucomannan Triacetate [b]	Per Cent Lignin Based on Unacetylated Glucomannan [b]	% Vanillin:% Syringaldehyde [c]
3(2)	60.6	1.82	3.19	95.7:4.3
2(1)	261	2.34	4.09	97.7:2.3
Insol'.	--[e]	3.11	5.40	94.6:5.4
Wood [d]	--	--	--	96.4:3.6

[a] Number average degree of polymerization.
[b] Corrected for ash content determined by ashing at 575 ± 25°C. for three hours. Fractions 3(2) and 2(1) had a negligible ash content and Fraction Insol'. had 3.03% ash.
[c] Based on total amount of vanillin and syringaldehyde.
[d] Black sprucewood.
[e] Insoluble fraction of apparent higher $\overline{DP}_n$.

The presence of lignin in three glucomannan triacetate fractions with widely separated degrees of polymerization is significant, particularly since these fractions have been extensively purified and carefully fractionated. An increasing trend in lignin content with increasing degree of polymerization is noticeable.

ACETYLATION, PURIFICATION, AND CHEMICAL CHARACTERIZATION OF VARIOUS ISOLATED GLUCOMANNANS AND GALACTOGLUCOMANNANS

GENERAL

In a study of this nature, the purity of the polymer is a prime requisite. Since losses occur in the isolation of pure glucomannan fractions it was impossible to carry out the isolation quantitatively and investigate the entire amount of glucomannan in the holocellulose. It is, therefore, important to know if the main Fractions 8 and 9 are representative of the entire glucomannan component of black spruce and also to understand the relationship of these fractions to the broad spectrum (with respect to sugar content, structure, and resistance to extraction from the holocellulose) of the mannose-containing polysaccharides of this wood. For this reason many other glucomannan and galactoglucomannan fractions which varied widely in their resistance to extraction and in their galactose content were studied following isolation from the 10% NaOH extract, 18% NaOH extract, and 18% NaOH-containing 4% H_3BO_3 extract.

ACETYLATION AND PURIFICATION OF THE VARIOUS GLUCOMANNANS AND GALACTOGLUCOMANNANS

The various glucomannan and galactoglucomannan fractions were acetylated by the procedure described in Appendix VI, p. 114, and the results are presented in Appendix X, p. 136. A portion of every acetylated fraction was insoluble in all solvents investigated. Since physical measurements were made on these acetylated fractions it was necessary to subject them to further purification in order to remove the insoluble material and the inorganic material that was present. The purification procedure and results are presented in Appendix X, p. 136. (The acetate derivatives before purification are designated by -A and the corresponding soluble and insoluble portions are designated by -S and -I, respectively.)

CHEMICAL CHARACTERIZATION OF THE VARIOUS ACETYLATED GLUCOMANNANS AND GALACTOGLUCOMANNANS

SUGAR CONTENT

Quantitative sugar analyses by the method of Saeman, et al. (23) are presented in Table III for the various acetylated glucomannan and galactoglucomannan fractions. From Table III, it is seen that the Fractions 8-S, 9-S, 13-S, 13-I, and 17-S are typical glucomannans which are chemically similar to the main glucomannan Fractions 8-A and 9-A. Fractions 6-7-S, 14-S, and 16-S have sugar ratios typical of galactoglucomannans, contaminated with 29.6, 9.1, and 9.0% xylose residues (based on the total sugar content), respectively.

Isolated galactoglucomannans from gymnosperms generally have the ratio of 0.5-1.2:1.0:1.4-3.7 of galactose:glucose:mannose residues (1:1:3 is the most common ratio) and are usually extracted from the holocellulose or pulp with water or dilute alkali (3). It is interesting that the galactoglucomannan Fractions 14-S and 16-S which have sugar ratios of 0.62:1.00:3.42 and 1.01:1.00:3.07 were extremely resistant to extraction and could only be extracted from the holocellulose with 18% sodium hydroxide containing 4% boric acid. These fractions are undoubtedly similar to the galactoglucomannan extracted from black spruce holocellulose with freezing 18% sodium hydroxide by Thompson (2). Comparison of the soluble fractions, 13-S and 17-S, with the corresponding insoluble fractions, 13-I and 17-I, shows that the insoluble component of the glucomannan triacetate fractions contains a greater amount of galactose, glucose, and xylose than the corresponding soluble component.

For all fractions investigated except Fraction 6-7-S which contains a considerable amount of xylose residues (29.6% based on the total sugar content) the ratio of galactose-to-xylose residues is 1.2 to 2.4. Thus, within these limits

TABLE III

QUANTITATIVE SUGAR CONTENTS OF THE VARIOUS ACETYLATED FRACTIONS

Fraction	Isolation	Sugar Ratio on Weight Basis[a]					Galactan: Xylan	Total Accounted for, %[b,c]
		Galactan	Glucan	Mannan	Xylan	Araban		
8-S	10% NaOH extraction - soluble as acetate	0.27	1.00	4.07	0.13	0	2.07	91.59[d]
9-S	10% NaOH extraction - soluble as acetate	0.23	1.00	3.82	0.11	0	2.12	92.82[d]
6-7-S	10% NaOH extraction - soluble as acetate	0.99	1.00	1.77	1.68	0.25	0.59	87.40[d]
13-S	18% NaOH extraction - soluble as acetate	0.16	1.00	4.38	0.07	0	2.36	94.89
13-I	18% NaOH extraction - insoluble as acetate	0.24	1.00	3.96	0.19	0	1.24	93.86
14-S	18% NaOH and 4% H_3BO_3 extraction - soluble as acetate	0.62	1.00	3.42	0.52	0.09	1.19	89.27
16-S	Water extraction after 18% NaOH and 4% H_3BO_3 - soluble as acetate	1.01	1.00	3.07	0.51	0.12	1.97	83.98[d]
17-S	Water extraction after 18% NaOH and 4% H_3BO_3 - soluble as acetate	0.27	1.00	3.89	0.21	0	1.26	94.97[d]
17-I	Water extraction after 18% NaOH and 4% H_3BO_3 - insoluble as acetate	0.35	1.00	2.54	0.28	0	1.23	70.36[d,e]

[a] The ratio of sugars is calculated on the basis of their polymerized state.
[b] Sum of sugar, acetyl, ash, and nitrobenzene lignin contents when available.
[c] The theoretical acetyl content of 44.78% was used. [d] Lignin content not included.
[e] Ash content not included. The ash content for this fraction is probably over 20%.

a relationship may exist between the amount of xylose and the amount of galactose present in the glucomannan fractions.

Qualitative sugar contents and spot area ratios of the sugars whose determination is described in Appendix IX, p. 132, were determined for all of the acetylated glucomannan and galactoglucomannan fractions. The results, presented in Appendix XI, p. 140, support the conclusions obtained from the more limited amount of quantitative data. A small amount of xylose was present in every fraction analyzed and no uronic acid was detected.

INFRARED SPECTRA

The infrared spectra of the various fractions were determined and analyzed with the objective of relating the spectra to the structure of the polysaccharides in order to elucidate the similarities and differences between these fractions. The infrared spectra of the unacetylated fractions were more informative than the spectra of the acetylated fractions due to the strong interference of the carbonyl and ester bands of the latter. A detailed analysis of the spectrum was made for the typical glucomannan, Fraction 8, and the spectra of the various other glucomannan and galactoglucomannan fractions were compared to this spectrum. The detailed infrared spectra analyses are presented in Appendix XII, p. 142. The spectra of the glucomannans, Fractions 8, 9, 13, and 17 are identical and have the characteristic bands for β-1,4 linked mannans or β-1,4 linked glucomannans. Since these glucomannan fractions had exhibited widely different resistances to extraction from the holocellulose it is significant that they are all structurally similar.

The spectra of the galactoglucomannan Fractions 7 and 16, have considerably diminished β-1,4 mannan bands and also differ from the glucomannan spectra in the

C-H, C-O, O-H, and C-O-C regions. The spectrum of the galactoglucomannan, Fraction 14, has the characteristic β-1,4 mannan bands but differs in the C-H and O-H regions. From the above results it is obvious that glucomannan fractions isolated and purified by various techniques all have a similar structure which apparently differs significantly from the galactoglucomannan structure as revealed by the infrared spectra. A portion of this structural difference is undoubtedly due to the large amount of α-1,6 linked galactose groups in galactoglucomannans but whether all the differences in the spectra can be attributed to these groups is unknown.

LIGNIN CONTENT

The lignin content determined by nitrobenzene oxidation of Fractions 13-S and 13-I (originally extracted with 18% sodium hydroxide) and Fractions 14, 14-S, and 14-I (originally extracted with 18% sodium hydroxide containing 4% boric acid) are presented in Table IV. Included in this table is the nitrobenzene lignin content of the unacetylated Fraction 14 to demonstrate that the determined lignin is not an artifact originating during acetylation. The lignin contents are substantially greater for the fractions which were initially more resistant to extraction from the holocellulose (Fractions 14, 14-S, and 14-I) than for the fractions which were less resistant to extraction (Fractions 13-S and 13-I). It is also significant that the insoluble fractions, 13-I and 14-I, have higher lignin contents than the corresponding soluble fractions, 13-S and 14-S.

THE SPECTRUM OF THE MANNOSE-CONTAINING POLYSACCHARIDES OF BLACK SPRUCE

Thompson (2) studied the noncellulosic polysaccharides of black spruce holocellulose and carried out a material balance for his extraction and isolation. He was able to account for the entire mannose content of the holocellulose. Thus,

TABLE IV

LIGNIN CONTENTS

Fraction	Isolation	Per Cent Lignin Based on Glucomannan Triacetate[a]	Per Cent Lignin Based on Unacetylated Glucomannan[a]	% Vanillin: % Syringaldehyde[b]
13-S	18% NaOH extraction, soluble as acetate	1.74	3.05	100:0
13-I	18% NaOH extraction, insoluble as acetate	3.28	5.69	90.2:9.8
14-S	18% NaOH-4% H_3BO_3 extraction, soluble as acetate	3.91	6.75	95.1:4.9
14-I	18% NaOH-4% H_3BO_3 extraction, insoluble as acetate	5.29	9.03	96.8:3.2
14	18% NaOH-4% H_3BO_3 extraction, unacetylated	--	7.17	86.9:13.1
Wood[c]	--	--	--	96.4:3.6

[a]Corrected for ash content determined by ashing at 575 ± 25°C. for three hours. Fractions 13-S and 14-S had negligible ash contents and Fractions 13-I, 14-I, and 14 had ash contents of 3.42, 14.51, and 21.6%, respectively.

[b]Based on total amount of vanillin and syringaldehyde.

[c]Black sprucewood.

comparison of the glucomannan and galactoglucomannan fractions isolated by Thompson with those studied in this investigation provides a clear picture of the relationship of these latter fractions to the entire spectrum of the mannose-containing polysaccharides of black spruce. From the comparison which is presented in Appendix XIII, p. 149, it is seen that the glucomannan Fractions 8 and 9 isolated from the 10% sodium hydroxide extract and on which the intensive study was carried out are typical of the major portion of the mannose-containing polysaccharides of black spruce. It is also apparent that various types of glucomannans and galactoglucomannans are present and that these polysaccharides which were isolated in this study are similar to those isolated by Thompson in his quantitative isolation and material balance. Therefore, conclusions based on the results of the intensive investigation of the main glucomannan Fractions 8 and 9 and the supplementary investigations of the other glucomannan and galactoglucomannan fractions in this study are applicable to the bulk of the mannose-containing polysaccharides of black spruce.

CONFIGURATION OF THE GLUCOMANNAN DETERMINED FROM THE MOLECULAR AND HYDRODYNAMIC PROPERTIES OF THE MAIN ACETYLATED GLUCOMANNAN FRACTIONS

MOLECULAR AND HYDRODYNAMIC PROPERTIES OF THE MAIN ACETYLATED GLUCOMANNAN FRACTIONS

The degrees of polymerization and hydrodynamic properties were determined for the fractions obtained by fractional precipitation of the acetylated glucomannans 8-A and 9-A. The number average degrees of polymerization, $\underline{DP}_n$, and the intrinsic viscosities in ml./g., $[\eta]$, determined on the fractions in 1,1,2-trichloroethane are listed in Table V. The analysis of $\underline{DP}_n$ with a Mechrolab High Speed Membrane Osmometer is described in Appendix XV, p. 154, and the determination of intrinsic viscosity made with a number 50 Cannon Ubbelohde semimicro dilution viscometer is described in Appendix XVI, p. 159. An attempt was made to determine the weight average molecular weights from light-scattering measurements but abnormally high molecular weights were obtained (see Appendix XVII, p. 164). This behavior was attributed to the presence of small amounts of very high molecular weight material (or aggregates) or the unusually large fluorescence correction that was involved.

Sedimentation equilibrium experiments were carried out with a Spinco Model E Analytical Ultracentrifuge, using the schlieren optical system, to determine the weight average degrees of polymerization, $\underline{DP}_w$, and the z-average degrees of polymerization, $\underline{DP}_z$, shown in Table V. This technique was particularly applicable since large particles or aggregates sediment to the bottom of the cell and have little effect on the determined degree of polymerization (25-27) and no error is incurred by fluorescence of the solutions. The measurements were made in acetophenone and the data were analyzed by the method of Lansing and Kraemer (28). The details of the calculations and experimental techniques are described in Appendix XVIII, p. 166.

TABLE V

MOLECULAR AND HYDRODYNAMIC PROPERTIES OF THE MAIN ACETYLATED GLUCOMANNAN FRACTIONS

Fraction	$\underline{DP}_n$ [a]	$\underline{DP}_w$ [b]	$\underline{DP}_z$ [b]	$[\eta]$ [c], ml./g.	$\underline{D}_\alpha \times 10^7$ [d,f], cm.^{2}/sec.	$\underline{s} \times 10^{14}$ [e,f], sec.
4	32.0	--	--	13.1	--	--
9-3	36.3	40.8	37.3	14.2	5.18	5.31
3(2)	60.6	82.4	95.8	23.4	--	--
9-2	82.2	132	157	29.7	3.37	9.95
3(1)	102.5	165	216	35.7	2.61	9.26
2(2)	123	257	452	44.6	2.45	12.3
9-1	155	--	--	44.0	--	--
I(2)	165	--	--	45.7	--	--
Insol.-1	205	--	--	47.6	--	--
2(1)	261	557	729	53.6	2.10	16.7

[a] Determined in 1,1,2-trichloroethane by osmometry. Based on the value of 288 for the triacetate monomer unit.

[b] Determined in acetophenone by sedimentation equilibrium. Based on the value of 288 for the triacetate monomer unit.

[c] Determined in 1,1,2-trichloroethane.

[d] Determined in acetophenone from transient state analysis of the sedimentation equilibrium experiments.

[e] Calculated from $\underline{M}_w$ and $\underline{D}_\alpha$.

[f] Determined at a concentration = 5×10^{-3} g./ml.

The diffusion coefficient, D_α, was determined from analysis of the transient state (approach to equilibrium) in the sedimentation equilibrium experiments (29) and the sedimentation coefficient, s, was calculated from the weight average molecular weight, diffusion coefficient, density, and partial specific volume. The determinations of the diffusion coefficients and sedimentation coefficients are described in Appendices XX, p. 193, and XXI, p. 203, respectively. The results of the determinations are summarized in Table V. These values are used in subsequent analyses. A measure of the heterogeneity of the fractions is given by the ratios of $\underline{DP}_w/\underline{DP}_n$ and $\underline{DP}_z/\underline{DP}_w$ presented in Table VI. Also presented in this table are the average values obtained by making the assumption that the Zimm-Schulz distribution applies (see Appendix XIX, p. 191).

TABLE VI

RATIO OF $\underline{DP}_n:\underline{DP}_w:\underline{DP}_z$

Fraction	Measured		"Averaged"[a]	
	$\underline{DP}_w/\underline{DP}_n$	$\underline{DP}_z/\underline{DP}_w$	$\underline{DP}_w/\underline{DP}_n$	$\underline{DP}_z/\underline{DP}_w$
9-3	1.12	0.916	1.05	1.05
3(2)	1.36	1.16	1.26	1.21
9-2	1.61	1.19	1.37	1.27
3(1)	1.61	1.31	1.53	1.35
2(2)	2.09	1.76	2.51	1.61
2(1)	2.13	1.31	1.71	1.41

[a]Average values obtained by making the assumption that Zimm-Schulz distribution applies.

CONFIGURATION OF THE GLUCOMANNAN DETERMINED FROM THE HYDRODYNAMIC PROPERTIES OF ITS TRIACETATE DERIVATIVE

INTRINSIC VISCOSITY-MOLECULAR WEIGHT RELATIONSHIP

The viscosity and molecular weight data can be represented by the empirical Mark-Houwink equation

$$[\eta] = KM^a \qquad (1)$$

where K and a are constants for a given polymer (30-32). This relationship was determined for the number average, weight average, and z-average molecular weights. The log $[\eta]$ versus log M plots are shown in Fig. 1. It is seen that these plots are not linear over the entire molecular weight range and exhibit a decreasing slope in the higher molecular weight region. Therefore, the constants of the Mark-Houwink equation were determined by the method of least squares from that data in the low molecular weight region and from the data in the high molecular weight region. These results are summarized in Table VII. Included in Table VII are values of K_1 for the intrinsic viscosity versus the molecular weight and K_2 for the intrinsic viscosity versus the degree of polymerization.

Linear polymers generally obey the Mark-Houwink equation and have a linear log $[\eta]$ versus log M relationship throughout a limited molecular weight range such as that employed in this investigation. A curvature in this plot which shows a progressively decreasing slope with increasing molecular weight is typical of branched molecules (32, 33). The abrupt change in slope exhibited in this study is indicative of a greater degree of branching or longer branches in the high molecular weight region than in the low molecular weight region.

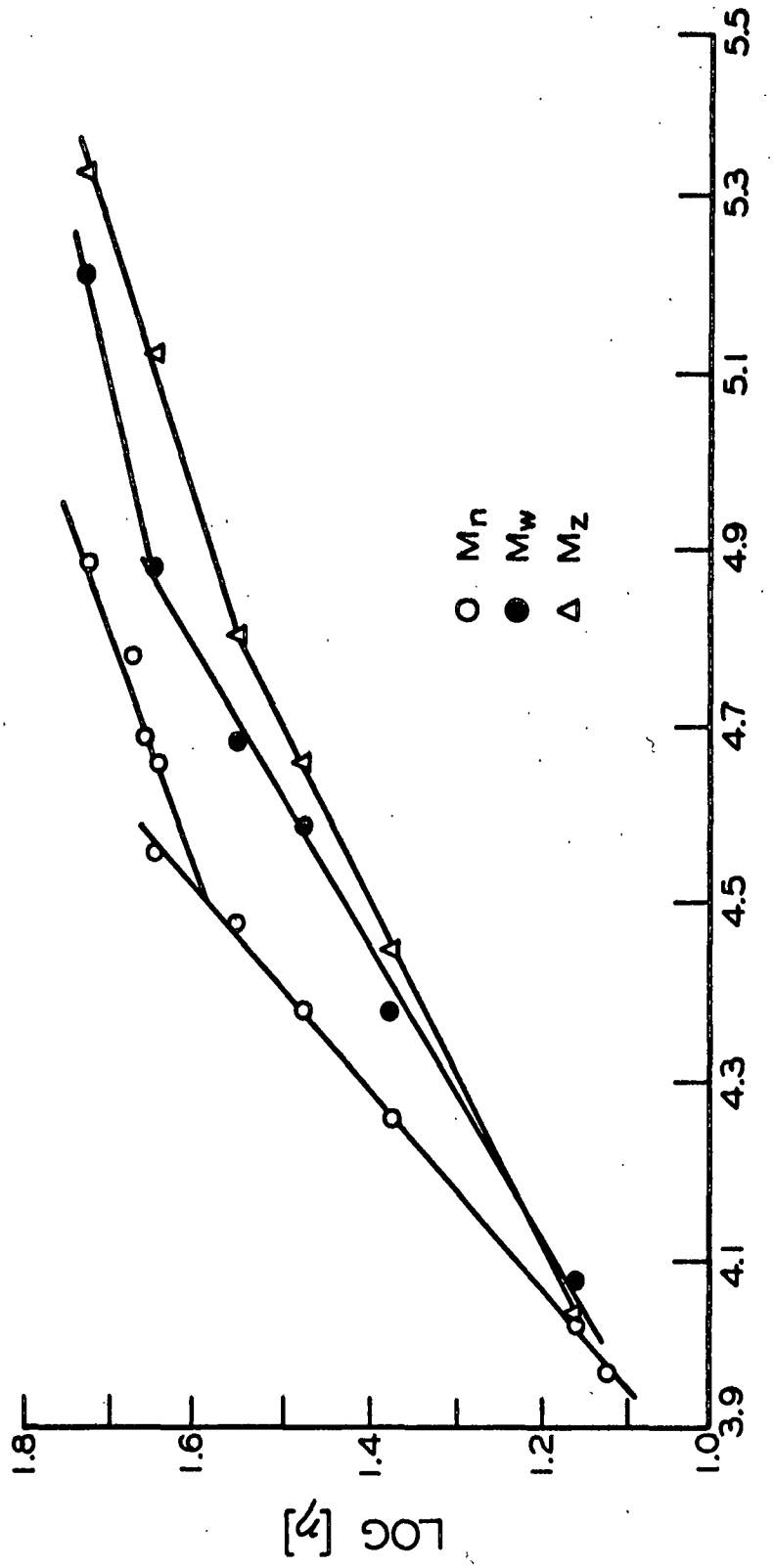

Figure 1. Log [η] Versus Log M

TABLE VII

CONSTANTS OF THE MARK-HOUWINK EQUATION

Molecular Weight Average	Range of Data Points	a	K_1 [a]	K_2 [b]
$\bar{M}_n$	First 6 points	0.897	3.60×10^{-3}	5.79×10^{-1}
$\bar{M}_n$	Last 4 points	0.355	9.80×10^{-1}	7.34
$\bar{M}_w$	First 5 points	0.622	4.30×10^{-2}	1.45
$\bar{M}_w$	Last 2 points	0.238	3.08	1.19×10
$\bar{M}_z$	First 4 points	0.521	1.13×10^{-1}	2.16
$\bar{M}_z$	Last 3 points	0.331	2.96×10^{-4}	1.93×10^{-3}

[a] Determined from the $[\eta]$, ml./g. versus M relationship.

[b] Determined from the $[\eta]$, ml./g. versus DP relationship.

The constant a is related to the configuration of the polymer molecule in solution and can be predicted theoretically by assuming various models. Theoretically, a equals zero for a rigid Einstein sphere (27, 38). For nondraining tightly packed coils $a = 0.5$, for loosely packed coils which exhibit complete free draining, $a = 1.0$ (30, 34-36) and a rigid rod exhibits a value of a equal to 2.0 (37-39). From Table VII, it is seen that the value of a in the high molecular weight region varies from 0.24 to 0.36. Thus, in this region the glucomannan triacetate molecule exhibits a behavior intermediate between an Einstein sphere and a nondraining coil. In the low molecular weight region the values of a are 0.90, 0.62, and 0.52 for the data from $\bar{M}_n$, $\bar{M}_w$, and $\bar{M}_z$, respectively. The viscosity average molecular weight is always considerably closer to the weight average molecular weight than to the number of z-average molecular weights when a is in the range of 0.5 to 1.0 (30-32). For this reason, all conclusions will be based on the value of a equal to 0.62 from the data for $\bar{M}_w$. This value of a indicates that

the glucomannan triacetate molecule approaches the behavior of a nondraining tightly packed coil in the low molecular weight region.

The exponent in the Mark-Houwink equation for various polysaccharides is given in Table L of Appendix XXII, p. 205. In every case listed in these tables the weight average molecular weights or the molecular weights from sedimentation diffusion were employed in the viscosity molecular weight relationship. From the values given in the tables, it is apparent that the β-1,4 linked linear polysaccharides exhibit a behavior typical of free draining or partially free-draining coils. In comparison to these polysaccharides, the wood glucomannan triacetate behaves as a relatively compact molecule. Considerable evidence exists in the literature which shows that coniferous glucomannans are composed primarily of β-1,4 links (3). Therefore, the relatively compact molecular structure of the glucomannan triacetate molecule must be due to branching.

The log-log plot of $[\eta]$ versus $\underline{\underline{DP}}_{\underline{w}}$ for various polysaccharides is shown in Fig. 2. The relatively compact structure of the glucomannan triacetate molecule from this study is indicated by the relatively low position of its curve in the figure. Cellulose in cadoxen, cellulose acetate, and cellulose trinitrate all have higher intrinsic viscosities at a given $\underline{\underline{DP}}_{\underline{w}}$ than the glucomannan triacetate from this study. The curves for a high molecular weight glucomannan triacetate from salep orchid tubers and guaran triacetate (a linear β-1,4 linked mannan backbone with single unit branches of α-1,6 linked galactose groups) are also above the glucomannan triacetate curve but pass through the two low $\underline{\underline{DP}}$ points in this study upon extrapolation into the low $\underline{\underline{DP}}$ region. The relationship of these two curves to the curve from this study can be interpreted as the wood glucomannan triacetate molecule having essentially a linear structure in the $\underline{\underline{DP}}_{\underline{w}}$ range of 40 to 80, slight branching occurring in the $\underline{\underline{DP}}_{\underline{w}}$ range of 80 to 250, and an

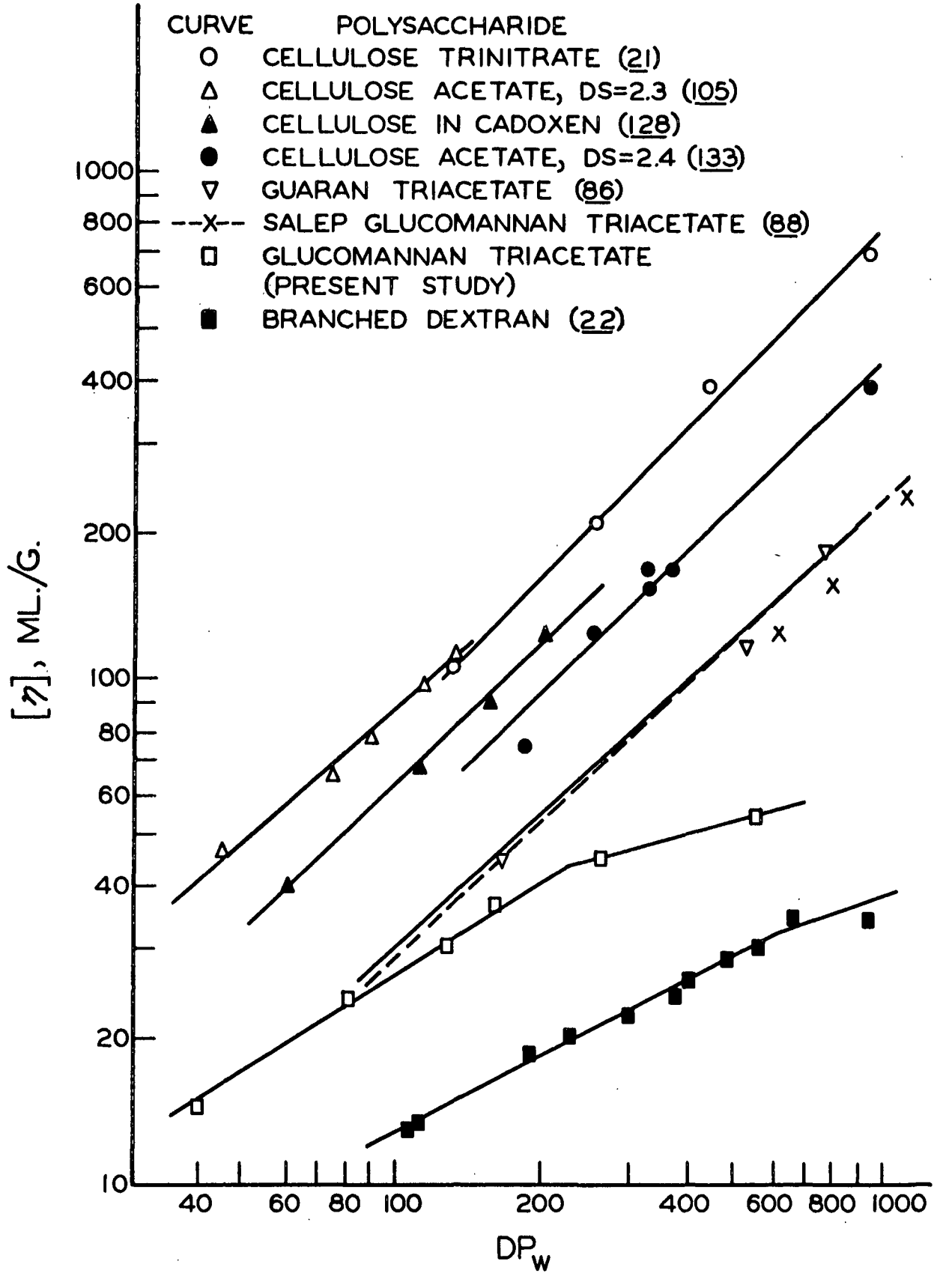

Figure 2. Log [η] Versus Log $\underline{DP}_{\underline{w}}$ for Various Polysaccharides

abrupt increase in the extent of branching above a $\underline{DP}_w$ of 250. The curve for the glucomannan triacetate is seen to lie above the curve for the more highly branched dextran.

DIFFUSION COEFFICIENT AND SEDIMENTATION COEFFICIENT VERSUS MOLECULAR WEIGHT RELATIONSHIPS

Values of log $\underline{D}_\alpha$ versus log $\underline{M}_w$ and log $\underline{s}$ versus log $\underline{M}_w$ are shown in Fig. 3 and 4, respectively. The corresponding equations in acetophenone are

$$D_\alpha = 3.39 \times 10^{-5} M_w^{-0.451} \quad (2)$$

$$s = 3.36 \times 10^{\pm 16} M_w^{0.543} \quad (3)$$

where $\underline{D}_\alpha$, $\underline{s}$, and $\underline{M}_w$ are at a concentration = 5×10^{-3} g./ml. For comparison purposes it is desirable to know the limits of the exponents in Equations (2) and (3). The $\underline{D}$ versus $\underline{M}_w$ relationship has exponents of -0.33, -0.50, and -0.67 to -1.00 for rigid (Einstein) spheres, tightly packed nondraining random coils, and loosely packed coils which exhibit free draining, respectively (30, 35). In the case of the corresponding sedimentation coefficient relationship the exponents are 0.67, 0.50, and 0.33, and 0 for rigid spheres, nondraining coils, free draining coils, and long rigid rods, respectively (30, 37). The exponent of the glucomannan triacetate lies between the exponents of a rigid sphere and a nondraining random coil.

Comparison with other polysaccharides according to Equations (2) and (3) is made in Tables LI and LII of Appendix XXII, p. 205. In contrast to the behavior of β-1,4 linked linear polysaccharides which have exponents typical of free draining or partially free-draining coils, the glucomannan triacetate behaves as a relatively compact molecule. The diffusion coefficients of the glucomannan triacetate fractions are higher than the values for β-1,4 linked linear

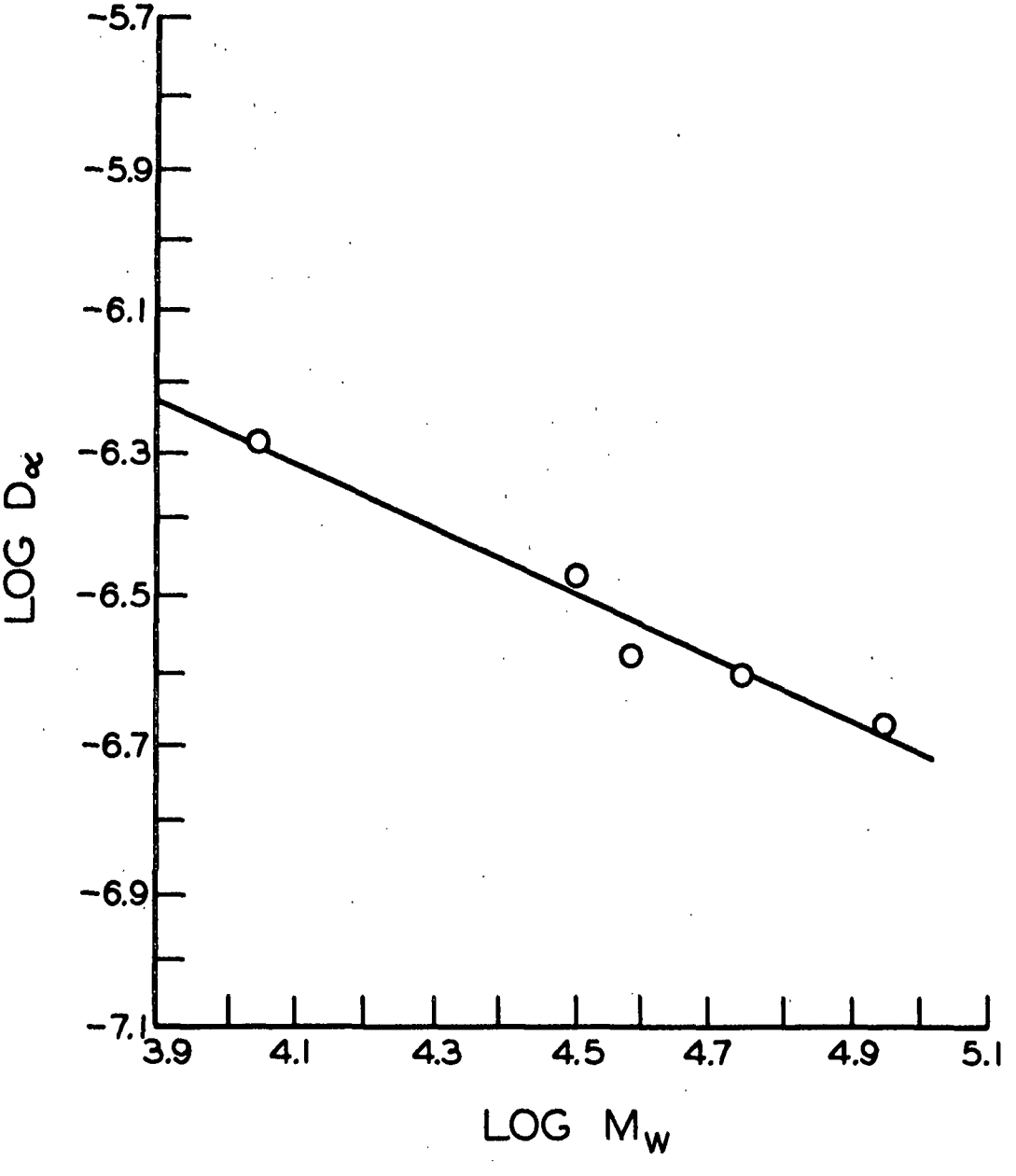

Figure 3. Log $\underline{D}_\alpha$ Versus Log $\underline{M}_{\underline{w}}$

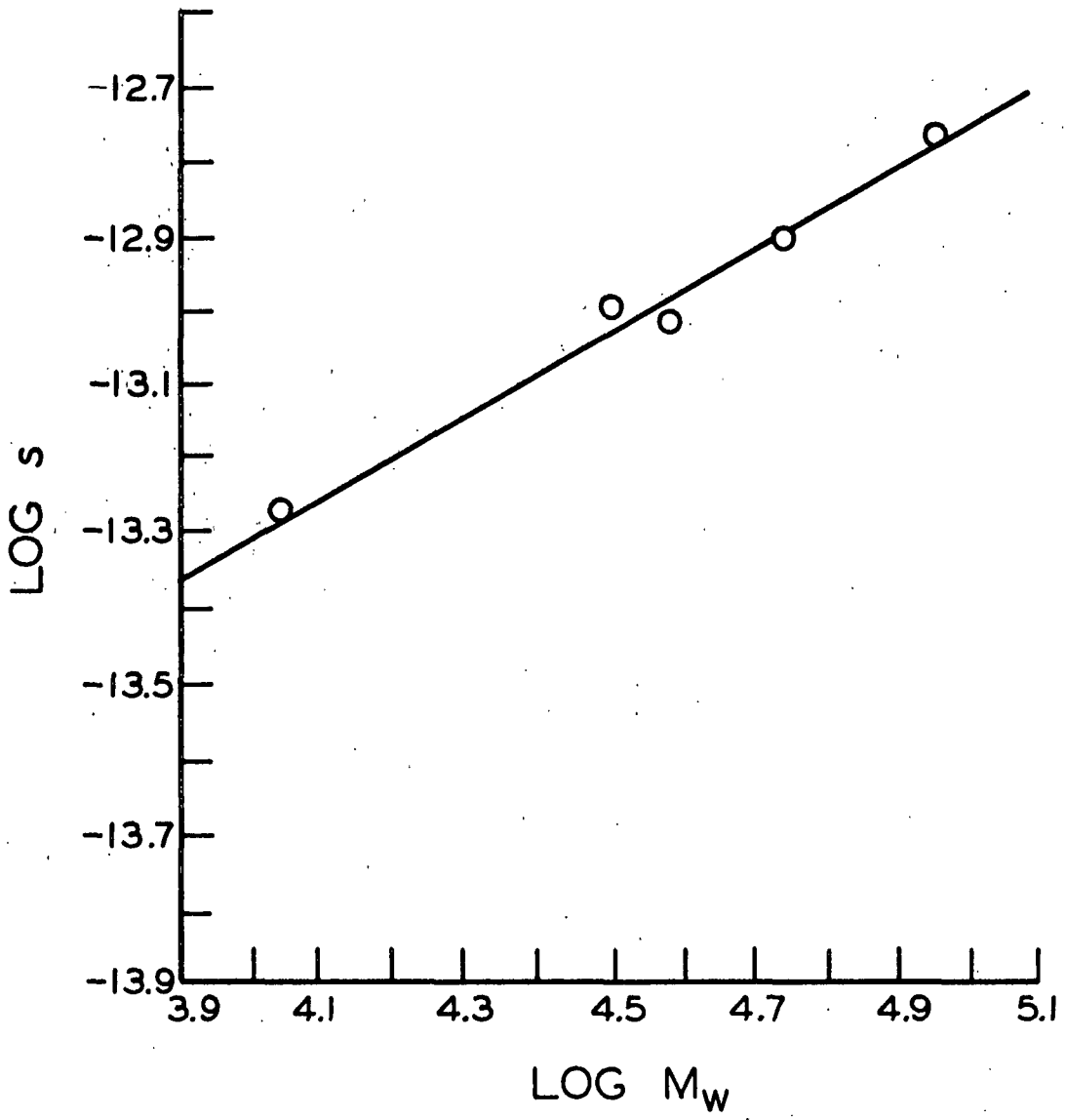

Figure 4. Log $\underline{s}$ Versus Log $\underline{M}_{\underline{w}}$

polysaccharides at a given molecular weight (see Table XLIII of Appendix XXII, p. 205). Thus, the molecular frictional coefficient, f, defined by (40) $f = kT/D$ (where k is the Boltzmann constant and T is the absolute temperature) is lower for the glucomannan triacetate than for β-1,4 linked linear polysaccharides. The relatively low value of the frictional coefficient is further evidence for a compact molecular configuration.

The above conclusions are further supported from an analysis of the diffusion coefficient data in which the ratio of the measured frictional coefficient to that of a hypothetical unsolvated sphere, f/f_{min}, is calculated (40). The deviation of f/f_{min} from 1.0 depends on two factors, solvation and asymmetry and is thus a measure of the configuration of the molecule in solution. The analysis of the data and a comparison of f/f_{min} with various polysaccharides is presented in Appendix XXIII, p. 210. The values of f/f_{min} for the glucomannan triacetate molecule are in the range of 1.9 and 2.5 which are considerably lower than the values for this parameter which have been found for β-1,4 linked linear polysaccharides. This behavior is due to a smaller molecular volume and/or to the more symmetrical shape of the glucomannan triacetate molecule in comparison to the linear polysaccharides and can be attributed to branching in the glucomannan.

THE EIZNER-PTITSYN THEORY

Eizner and Ptitsyn (41, 42) have derived equations describing the hydrodynamic properties of semirigid linear polymers. By application of their theory to intrinsic viscosity data the persistence length, a, which is a measure of chain stiffness can be calculated (42). The theory describes the experimental results obtained on semirigid β-1,4 linked linear polysaccharides more adequately than any of the other existing polymer theories (41-45). The persistence length determined from the theory is generally in the range of 50 to 70 A. for β-1,4 linked

linear polysaccharides, with the one exception of $\underline{a}$ = 132 A. for cellulose nitrate (45). Thus, the generalization can be made that if a polysaccharide has a linear β-1,4 linked structure then it has a persistence length greater than 50 A. The glucomannan triacetate from this study had a persistence length of 20.2 A. determined by analysis of the intrinsic viscosity and molecular weight data according to the Eizner-Ptitsyn theory. (The theory, analysis, and results are presented in Appendix XXIV, p. 214). Since coniferous glucomannans are composed primarily of β-1,4 links (3), one arrives at the conclusion that the glucomannan in this study is branched.

The experimental diffusion and sedimentation coefficients deviated from the theoretical values calculated from the Eizner-Ptitsyn theory (41) by 3 to 18% (see Appendix XXIV, p. 214). Thus, it appears that the gross behavior of the molecule in solution is adequately described within about 20% by the theory regardless of the detailed structure of the molecule. In other words, a low value of the persistence length obtained from the theory indicates that the molecule has a relatively compact configuration in solution and it is apparently not important whether this compact configuration results from a flexible linear molecule or a branched molecule made up of semirigid chains.

A convenient method for comparing the configuration of polymers in solution is to plot log $[(\overline{s^2}_z)^{1/2}/L_{max}]$ versus log L_{max} (45). The contour length, L_{max}, is the product of DP_w and 5.15 x 10^{-8} cm., the length of the monomer unit and $\overline{s^2}_z$ is the z-average mean square radius of gyration. (The value $\overline{s^2}_z$ is determined from the Eizner-Ptitsyn theory in Appendix XXIV, p. 214.) This type of plot was recently made for various polysaccharides by Swenson (45) and is shown in Fig. 5. The results for the glucomannan triacetate in this study were also plotted. This curve lies considerably below the family of curves for the linear β-1,4 linked

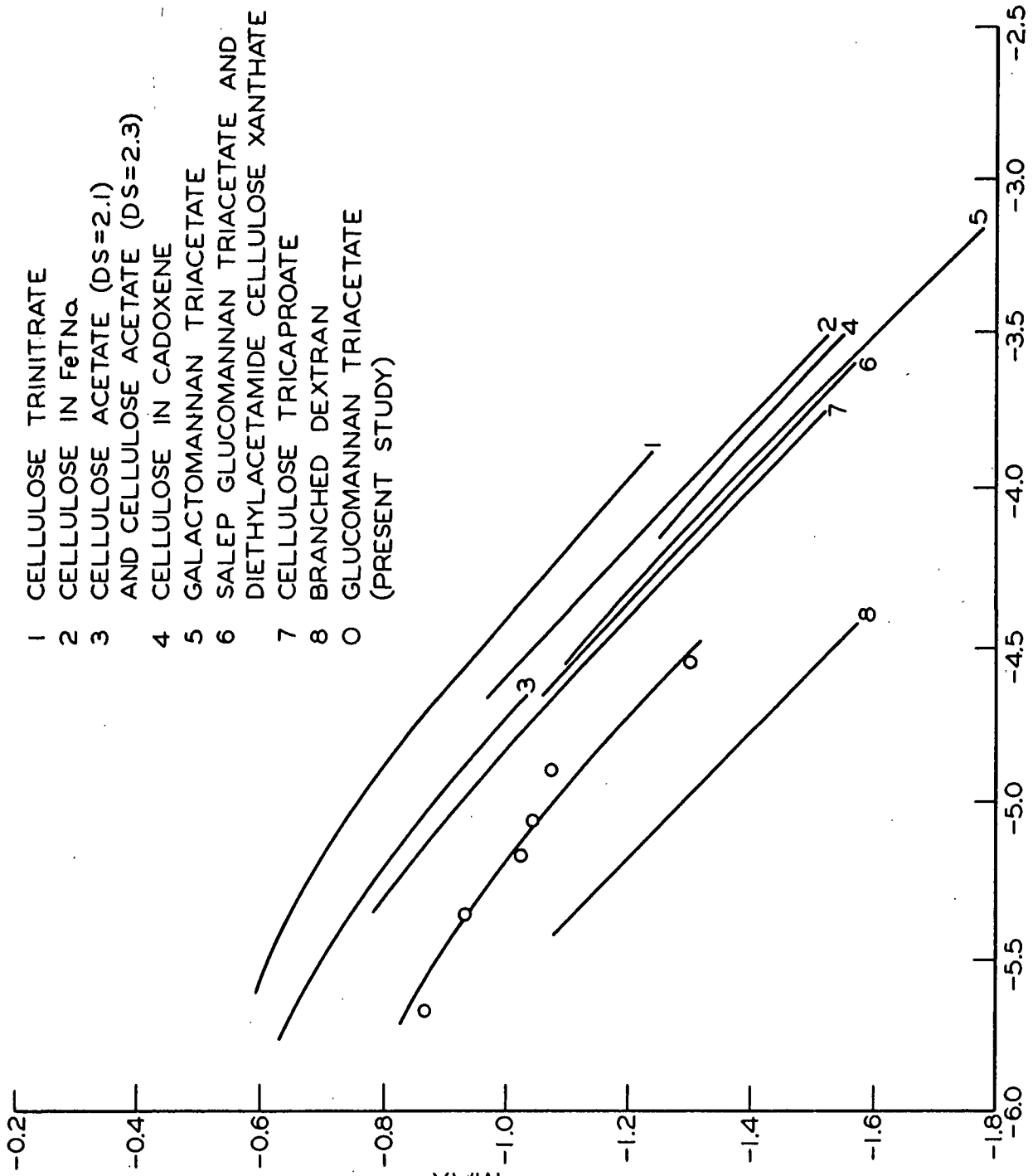

Figure 5. Log $(\overline{s_z^2})^{1/2}/L_{max}$ Versus Log L_{max}

polysaccharides, thereby demonstrating the compactness of the glucomannan triacetate molecule and strongly indicating a branched structure.

DISCUSSION

Analysis of the hydrodynamic properties has definitely shown that the glucomannan triacetate molecule has a relatively compact configuration in comparison to β-1,4 linked linear polysaccharides. A compact configuration is also indicated from analyses of the second virial coefficient, $\underline{A}_2$, from osmometry and the Huggins constant, $\underline{K}_1$, from viscometry presented in Appendices XXV, p. 229, and XXVI, p. 231, respectively.

In light of the solubility difficulties that were encountered, it is important to consider the possibility of association or aggregation of the glucomannan triacetate molecules in solution. An apparent compact molecular configuration in solution might arise from association of polymer molecules. This type of behavior in which it is possible to get extensive aggregation accompanied by a relatively small increase in viscosity would be brought about by indiscriminate or random association to form gel-like aggregates in contrast to association at the ends of the molecule which can result in a tremendous increase in viscosity (46). The following discussion is presented to show that aggregation is not an important factor in this investigation and the results indicating a compact configuration are due to the properties of the molecules and not of aggregation.

The number average molecular weight determined by osmometry was reproducible to within 1.4% in two different solvents for Fraction 3(2) which is strong evidence that association is not occurring (see Appendix XV, p. 154). The extrapolation of the osmotic pressure and the viscosity data to zero concentration gave extremely good linear correlations with high correlation coefficients (see Appendices XV,

p. 154, and XVI, p. 159). If aggregation was a factor one would expect scatter in the data and a relative increase in π/c with dilution which did not occur. The osmotic pressure second virial coefficients were positive and had reasonably high values (Appendix XV, p. 154). Since association of solute molecules is known to decrease the virial coefficient to negative values (40) this evidence is further support for the absence of association in this study.

The extrapolation of the apparent molecular weights from sedimentation equilibrium to obtain M_w and M_z for Fraction 3(2) had little scatter and positive second virial coefficients of the same order of magnitude as those from osmometry (Appendix XVIII, p. 166). The agreement between M_n, M_w, and M_z was reasonable and if association was a factor one would expect to find greater differences in these values than was found. The agreement between the molecular weights and the second virial coefficients determined by osmometry and by sedimentation equilibrium is particularly significant since different solvents were used in these determinations. Furthermore, any aggregates that are present are effectively removed in the sedimentation equilibrium determination (25-27).

From the above discussion, it is apparent that association is not an important factor in this study. This conclusion is further supported by the relatively low scatter in the log-log plots of molecular weight versus intrinsic viscosity since aggregation would contribute to scatter in these plots. The results, indicating a compact configuration, therefore, show that the glucomannan in this study is branched and that long-chain branching is present since there is a substantial effect on the hydrodynamic properties.

MOLECULAR PROPERTIES OF THE VARIOUS GLUCOMANNANS AND GALACTOGLUCOMANNANS

DEGREE OF POLYMERIZATION IN RELATION TO RESISTANCE TO EXTRACTION FROM THE HOLOCELLULOSE

In order to determine whether the degree of polymerization of the isolated glucomannan and galactoglucomannan fractions increased with increasing resistance to extraction from the holocellulose, intrinsic viscosities in cupriethylenediamine (cuene) were determined for Fraction 8 isolated from the 10% sodium hydroxide extract, Fraction 13 isolated from the 18% sodium hydroxide extract, and Fraction 14 isolated from the 18% sodium hydroxide containing 4% boric acid extract. These intrinsic viscosity values were then converted to the weight average degrees of polymerization, $\underline{\underline{DP}}_w$, using a log $[\eta]$ versus log $\underline{\underline{DP}}_w$ curve determined for the main glucomannan fractions. This curve was constructed by using the intrinsic viscosities in cuene determined for the main acetylated glucomannan Fractions 3(2), 3(1), and 2(1) and the previously determined values of $\underline{\underline{DP}}_w$ for these fractions. This is a valid procedure since complete deacetylation takes place in cuene solutions (47, 48). Details of the determination are presented in Appendix XXVII, p. 237, and the results are presented in Table VIII.

TABLE VIII

CUENE VISCOSITIES AND DEGREES OF POLYMERIZATION OF UNACETYLATED FRACTIONS

Fraction	Solution Used to Extract from Holocellulose	$[\eta]$, ml./g.	$\underline{\underline{DP}}_w$
8	10% NaOH	37.96	111
13	18% NaOH	40.52	130
14	18% NaOH-4% H_3BO_3	46.20	374[a]

[a]The large increase in $\underline{\underline{DP}}_w$ with respect to the relatively small increase in $[\eta]$ is due to the progressively decreasing slope of the log $[\eta]$ versus log $\underline{\underline{DP}}_w$ plot shown in Fig. 38 of Appendix XXVII, p. 237. This type of behavior is typical of branched molecules.

It is apparent from the results presented in Table VIII that $\underline{\underline{DP}}_w$ increases with increasing resistance to extraction. This increase in $\underline{\underline{DP}}_w$ is particularly noticeable for Fraction 14 which could only be extracted from the holocellulose with 18% sodium hydroxide containing 4% boric acid. The $\underline{\underline{DP}}_w$ of Fraction 14 is three times greater than the $\underline{\underline{DP}}_w$ of Fraction 8 from the 10% sodium hydroxide extraction. It should be pointed out, however, that there is only a small increase in $[\eta]$ and the large increase in $\underline{\underline{DP}}_w$ depends on the extremely low slope of the log $[\eta]$ versus log $\underline{\underline{DP}}_w$ curve. This relatively small increase in $[\eta]$ with respect to an increase in $\underline{\underline{DP}}_w$ is typical of branched molecules (32, 33).

MOLECULAR PROPERTIES OF VARIOUS ACETYLATED GLUCOMANNANS AND GALACTOGLUCOMANNANS

The number average molecular weights, $\underline{M}_n$, and intrinsic viscosities, $[\eta]$, in 1,1,2-trichloroethane were determined for the soluble portions of the various acetylated glucomannans and galactoglucomannans. The determinations are described in Appendices XV, p. 154, and XVI, p. 159, and the results are presented in Table IX.

TABLE IX

$\underline{M}_n$ AND $[\eta]$ OF VARIOUS ACETYLATED GLUCOMANNANS AND GALACTOGLUCOMANNANS

Fraction	Extraction Solution[a]	Type of Polymer	$\underline{M}_n$	$[\eta]$, ml./g.
8-S	10% NaOH	G.M.[b]	23,400	35.09
9-S	10% NaOH	G.M.	24,700	38.41
6-7-S	10% NaOH	Gal.G.M.[c]	25,900	32.65
13-S	18% NaOH	G.M.	23,500	38.65
14-S	18% NaOH-4% H_3BO_3	Gal.G.M.	28,300	35.84
16-S	Wash solution[d]	Gal.G.M.	26,900	34.96
17-S	Wash solution	G.M.	25,500	38.22

[a] Solution used to extract the polymer from the holocellulose.
[b] G.M. = glucomannan.
[c] Gal.G.M. = galactoglucomannan.
[d] Wash solution = water wash after 18% NaOH containing 4% H_3BO_3 extraction.

In Fig. 6 the relationship of these fractions to the log [η] versus log $\underline{M}_n$ curve for the main acetylated glucomannan fractions is shown. The fact that the points for all the fractions lie close to the main curve indicates that the chain structures of the various glucomannans and galactoglucomannans from black spruce do not differ in any gross characteristic. It should be emphasized that this is only an approximate generalization since exact interpretation of the data is impossible due to the heterogeneity of the fractions. However, it does appear that all the fractions have a similar hydrodynamic volume and thus probably have similar long-chain branching.

The narrow molecular weight range (23,400 to 28,300) of the fractions is quite remarkable since they had been isolated under widely varying conditions. These fractions are the soluble portions of the acetate derivatives and this narrow $\underline{M}_n$ range indicates that fractionation into soluble and insoluble fractions (Appendix X, p. 136) is controlled primarily by molecular weight, with insolubility occurring above a given molecular weight. Therefore, the $\underline{DP}_n$ of a portion of glucomannan molecules in the main acetylated Fraction 8-A is even greater than the value of 261 determined on the highest molecular weight soluble fraction (Appendix XV, p. 154) since 25% of Fraction 8-A was insoluble (Appendix VIII, p. 125). This is an interesting conclusion because the value of 261 is the highest reported number average degree of polymerization for wood glucomannans.

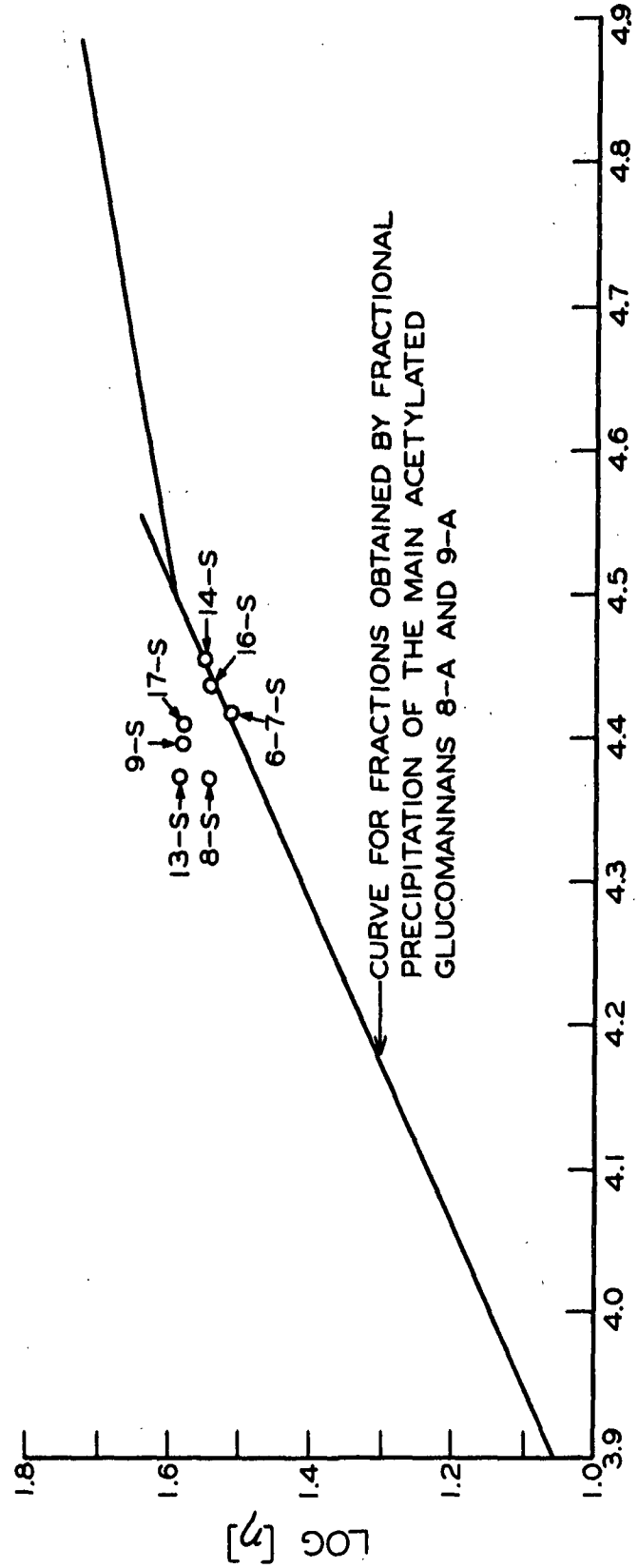

Figure 6. Log [η] Versus Log $\underline{M}_n$ for Various Acetylated Glucomannans and Galactoglucomannans

DISCUSSION OF THE LIGNIN-GLUCOMANNAN LINKAGE

INTRODUCTION

The first indication that lignin might be present in the isolated glucomannan and galactoglucomannan fractions came from infrared spectra studies of the fractions. Every fraction investigated contained a weak band at about 1515 $cm.^{-1}$ which was attributed to the aromatic groups of lignin. Some fractions contained other bands which could also be explained by the presence of lignin. Further evidence indicating the presence of lignin came from the qualitative sugar analysis. During hydrolysis with 72% sulfuric acid, it was noticed that all fractions contained a small amount of insoluble material. This material had the appearance of Klason lignin and undoubtedly would show up in a Klason lignin analysis. The above results, indicating the presence of lignin, were corroborated from nitrobenzene lignin analyses on a few selected fractions which showed that the lignin content based on the unacetylated glucomannan varied from 3 to 9% (see Tables II and IV).

INDICATION OF LIGNIN-CARBOHYDRATE LINKAGE

A summary of the behavior of the lignin during isolation of the glucomannan and galactoglucomannan fractions is presented in Fig. 7. The presence of lignin after the fractions have been extensively purified indicates that this lignin may be chemically linked to the glucomannan. In particular, lignin is found in widely separated fractions obtained by careful fractional precipitation of the main glucomannan triacetate. The large ratio of the volume of solvent to the weight of polymer used minimizes occlusion by polymer species present as impurities during fractional precipitation. Thus, the presence of lignin in an insoluble fraction (Fraction Insol'.), a fraction of $\underline{DP}_n$ = 261, [Fraction 2(1)], and a fraction of $\underline{DP}_n$ = 61 [Fraction 3(2)] is very significant.

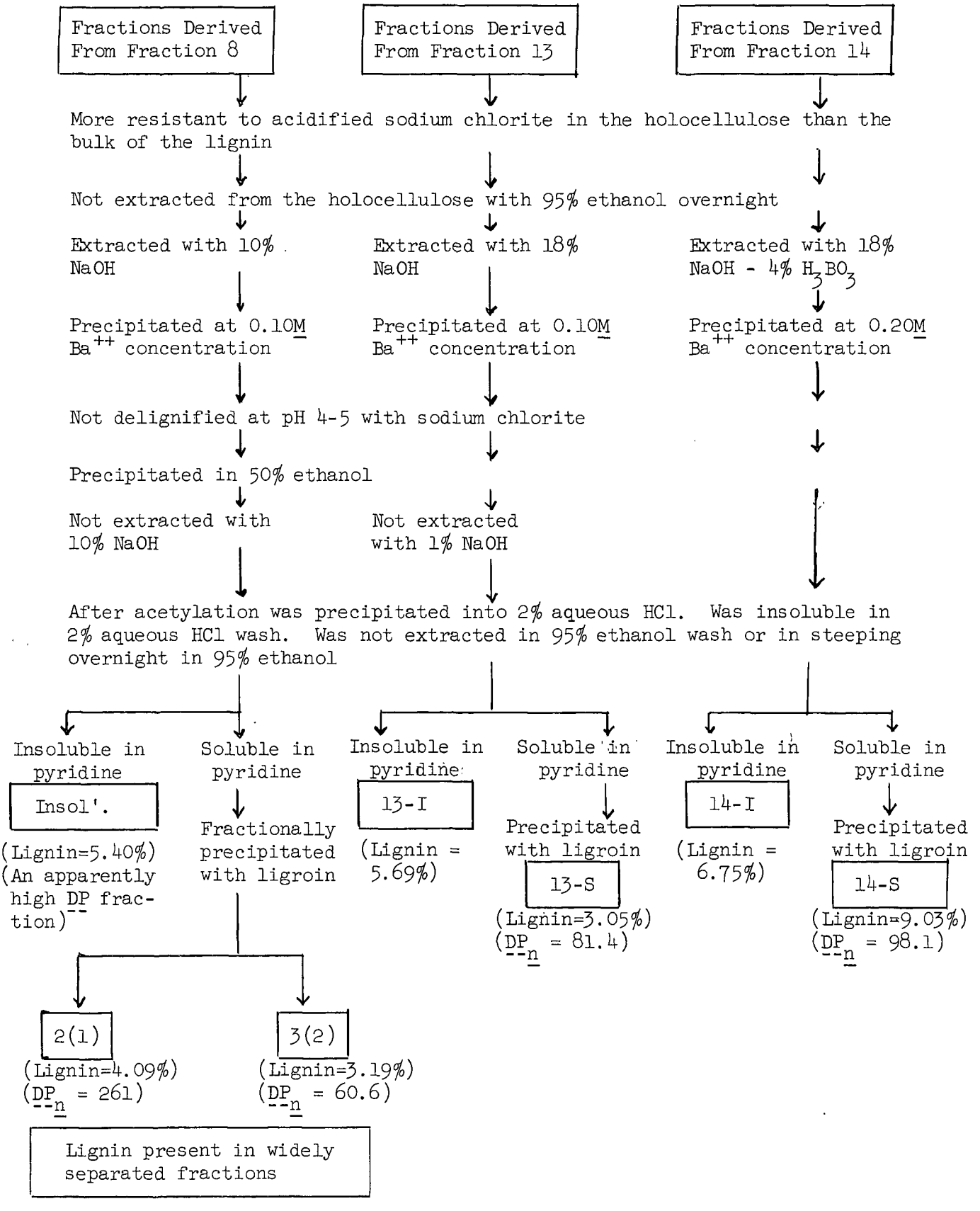

Figure 7. Behavior of the Lignin in the Glucomannan and Galactoglucomannan Fractions During Isolation

This lignin was more resistant to the action of acidified sodium chlorite than the bulk of the lignin in the holocellulose and also was not destroyed in the isolated fractions by dilute aqueous sodium chlorite at pH 4 to 5 at room temperature. Chlorine dioxide which is produced from acidified sodium chlorite destroys the aromatic nature of lignin (see Appendix II, p. 88). Since nitrobenzene oxidation of the lignin in the fractions gave vanillin and syringaldehyde, it is obvious that the aromatic nature of this lignin remained intact. The resistance of this lignin to reaction with acidified sodium chlorite may be due to the presence of a lignin-carbohydrate linkage. This resistant lignin was not extracted from either the holocellulose or the isolated lignin fractions with ethanol. Since some isolated lignin fractions are soluble in alcohol (49-52) the insolubility of this lignin may be due to a lignin-carbohydrate linkage. To summarize the information in Fig. 7, the fact that lignin is present in widely separated glucomannan fractions, while the solubility properties of lignin differ considerably from glucomannans indicates that the lignin may be chemically linked to the glucomannan. A literature review of the lignin-carbohydrate linkage presented in Appendix I, p. 80, reveals that there is a considerable amount of experimental evidence supporting the existence of this type of linkage. Therefore, the hypothesis is made that the lignin is chemically linked to the isolated glucomannan and galactoglucomannan fractions and the results of this investigation are reviewed in light of this concept.

LIGNIN IN RELATIONSHIP TO SOLUBILITY AND MOLECULAR SIZE OF THE GLUCOMANNAN AND GALACTOGLUCOMANNAN FRACTIONS

It is seen from Tables II and IV that the insoluble acetylated Fractions Insol'., 13-I, and 14-I have higher lignin contents than the corresponding soluble acetylated fractions, 3(2) and 2(1), 13-S and 14-S. This can be explained by a cross-linking of glucomannan molecules through a common lignin molecule.

This cross-linked molecule would have a higher molecular weight and probably would be less soluble than a glucomannan molecule not linked to lignin. The higher the lignin content in a glucomannan fraction, the higher the probability of cross-linking which may explain the greater lignin contents in the insoluble fractions as compared to the soluble fractions. Some evidence which indicates the insoluble fractions have higher molecular weights than the corresponding soluble fractions is presented in the Molecular Properties of Various Glucomannans and Galactoglucomannans section, p. 38.

Further evidence is obtained from the magnitude of the molecular weights found for the glucomannan fractions investigated in this study. For the fractions obtained from fractional precipitation, the range for $\underline{DP}_n$ is 32 to 261, the range for $\underline{DP}_w$ is 41 to 557, and the range for $\underline{DP}_z$ is 37 to 729. The degrees of polymerization at the upper end of the ranges are considerably greater than the values reported for wood glucomannans in the literature. The greater molecular weights found in this study are probably due to a lignin-glucomannan linkage as discussed above. This concept is further supported by the greater lignin content of Fraction 2(1) with $\underline{DP}_n$ of 261 as compared with Fraction 3(2) with $\underline{DP}_n$ of 61. Further evidence indicating a trend in increasing molecular weight with increasing lignin content is given in the following section on the relationship of the lignin content to the extraction sequence.

The hypothesis that two or more glucomannan molecules are joined to a common lignin moiety, giving a branched lignin-carbohydrate complex explains the relatively compact molecular structure of the glucomannan fractions found in this study. It has been shown previously that the relatively high molecular weight Fraction 2(1) has a more compact structure than the lower molecular weight fractions such as Fraction 3(2). If the above hypothesis is correct, one would expect to find

a greater lignin content in Fraction 2(1) than in Fraction 3(2). The lignin contents in Fractions 2(1) and 3(2) are 4.09 and 3.19%, respectively (based on the unacetylated glucomannan); thus, the above prediction is substantiated. Although the lignin-carbohydrate linkage appears to contribute toward the compact structure of the glucomannan molecule it is not the only possible cause. Other investigators have found evidence that some glucomannans from gymnosperms contain carbohydrate branches (3). Thus, it is possible that both lignin-carbohydrate linkages and carbohydrate branches are contributing toward the compact structure.

A great deal of difficulty was encountered in attempting to find a solvent which would completely dissolve the main acetylated glucomannan 8-A (Appendices VII, p. 118, and VIII, p. 125). In light of the preceding discussion on the lignin-carbohydrate linkage it is a good possibility that this type of linkage is responsible for the insolubility of a portion of the glucomannan triacetate fractions in many organic solvents. This phenomenon may be similar to the reported insolubility of nitrated wood in acetone although nitrocellulose and nitrolignin are known to be soluble in acetone (53, 54).

The question arises, why haven't other workers found high molecular weights for isolated glucomannan fractions if the probability of a lignin-carbohydrate linkage is so high? As was discussed above, solubility problems are encountered with the acetate derivative of glucomannans. For this reason, most investigators have made molecular weight measurements on the nitrate derivative of glucomannans. Meier (5) found that nitration of a lignin-glucomannan complex resulted in complete delignification. Therefore, molecular weight measurements on a glucomannan nitrate give a value for the glucomannan molecule and not the lignin-glucomannan complex even though the original glucomannan fraction may have contained lignin. Viscosity measurements alone on the original lignin-glucomannan complex would not

reveal a relatively high molecular weight since the viscosity would increase very little with an increase in molecular weight resulting from a cross-linked lignin-glucomannan complex. The probability of isolating a lignin-glucomannan complex was enhanced in this study due to the extremely mild conditions employed in the holocellulose preparation (Appendix II, p. 88). Although, the mild chlorite delignification at room temperature reduced the Klason lignin content in the holocellulose to 2.3%, the acid-soluble lignin content was 14.0% and much of this lignin may have been involved in lignin-carbohydrate linkages.

RELATIONSHIP OF LIGNIN CONTENT TO RESISTANCE TO EXTRACTION OF GLUCOMANNANS AND GALACTOGLUCOMANNANS

The lignin contents of the unacetylated Fractions 8, 13, and 14 were estimated from a material balance on the acetylated fractions derived from them. The calculation of these values is presented in Appendix XXVIII, p. 242, and the results along with the measured lignin content of Fraction 14 are presented in Table X.

TABLE X

LIGNIN CONTENT IN RELATION TO RESISTANCE TO EXTRACTION

Fraction	Extraction Solution	Lignin Content, (based on unacetylated glucomannan), %
8	10% NaOH	4.23[a]
13	18% NaOH	4.53[a]
14	18% NaOH-4% H_3BO_3	8.47[a]
14	18% NaOH-4% H_3BO_3	7.17[b]

[a]Estimated lignin content from material balance.

[b]Measured lignin content.

From Table X it is seen that there is a slight increase in the lignin content from Fraction 8 to Fraction 13 and a substantial increase in the lignin content in Fraction 14 which could only be extracted with 18% sodium hydroxide containing 4% boric acid. This trend to an increased lignin content with an increased resistance to extraction for the glucomannan fractions can be explained by a strong association of the lignin with the glucomannan in the holocellulose, perhaps through a chemical linkage. Many investigators have explained the resistance of the glucomannan to extraction by its close association with the cellulose in the fiber. From the results of this investigation, it is hypothesized that the cellulose-glucomannan association is only one factor and that the lignin-glucomannan association in the fiber also plays an important role in the glucomannan's resistance to extraction.

The physical picture is similar to that suggested by Lindberg (55) in which the lignin and the carbohydrates are present in a solid solution containing many hydrogen bonds and occasional chemical linkages between lignin and carbohydrate molecules, resulting in a cross-linked network. The extraction of resistant glucomannan fractions at higher alkali concentrations is then pictured as the result of a combination of increased solubility, increased accessibility due to swelling and partial disruption of the fiber structure, and destruction of occasional lignin-carbohydrate linkages. This hypothesis agrees well with the fact that a considerable amount of carbohydrate material is removed as the last 2 or 3% lignin is removed from a holocellulose (56, 57).

The hypothesis given above predicts that the more resistant glucomannan fractions, containing a greater lignin content should have a higher molecular weight than the easily extractable glucomannan fractions with a lower lignin content since the probability of cross-linking increases with increasing lignin

content. This behavior was found from a determination of the intrinsic viscosities in cupriethylenediamine. The calculated weight average degrees of polymerization were 111, 130, and 374 for Fractions 8, 13, and 14, respectively.

From the results of a material balance on the holocellulose and the extracted residue, it was shown that the ratio of lignin to hemicellulose was constant in the holocellulose, the sum of the extracts, and the extracted residue (Appendix IV, p. 105). This type of behavior is consistent with the existence of a lignin-hemicellulose linkage.

RELATIONSHIP OF LIGNIN CONTENT TO SUGAR CONTENT

From the quantitative and the qualitative sugar analyses, it is seen that the galactose and xylose content is greater in Fraction 14 from the 18% sodium hydroxide containing 4% borate extract than in Fractions 8 and 13 from the 10 and 18% sodium hydroxide extracts, respectively. Since Fraction 14 contains more lignin than the other two fractions, the greater content of galactose and xylose in this fraction may be due to the presence of a lignin-carbohydrate linkage of the type suggested by Meier (5, 7). Meier found that a glucomannan fraction from pine contained xylose and galactose residues which could not be separated before delignification but were easily removed after delignification. From these results and from electrophoresis studies, Meier concluded that different polysaccharides, glucomannans and xylans, as well as galactans or arabogalactans, may be linked to the same lignin molecule. The presence of a small amount of xylose in every fraction investigated in this study may be due to this type of linkage.

DEGREE OF BRANCHING AND NATURE OF THE BRANCH POINTS

POSSIBLE STRUCTURES

The results of this investigation have shown that the glucomannan from black spruce has a significant degree of branching which results in a considerable decrease in its molecular hydrodynamic volume. Evidence has also been found that lignin is closely associated with the glucomannan molecule and it appears that lignin may be involved in the branching. The possible branched structures are presented in Fig. 8. In a linear chain all monomer units are attached to only one or two other monomer units but in a branched chain, certain monomer units may be attached to three or more monomer units. These monomer units are called branch units. The number of monomer units attached to a branch unit is defined as the functionality of the branch unit.

In Fig. 8 two basic types of branching are considered. The first type of branching involves only sugar branch units which are considered to occur only as trifunctional units. The restriction to trifunctional branch units is necessary because the occurrence of four bulky chains linked to one sugar monomer unit is highly improbable and no evidence for tetrafunctional sugar units in glucomannans has been found from methylation studies reported in the literature. The branching would occur through glycosidic linkages. Structures A and C represent the two possibilities of branching onto a linear backbone and branching resulting in a highly ramified structure. The second type of branching that is considered involves lignin in which sugar units from separate glucomannan chains are linked to a common lignin moiety, thus resulting in a branch point. The branch unit in this case is the lignin moiety and the sugar units from the separate chains which are combined to the lignin moiety. Structures B and D represent the case of trifunctional branch units. It is felt that these types

TRIFUNCTIONAL BRANCH UNITS - LINEAR BACKBONE:

A

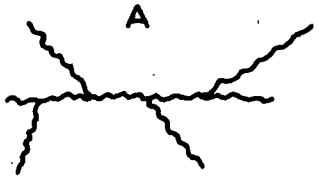

B

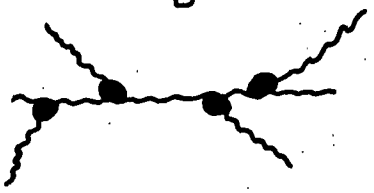

TRIFUNCTIONAL BRANCH UNITS - HIGHLY RAMIFIED STRUCTURE:

C

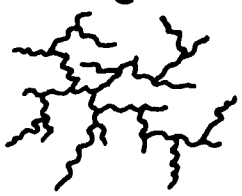

D

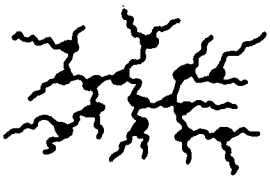

TETRAFUNCTIONAL BRANCH UNITS - LINEAR CHAINS LINKED TOGETHER IN RANDOM MANNER:

E

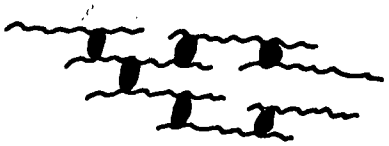

ONE MULTIFUNCTIONAL BRANCH UNIT:

F

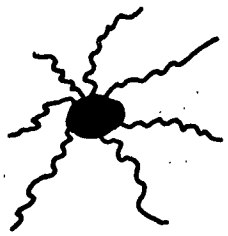

~~~~ LINEAR CHAIN

● LIGNIN MOIETY

Figure 8. Possible Structures of the Branched Glucomannan Molecule
~~~~

of structures are improbable since they would occur only from the rather special case of a glycosidic linkage from a sugar monomer unit of one chain to a lignin hydroxyl group and a linkage of hydroxyl group from a sugar unit in the second chain to either a lignin hydroxyl group or carbonyl group. Since the glycosidic linkage could only occur at the reducing end group, one chain would be linked to the lignin moiety at the end of the chain and the other chain would be linked to the lignin at any point along its chain. Structure F is another special case in which only sugar glycosidic linkages to lignin hydroxyl groups occur. In this case, the branching would result in a star-shaped molecule with many linear chains attached to a common lignin moiety at their reducing end groups.

A more general type of branching would occur if the hydroxyl groups on all sugar monomer units could link with equal probability to lignin hydroxyl or carbonyl groups. In this case linear chains would be cross-linked in a random manner by common lignin moieties resulting in tetrafunctional branch units made up of the lignin moiety and the two sugar units to which it is linked. This type of branching is represented by Structure E and from the ideas formulated in this study this structure is the most probable result of a lignin-carbohydrate linkage. This type of cross-linking could easily result in a continuous lignin-hemicellulose matrix in the fiber. Structures similar to E with multifunctional branch units greater than tetrafunctional are also possible but will not be considered because of the greater probability of two chains linked to a common lignin moiety than three or more chains at the low lignin levels of 3 to 4%. Of course, combinations of the above structures are possible but will not be considered because of the lack of exact information and the simplicity of the above idealized models.

DEGREE OF BRANCHING

A branched molecule has a smaller hydrodynamic volume and consequently a lower intrinsic viscosity than a linear molecule at the same molecular weight (33, 58-69). The decrease in the mean square radius of gyration with branching has been treated theoretically by Zimm and Stockmayer (59) and they present tables relating the ratio g of the mean square radius of gyration of a branched to a linear molecule of the same molecular weight to the degree of branching for various branched models. Various relationships have been suggested relating the ratio g' of the intrinsic viscosity of a branched polymer to that of a linear polymer of the same molecular weight to the ratio g (59-62) and the most satisfactory relationship to date is $g' = g^{1/2}$ (61, 62). Kilb (62) has used this relationship and theoretically treated the case of a polydisperse polymer with a random distribution of tetrafunctional cross-links. His model is a polymer which is composed of linear chains with an initial molecular weight distribution such that $M_w/M_n = 2$. These chains have then been linked together randomly through tetrafunctional cross-links to give a polydisperse branched polymer.

The model that Kilb treated is similar to Structure E of Fig. 8, which is considered to be the most probable structure of the branched glucomannan molecule in this investigation. The one questionable point in applying Kilb's model to the present case is the necessary assumption that the primary linear chains (the linear chains remaining if all the cross-links were broken) and the branched cross-linked glucomannan molecule have molecular weight distributions which are adequately described by the distribution function employed by Kilb. However, Kilb was able to show that his treatment was not very sensitive to the exact distribution function as long as the ratio g' is calculated by comparing the intrinsic viscosities of the branched and linear molecules at the same weight average degree of polymerization. Therefore, Kilb's model should adequately apply to Structure E by

calculating g' at the same weight average degree of polymerization, thus minimizing the effect of the molecular weight distribution. The degree of branching is calculated in the following manner. The branching parameter, γ, is calculated from tables relating the intrinsic viscosity ratio g' to the branching parameter γ at various values of the exponent, a, in the viscosity-molecular weight relationship for the corresponding linear polymer, $[\eta]_{linear} = K\overline{M}_w^a$. Then the weight average number of cross-links per molecule, $\overline{m}_w$, is calculated with Equation (4).

$$\overline{m}_w = \frac{\gamma}{(1 - \gamma)} \qquad (4).$$

The weight average degree of polymerization of the primary linear molecules, Primary $\overline{DP}_w$, is given by Equation (5).

$$\text{Primary } \overline{DP}_w = \overline{DP}_w (1 - \gamma) \qquad (5)$$

where $\overline{DP}_w$ is the weight average degree of polymerization of the cross-linked molecule.

To apply the above theory it is necessary to have an $[\eta]$ versus $\overline{DP}_w$ relationship for a linear glucomannan triacetate. Juers's (43) data for a linear high molecular weight salep glucomannan triacetate is shown in the log $[\eta]$ versus log $\overline{DP}_w$ plot of Fig. 2. It is necessary to extrapolate his data into the lower molecular weight region of this study. The salep glucomannan triacetate curve and the guaran triacetate (21) curve essentially coincide and both curves pass through the two lowest molecular weight points of the wood glucomannan triacetate in this study. Guaran is a linear β-1,4-linked mannan with single unit side chains of galactose linked α-1,6. The curve for guaran triacetate (the $\overline{DP}_w$ employed is that of the mannan backbone) was used as a reference in this study rather than the salep glucomannan triacetate curve since the data points of the former curve extend into the molecular weight region of this study and, therefore, are probably

more accurate than the extrapolated salep glucomannan triacetate curve. Due to the similarity of the two curves, essentially the same results would have been obtained if the salep glucomannan triacetate curve had been used for the reference linear glucomannan. Since different solvents were used to measure the intrinsic viscosities of the guaran triacetate fractions than the glucomannan triacetate fractions, the assumption is made that the solvent effects are negligible. This is a reasonable assumption since the intrinsic viscosities of β-1,4-linked polysaccharides are less affected by polymer-solvent interaction than flexible polymers (45).

Before calculations were made of the long-chain branching by Kilb's treatment, it was necessary to first correct for the presence of short-chain branching. It is believed that the galactose groups are present as unit side chains linked to the main glucomannan chain (3). It was assumed that the small amount of xylose in the fractions was also present as unit side chains and a correction was made for the galactose and xylose side groups in the following manner. The following equation derived by Stockmayer (70) for a monodisperse system with equally spaced short branches was used to calculate g.

$$g = \frac{1}{s + 1} [1 + s(1 - 2f + 2f^2 - 2f^3) + s^2(-f + 4f^2 - f^3)] \qquad (6)$$

where s is the number of branches per molecule and f is the fractional length of a branch. The average mole ratio of sugar residues for Fractions 3(2), 3(1), 2(2), and 2(1) is galactose:glucose:mannose:xylose:arabinose = 0.21:1.00:3.97:0.16:0. Since the mole ratio of galactose and xylose residues is 6.9% of the neutral sugar content, $s = (0.069)(\underline{DP}_w)$ and $f = 1/\underline{DP}_w$. The ratio $g'_{\text{short branches}}$ for short-chain branching is calculated from $g' = g^{1/2}$ (61). The value of g' corrected for short-chain branching, $g'_{\text{corrected}}$, is then calculated with Equation (7).

$$g'_{corrected} = \frac{g'_{experimental}}{g'_{short\ branches}} \qquad (7).$$

From the results presented in Table XI, it is seen that the reduction in intrinsic viscosity due to the unit side chains of galactose and xylose groups is less than 4%.

The corrected ratio, $g'_{corrected}$, was used in the treatment of Kilb and the results are presented in Table XI. The weight average number of branch points per molecule increases from 0.1 for the low DP Fraction 3(2) to 7.1 for the high DP Fraction 2(1). These values are considerably more reasonable than the corresponding values calculated by assuming trifunctional branched models. In the latter case the number of branch points per molecule are unrealistically large, thus lending support to the validity of the randomly branched tetrafunctional model that was chosen. The DP_w of the primary chains are reasonably constant within the range of 69 to 82, and have an average value of 77. This fairly constant value of Primary DP_w regardless of the DP of the entire cross-linked molecule is good support for the validity of the branching theory and the branched model employed in this treatment. It should be mentioned that reasonably close results and essentially the same conclusions would have been obtained if the correction for short-chain branching had not been applied.

THE STRUCTURE OF THE GLUCOMANNAN FRACTIONS AND THE NATURE OF THE BRANCH POINTS

The average mole per cent of galactose and xylose residues is 3.9 and 3.0%, respectively. Therefore, each primary chain with a DP_w of 77 has on the average 3.0 galactose residues and 2.3 xylose residues attached as unit side groups to a linear chain of 72 glucose and mannose residues. These primary chains are linked together by lignin through tetrafunctional cross-links as shown in Fig. 9.

TABLE XI

DEGREE OF BRANCHING

Fraction	$\underline{g}'_{experimental}$ [a]	$\underline{g}'_{short\ branches}$ [b]	$\underline{g}'_{corrected}$ [c]	γ [d]	$\eta_{\underline{w}}$ [e]	Primary $\underline{DP}_{\underline{w}}$ [f]
3(2)	0.934	0.961	0.972	0.093	0.10	75
9-2	0.820	0.962	0.852	0.430	0.75	75
3(1)	0.779	0.963	0.809	0.501	1.00	82
2(2)	0.644	0.964	0.668	0.681	2.14	82
2(1)	0.412	0.964	0.427	0.876	7.06	69

[a] Experimental $[\eta]_{branched}/[\eta]_{linear}$.

[b] Theoretical $[\eta]_{branched}/[\eta]_{linear}$ for galactose and xylose unit side chains.

[c] $[\eta]_{branched}/[\eta]_{linear}$ corrected for galactose and xylose unit side chains.

[d] Branching parameter.

[e] Weight average number of branch points per molecule.

[f] $\underline{DP}_{\underline{w}}$ of primary linear chain, including the galactose and xylose side groups.

FRACTION 3(2)
$DP_w = 82.4$
$M_w = 0.10$

FRACTION 9-2
$DP_w = 132$
$M_w = 0.75$

AND

FRACTION 3(1)
$DP_w = 165$
$M_w = 1.00$

FRACTION 2(2)
$DP_w = 257$
$M_w = 2.14$

FRACTION 2(1)
$DP_w = 557$
$M_w = 7.06$

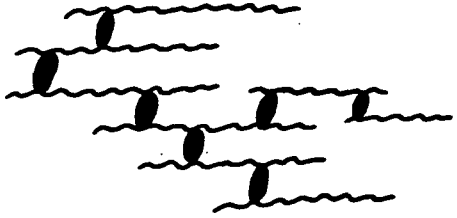

~~~~ LINEAR CHAIN

● LIGNIN MOIETY

DP_w = WEIGHT AVERAGE DEGREE OF POLYMERIZATION

M_w = WEIGHT AVERAGE NUMBER OF BRANCH POINTS PER MOLECULE

Figure 9. Structure of the Glucomannan Fractions
~~~~

The degree of branching varies from the essentially linear structure of the low DP Fraction 3(2) to the highly branched structure of the high DP Fraction 2(1) which contains approximately 7 cross-links and 8 primary chains per molecule. All the fractions are considered to be artifacts occurring from the cleavage of the lignin-carbohydrate linkages of a continuous lignin-hemicellulose matrix within the fiber.

The number average degrees of polymerization of isolated glucomannans from coniferous woods vary from 35 to 140 but most are in the range of 70 to 110 (3). It is felt that the DP_w of 77 obtained for the primary chain in this study is quite reasonable in comparison to these values. It should be pointed out that the branching theories are not exact and the actual DP of the primary chain could easily be approximately 100 which would agree with the DP_n of many isolated glucomannans in the literature (3). Although it is impossible to tell if the isolated glucomannans in the literature were completely delignified, they probably contained less lignin than the fractions in this study and, therefore, should have a DP closer to that of the primary chain than the relatively high DP Fractions 2(2) and 2(1) of this study.

For randomly cross-linked polymers the branching parameter γ is unity at incipient gelation (62, 71, 72). The value of γ for Fraction 2(1) is 0.876. This value of γ close to unity might explain the substantial amount of insoluble material that was present in all the acetylated fractions before purification. If this explanation is correct then the insoluble material consists of primary chains cross-linked to such an extent that the molecule has a value of γ close to unity and, therefore, has solubility properties similar to a gel.

In order to obtain an idea of the type of lignin moiety involved in the cross-linking sites the DP_w of the lignin present was calculated for Fractions 3(2)

and 2(1). The $\underline{DP}_w$ of the lignin present was calculated by multiplying $\underline{M}_w$ by the fraction of lignin present and dividing by 185 where 185 is the average molecular weight of the phenylpropane unit (73, 74), considered to be the basic monomer unit of lignin (75, 76). The results are presented in Table XII. The $\underline{DP}_w$ of the lignin per branch point and the $\underline{DP}_w$ of the lignin per primary chain are also calculated.

TABLE XII

LIGNIN IN RELATION TO BRANCH UNITS

Fraction	$\underline{DP}_w$	Number of Branch Units Per Molecule	Per Cent Lignin (on Glucomannan Triacetate)	$\underline{DP}_w$ of Lignin Present	Lignin $\underline{DP}_w$ Per Branch Unit	Lignin $\underline{DP}_w$ Per Primary Chain
3(2)	82.4	0.10	1.82	2.33	--	2.12
2(1)	557	7.06	2.34	20.4	2.89	2.53

Both fractions have approximately two phenylpropane units per primary chain. The similar lignin contents of the two fractions are consistent with the concept that the low $\underline{DP}$ Fraction 3(2) was derived by cleavage of the lignin-carbohydrate branch points of a fraction similar to the high $\underline{DP}$ Fraction 2(1). A slightly greater lignin content for Fraction 2(1) is expected since some of the lignin in Fraction 3(2) has undoubtedly been removed completely from the chains due to degradation. Since Fraction 3(2) is essentially linear, the major part of the lignin in this fraction is not involved in branching. The lignin $\underline{DP}_w$ per branch unit for Fraction 2(1) is 2.9. Experimental evidence exists that lignin is made up of basic "building units" which contain about five phenylpropane units (76). Thus, it is possible that in Fraction 2(1) and perhaps the other branched fractions each branch unit may be composed of approximately one "lignin building unit."

After lignin has reacted with acidified sodium chlorite it is modified so that it does not yield vanillin on oxidation with alkaline nitrobenzene (see Appendix II, p. 88). The sum of the sugar, acetyl, ash, and nitrobenzene lignin contents for Fractions 3(2) and 2(1) are 94%. Thus, 6% of the fractions is unaccounted for and since acidified sodium chlorite modifies the lignin there may be additional lignin fragments present in the molecule which have not been detected. The basic aromatic nature of these fragments has probably been destroyed if they are present.

The model employed in this study is based on linkages occurring between lignin and the hydroxyl groups of the glucomannan chain. From methylation studies in the literature (3) it appears that the hydroxyl groups at the Number 2, 3, or 6 carbon atoms of the glucose or mannose residues are all possible branching sites. These hydroxyl groups may be involved in an ether linkage with a phenolic hydroxyl group or an aliphatic hydroxyl group on the propane chain of lignin. Lignin contains one carbonyl group per lignin building unit (53) and the sugar hydroxyl groups also may be involved in an acetal or hemiacetal linkage with this carbonyl group. From evidence obtained from Fraction 2(1) it is possible that two glucomannan chains may be linked to a lignin building unit containing approximately five phenylpropane units.

CONCLUSIONS

A glucomannan isolated by a mild process from black spruce was shown to contain long-chain branches. Previous chemical investigations have presented contradictory evidence for and against branching in coniferous glucomannans but have provided no insight into the length of the branches. The relatively compact configuration of the fully acetylated glucomannan as revealed by its hydrodynamic properties clearly demonstrated the presence of long-chain branches.

Lignin was found to be tenaciously associated with glucomannan fractions which had been extensively purified and the hypothesis was made that this lignin may be involved in the long-chain branching. A detailed inspection of the behavior of the glucomannan fractions in relationship to the lignin content, molecular properties, solubility properties, and ease of extraction and a critical review of the literature indicated that the lignin was quite probably chemically linked to the glucomannan chains.

Theoretical treatment of the viscosity-molecular weight results in order to obtain a measure of the degree of branching showed the results were best described by a model involving cross-linking of linear chains. This model adequately described the abrupt decreasing slope of the log $[\eta]$ versus log $\underline{\underline{DP}}_{\underline{w}}$ plot and gave consistent results when applied to the data. In particular, the calculated $\underline{\underline{DP}}$ of the linear chains which are cross-linked together was constant for all fractions, regardless of the $\underline{\underline{DP}}$ of the entire cross-linked molecule. The hypothesis was then made that lignin was the cross-linking unit between essentially linear or slight branched glucomannan chains.

This model, which involves a cross-linked matrix of lignin and glucomannan within the fiber, adequately described all the results of this investigation.

It implies that all isolated glucomannans from gymnosperms are actually artifacts originating from the original lignin-glucomannan complex. If delignification is complete then isolated glucomannans from different investigations should have similar properties; however, if lignin is present in the isolated fractions then the glucomannans can have widely varying properties such as degree of polymerization, degree of branching, solubility, and perhaps sugar content. These latter properties would depend on the degree and nature of lignin-carbohydrate linkages. Thus, the relatively high degrees of polymerization found in this study are readily explained. This may also be a partial explanation of the contradictory literature evidence concerning branching in coniferous glucomannans. The concept of a cross-linked lignin-carbohydrate matrix is applicable to various areas of wood chemistry and the pulp and paper industry and a brief discussion of possible applications is presented in Appendix XXIX, p. 243.

NOMENCLATURE

a = constant in Mark-Houwink equation

a = persistence length

a = value of x at the solution-air meniscus

a/b = axial ratio of a prolate ellipsoid

A = area under schlieren curve

A_2 = second virial coefficient

b = length of the monomer unit equal to 5.15×10^{-8} cm.

b = value of x at the solution-oil meniscus

B_{SD}, B'_{SD} = weight average and z-average sedimentation equilibrium second virial coefficients, respectively

B_{OS}, B_{LS} = theoretical osmotic pressure and light scattering second virial coefficients, respectively

c = concentration

c^o = initial concentration of the solution

c_x = concentration at point x in ultracentrifuge cell

dn/dc = refractive index gradient of the solute

d_a = density of air

d_n = density of liquid in pycnometer

d_w = density of weights

DP = degree of polymerization

DP_n = number average degree of polymerization

DP_w = weight average degree of polymerization

DP_z = z-average degree of polymerization

D = diffusion coefficient

D_α = diffusion coefficient

f = fractional length of a short branch

f = molecular frictional coefficient

f_o = frictional coefficient of hypothetical solvated sphere

f_{min} = molecular frictional coefficient of a hypothetical unsolvated sphere

$f(M)$ = normalized weight distribution of the molecular weight, M

g = ratio of the mean square radius of gyration of a branched to a linear polymer

g' = ratio of the intrinsic viscosity of a branched to a linear polymer

h = adjustable parameter in the Zimm-Schulz distribution

h = thickness of the solution in the centrifuge cell perpendicular to the plane of rotation

J = number of Rayleigh fringes

J = flux of particles in Fick's first law of diffusion

k = Boltzmann constant

K, K_1, K_2 = constants in Mark-Houwink equation

K_1, K_2, K_3 = viscosity extrapolation constants

L_{max} = contour length

L = optical lever arm

m_w = weight average number of cross-links per molecule

m_x = magnification factor for the camera in the radial direction

m_z = magnification of the cylinder lens

M = molarity of chemical solutions

M = molecular weight

M_n = number average molecular weight

M_w = weight average molecular weight

M_z = z-average molecular weight

M_{wx} = weight average molecular weight at point x in ultracentrifuge cell

M_{zx} = z-average molecular weight at point x in ultracentrifuge cell

N = normality of chemical solutions

N = degree of polymerization in Eizner-Ptitsyn theory

$\underline{N}$ = Avogadro's number

$\underline{N_n}$, $\underline{N_w}$, $\underline{N_z}$ = number average, weight average, and z-average degrees of polymerization, respectively

Primary $\underline{DP_w}$ = weight average degree of polymerization of the primary linear molecules

$\underline{p}$ = adjustable parameter in the Zimm-Schulz distribution

$\underline{p}$ = solute concentration

$\underline{q_o}$ = a factor to correct for sample heterogeneity for Flory coefficient

$\underline{r_o}$ = hydrodynamic radius of the monomer unit

$\underline{r_H}$ = distance from the center of rotation to the boundary position in the ultracentrifuge cell

$\underline{\bar{r}}$ = distance of the center of the solution column from the center of rotation in the ultracentrifuge cell

$\underline{R}$ = gas constant

$\underline{R_o}$ = radius of hypothetical solvated sphere

$\underline{R_s}$ = maximum radius of hypothetical solvated sphere

$\underline{s}$ = sedimentation coefficient

$\underline{\overline{s^2}_z}$ = z-average mean square radius of gyration

$\underline{s}$ = number of short branches per molecule

$\underline{t}$ = time of ultracentrifugation run

$\underline{T}$ = absolute temperature, °K.

$\underline{\bar{v}}$ = the partial specific volume of the solute

$\underline{v_1^o}$ = specific volume of pure solvent

$\underline{v_2}$ = partial specific volume of polymer

$\underline{W}$ = true weights

$\underline{W'}$ = weights used

$\underline{x}$, $\underline{x_1}$, $\underline{x_2}$ = distance from center of rotation in ultracentrifuge cell

$\underline{\bar{x}}$ = average $\underline{x} = (\underline{x_1} + \underline{x_2})/2$

$\underline{Z}$ = the ordinate of the photographic plate obtained with the schlieren optical system

α = type of linkage

β = type of linkage

γ = branching parameter

Γ = gamma function

Γ_2 = a parameter which depends on polymer-solvent interaction

δ_1 = an empirical degree of solvation

$\Delta\underline{c}$ = difference in concentration across ultracentrifuge cell

$\Delta\underline{F}$ = change in free energy

$\Delta\underline{H}$ = resultant of energy absorbed in breaking polymer – polymer and solvent – solvent bonds and the energy emitted in forming polymer – solvent bonds in solution processes

$\Delta\underline{S}$ = change in entropy

ϵ = a measure of the departure from equilibrium in ultracentrifugation

η = solution viscosity

η_o = solvent viscosity

$[\eta]$ = intrinsic viscosity

Θ = phase plate angle

λ = wavelength of light

λ = ratio of $\underline{a}$ to $\underline{b}$ in Eizner-Ptitsyn theory

π = osmotic pressure

ρ = density of solution

ρ_o = density of solvent

ϕ_1 = apparent specific volume

Φ, Φ_o = Flory coefficient

$\phi(\lambda,\underline{N})$ = hydrodynamic function of $\underline{N}$ and λ in Eizner-Ptitsyn theory

χ = geometric function of $\underline{N}$ and λ in Eizner-Ptitsyn theory

ω = angular velocity

ACKNOWLEDGMENTS

The author would like to express his appreciation to all the individual members of the faculty and staff at The Institute of Paper Chemistry who have contributed assistance or advice during the progress of this thesis. Sincere thanks are extended to Mr. H. A. Swenson, chairman of the thesis advisory committee, Dr. N. S. Thompson and Dr. S. F. Kurath, committee members for their advice and criticism throughout the course of this work. Appreciation is also expressed to Mr. E. E. Dickey and Dr. L. E. Wise who took an active interest in the progress of this thesis.

The aid of the following is also gratefully acknowledged: L. G. Borchardt for analyses, L. O. Sell for operation of the spectrophotometer, and J. A. Carlson for operation of the ultracentrifuge and electrophoresis apparatus.

Finally, I would like to express my deepest appreciation to my wife, Rose, for her expert typing and proofreading of all progress reports and the thesis. I am particularly grateful for her continual encouragement and support which made the completion of this thesis possible.

LITERATURE CITED

1. Hamilton, J. K., and Thompson, N. S., Tappi 42:752-60(1959); Hamilton, J. K., and Thompson, N. S., Pulp Paper Mag. Can. 59:233-41(1958).

2. Thompson, N. S., and Kaustinen, O. A., Paperi Puu 46:637-50(1964).

3. Timell, T. E. To be published in Advances of Carbohydrate Chemistry, 1965.

4. Croon, I., and Lindberg, B., Acta Chem. Scand. 12:453-8(1958).

5. Meier, H., Acta Chem. Scand. 12:1911-18(1958).

6. Lindgren, B. O., Acta Chem. Scand. 12:447-52(1958).

7. Croon, I., Lindberg, B., and Meier, H., Acta Chem. Scand. 13:1299-1304(1959).

8. Immergut, B., and Ranby, B. G., Svensk Papperstid. 60:573-81(1957).

9. Jayme, G., and Kringstad, K., Papier 15:500-6(1961).

10. Mills, A. R., and Timell, T. E., Can. J. Chem. 41:1389-95(1963).

11. Timell, T. E., and Tyminski, A., Tappi 40:519-22(1957).

12. Tyminski, A., and Timell, T. E., J. Am. Chem. Soc. 82:2823-7(1960).

13. Aspinall, G. O., Laidlaw, R. A., and Rashbrook, R. B., J. Chem. Soc. 1957:4444-8.

14. Dutton, G. G. S., and Hunt, K., J. Am. Chem. Soc. 80:5697-701(1958).

15. Vaughan, J. M., and Dickey, E. E., Tappi 47:142-3(1964).

16. Vaughan, J. M., and Dickey, E. E., J. Org. Chem. 29:715-18(1964).

17. Thompson, N. S., and Kaustinen, O. A., Tappi 47:157-62(1964).

18. Katz, Gerald. The location and significance of the O-acetyl groups in a glucomannan from Paraña pine. Doctor's Dissertation. Appleton, Wis., The Institute of Paper Chemistry, 1964. 85 p.

19. Ott, E., Spurlin, H. M., and Grafflin, M. W. Cellulose and cellulose derivatives. Part II. p. 511-1055. New York, Interscience, 1955.

20. Carson, J. F., and Maclay, W. D., J. Am. Chem. Soc. 70:293-5(1948).

21. Koleske, Joseph V. The configuration and hydrodynamic properties of fully acetylated guaran. Doctor's Dissertation. Appleton, Wis., The Institute of Paper Chemistry, 1963. 175 p.

22. Hamilton, J. K., and Kircher, H. W., J. Am. Chem. Soc. 80:4703-9(1958).

23. Saeman, J. F., Moore, W. E., Mitchell, R. L., and Millett, M. A., Tappi 37:336(1954).

24. Stone, J. E., and Blundell, M. J., Anal. Chem. 23:771-4(1951).

25. Schachman, Howard K. Ultracentrifugation in biochemistry. New York, Academic Press, 1959. 272 p.

26. Baldwin, R. L., and Van Holde, K. K., Fortschr. Hochpolymer. Forsch. Bd. 1. S:451-511(1960).

27. Goring, D. A. I., Pure Appl. Chem. 5:233-54(1962).

28. Lansing, W. D., and Kraemer, E. O., J. Am. Chem. Soc. 57:1369-77(1935).

29. Van Holde, K. E., and Baldwin, R. L., J. Phys. Chem. 62:734-43(1958).

30. Flory, Paul J. Principles of polymer chemistry. Ithaca, New York, Cornell University Press, 1963. 672 p.

31. Tompa, H. Polymer solutions. London, Butterworth's, Inc. 1956. 325 p.

32. Onyon, P. F. Viscometry. In Allen's Techniques of polymer characterization. p. 171. London, Butterworth's, 1959.

33. Senti, F. R., Hellman, N. N., Ludwig, N. H., Babcock, G. E., Tobin, R., Glass, C. A., and Lamberts, B. L., J. Polymer Sci. 17:527-46(1955).

34. Cowie, J. M. G., and Toporowski, P. M., Polymer 5:601-10(1964).

35. Henley, D., Arkiv für Kemi 18:327-92(1961).

36. Kirkwood, J. G., and Riseman, J., J. Chem. Phys. 16:565-73(1948).

37. Sitaramaiah, G., and Goring, D. A. I., J. Polymer Sci. 58:1107-31(1962).

38. Immergut, E. H., and Eirich, F. R., Ind. Eng. Chem. 45:2500-11(1953).

39. Riseman, J., and Kirkwood, J. G., J. Chem. Phys. 18:512-16(1950).

40. Tanford, Charles. Physical chemistry of macromolecules. New York, John Wiley and Sons, Inc., 1963. 710 p.

41. Ptitsyn, O. B., and Eizner, Yu. E., Vysokomol. Soed. 3:1863-9(1961).

42. Eizner, Yu. E., and Ptitsyn, O. B., Vysokomol. Soed. 4:1725-31(1962).

43. Juers, D. H. The configuration and hydrodynamic properties of fully acetylated salep glucomannan. Doctor's Dissertation. Appleton, Wis., The Institute of Paper Chemistry, 1965. 85 p.

44. Kurath, S. F., Schmitt, C. A., and Bachhuber, J. J. J. Polymer Sci. 3A:1825-32(1965).

45. Swenson, H. A., Schmitt, C. A., and Thompson, N. S. In press.

46. Doty, P., Bradbury, J. H., and Holtzer, A. M., J. Am. Chem. Soc. 78:947-54(1956).

47. LeBel, R. G., Goring, D. A. I., Timell, T. E., J. Polymer Sci. Part C: 9-28(1963).

48. Peterson, F. C., Barry, A. J., Unkauf, H., and Wise, L. E., J. Am. Chem. Soc. 62:2361-5(1940).

49. Wacek, A. V., and Schroth, D., Papier 4:410-14(1950).

50. Schubert, W. J., and Nord, F. F., J. Am. Chem. Soc. 72:977-81(1950).

51. Schubert, W. J., and Nord, F. F., J. Am. Chem. Soc. 72:3835-8(1950).

52. Leopold, B., Svensk Kem. Tidskr. 63:260-71(1951).

53. Merewether, J. W. T. The linkage of lignin in the plant. In Brauns and Brauns' The chemistry of lignin. Supplement Volume. p. 630. New York, Academic Press, 1960.

54. Abadie-Maumert, F. A., Papeterie 77:255(1955).

55. Lindberg, J. J., Paperi Puu 42, no. 4a:193-6(1960).

56. Wise, L. E., Murphy, M., and D'Addieco, A. A., Paper Trade J. 35, no. 2:122(1946).

57. Jayme, G., and Wettstein, R., Papier Fabr. 36:519(1938).

58. Granath, K. A., J. Colloid Sci. 13:308-28(1958).

59. Zimm, B. H., and Stockmayer, W. H., J. Chem. Phys. 17:1301-14(1949).

60. Stockmayer, W. H., and Fixman, M., Ann. N. Y. Acad. Sci. 57:334(1953).

61. Zimm, B. H., and Kilb, R. W., J. Polymer Sci. 37:19-42(1959).

62. Kilb, R. W., J. Polymer Sci. 38:403-15(1959).

63. Atkins, J. T., and Billmeyer, F. W., J. Phys. Chem. 63:1966-8(1958).

64. Billmeyer, F. W., Jr., J. Am. Chem. Soc. 75:6118-22(1953).

65. Trementozzi, Q. A., J. Polymer Sci. 22:187-9(1956).

66. Thurmond, C. D., and Zimm, B. H., J. Polymer Sci. 8:477-94(1952).

67. Krigbaum, W. R., and Trementozzi, Q. A., J. Polymer Sci. 28:295-307(1958).

68. Pao, Yoh-Han, J. Polymer Sci. 61:413-48(1962).

69. Wales, M., Marshall, P. A., Weissberg, S. G., J. Polymer Sci. 10:229-40(1953).

70. Stockmayer, W. H. Private communication, 1947, to Billmeyer, F. W., J. Am. Chem. Soc. 75:6118-22(1953).

71. Stockmayer, W. H., J. Chem. Phys. 12:125-31(1944).

72. Flory, P. J., J. Am. Chem. Soc. 63:3096-100(1941).

73. Björkman, A., and Person, B., Svensk Papperstid. 60:158-69(1957).

74. Freudenberg, K., Ann. Rev. Biochem. 8:81-112(1939).

75. Brauns, F. E. The chemistry of lignin. New York, Academic Press, Inc., 1952. 808 p.

76. Brauns, F. E., and Brauns, D. A. The chemistry of lignin. Supplement Volume. New York, Academic Press, 1960. 804 p.

77. Merewether, J. W. T., Holzforsch. 11:65-80(1957).

78. Aaltio, E., and Roschier, R. H., Paperi Puu 36:157(1954).

79. Harris, E. E., Tappi 36:402(1953).

80. Traynard, P., and Eymery, A., Holzforsch. 9:172(1955).

81. Staudinger, M., Holz Roh- Werkstoff 5:193-200(1942).

82. Lange, P. W., Svensk Papperstid. 48:241-5(1945).

83. Prey, V., Waldmann, E., and Swoboda, H., Holzforsch. 9:10-14(1955).

84. Freudenberg, K., Harder, M., and Markert, L., Ber. 61:1760-5(1928).

85. Freudenberg, K., Zocher, H., and Durr, W., Ber. 62:1814-23(1929).

86. Staudinger, H., Dreher, E., and Ekenstam, A., Ber. 69:1099-100(1936).

87. Konkin, A. A., and Rogovin, Z. A., Bumazh. Prom. 28, no. 9:15-19(1953).

88. Hachihama, Y., and Takamuku, S., J. Chem. Soc. Ind. Chem. Sect. 63:1043 (1960); Ref. Zh. Khim., no. 9:435(1961).

89. Virtanen, A. I., and Koistinen, O. A., Svensk Kem. Tidskr. 56:391(1944).

90. Virtanen, A. I., and Nikkila, O. E., Suomen Kem. 19B:3(1946).

91. Ploetz, T., Ber. 72:1885-9(1939).

92. Björkman, A., Svensk Papperstid. 59:477-85(1956).

93. Björkman, A., Svensk Papperstid. 60:243-51(1957).

94. McPherson, J. A., Acta Chem. Scand. 12:779-80(1958).

95. Fisher, J. H., Hawkins, W. L., and Hibbert, H., J. Am. Chem. Soc. 63:3031-5 (1941).

96. Sawyer, N., and Chidester, G. H. Manufacture of wood pulp. In Browning's The chemistry of wood. 1st ed. p. 450. New York, John Wiley & Sons, Inc. 1963.

97. Lindgren, B. O., Svensk Papperstid. 61:669-74(1958).

98. Freudenberg, K., and Harkin, J. M., Chem. Ber. 93:2814-19(1960).

99. Holmberg, B., and Runius, S., Svensk Kem. Tidskr. 37:189-97(1925).

100. Isenberg, I. H. Personal communication, 1963.

101. Casey, James P. Pulp and Paper. Vol. 1. Pulping and bleaching. 2nd ed. New York, Interscience, 1960. 580 p.

102. Giertz, H. W., Tappi 34:209-15(1951).

103. Rapson, W. H., Tappi 39:284-95(1956).

104. Samuelson, O., and Hartler, N., Svensk Kem. Tidskr. 62:197-204(1950).

105. Leopold, B., Tappi 44:230-2(1961).

106. Ball, D. H., Jones, J. K. N., Nicholson, W. H., and Painter, T. J., Tappi 39:438-43(1956).

107. Dence, C. W., Gupta, M. K., and Sarkanen, K. V., Tappi 45:29-38(1962).

108. Gianola, G., and Meybeck, J., J. Assoc. Tech. Ind. Papetiere, Bull. no. 1:25-31(1960).

109. Levitin, N., Thompson, N. S., and Purves, C. B., Pulp Paper Mag. Can. 56:117-30(1955).

110. Meier, H., Acta Chem. Scand. 12, no. 3:144-6(1958).

111. Vaughan, John M. The oxidation of a spruce glucomannan with lead tetra-acetate. Doctor's Dissertation. Appleton, Wis., Institute of Paper Chemistry, 1963. 65 p.

112. Bier, Milan. Electrophoresis. New York, Academic Press, Inc., 1959. 563 p.

113. Beckman/Spinco Model H. Electrophoresis — Diffusion Instrument. Instrumentation Manual. 72 p.

114. Timell, T. E., Tappi 44:88-96(1961).

115. Fuller, K. W., and Northcate, D. H., Biochem. J. 64:657-63(1956).

116. Northcate, D. H., Biochem. J. 58:353-8(1954).

117. Malcolm, E. W., Green, J. W., and Swenson, H. A., J. Chem. Soc., Dec., 1964:4669-76.

118. Genung, L. B., and Mallatt, R. C., Ind Eng. Chem. 13:369-74(1931).

119. Wilson, H. N., and Hughes, W. C., J. Soc. Chem. Ind. 58:Transactions 74-7(1939).

120. Burrell, H., Interchem. Rev. 14, no. 1:3-16; 14, no. 2:31-46(1955).

121. Allen, P. W. Techniques of polymer characterization. London, Butterworths Sci. Publishers, 1959.

122. Moore, W. R., and Russell, J., J. Colloid Sci. 8:243-51(1953).

123. Howlett, F., and Urquhart, A. R., Chem. Ind. (London) 1957:82-7.

124. Mardles, E. W. J., In Alexander's Colloid chemistry. Vol. 4. p. 87. New York, The Chemical Catalog Co., 1932.

125. Ott, E., Spurlin, H. M., and Grafflin, M. W. Cellulose and cellulose derivatives. Part III. p. 1507-1601. New York, Interscience, 1955.

126. Moore, W. R., and Russell, J., J. Colloid Sci. 9:338-46(1954).

127. Cragg, L. H., and Hammerschlag, H., Chem. Revs. 39:79-139(1946).

128. Flory, P. J. Principles of polymer chemistry. Ithaca, New York, Cornell University Press, 1953. 672 p.

129. Scott, Robert L., Ind. Eng. Chem. 45:2532-7(1953).

130. Conrad, Carl M., Ind. Eng. Chem. 45:2511-17(1953).

131. Kline, Gordon M. Analytical chemistry of polymers. Part II. Analysis of molecular structure and chemical groups. New York, Interscience, 1962. 619 p.

132. Huggins, Maurice L. Physical chemistry of high polymers. New York, John Wiley & Sons, Inc., 1958. 175 p.

133. Mark, H., Paper Trade J., Tappi 113:28-34(1941).

134. Mitchell, R. L., Ind. Eng. Chem. 45:2527-31(1953).

135. Tung, L. H., J. Polymer Sci. 61:449-61(1962).

136. Flodin, Per. Dextran gels and their applications in gel filtration. Uppsala, 1962. 85 p.

137. Granath, Kirsti, and Flodin, Per, Makromol. Chem. 48:160-71(1961).

138. Chem. Eng. News 40, no. 51:43-4(1962).

139. Vink, Hans, Arkiv Kemi 19:531-48(1962).

140. Sihtola, H., Kaila, E., and Virkola, N. Makromol. Chem. 11:70-8(1953).

141. Doolittle, A. K., Ind. Eng. Chem. 36:239-44(1944).

142. Moore, W. R., Trans. Faraday Soc. 43:543-52(1947).

143. Billmeyer, Fred W., Jr. Textbook of polymer chemistry. New York, Interscience, 1957. 518 p.

144. Okamoto, H., and Sakikawa, K., J. Polymer Sci. 55:597-607(1961).

145. Swenson, H. A. Molecular size distribution in cellulose. In Whistler's Methods in carbohydrate chemistry, Vol. III. p. 91. New York, Academic Press, 1963.

146. Morey, D. R., and Tamblyn, J. W., J. Phys. Chem. 50:12-22(1946).

147. Sookne, A. M., Rutherford, H. A., Mark, H., and Harris, M., J. Res. Natl. Bur. Std. A29:123-30(1942).

148. Staudinger, H., and Eder, K., J. Prakt. Chem. 159:39-69(1941).

149. Rosenthal, A. J., and White, B. B., Ind. Eng. Chem. 44:2693-6(1952).

150. Howlett, F., and Urquhart, A. R., J. Text. Inst. 37T:89-112(1946).

151. Lambert, R. Personal communication, 1964.

152. Hamilton, J. K., Partlow, E. V., and Thompson, N. S., J. Am. Chem. Soc. 82:451-7(1960).

153. Weissberger, Arnold. Chemical applications of spectroscopy. Vol. IX. New York, Interscience, 1956. 787 p.

154. Bellamy, L. J. The infrared spectra of complex molecules. New York, John Wiley & Sons, Inc., 1958. 425 p.

155. Nakanishi, Kaji. Infrared absorption spectroscopy - practical. San Francisco, Holden Day, Inc., 1962. 233 p.

156. Marchessault, R. H., Pure Appl. Chem. 5:107-29(1962).

157. Higgins, H. G., Stewart, C. M., and Harrington, K. J., J. Polymer Sci. 51:59-84(1961).

158. O'Connor, R. T., DuPre, E., and McCall, E. R., Textile Res. 28:542-54(1958).

159. O'Connor, R. T., DuPre, E. F., and McCall, E. R., Anal. Chem. 29:998-1005 (1957).

160. Barker, S. A., Bourne, E. J., Stacey, M., and Whiffen, D. H., J. Chem. Soc., 1954:171-6, 3468-73.

161. Liang, C. Y., Bassett, K. H., McGinnes, E. A., and Marchessault, R. H., Tappi 43:1017-24(1960).

162. Thompson, N. S. Personal communication, 1965.

163. Mechrolab, Inc. Model 501 high speed membrane osmometer. Operation manual. Mountain View, California.

164. Staverman, A. J., Rec. Trav. Chim. 70:344-52(1951).

165. Staverman, A. J., Pals, D. T. F., and Krvissink, C. H. A., J. Polymer Sci. 23:57-68(1957).

166. Hookway, H. T. Number-average molecular weights by osmometry. In Allen's Techniques of polymer characterization. p. 68. London, Butterworth's Sci. Publishers, 1959.

167. Tung, L. H., J. Polymer Sci. 32:477-85(1958).

168. Cannon, M. R., Manning, R. E., and Bell, J. D., Anal. Chem. 32:355-8 (1960).

169. Timell, T. E., Svensk Papperstid. 57:777-88(1954).

170. International Union of Pure and Applied Chemistry, J. Polymer Sci. 8:257-77(1952).

171. Manley, R. St. J., Arkiv Kemi 9:519(1956).

172. Abe, H., and Prins, W., Makromol. Chem. 42:216(1961).

173. Schulz, W. J., Papier 14:518(1960).

174. LeBel, R. G., and Goring, D. A. I., J. Polymer Sci., Part C:29-48(1963).

175. Swenson, H. A., Morak, A. J., and Kurath, S., J. Polymer Sci. 51:231-45 (1961).

176. Goring, D. A. I., and Timell, T. E., J. Phys. Chem. 64:1426-30(1960).

177. Instruction Manual E-1 M-3. Beckman Model E. Analytical Ultracentrifuge Spinco Division, Beckman Instruments, Inc. Palo Alto, California, May, 1964.

178. Svedberg, T., and Pedersen, Kai O. The ultracentrifuge. Oxford, Clarendon Press, 1940. 478 p.

179. Trautman, Rodes. Ultracentrifugation. In Newman's Instrumental methods of experimental biology. p. 211. New York, Macmillan Company, 1964.

180. Williams, J. W. Ultracentrifugal analysis in theory and experiment. New York, Academic Press, 1963. 282 p.

181. Fujita, Hiroshi. Mathematical theory of sedimentation analysis. New New York, Academic Press, 1962. 315 p.

182. Van Holde, K. E., and Baldwin, R. L., J. Phys. Chem. 62:734-43(1958).

183. Lansing, W. D., and Kraemer, E. O., J. Am. Chem. Soc. 57:1369-77(1935).

184. Johnson, J. S., Kraus, K. A., and Young, T. F., J. Am. Chem. Soc. 76:1436-43(1954).

185. Beckman Technical Bulletin. E-TB-0030 Calibration cell for the Model E Analytical Ultracentrifuge. February, 1963.

186. Carlson, J. Personal communication, 1965.

187. Tostevin, J. Personal communication, 1965.

188. Swenson, H. A. Personal communication, 1965.

189. Bauer, N., and Lewin, S. Z. Determination of density. In Weissberg's Physical methods of organic chemistry. Vol. I, Part I. p. 131. New York, Interscience, 1959.

190. Zimm, B. H., J. Chem. Phys. 16:1093-9(1948); J. Chem. Phys. 16:1099-116 (1948).

191. Schulz, G. V., Z. Phys. Chem. B43:25-46(1924).

192. Mason, M., and Weaver, W., Phys. Rev. 23:412(1924).

193. LaBar, F. E., and Baldwin, R. L., J. Phys. Chem. 66:1952-9(1962).

194. Brown, W., and Wikstrom, R., European Polymer J. 1:1-10(1965).

195. Marx, M., Makromol. Chem. 16:157-76(1955).

196. Claesson, Von S., Bergmann, W., and Jayme, G., Svensk Papperstid. 62:141-55(1959).

197. Huque, M. M., Goring, D. A. I., and Mason, S. G., Can. J. Chem. 36:952-69(1958).

198. Meyerhoff, G., J. Polymer Sci. 29:399-410(1958).

199. Hunt, M. L., Newman, S., Scheraga, H. A., and Flory, P. J., J. Phys. Chem. 60:1278-90(1956).

200. Holtzer, A. M., Benoit, H., and Doty, P., J. Phys. Chem. 58:624-34(1954).

201. Kraemer, E. O., Ind. Eng. Chem. 30:1200-3(1938).

202. Uda, K., and Meyerhoff, F., Makromol. Chem. 47:168-84(1961).

203. Scherer, P. C., Tanebaum, A., and Levi, D. W., J. Polymer Sci. 43:531-5 (1960).

204. Brown, W., Henley, D., and Ohman, J., Makromol. Chem. 64:49-67(1963).

205. Brown, W., Arkiv Kemi 18:227-84(1961).

206. Brown, W., Henley, D., and Ohman, J., Makromol. Chem. 62:164-82(1963).

207. Brown, W., and Henley, D., Makromol. Chem. 79:68-88(1964).

208. Cowie, J. M. G., Makromol. Chem. 42:230-47(1947).

209. Cowie, J. M. G., J. Polymer Sci. 49:455-71(1961).

210. Gralén, Nils. Sedimentation and diffusion measurements on cellulose and cellulose derivatives. Uppsala, Sweden, Institute of Physical Chemistry, 1944. 115 p.

211. Jullander, Ingvar, Arkiv Kemi, Mineralogi och Geologi 21A:1-142(1945).

212. Bevilacqua, E. M., Bevilacqua, E. B., Bender, M. M., and Williams, J. W., Ann. N. Y. Acad. Sci. 46:309-27(1945).

213. Kratky, O., and Porod, G., Rec. Trav. Chim. 68:1106-22(1949).

214. Kirkwood, J. G., J. Polymer Sci. 12:1-14(1954).

215. Peterlin, A., J. Polymer Sci. 5:473-83(1950).

216. Peterlin, A., J. Chem. Phys. 33:1799-802(1960).

217. Flory, P. J., and Fox, T. G., Jr., J. Am. Chem. Soc. 73:1904-7(1951).

218. Newman, S., Krigbaum, W. R., Laugier, C., and Flory, P. J., J. Polymer Sci. 14:451-62(1954).

219. Krigbaum, W. R., and Sperling, L. H., J. Phys. Chem. 64:99-108(1960).

220. Krigbaum, W. R., and Carpenter, D. K., J. Phys. Chem. 59:1166-72(1955).

221. Benoit, H., and Doty, P., J. Phys. Chem. 57:958-63(1953).

222. Wagner, R. H., and Moore, L. D., Jr. Determination of osmotic pressure. In Weissberger's Physical methods of organic chemistry. Part I. Vol. I. New York, Interscience, 1959. 815 p.

223. Spencer, R. S., and Boyer, R. F., Polymer Bull. 1:129-39(1945).

224. Cragg, L. H., and Manson, J. A., J. Polymer Sci. 9:265-78(1952).

225. Manson, J. A., and Cragg, L. H., Can. J. Chem. 30:482-96(1952).

226. Speiser, R., and Whittenberger, R. T., J. Chem. Phys. 13:349-50(1945).

227. Eirich, F., and Riseman, J., J. Polymer Sci. 4:417-34(1949).

228. Bawn, C. E. H., Freeman, R. F. J., and Kamaliddin, A. R., Trans. Faraday Soc. 46:1107-12(1950).

229. Heller, W., J. Colloid Sci. 9:547-73(1954).

230. Annergren, G. E., and Rydholm, S. A., Svensk Papperstid. 63:591-600(1960).

231. Annergren, G. E., and Rydholm, S. A., Svensk Papperstid. 62:737-46(1959).

232. Bradway, K. E., Tappi 37:440-6(1954).

233. Steinmann, H. W., and White, B. B., Tappi 37:225-32(1954).

234. Watson, J. K., and Henderson, D. R., Tappi 40:686-90(1957).

235. Polglase, W. J., Polysaccharides associated with cellulose. In Advances of carbohydrate chemistry. Vol. 10. p. 283. New York, Academic Press, 1955.

236. Matsuzaki, Kei, and Ward, K., Tappi 41:396-402(1958).

237. Leopold, B., Tappi 44:232-5(1961).

238. Wise, L. E., Paper Ind. 29:825-9(1947).

239. Most, D. S., Tappi 40:705-12(1957).

240. Guzman, G. M., and Gomey-Fatav, J. M., Anales de la Real Sociedad Espanola de Fisica y Quimica 53B:669(1957).

241. Cornell, R. H., and Swenson, H. A., J. Appl. Polymer Sci. 5:641(1961).

APPENDIX I

LITERATURE ON THE LIGNIN-CARBOHYDRATE LINKAGE

INTRODUCTION

Much work has been carried out on the problem of the lignin-carbohydrate linkage and the subject has been reviewed by various workers (53, 75, 77-80).

In summarizing the evidence for and against the existence of a lignin-carbohydrate bond, Merewether (53) states, "The considerable volume of evidence for the existence of lignin-carbohydrate complexes in wood that has been subjected to a variety of chemical and physical treatments leaves one in no doubt as to their existence, and the question is no longer whether there is a lignin-carbohydrate linkage, but whether all the lignin is combined with carbohydrate and whether all the carbohydrate is combined with lignin." The existence of a lignin-carbohydrate linkage in coniferous woods has an important bearing on this study and some of the literature supporting this linkage will be presented. The presence of this linkage in sprucewood and between lignin and glucomannans will be emphasized.

THE POSSIBILITY OF THE LINKAGE ON MORPHOLOGICAL GROUNDS

The first point which must be clarified is whether a lignin-carbohydrate linkage is possible on morphological grounds. Staudinger (81) completely delignified woods with chlorine dioxide and in a separate experiment completely removed the carbohydrates with alternate treatments of sulfuric acid and cuprammonium hydroxide. He then compared photographs of these sections and the untreated wood and was able to show that in softwoods the lignin skeleton was distributed throughout the fiber wall as well as in the middle lamella. Lange (82) employed a method of ultraviolet microscopy to study the distribution of

lignin in the fiber walls of spruce. His results showed that although 70% of the lignin is located in the compound middle lamella, the lignin is continuously distributed in the fiber walls. The lignin decreases from a high concentration in the middle lamella to a very low concentration at the lumen, but the concentration never reaches zero. Lange's results also indicated that the lignin is partly oriented in stratification in the cell. Lange claimed this is evidence for some form of bonding between the lignin and the more oriented carbohydrate. Merewether (77) summarizes the evidence by stating that there can be no objection on morphological grounds in the postulation of a lignin-carbohydrate complex since lignin occurs in the secondary wall and the middle lamella contains approximately 25% of material which is not lignin.

EVIDENCE BASED ON THE SOLUBILITY OF THE POLYSACCHARIDE COMPONENT OF WOOD

The simultaneous removal of carbohydrates with the last few per cent of lignin from a holocellulose is often explained by the presence of a lignin-carbohydrate linkage. Wise and co-workers (56) found that if a chlorite holocellulose was delignified below about 3% Klason lignin, a marked loss of hemicelluloses occurred. Jayme and Wettstein (57) have shown that when the last portion of lignin was removed from a coniferous Asplund pulp by chlorination, an appreciable amount of carbohydrate was also removed. Complete delignification also increased the amount of carbohydrate which could be extracted by alkali. Since there was no increase in the copper number, it was inferred that there was no degradation of the carbohydrate. Jayme suggested that the data are best explained by the existence of complexes of lignin with comparatively small polysaccharide units. These complexes would be sufficiently large to be insoluble in alkali, but would become alkali-soluble after removal of the lignin.

The insolubility of the polysaccharide component of wood prior to delignification or hydrolysis indicates the presence of a lignin-carbohydrate linkage. Extraction of sprucewood with cold 4% aqueous sodium hydroxide extracts only 0.5% hemicellulose while extraction of spruce holocellulose with the same solvent extracts 8.9% hemicellulose (83). It, therefore, appears that a hemicellulose-lignin complex is decomposed during the preparation of the holocellulose. Cuoxam lignin is prepared by alternately treating wood with boiling 1% sulfuric acid and cold cuprammonium hydroxide (84, 85). The acid hydrolysis is an essential step and only a small amount of polysaccharide is removed when the hydrolysis is not made. Delignification also renders the carbohydrate component of wood soluble in cuprammonium hydroxide. Staudinger, et al. (86) found that in forty-eight hours only 3.6% of sprucewood dissolved in this solvent, whereas a bleached wood pulp readily dissolves in cuprammonium hydroxide. Merewether (77) reviews other studies on the solubility of the carbohydrate component of wood and concludes that whether wood is extracted with cuprammonium or cupriethylenediamine or whether it is xanthated, it is impossible to separate the carbohydrate and the lignin. Even when some of the wood is dissolved, this dissolved material is not pure carbohydrate and always contains lignin.

Experiments involving the nitration of wood support the concept of a lignin-carbohydrate linkage. When wood is nitrated, a portion of this nitrate is insoluble in acetone. It is known that both nitrocellulose and nitrolignin are soluble in acetone; therefore, the insolubility of wood nitrate is interpreted as the result of a nitrated lignin-carbohydrate complex which is insoluble in acetone (53). Hydrolysis of wood before nitration will decrease the amount of insoluble material considerably. Abadie-Maumert (54) found that the nitration of sprucewood gave a product, of which 59% was insoluble in acetone. When the wood was boiled with water for fifty days prior to the nitration the

yield of acetone-insoluble nitrate was only 4%. It is quite plausible that a lignin-carbohydrate bond was broken by this hydrolysis.

EVIDENCE BASED ON THE SOLUBILITY OF THE LIGNIN COMPONENT OF WOOD

Evidence on the solubility of lignin as well as the solubility of the carbohydrate component of wood indicates the existence of a lignin-carbohydrate linkage. Wacek and Schroth (49) obtained a lignin fraction from spruce holocellulose which became alcohol soluble after isolation, but could not be extracted from the holocellulose with alcohol prior to isolation. The lignin fraction was removed with the hemicelluloses by alkaline extraction of the holocellulose and remained in solution when the hemicelluloses were precipitated. One explanation of the solubility of this lignin fraction in alcohol only after isolation and the fact that it was relatively resistant to the action of chlorite, in contrast to the remainder of the lignin, is that it was chemically combined with carbohydrate in the holocellulose.

Lindberg (55) studied the digestion of wood meal with dimethylsulfoxide at 100°C. He reasoned that the properties of dimethylsulfoxide were such that if only hydrogen bonds existed between the lignin and the carbohydrates in wood, an appreciable amount of lignin would be dissolved under these conditions. Since very little lignin was dissolved, Lindberg concluded that real chemical bonds exist between the lignin and the carbohydrates in wood. He suggested that the bonding state of the lignin-carbohydrate complex is a solid solution containing chemical bonds interspersed and embedded in the hydrogen bond network.

Only a trace of lignin is extracted from sprucewood with ethylene glycol at 160°C. However, boiling the wood with 1% hydrochloric acid for two hours renders 55% of the lignin soluble on subsequent extraction under the above

conditions (87). The solubility of the lignin might arise from the decomposition of a lignin-carbohydrate complex. Hachihama and Takamuku (88) found that the solubility of lignin was increased by irradiating pinewood with varying doses of γ-rays in the presence of air but the properties of the lignins were not different. The authors explained the increased solubility by a splitting of the lignin-carbohydrate complex.

EVIDENCE FROM THE MICROBIOLOGICAL DEGRADATION OF WOOD

Studies involving the microbiological degradation of wood have given good evidence for the existence of a lignin-carbohydrate linkage. An interesting approach is to first extract wood with ethanol to remove the 2 to 3% soluble lignin and then decay the extracted wood with brown rot fungi which preferentially attacks the carbohydrate components of the wood, leaving the lignin essentially unaffected. When Schubert and Nord (50, 51) subjected coniferous woods to this decay, an additional amount of alcohol-soluble lignin was liberated. This behavior indicates that a lignin-carbohydrate linkage is destroyed by the microbiological degradation of the carbohydrate components of wood. Leopold (52) studied sprucewood and also found an increased yield of alcohol-soluble lignin resulting from the decay by brown rot fungi. He also reported that complete delignification occurred when this brown-rotted sprucewood was sulfonated at pH 5.3 and 135°C. while under similar conditions sound wood gave only 30% delignification.

The evidence from fermentation of wood supports the view that a chemical linkage exists between lignin and carbohydrate. Virtanen, et al. (89, 90) and Ploetz (91) in separate investigations found that, when pulp or wood is fermented, the fermentation ceases after a certain stage has been reached, leaving an

unfermentable residue containing both lignin and carbohydrate. Only half of the cellulose of coniferous woods and two-thirds of the cellulose of hardwoods were fermented by thermophilic cellulose bacteria (90). This behavior can be explained by the existence of a chemical linkage between the lignin and the carbohydrate which is resistant to fermentation. It is also of interest to note that the loss of carbohydrate during fermentation was accompanied by a loss of lignin.

ISOLATED LIGNIN-CARBOHYDRATE COMPLEXES

The most direct evidence for a lignin-carbohydrate linkage comes from the isolation and subsequent investigation of lignin-carbohydrate complexes. Björkman (73, 92, 93) extracted lignin-carbohydrate complexes (L.C.C.) from sprucewood which had been milled vigorously under nonswelling conditions. He first extracted the milled sprucewood with aqueous dioxane to obtain a material which contained primarily lignin and which he called milled wood lignin (M.W.L.). Then extraction of the residue with acetic acid or dimethylformamide gave lignin-carbohydrate complexes which contained 1 part of lignin to 3 to 4 parts of carbohydrate. The carbohydrate composition in L.C.C. corresponded very closely with the relative amounts of sugars in the hemicellulose components of the sprucewood. Thus, it appears plausible that the carbohydrates involved in the lignin-carbohydrate linkage of sprucewood are the hemicelluloses. The lignin in L.C.C. appeared to be identical with M.W.L. and upon further milling of L.C.C. more "free" lignin was liberated which was soluble in dioxane. Since this lignin could not be separated from L.C.C. and was not soluble in dioxane before milling, Björkman explained the above behavior by a splitting of a lignin-carbohydrate bond during milling.

Lindgren (6) studied Björkman's fractions with paper and free boundary electrophoresis. The fraction L.C.C. could be separated into two subfractions having different electrophoretic mobilities. The slower subfraction contained only carbohydrate and the faster subfraction contained both carbohydrate and lignin materials in approximately equal amounts. This latter fraction moved more slowly than did the lignin in the M.W.L. fraction. The mobility of the subfraction containing lignin and carbohydrate materials strongly supports Björkman's hypothesis of a lignin carbohydrate linkage.

Meier (5) has obtained good evidence for a lignin-carbohydrate linkage in isolated glucomannan fractions from pine. Two glucomannan fractions were studied with paper electrophoresis. One fraction contained about 6% lignin and had a mobility distinctly different from the other glucomannan fraction which contained only a trace of lignin. He, therefore, concluded that the mannose residues in the former fraction must either have been present in a different type of molecule, or be in a glucomannan chemically bound to some other species. After complete delignification this fraction had a mobility similar to the fraction which originally contained only a trace amount of lignin. This indicates that a lignin-carbohydrate complex was involved. Furthermore, it was found that glucomannan fractions with about 5% lignin contained 11% galactose and 5.5% xylose which could not be separated by conventional methods. After delignification to 0.3% lignin, the galactose residues could be reduced to 1 to 2% and the xylose residues to traces (7). It was concluded that different polysaccharides, glucomannans, and xylans, as well as galactans or arabogalactans may be linked to the same lignin molecule. It is of interest to note that Meier (5) found that nitration of the glucomannan fractions resulted in complete delignification and therefore molecular weight determinations on glucomannan nitrates gave values for the glucomannan molecule and not the glucomannan-lignin complex.

McPherson (94) obtained a series of lignin-carbohydrate complexes along with relatively pure lignin and hemicellulose fractions from milled sprucewood by successive extraction, fractional precipitation, and separation on various columns.

THE NATURE OF THE LIGNIN-CARBOHYDRATE LINKAGE

The type of chemical bond between lignin and carbohydrate has not been established. The favored linkage is a β-phenyl glycosidic bond because of the sensitivity of this type of bond to acid, alkali, and heat treatments and its abundance in plants (95, 96). Lindgren (97) reviewed the research in this field and suggested that the most likely linkage is a β-phenyl glycoside or a benzyl ether bond. An ether linkage at the β-carbon of the propyl group (98) or an acetal linkage in which the carbonyl group comes from the lignin (99) are also possible. Brauns (75) discusses the various possible lignin-carbohydrate linkages.

SUMMARY

From the evidence presented above, it is seen that a chemical linkage between the glucomannan and the lignin component of sprucewood is not only possible but it is highly probable. Considerably more evidence is available from investigations based on extraction of cell wall components, microbiological degradation of wood, alkaline hydrolysis of wood, acid hydrolysis of wood, holocellulose preparation, alkylation of wood, alcoholysis of wood, acetylation and acetolysis of wood, nitration of wood, sulfonation of wood, and other miscellaneous reactions (53, 77).

APPENDIX II

HOLOCELLULOSE PREPARATION

WOOD

Two eight-foot logs were obtained from Consolidated Papers, Inc., Appleton, Wis., and identified as black spruce by Irving H. Isenberg (100). The logs were debarked, chipped, and screened, Chips that passed through a one-half inch screen and were retained on a one-fourth inch screen were saved for delignification.

GENERAL ON PREPARATION AND THEORY OF DELIGNIFICATION

In order to minimize degradation of the polysaccharides during delignification, a room temperature chloriting process was employed similar to that recently described by Thompson and Kaustinen (17). Several modifications were employed in this study to shorten the reaction time of Thompson's process of three to four weeks: (1) small (one-fourth inch) chips were employed rather than wood blocks, (2) the chips were evacuated prior to contact with the solution to aid in penetration, (3) a sodium chlorite concentration of 200 g./l. was used in contrast to the 45 g./l. employed by Thompson, and (4) as soon as possible the chips were defibered in order to improve the accessibility of the lignin and the delignification allowed to proceed at a lower concentration. These modifications reduced the reaction time to less than 6 days.

The delignification of an acidic sodium chlorite solution is due to the reaction of chlorine dioxide with lignin (101, 102). The chlorine dioxide specifically attacks the lignin compounds but does not react with the carbohydrates (101, 102). In acid solutions containing pulp the chlorite ion reacts to form chlorine dioxide according to the simplified reaction (101, 102), $5ClO_2^- +$

$4H^+ \rightarrow 4ClO_2 + Cl^- + 2H_2O$. The chlorite ions do not form chlorine dioxide above pH 7 and thus are not reactive toward lignin above this pH. However, as the pH drops to four, the chlorite ions become increasingly reactive (102, 103). The chlorite ion will attack carbohydrates by oxidizing the aldehyde group on an end group reducing sugar to a carboxyl group (104-106).

When acidified sodium chlorite or chlorine dioxide reacts with compounds having a guaiacyl nucleus, oxidation and splitting of the benzene ring take place between the methoxyl and hydroxyl groups (108, 109). This type of reaction may occur when acidified sodium chlorite or chlorine dioxide reacts with coniferous woods since the lignin in these woods is composed primarily of phenylpropane units containing the guaiacyl nucleus. It is probable that the aromatic nature of the lignin is destroyed by reaction with acidified sodium chlorite since spruce periodate lignin which has been treated with acidified sodium chlorite does not yield vanillin upon alkaline nitrobenzene oxidation whereas the untreated periodate lignin does yield vanillin, similar to the behavior of other lignins (109). Lignin also undergoes some demethoxylation when it is reacted with acidified sodium chlorite or chlorine dioxide (108, 109).

A slight modification of this delignification from that described by Thompson and Kaustinen (17) is that the sodium chlorite solution in this procedure was not acidified to pH 4 before reaction with the wood. The initial pH of the chlorite solution was 12.4; thus, little delignification will occur at first. This results in a greater penetration of the chips by the solution before the delignification reaction begins and thus supposedly a more uniform delignification. As the chlorite solution penetrates the chips, wood acids and carboxyl groups are formed. These acids initiate the formation of chlorine dioxide and the reaction of chlorine dioxide and lignin creates more acids and thus the pH drops. The pH

does not drop below pH 4, however, due to the buffering action of the salts of the organic acids (17). Thus, the reaction is self-initiating and also self-buffered, preventing the formation of a dangerously low pH. The pH of the solution quickly drops as indicated by the evolution of chlorine dioxide a few hours after contact of the chips with the chlorite solution. The pH of the final solution was 5.4 to 5.6. Rapson (103) claims that optimum bleaching with chlorine dioxide occurs between pH 5-7. It can be inferred that this delignification behaves in the same manner since chlorine dioxide is the active agent and since bleaching is primarily a delignification reaction.

The resulting holocellulose should contain polysaccharide material that has been subjected to a minimum of degradation due to the low temperature of delignification and the specificity of the chlorine dioxide for lignin. Furthermore, the presence of a nonreducing carboxyl end-group (introduced by the chlorite ion oxidation) on the polysaccharide chain retards degradation of the polysaccharide under alkaline conditions. This is a definite advantage as subsequent isolation of the glucomannan from the holocellulose was carried out by alkaline extraction. In addition to minimizing degradation, the room temperature chloriting process made it feasible to prepare kilogram quantities of holocellulose. Since heat was not applied in this process, degradation due to local overheating which occurs in large-scale preparations of other holocelluloses was prevented in this holocellulose preparation. Wood chips rather than wood meal were used in order to preserve the fibrous structure since this undoubtedly influences the sequence of hemicellulose extraction.

PROCEDURE OF HOLOCELLULOSE PREPARATION

Four kilograms of one-quarter inch black spruce chips (3.20 kg. of ovendry wood) were delignified. Nonextracted wood was used as it has been found

unnecessary to extract sprucewood when using the room temperature chloriting procedure (17). The chips were placed in 6 ten-inch vacuum desiccators and 4 eight-inch vacuum desiccators and evacuated. The chips were then delignified with an 8:1 (volume to weight) ratio of liquor to wood. The delignification solution was made up with 200 grams of sodium chlorite to every liter of H_2O. Initial pH of solution was 12.40. The delignification was then allowed to proceed at ambient temperature for five days. The pH of the solution after this first reaction stage was 5.43.

The liquor was then filtered from the chips and the chips were defibered in a Waring Blendor for 50 seconds. The chips were defibered in order to speed up the final delignification by aiding diffusion of chemicals into and lignin reaction products out of the fibers and to provide for a more uniform reaction in the final delignification. A uniform reaction is probably more critical in the final stage when the fibers are not protected by the lignin. In the final stage the solution from the first stage was diluted to one-third of its volume. Assuming 50% of the sodium chlorite on the basis of ovendry wood had reacted during the first stage (17), this diluted solution would be at a concentration of approximately 50 grams of sodium chlorite per liter. The solution and fibers were then placed in the desiccators at an 8:1 ratio. This second-stage delignification was allowed to proceed for 22 hours. The final pH of the solution was 5.67.

At the end of the second stage the fibers were washed well with water, steeped in water overnight, washed again with excess water, pressed, and steeped in 95% ethanol overnight. The fibers were then pressed and air dried. The final ethanol washing was to give a holocellulose which would be readily dispersed in a 0.1N sodium hydroxide solution in the following extraction experiments. The final air-dried product weighed 2,616 grams and had a slight yellow tint. The ovendry yield was 2,404 grams or 75.1% based on the ovendry wood.

APPENDIX III

EXTRACTION AND PURIFICATION OF THE GLUCOMANNAN FRACTIONS

PRELIMINARY INVESTIGATION

Preliminary experiments were carried out to determine the best method of isolating pure glucomannan fractions from the holocellulose in fairly large quantities with a minimum of degradation. Two preliminary experiments were run in which the extraction sequences were similar but the methods of precipitation and purification were different. The extraction sequence employed was 0.1N sodium hydroxide, 10% sodium hydroxide, 18% sodium hydroxide, and 18% sodium hydroxide containing 4% boric acid.

In the first series of experiments the initial precipitates were isolated by neutralizing the extracts and, in the second series of experiments, barium acetate was added to the extracts to cause precipitation. Further purification of the initial fractions gave 56 final fractions. Determination of the yields and qualitative sugar contents of these fractions showed that the second method of isolation was superior to the first method. The second method was simpler and faster to carry out than the first method and gave higher yields with less chance of degradation.

Barium precipitation was shown to be a highly effective method of isolating glucomannan fractions. Meier (110) first discovered that barium ions would precipitate glucomannans from alkaline solutions and postulated that barium ions form a complex with the cis-hydroxyl groups on carbon atoms 2 and 3 of the mannose units. From this series of experiments, it has been found that the selectivity of the barium ion for mannose-containing polysaccharides can be enhanced through a fractional precipitation scheme. It was shown that up to

about 0.08 to 0.10M in barium ion concentration the glucomannan is selectively precipitated while the xylan remains in solution, but in the range of 0.10 to 0.20M the xylans are also precipitated.

LARGE-SCALE ISOLATION

GENERAL

Direct barium precipitation of the extracts was employed. Solutions of barium acetate were used to cause precipitation rather than the conventional barium hydroxide because of the greater solubility of the former which enabled solution volumes to be kept to a minimum (111). By precipitating the hemicellulose fractions immediately after extraction, excessive degradation should be prevented by minimizing the contact time between the alkaline solution and the hemicelluloses.

The 0.1N, 10%, and 18% extraction solutions were made 0.10M in barium ion concentration and the 18 and 4% and wash solutions were made 0.20M in barium ion concentration to cause precipitation. This was done to minimize the precipitation of xylans (which is appreciable above 0.10M barium ion concentration) in the 0.1N, 10, and 18% solutions. Less xylan is extracted by the 18 and 4% and wash solutions, permitting the use of a higher concentration of barium ion. Also, Vaughan (111) claims that an excess of barium ion is needed to precipitate glucomannans in the presence of borate ions. Due to the large amount of holocellulose being extracted, it was necessary to divide it into two batches. A summary of the isolation and purification procedures are given in Fig. 10 and 11.

EXTRACTION AND PRECIPITATION

A total of 2,200 grams of ovendry holocellulose were extracted. The extraction was carried out in two batches of 1,100 grams each. The extraction and

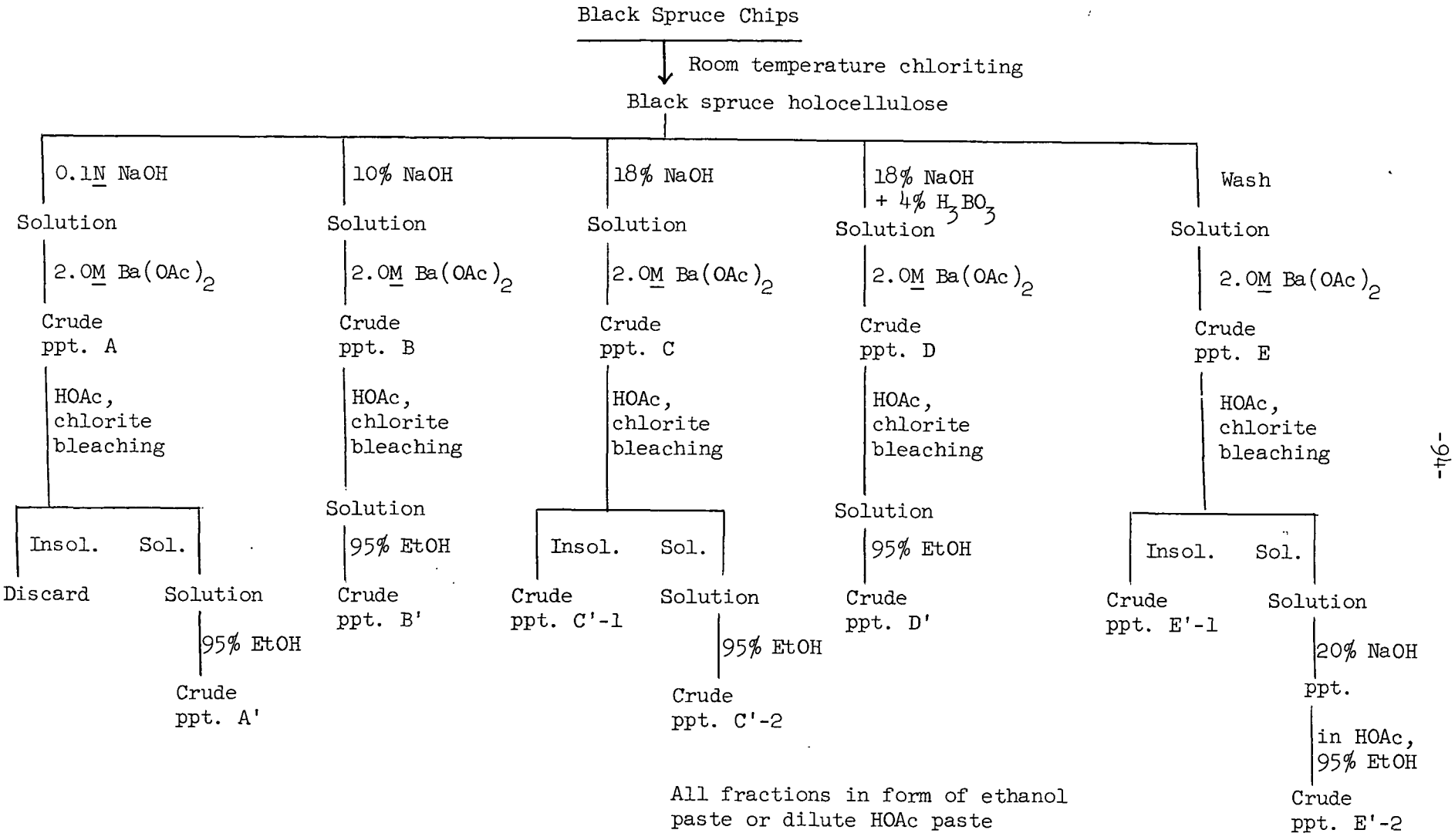

Figure 10. Isolation of Crude Fractions

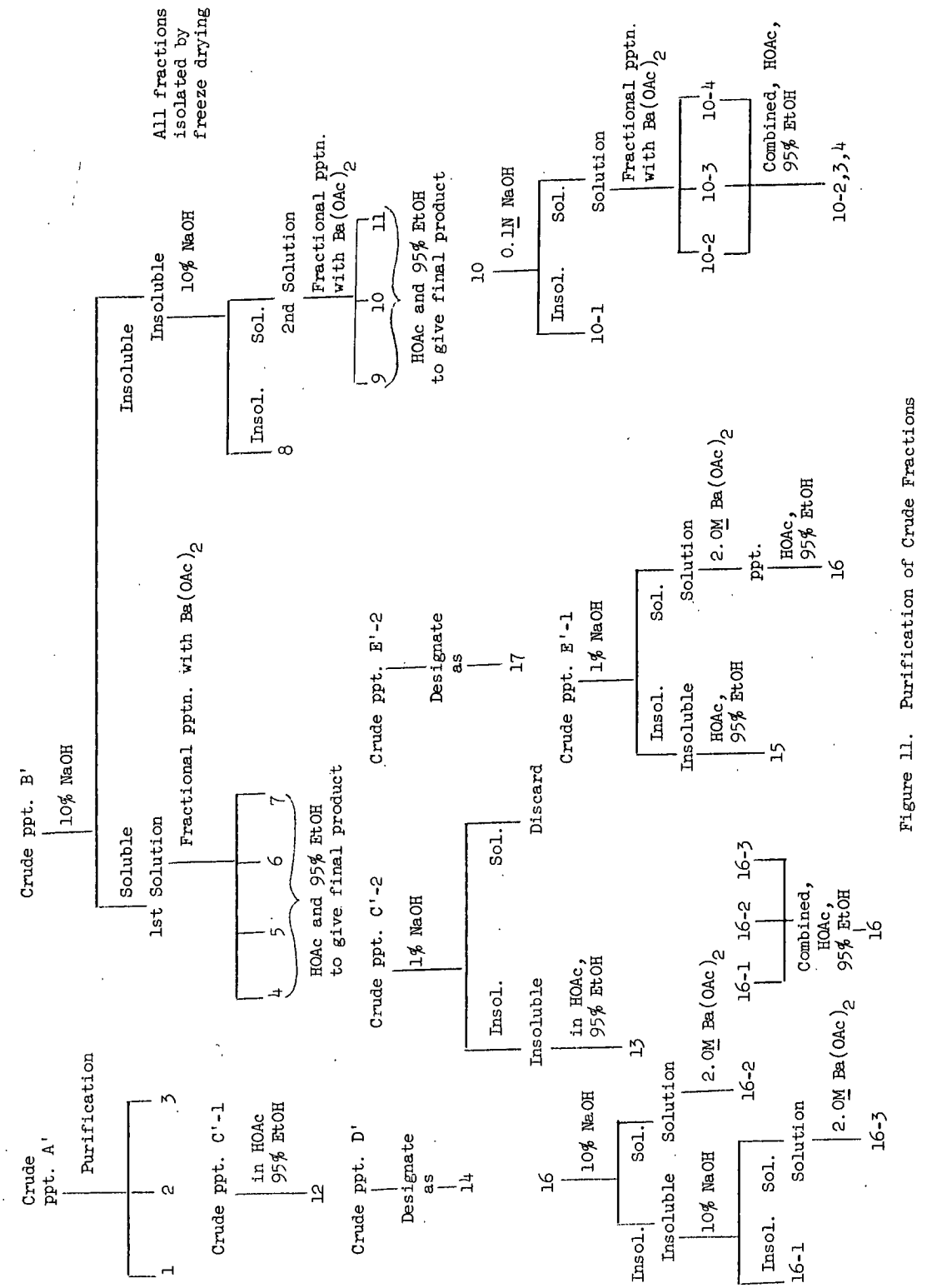

Figure 11. Purification of Crude Fractions

immediate precipitation procedures were identical for each batch. The holocellulose from each batch was placed in 2 ten-inch vacuum desiccators. Three extractions for one-half hour each were carried out for each of the following concentrations: (1) 0.1N NaOH, (2) 10% NaOH, (3) 18% NaOH, (4) 18% NaOH and 4% H_3BO_3, and (5) wash water. The volume-to-weight ratio of the solution to ovendry holocellulose was 10:1. A vacuum was applied during all extractions in order to aid in penetration and minimize degradation.

After each extraction, the solution was removed from the holocellulose by filtration on a large bench Buchner funnel without filter paper and the fines removed from this solution by filtration on a large fritted glass funnel. This procedure markedly decreased the filtration time and allowed a one-half hour extraction schedule to be maintained. A yield of the large-scale residue was not determined but in an identical small-scale experiment 40.2% of the ovendry holocellulose was extracted.

Immediately after each extraction, 2.0M barium acetate solution was added to cause precipitation. The resulting barium ion concentrations were 0.10M, 0.10M, 0.10M, 0.20M, and 0.20M for the 0.1N sodium hydroxide solution, 10% sodium hydroxide solution, 18% sodium hydroxide solution, 18% sodium hydroxide containing 4% boric acid solution, and the final water wash, respectively. The three extraction solutions for each concentration were then placed in a five-gallon pickle jar and the precipitates allowed to settle for about 12 hours. The top solution was then siphoned off and the remaining precipitate filtered. A large bench Buchner funnel covered with coarse filter paper sandwiched between two sheets of nylon allowed for fairly rapid filtration. Only a small amount of the 0.1N precipitate was collected due to the difficulty of filtering. The 10% precipitate was centrifuged rather than filtered to prevent mechanical losses.

The barium precipitates were then slurried in acetic acid solutions maintained at pH 4-5 by addition of glacial acetic acid. Ice was added to prevent the temperature from rising considerably above room temperature. The following amounts of sodium chlorite were then added for each batch: 0.1N (11.00 g.), 10% (5.50 g.), 18% (1.10 g.), 18 and 4% (1.10 g.), wash (1.10 g.). The delignification reaction was carried out overnight.

The "crude" precipitates were then isolated. The insoluble precipitates were centrifuged from the 0.1N and the 18% solutions and the soluble fractions were collected by precipitating with addition of an equal volume of 95% ethanol. The 10 and 18% and 4% solutions contained very little insoluble precipitate and, therefore, the entire soluble fractions were collected by addition of an equal volume of 95% ethanol. The insoluble precipitate from the wash solution was removed by centrifugation and the supernatant was made about 10% in NaOH by addition of 20% NaOH solution. The resulting precipitate was removed by centrifugation, slurried in 1N acetic acid, and reprecipitated with 95% ethanol.

PURIFICATION OF "CRUDE" FRACTIONS

Purification of 0.1N Precipitate

An attempt was made to obtain a galactoglucomannan from this precipitate by dissolving in a 1% sodium hydroxide solution and adding an equal volume of Fehling solution. However, the attempt failed and no precipitate was obtained upon standing overnight. Apparently, the galactoglucomannan was not present in sufficient quantity to form a precipitate. A rather involved procedure employing precipitation with barium acetate and Fehling solution was then used to obtain three fractions designated as Fractions 1, 2, and 3.

Purification of the 10% Precipitate

The 10% precipitate was the largest fraction. It was decided to precipitate the hemicelluloses fractionally from an alkaline solution and to divide the 10% precipitate into two batches in order to keep the time of contact between the hemicellulose and the solution to a minimum. The precipitate was first slurried in 2.2 liters of 10% NaOH solution for one-half hour. The insoluble precipitate was then removed and reslurried in 2.2 liters of 10% NaOH solution to give a second solution. After 2-1/2 hours the insoluble precipitate (which constituted the bulk of the original precipitate) was removed by centrifugation from the second solution. Fractional precipitation was then carried out on both solutions by the gradual addition of 2.0M barium acetate solution. The fractionation sequence is reported in Table XIII.

TABLE XIII

FRACTIONATION OF 10% PRECIPITATE

1st Solution

Fraction	Reslurried	4	5	6	7
Resulting Ba^{++} concn.	Insol.	0.035M	0.08M	0.15M	0.20M

2nd Solution

Fraction	8	9	10	11
Resulting Ba^{++} concn.	Insol.	0.03M	0.15M	0.20M

All precipitates were slurried in acetic acid solution maintained at pH 4-5 and reprecipitated by addition of an equal volume of 95% ethanol. The dilute acetic acid solution of Fraction 8 contained a small amount of insoluble precipitate and this was removed by centrifugation and discarded before the ethanol addition.

Purification of 18% Precipitates

The insoluble 18% precipitate was slurried in 1N acetic acid and reprecipitated by the addition of an equal volume of 95% ethanol. This fraction was designated as Fraction 12.

The soluble 18% precipitate was slurried in 4.4 liters of 1% NaOH solution. After standing for two hours, the insoluble fraction (which constituted the bulk of the original precipitate) was removed by centrifugation, slurried in 1N acetic acid, and reprecipitated by addition of an equal volume of 95% ethanol. This fraction was designated as Fraction 13.

The supernatant from the 1% NaOH solution was made 0.05M in barium ion concentration. The solution was discarded since only a small amount of precipitate was formed.

Purification of 18 and 4% Precipitate

The 18 and 4% precipitate was considered in a sufficiently pure state and therefore no further purification was carried out. This fraction was designated as Fraction 14.

Purification of Wash Precipitates

The insoluble wash precipitate was slurried in 4.4 liters of 1% NaOH solution for six hours. The insoluble fraction was then removed by centrifugation, slurried in 1N acetic acid, and reprecipitated by addition of an equal volume of 95% ethanol. This fraction was designated as Fraction 15.

The 1% NaOH supernatant was made 0.05M in barium ion concentration by addition of 2.0M barium acetate solution. This caused the formation of precipitate which was collected by centrifugation, slurried in 1N acetic acid, and reprecipitated by the addition of 95% ethanol. This fraction was designated as Fraction 16. The above supernatant was tested by making the solution 0.20M in barium

ion concentration but only a small amount of precipitate was formed and the solution was therefore discarded.

The original soluble wash precipitate was in a sufficiently pure state and was not treated any further. This fraction was designated as Fraction 17.

CHARACTERIZATION OF THE PURIFIED FRACTIONS

The Fractions 1 through 17 were then hydrolyzed with 72% sulfuric acid (23) and subjected to qualitative sugar analysis on a chromatogram. From the results of this analysis it was decided to attempt a further purification of Fractions 10 and 16 and they were set aside for further study. The quantity of Fraction 2 was so minute that it was completely used up in the qualitative analysis. The other fractions were slurried in acetic acid solution maintained at pH 3-5 and dialyzed in cellophane bags against distilled water for 12 to 18 days (the distilled water was acidified the first night in order to facilitate removal of inorganic salts). After dialysis, the solutions were concentrated by evaporation and freeze dried.

All fractions appeared white or a shade of white after freeze drying. Fractions 1 and 3 had a gritty feel, while all other fractions were in a light fluffy state. Although no change in sugar content was expected during dialysis, evaporation, and freeze drying, a check was made by reanalyzing Fraction 7 and Fraction 8 after freeze drying. As was expected, no change in sugar content occurred. Fraction 3 failed to give a spot on a chromatogram after hydrolyzing as the ethanol paste and was analyzed again after freeze drying. It again failed to give a spot and this evidence, coupled with its gritty feel indicated it was an inorganic material. Moisture contents and ovendry yields were then determined and are reported in Table XIV along with appearances of the ethanol pastes and qualitative sugar analyses.

TABLE XIV

CHARACTERIZATION OF PURIFIED FRACTIONS

Extraction solution	0.1N NaOH			10% NaOH								18% NaOH		18% NaOH + 4% H_3BO_3	Wash		
Designation of fraction	1	2	3	4	5	6	7	8	9	10	11	12	13	14	15	16	17
Appearance of ethanol pastes	light yellow	light yellow	white with yellow tinge	white with yellow tinge	white with yellow tinge	light yellow	light yellow	white with yellow tinge	white with yellow tinge	light yellow	light yellow	gray	cream	light brown	light brown	cream	white
Sugar analysis (qual.)	Gal. >[a] X. > M. > Gl. > A.(T)	M. ~[b] Gl.	None	M. > Gl. > Gal.(T)	M. > Gl. > Gal. > X. (T)	X. > Gal. > M. ~ Gl. > A.(T)	X. > Gal. > Gl. ~ M. > A.	M. > Gl. > Gal. > X.(T)	M. > Gl. > Gal. > X.(T)	M. > Gl. ~ Gal. > X. > A.(T)	Gal. ~ Gl. > M. > X. > A.(T)	Gl. > M. > Gal.	M. > Gl. > Gal. > X.(T)	M. > Gl. > Gal. > X.(T)	Gl. > M. ~ Gal. > X. > A.(T)	M. > Gal. ~ Gl. > X.(T) > A.(T)	M. > Gl. > Gal. > X.(T)
O.D. yield, g. (freeze dried)	9.0	All used in sugar analysis	0.8	2.1	0.1	1.1	5.9	38.7	9.7	Purified further	0.6	0.5	17.1	8.5	5.9	Purified further	3.1
Moisture content, % (freeze dried)	0.953	--	1.93	6.79	16.2	8.36	7.14	5.94	4.90	--	8.10	5.92	2.48	8.39	2.56	--	4.70
Rating				e	c	g	g	c	c	g			c	d		f	c to d

[a] > Designates greater than.
[b] ~ Designates similar to.
The columns in the table are read vertically.
[c] Glucomannan with normal (low) galactose content.
[d] Glucomannan with high galactose content.
[e] Glucomannan with only trace level of galactose.
[f] Glucomannan rich in galactose or galactoglucomannan.
[g] Potential galactoglucomannan contaminated with xylose.

FURTHER PURIFICATION OF FRACTIONS 10 AND 16

Purification of Fraction 10

Fraction 10 was a galactoglucomannan with a xylose impurity. An attempt was made to remove the xylose impurity with the following fractionation procedure. Fraction 10 was slurried in a 0.1N NaOH solution, the insoluble portion was removed by centrifugation, and 2.0M barium acetate solution added to obtain a total of 4 fractions. The precipitates were slurried in 1N acetic acid, reprecipitated by addition of 95% ethanol, collected, and analyzed qualitatively for sugar content. The Fractions 10-2, 10-3, and 10-4 were identical and thus were combined, dialyzed, concentrated, and freeze dried. The results, together with moisture content and ovendry yield, are reported in Table XV.

TABLE XV

REFRACTIONATION OF FRACTION 10

Fraction	10-1	10-2	10-3	10-4
Resulting concn. of barium ion	Insol.	0.10M	0.15M	0.20M
Appearance of ethanol paste	cream	light yellow	light yellow	light yellow
Qual. sugar analysis	Gl. ~ [a] Gal. > [b] M. > X. > A.(T)	M. > Gl. ~ Gal. > X. > A.(T)	M. > Gl. ~ Gal. > X. > A.(T)	M. > Gl. ~ Gal. > X. > A.(T)
Redesignation of fractions	--		10-2,3,4	
O.D. yield (freeze dried)	--		0.4 g.	
Moisture content (freeze dried)	--		9.60%	

[a] ~ Designates similar to.
[b] > Designates greater than.
Columns in the table are read vertically.

The conclusion is that the fractionation did not result in a change in the original sugar content and the Fraction 10-2,3,4 is a galactoglucomannan with a xylose impurity.

Purification of Fraction 16

Fraction 16 was a galactose-rich glucomannan with a possible glucose impurity. An attempt was made to remove the glucose impurity with the following fractionation procedure. Fraction 16 was slurried in a 10% NaOH solution. The insoluble portion was removed by centrifugation and reslurried in a 10% NaOH solution to give a second solution. The insoluble precipitate from the second solution was removed and designated as 16-1.

The centrifugate from the first solution was made 0.18M in barium ion concentration and the resulting precipitate removed and designated as 16-2. The centrifugate from the second solution was made 0.15M in barium ion concentration and the resulting precipitate removed and designated as 16-3. All precipitates were slurried in 1N acetic acid, reprecipitated by addition of 95% ethanol, collected, and analyzed for qualitative sugar content. The three fractions were identical in sugar content and they were combined, dialyzed, concentrated, and freeze dried. The results, together with moisture contents and ovendry yields are reported in Table XVI.

The conclusion is that the fractionation did not result in a change in the original sugar content and the Fraction 16-1,2,3 is galactose-rich glucomannan with a small amount of xylose impurity.

TABLE XVI

REFRACTIONATION OF FRACTION 16

Fraction	16-1	16-2	16-3
Appearance of ethanol paste	light brown	light yellow	cream
Qual. sugar analysis	M. $>^{a}$ Gal. $\sim^{b}$ Gl. > X. > A.(T)	M. > Gal. $\sim$ Gl. > X. > A.(T)	M. > Gal. $\sim$ Gl. > X. > A.(T)
Redesignation of fractions		16-1,2,3	
O.D. yield, g. (freeze dried)		2.2	
Moisture content, % (freeze dried)		4.80	

$^{a}>$ Designates greater than.
$^{b}\sim$ Designates similar to.
Columns in the table are read vertically.

APPENDIX IV

CHARACTERIZATION OF HOLOCELLULOSE AND EXTRACTED RESIDUE

The results of the characterization of the holocellulose are presented in Tables XVII and XVIII. The paper tests were carried out according to TAPPI Standard T 220 m-60. The following analytical procedures were used: Klason lignin (I.M. 13), sulfated ash (ignited at 650°C.), sugar analysis [Saeman, J. F., et al. (23)], carboxyl [Davidson, G. J., and Nevell, T. P., J. Textile Institute 39:T93(1948)], carbonyl [Gladding, E. K., and Purves, C. B., Paper Trade J. 116, no. 14:26(1943)], methoxyl (TAPPI T 209 m-45), viscosity (TAPPI T 230 sm-50), soluble lignin [Hess, C. L., Tappi 35, no. 7:312-20(July, 1952)] - Absorbance at 280 mμ divided by factor of 18, burst (TAPPI T 403 m), tear (TAPPI T 414), Instron tensile (TAPPI T 404 in which an I.P.C. line-type specimen clamp was employed), zero-span tensile (TAPPI T 231 sm-60 modified by Wink, et al., Tappi, in press) and z-direction tensile. In order to form a handsheet for strength measurements it was necessary to steep the fibers in 0.1N sodium hydroxide for 4-1/2 hours. Thompson (17) has found that this procedure does not effect the strength properties of the handsheet.

The mannose content and the arabinose content are slightly less and the glucose content slightly greater than the corresponding sugar contents of a black spruce holocellulose prepared by Thompson (17) in a similar manner. The Klason lignin content of the holocellulose prepared in this study was a little greater than that of Thompson's holocellulose (1.1%) and the soluble lignin content was in the 7-15% range obtained by Thompson.

In general, the holocellulose prepared in this study is similar to the black spruce holocellulose prepared by Thompson. The carboxyl content obtained in this study was close to the value 27 mmol./100 g. for Thompson's holocellulose. These

TABLE XVII

CHEMICAL CHARACTERIZATION OF HOLOCELLULOSE

Yield, %	75.1	
Galactan, %	3.42	(4.22)[a]
Glucan, %	56.2	(69.26)
Mannan, %	12.4	(15.28)
Xylan, %	7.78	(9.59)
Araban, %	1.34	(1.65)
Total carbohydrate content, %		81.14
Klason lignin, %		2.30
Soluble lignin, %		14.0
Total lignin content, %		16.3
Sulfated ash (as sodium chlorite), %		5.77
Total accounted for, %		103.2[b]
Carboxyl content, mmol./100 g.		22.8
Carbonyl content, mmol./100 g.		22.3
Methoxyl, %		1.76
Methoxyl of total lignin, %		10.80[c]
Viscosity		did not dissolve completely in cupriethylenediamine

[a] ( ) = based on neutral carbohydrate content.

[b] Sum of the sugar content, the total lignin content, and the ash content.

[c] Assumes that the entire methoxyl content of the holocellulose is due to the total lignin content.

TABLE XVIII

PHYSICAL CHARACTERIZATION OF HOLOCELLULOSE

Burst = 133 points/100 lb.

Tear factor = 0.89

Instron tensile = 37.0 lb./inch

Zero-span tensile = 63.4 lb./inch

z-Direction tensile = 16.8 kg./sq. cm.

relatively high values of carboxyl content are characteristic of the room temperature sodium chlorite holocellulose and may be due to the high retention of hemicelluloses containing uronic acid groups and terminal oxidized end groups (17). The strength properties of the holocellulose in this study are comparable to the values which were obtained by Thompson.

The results from the characterization of the residue remaining after extraction are presented in Table XIX. The per cent of material extracted based on the total amount of holocellulose for the individual sugar residues and the Klason and soluble lignin is presented in Table XX. Also presented in this table is the per cent of each individual component extracted based on the amount of that component originally present in the holocellulose. The values presented in this table were calculated from a material balance on the holocellulose and residue.

Galactose is more resistant to extraction than the other hemicellulose sugars, excluding the 17.4% of glucose extracted, and only 57.0% of the galactose residues were extracted from the holocellulose by the exhaustive extraction procedure employed. In contrast to this behavior, 86.1% of the xylose residues were extracted. The sugar ratios for the holocellulose, the extract, the residue, and a typical glucomannan fraction from this study are presented in Table XXI.

TABLE XIX

CHEMICAL CHARACTERIZATION OF RESIDUE

Yield, %	59.8[a]		
Galactan, %	2.46	(2.76)[b]	
Glucan, %	77.6	(87.16)	
Mannan, %	6.66	(7.48)	
Xylan, %	1.81	(2.03)	
Araban, %	0.50	(0.56)	
Total carbohydrate content, %			89.03
Klason lignin, %			0.80
Soluble lignin, %			4.72
Total lignin content, %			5.52
Sulfated ash (as sodium chlorite), %			1.94
Total accounted for, %			96.49[c]

[a]Based on holocellulose.
[b]( ) = based on neutral carbohydrate content.
[c]Sum of the sugar content, the total lignin content, and the ash content.

TABLE XX

AMOUNT OF MATERIAL EXTRACTED FROM HOLOCELLULOSE

Component	Holocellulose Extracted, %	Original Component Extracted, %[a]
Galactan, %	1.95	57.02
Glucan, %	9.80	17.44
Mannan, %	8.42	67.90
Xylan, %	6.70	86.12
Araban, %	1.04	77.61
Total carbohydrates, %	27.90	34.39
Klason lignin, %	1.82	79.13
Soluble lignin, %	11.18	79.86
Total lignin, %	13.00	79.75
Total carbohydrates and lignin, %	40.90	41.97

[a]Based on the amount of component originally present in the holocellulose.

TABLE XXI

SUGAR RATIOS OF HOLOCELLULOSE, EXTRACT, AND RESIDUE

Sugar Residue	Sugar Ratio of Holocellulose	Sugar Ratio of Extract[b]	Sugar Ratio of Residue	Sugar Ratio of Fraction 2(1)
Galactan	1.05	0.88	1.40	0.21
Glucan	?[a]	4.42	?[a]	1.00
Mannan	3.80[c]	3.80[c]	3.80[c]	3.88
Xylan	2.38	3.02	1.03	0.12
Araban	0.41	0.47	0.29	0

[a]No estimate is available of the amount of noncellulosic glucose residues present.
[b]Calculated from a material balance.
[c]Assumed 3.80 to compare with the typical sugar ratio of Fraction 2(1).

From this table it is seen that a relatively high amount of galactose remains in the residue after extraction. These resistant galactose residues may be present in the form of a galactose-rich glucomannan such as Fraction 14 which could only be extracted with 18% NaOH containing 4% H_3BO_3. The assumption is made that all the resistant mannose and galactose in the extracted residue are present in the form of a glucomannan with a glucose:mannose ratio of 1:3.8 which is typical of most of the purified glucomannan fractions in this study. Then it can be concluded that a glucomannan with galactose:glucose:mannose = 1.4:1.0:3.8 and accounting for 32.1% of the mannose residues in the holocellulose is extremely resistant to extraction. Also extremely resistant to extraction are xylose and arabinose residues which amount to 17.5% of the resistant hemicelluloses in the extracted residue. These xylose residues account for 13.9% of the xylose originally present in the holocellulose.

From Table XXI it can be seen that the extract contains considerably more glucose than the typical amount present in glucomannans and galactoglucomannans

which generally have a glucose:mannose ratio of 1:3.0 to 4:4. Since glucomannans and galactoglucomannans are the only known glucose-containing hemicelluloses in gymnosperms, the major portion of these extracted glucose residues are probably present in the form of glucans.

It is interesting to note from Table XX that the per cent of Klason lignin and acid-soluble lignin extracted based on the amount of each component originally present in the holocellulose were essentially the same with values of 79.1 and 79.9%, respectively. In Appendix I, p. 80, the possibility of the hemicelluloses being chemically combined with the lignin is discussed. In order to check for a correlation between the total lignin content and the hemicellulose content, the per cent lignin based on the sum of the hemicellulose and lignin content in the holocellulose, in the extract, and in the residue was calculated as follows: The total noncellulosic sugar content was calculated by making the assumption that the ratio of the noncellulosic glucose units to the mannose units in the holocellulose and the residue is equal to the glucose-to-mannose ratio in the extract. The per cent lignin calculated in this manner is 30.2, 31.8, and 22.4% for the holocellulose, extract, and residue, respectively. If the assumption is made that the noncellulosic glucose units in the residue are all present in the form of a glucomannan with glucose:mannose = 1.0:3.8 then the per cent lignin based on the sum of the lignin and hemicellulose content in the residue is 29.5%. It thus appears that the lignin and the hemicellulose are removed together and that there may be a close association of the lignin and the hemicellulose components in the black spruce holocellulose. Furthermore, this lignin contains the same relative amounts of Klason lignin and soluble lignin in the holocellulose, extract, and residue as seen by the ratios of soluble lignin to Klason lignin of 6.09, 6.14, and 5.90, respectively. The above discussion leads to the speculation that the resistant hemicelluloses in the residue cannot be

readily extracted because they are chemically linked to the residual lignin in the residue.

APPENDIX V

ELECTROPHORESIS

EXPERIMENTAL

Free boundary electrophoresis experiments were carried out on Fractions 8 and 9 in order to determine the extent of chemical homogeneity of these fractions. In order to obtain a complete solution of the glucomannan fractions at not too high a pH, it was necessary first to dissolve them in 2M NaOH and 1M H_3BO_3 (at pH 12.6) and then to dilute with 0.6M H_3BO_3 and water to give a resulting solution of 0.296M in borate ion (III). The pH of this final solution was 9.2 and the concentration of glucomannan was 0.5 g./100 ml. This procedure was necessary as the glucomannan fractions, if added directly, could not be completely dissolved in sodium borate solutions in the pH range of 9 to 10. The temperature was 30.0°C. and the current applied across the Tiselius cell was 16 ma. The runs were continued for five hours until the boundaries were out of view.

RESULTS

The results of electrophoresis of Fractions 8 and 9 were very similar. The ascending boundary of 8 on careful examination shows five small faster moving peaks (two of which can reasonably be grouped together and three which can reasonably be grouped together) and one small, very sharp slower moving peak. The descending boundary of Fraction 8 has a small faster moving peak and a small slower moving peak. The ascending boundary of 9 has at least two small faster moving peaks and one small, fairly sharp slower moving peak. The descending boundary of 9 has a small faster moving peak and a small slower moving peak.

The area under each peak is proportional to the concentration of the migrating material (112, 113). A photograph of the schlieren pattern was enlarged ten times and the area under each peak measured with a planimeter. The percentage of each peak for the ascending and descending boundaries of Fractions 8 and 9 are given in Table XXII.

TABLE XXII

PERCENTAGE OF DIFFERENT POLYSACCHARIDES IN FRACTIONS 8 AND 9 DETERMINED BY ELECTROPHORESIS

Fraction	Boundary	Percentage of Peak		
		Fastest	Middle	Slowest
8	Ascending	3.3 (1st 2 peaks) 2.9 (2nd 3 peaks)	89.7	4.1
8	Descending	2.1	97.2	0.7
9	Ascending	3.6 (1st) 2.6 (2nd)	90.0	3.8
9	Descending	3.4	95.7	0.9

INTERPRETATION OF RESULTS

The faster moving peaks may be due to impurities of one or more of the following polysaccharides which are known to move faster on electrophoresis in a borate buffer than a glucomannan, xylan, galactan, and/or galactoglucomannan (114-116). This amounts to 2 to 6% in Fraction 8 and 3 to 6% in Fraction 9. The slower moving peaks might be due to a glucan impurity. This amounts to 1 to 4% in Fraction 8 and 1 to 4% in Fraction 9. The slower moving peaks can also be explained through the formation of aggregates, possibly due to cross-linking by means of a borate complex (117). This explanation would account for the fact that the trailing peaks are sharper and larger for the ascending boundary than the descending boundary.

APPENDIX VI

ACETYLATION OF THE MAIN GLUCOMANNAN FRACTIONS

PRELIMINARY ACETYLATIONS

It was initially attempted to acetylate Fraction 8 according to the method employed by Koleske (21). This resulted in a low yield and low acetyl content and therefore it was necessary to carry out a series of trial acetylations in order to determine which method would give a fully acetylated glucomannan in sufficient yield. The procedures were modifications of the method used by Koleske which is described as follows on a one gram of polysaccharide basis. One gram of glucomannan is shaken in 17.5 milliliters of formamide for three hours. Pyridine (32.5 ml.) is added and the mixture is shaken for two hours. Acetic anhydride (25.0 ml.) is added over three hours with shaking. The reaction mixture is allowed to stand for fourteen hours and then the glucomannan acetate is precipitated in a 5% methanol solution to which ice has been added. The precipitate is washed successively with 2% hydrochloric acid in distilled water, 95% ethanol, absolute ethanol, petroleum ether, and finally dried. Modifications included increases in the reaction time, increases in the amount of acetic anhydride, changes in the precipitation solution, collection of the precipitate by centrifugation rather than filtration, and changes in the washing solutions. The results are presented in Table XXIII.

The conclusions from these acetylations are: (1) Centrifugation is superior to filtration as some polysaccharide is lost through the filter and the filter becomes clogged quickly. (2) Length of reaction time is the important variable in obtaining complete acetylation. A reaction time of four additional days gave a sufficiently high acetyl content. (3) A methanol wash is superior to a water wash as the glucomannan acetate is peptized to a finely divided state in water

and cannot be completely collected. (4) Preliminary experiments on freeze drying the glucomannan acetate from a water slurry indicated that the products obtained by solvent exchanging and by freeze drying were similar in their dried state and solubility properties.

TABLE XXIII

TRIAL ACETYLATIONS OF THE MAIN GLUCOMANNAN FRACTION 8

Sample	Change from Koleske's Procedure	% of Theoretical Yield[a]	Acetyl, %[b]
1	None	57.3[c]	20.14[c]
2	(1) Ppt. into 44.5% ethanol with ice. (2) Collect ppt. by centrifugation.	39.5	39.84
3	(1) Reacts 1 additional day. (2) Ppt. into 2% HCl solution with ice. (3) Collect ppt. by centrifugation.	51.1[d]	40.46[d]
4	(1) Reacts 4 additional days. (2) Ppt. into 2% HCl solution with ice. (3) Collect ppt. by centrifugation. (4) Wash with methanol instead of water.	74.0	43.00
5	(1) Reacts 4 additional days. (2) Ppt. into 100% methanol with ice. (3) Collect ppt. by centrifugation. (4) Wash with 2% HCl in methanol. (5) Wash with methanol instead of water.	68.2	42.69
6	(1) Amount of acetic anhydride increased 1.5 times. (2) Reacts 4 additional days. (3) Ppt. into 2% HCl solution with ice. (4) Collect ppt. by centrifugation. (5) Wash with methanol instead of water.	74.7	42.78

[a] Based on the triacetate.
[b] Doesn't consider ash content.
[c] Appeared to have some grit from glass filter which would result in too high a determined yield and too low a determined acetyl content.
[d] Ash = 0.61%.

ACETYL ANALYSIS

Acetyl contents were determined by the method of Eberstadt as modified by Genung and Mallatt (118). This method involves a saponification of the acetate groups with sodium hydroxide and effectively measures any other acid groups present as well as the acetate groups. Since the glucomannan fractions should not contain any appreciable amount of carboxyl groups this error is negligible.

In order to conserve on material, the sample size was reduced from the suggested 1 g. to 0.2 g. and all other quantities correspondingly reduced. The accuracy was checked on standard cellulose acetate (40.5% acetyl). The measured acetyl content was 40.4% with a precision of $\pm$ 0.1% on duplicate samples. The burets were calibrated but this was found to have only a small effect on the determined acetyl contents and the calibrations were not used.

LARGE-SCALE ACETYLATION

The large-scale acetylations were carried out by the procedure used for Sample 6 of the trial acetylations with the exception that a 95% ethanol wash was used instead of the methanol wash and the precipitates were isolated by freeze drying from a water slurry instead of solvent exchanging. The results of the acetylations are presented in Table XXIV. The fully acetylated derivatives were obtained in yields of 19.8 grams and 5.10 grams for Fractions 8 and 9, respectively. The triacetate derivatives are designated as 8-A and 9-A.

Color formation was appreciable in all the acetylation solutions and after the first 14 hours of reaction the solutions were very dark. Although some of this color is removed in the following washing steps, much of it remained with the isolated fractions, giving them a light brown tint. The same color formation occurs in the acetylation of higher molecular weight polysaccharides but

in those cases it is readily removed with washing. In order to determine if the color formation is due to the presence of the glucomannan, a blank acetylation was carried out. Color formation occurred in the absence of a polysaccharide but at a lower rate. However, after four days of reaction the blank solution was very dark.

TABLE XXIV

LARGE-SCALE ACETYLATION

Fraction	Per Cent of Theoretical Yield[a,b]	Ash, %	Acetyl, %[c]	DS[d]
8-A	75.2	2.28	44.25	2.97
9-A	72.6	2.53	44.61	2.98

[a]Ash content not taken into account.
[b]Based on the triacetate.
[c]Ash content taken into account.
[d]Degree of substitution.

The mechanism of color formation is not known but it is probably due to a reaction of pyridine. Wilson and Hughes (119) found that dry pyridine reacts with dry acetic anhydride to give a dark resinous condensation product; however, this undesirable side reaction could be prevented if water was present in an amount of 0.3 to 0.5% and the pyridine was previously purified. Thus, in future acetylations of polysaccharides it appears possible to eliminate the color formation in cases where this may be detrimental.

APPENDIX VII

SOLUBILITY OF THE GLUCOMANNAN TRIACETATE

THEORY

No satisfactory quantitative theory exists for the solubility of polysaccharides and polysaccharide derivatives. A quantitative theory has been developed for nonpolar polymers like rubber or polystyrene which is based on the concept of the cohesive energy density (energy of vaporization per cubic centimeter) of the polymer and solvent (120). Nonpolar polymers are found to be soluble in solvents with a similar cohesive energy density but the theory does not yield consistent results when applied to polysaccharide derivatives (21, 120). This behavior is due to the polar nature of the polysaccharide molecule. In order that a polymer containing polar groups be made soluble, it is necessary to solvate these groups through some kind of positive interaction between the polymer and the solvent (121-125). For polysaccharide acetates the important polar group is the carbonyl group of the ester (123, 125). This group behaves as a proton acceptor and therefore it is found that solvents for polysaccharide acetates are generally proton donors.

This discussion, which is taken from a review article by Howlett and Urquhart (123), is presented to explain the necessity of a polymer-solvent interaction in order to dissolve polysaccharides and their derivatives.

In order to dissolve, a polymer must have a decrease in free energy, $\Delta F = \Delta H - T\,\Delta S$. The product of the temperature, T, and the entropy, ΔS, is always positive in solution processes. The rigidity of the polysaccharide chain minimizes the entropy term and thus the problem is one of keeping the heat term, ΔH, at as low a value as possible. The term ΔH is the resultant of the energy

absorbed in breaking polymer-polymer and solvent-solvent bonds and the energy emitted in forming polymer-solvent bonds. The energy involved in solvent-solvent bonds is small; however, for polysaccharides and their derivatives a large amount of energy is required in breaking polymer-polymer bonds. Therefore, in order to keep ΔH at a low positive or negative value, a large amount of energy must be liberated in the formation of the polymer-solvent bonds.

This, in effect, means that a relatively strong interaction between solvent and polymer, commonly called solvation, is a prerequisite to solution of polysaccharides and their derivatives. This behavior is quite different from the solubility behavior of nonpolar synthetic polymers in which only a small amount of energy is necessary to break polymer-polymer bonds.

RESULTS

The solubility of Fraction 8-A was investigated in 172 solvents. The concentration was 0.005 g./ml. The solutions were shaken overnight in small test tubes containing glass rods to insure complete dispersion of the polymer in the solvent. Solubility ratings were then made according to the appearance of the solution. The classifications in order of decreasing solubility are S = soluble by eye (clear solution), S-AS' = slight cloudiness or a few fine particles visible, AS' = hazy, AS = almost soluble but a little insoluble, P = partially soluble, and I = insoluble.

In order to interpret the results, solvents having a classification of S, S-AS', and AS' were considered as having a relatively high degree of solvent power and solvents with the classification of I were considered as nonsolvents. It was found that the data could be correlated quite well using the concept that in order to be a solvent, a compound must be able to donate a proton in the form of a plus dipole to the carbonyl group of the ester. Of the 53 solvents with a

high degree of solvent power (S, S-AS', and AS'), 46 could be placed in classes of compounds that are known to have some plus dipole character, generally in the form of a proton. The plus dipole character of many of the classes is obvious. For example phenols, cyanides, aromatic nitro compounds, chlorinated aliphatic compounds, alcohols substituted with electron attracting groups, and aromatic rings substituted with electron attracting groups are known to have some proton donating character. Others such as conjugated ketones and aldehydes, pyridine rings, amides, and phenylamines are amphoteric and their plus dipole character is apparent when the resonance forms are considered. For example, the resonance forms of phenylamine can be shown to have a plus dipole character:

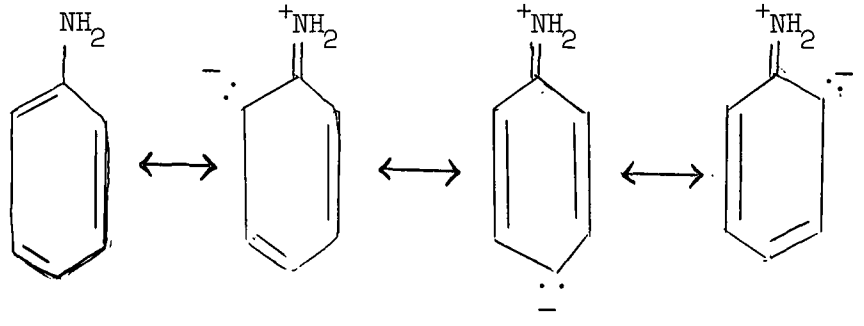

All of the nonsolvents (I) could be placed in classes which were either inert compounds such as hydrocarbons or compounds whose primary behavior was that of an electron donor such as ethers, esters, alcohols, aliphatic amines, or non-conjugated ketones. In any case not one of the nonsolvents exhibited appreciable proton donating character. No attempt was made to classify the partial solvents (AS and P).

Table XXV lists compounds with a relatively high degree of solvent power, Table XXVI nonsolvents, and Table XXVII partial solvents.

TABLE XXV

COMPOUNDS WITH A RELATIVELY HIGH DEGREE OF SOLVENT POWER (S, S-AS', AND AS')

Phenols

p-chlorophenol (S)
m-cresol (S-AS')
2-methoxy-4-methylphenol (S-AS')
o-chlorophenol (S-AS')
3-trifluoromethylphenol (S-AS')
eugenol (AS')
o-bromphenol (AS')

Alcohols Substituted with Electron Attracting Groups

furfuryl alcohol (S)
2-phenoxylethanol (S)
benzyl alcohol (AS')

Conjugated Aldehydes & Ketones

furfural (S)
benzaldehyde (S-AS')
acetophenone (S-AS')
anisaldehyde (AS')
acetylacetone (AS')
cyclohexanone (AS')
carvone (AS')

Amides

formamide (S-AS')

Unsymmetrical Substituted Double Bond Compounds

amylene (AS')
limonene (AS')

Pyridine Rings

pyridine (S-AS')
α-picoline (S-AS')
β-picoline (S-AS')
γ-picoline (S-AS')
2-amino-3-methyl pyridine (AS')

Cyanides

benzyl cyanide (S-AS')
benzonitrile (AS')

Aromatic Nitro Compounds

nitrobenzene (AS')

Chlorinated Aliphatic Compounds

1,2,3-trichloropropane (S)
1,3-dichloro-2-propanol (S)
1,1,2,2-tetrachloroethane (S-AS')
1,1,2-trichloroethane (S-AS')
chloroform (AS')
1,2-dichloroethane (AS')
2-chloroethanol (AS')
dichloroethylether (AS')

Esters & Ethers Substituted on Aromatic Ring

phenyl acetate (S-AS')
ethyl benzenesulfonate (AS')
ethyl benzoate (AS')
methyl benzoate (AS')
phenetole (AS')

Phenyl Amines

2-amino picoline (S)
phenyl hydrazine (S)
aniline (S-AS')
m-toluidine (S-AS')

Sulfoxides

dimethyl sulfoxide (S-AS')

Compounds Not Readily Explainable

Amines: ethanolamine (S); morpholine (S); benzylamine (S-AS'); cyclohexylamine (S-AS')

Benzene Derivatives: benzene (S-AS'); toluene (S-AS'); xylene (S-AS')

TABLE XXVI

NONSOLVENTS (I)

Esters

triethyl citrate
dibutyl phthalate
butyl acetate
diethyl carbonate
n-propyl acetate
n-butyl d-tartrate
n-butyl oxalate
ethyl propionate
octyl acetate
ethyl butyrate

Ethers

benzyl ether
iso-amyl ether
n-hexyl ether
phenyl ether
1,1,3,3-tetraethoxypropane
diethylether
petroleum ether

Nonconjugated Aldehydes and Ketones

formaldehyde
di-isopropyl ketone
diethyl ketone
methyl n-amyl ketone

Acetals

diethyl acetal
dimethyl acetal

Mono-Halides

ethyl bromide
butyl bromide
α-bromonaphthalene

Alcohols

isopropyl alcohol
terpineol
diethyl carbinol
iso-amyl alcohol
butanol
methyl cellosolve
ethylene glycol
allyl alcohol
1,3-propane diol
ethyl alcohol
methyl alcohol
octanol
glycerine
water[a]

Aliphatic Amines

diethyl amine
diethyl aniline
di-n-propylamine

Aliphatic Hydrocarbons

n-decane
n-heptane
diphenylmethane

Aromatic Hydrocarbons

1,2,3,4-tetra hydronaphthalene
1-chloronaphthalene
o-dichlorobenzene
m-dichlorobenzene

Sulfides

carbon disulfide

Isocyanates

phenyl isothiocyanate

[a]Although water is not an alcohol it is included in this class.

TABLE XXVII

PARTIAL SOLVENTS (AS AND P)

AS

diethyl oxalate	ethyl lactate	N,N-dimethyl formamide
acetic acid	dichloromethane	chloracetonitrile
ethylene dichloride	nitromethane	ethyl iodide
anisole	dioxane	ethyl malonate
chlorobenzene	acetonyl acetone	propiophenone
phenyl ethyl alcohol	diacetone alcohol	trimethylene
mesitylene	ethylene dichloride	epichlorohydrin

P

trifluoroethanol	acetonitrile	tetrahydrofuran
chlorobenzene	acetic anhydride	acetone
ethyl acetate	nitroethane	carbon tetrachloride
cyclohexane	hydroxymethyl-furfural	methyl salicylate
3-bromo-1-propanol	ethylene diamine	vinyl acetate
n-butylamine	methyl acetate	triethylphosphate
cyclohexanol	methyl-iodide	quinoline
acrylonitrile	methyl-ethyl ketone	ethylidene chloride
methyl isopropyl ketone	cinnamaldehyde	propionaldehyde
acetal safrole	frenchone	methyl propyl ketone
dihydro pyran	tripropionin	trimethylene chlorohydrin
cyclohexene	dicyclohexylamine	diethanolamine
o-nitrotoluene	benzyl chloride	cineole
ammonium hydroxide (28-30%)	2,2,3,3-tetrafluropropanol	1,3-difluoro-2-propanol
	1,1,1-trifluoro-2-propanol	

DISCUSSION

The data indicate that the factor of primary importance in dissolving the glucomannan triacetate (Fraction 8-A) is the solvation of the polymer in which an oxygen atom such as that of the ester carbonyl group forms a hydrogen bond with a proton donated by the solvent. In further support of this hypothesis examples are given in Table XXVIII of pairs of compounds which differ only in their capacity to donate a proton and in all instances the better proton donor is the better solvent.

TABLE XXVIII

EVIDENCE FOR PROTON DONOR THEORY OF SOLVATION

Better Solvent and Better Proton Donor	Poorer Solvent	Reason Why Poorer Solvent is Poorer Proton Donor
(1) $CH\text{-}Cl_3$ (AS')	$C\text{-}Cl_4$ (P)	No H available
(2) $Cl\text{-}CH_2\text{-}CH_2\text{-}OH$ (AS')	CH_3CH_2OH (I)	Desirable inductive effect of Cl group is absent
(3) 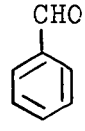 (S-AS')	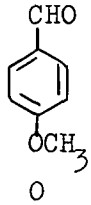 (AS')	The OCH group has an undesirable inductive effect on the carbonyl resonance with the ring
(4) $CH_3\text{-}C(=O)\text{-}CH_2\text{-}C(=O)\text{-}CH_3$ (AS')	$CH_3\text{-}C(=O)\text{-}CH_3$ (P)	Conjugation to the enol form is not possible as with the β-diketone
(5) 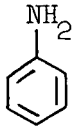 (S-AS')	$CH_3\text{-}CH_2\text{-}CH_2\text{-}CH_2\text{-}NH_2$ (P)	The aliphatic amine cannot exist in a resonance form like aromatic amine
(6) 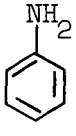 (S-AS')	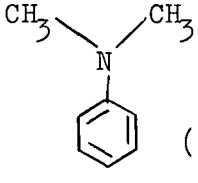 (I)	No H available on the nitrogen group
(7) $Cl\text{-}CH_2\text{-}CH_2\text{-}O\text{-}CH_2\text{-}CH_2Cl$ (S-AS')	$CH_3\text{-}CH_2\text{-}O\text{-}CH_2\text{-}CH_3$ (I)	Desirable inductive effect of Cl groups is absent

APPENDIX VIII

FRACTIONATION OF THE GLUCOMANNAN TRIACETATE

PRELIMINARY INVESTIGATION OF SOLVENTS AND PRECIPITANTS

A preliminary investigation of nine promising solvents and six precipitants for the glucomannan triacetate fraction 8-A was carried out in order to determine which solvent and precipitant combination would be desirable for fractionation. A portion of the acetylated glucomannan was insoluble in all solvents investigated. The amount insoluble varied from 13 to 30% and the ash content of the insoluble material was about 2%. A measure of the relative size of the molecules going into solution was obtained from intrinsic viscosity* determinations of the soluble material which varied from 34 to 48 ml./g. in the various solvents. The effectiveness of various precipitants was investigated by determining (1) the initial turbidity point (122, 126), and (2) the amount of soluble polymer recovered by addition of a given volume of precipitant. The solvent finally chosen for the large-scale fractionation was pyridine and the precipitant was ligroin (65 to 90°C.).

THEORY

There is a large volume of literature on the theoretical and practical aspects of polymer fractionation (19, 127-145) and in particular much experimental work has been done on cellulose acetate (19, 146-150). It was concluded from these references that fractional precipitation will be employed since for any new polymer, this technique requires a minimum of trial and error to achieve satisfactory fractionation.

*Intrinsic viscosity reported in ml./g. rather than the customary 100 ml./g.

Fractional precipitation consists of the slow addition of a precipitant to a polymer solution until turbidity occurs, at which point the precipitated polymer is removed. Fractionation according to molecular weight results from the separation of the solution into a polymer-rich precipitated phase and a supernatant phase (31, 125, 128, 131, 143). Every polymer species is more soluble in the precipitated phase but the higher the molecular weight of the polymer the greater is the solubility in this phase. This is because the lower molecular weight species have fewer units per molecule to interact with the less favorable environment of the supernatant phase and consequently are distributed at more nearly equal concentrations in the two phases. It is desirable that the polymer precipitate in an amorphous form. If crystallization or aggregation occurs, fractionation according to molecular weight will be hindered (121, 125, 128). This is due to the slower rate of crystallization of the higher molecular weight species.

FRACTIONATION PROCEDURE AND RESULTS

The only complete fractionation of a glucomannan acetate in the literature was accomplished by the addition of methanol to a 9:1 tetrachloroethane:ethanol solution (22). A successful trial fractionation was carried out from tetrachloroethane by the addition of ethanol in this investigation, but the high density of tetrachloroethane made it difficult to collect the first few fractions quantitatively by centrifugation. This difficulty was not encountered with the solvent pyridine and the precipitant ligroin (65-90°C.). A fairly dilute solution is necessary in order to get efficient fractionation. However, for a low molecular weight polymer, satisfactory fractionation can be achieved at a higher initial concentration than for a higher molecular weight polymer (128). Twelve grams of the acetylated glucomannan Fraction 8-A were fractionated

from a pyridine solution at an initial concentration of 0.5 g./100 ml., which should be satisfactory for the relatively low molecular weight glucomannan. In order to keep the insoluble material to a minimum, the solution was stirred and shaken vigorously for two days and heated to 49°C. prior to fractionation.

For the first three fractions collected, the solution was warmed after the turbid point was reached and allowed to cool slowly overnight with stirring before collecting the precipitate. This was done in order to insure equilibrium between the supernatant solution and the precipitate when it forms. However, on standing for any length of time, the turbid solution formed agglomerates. Therefore, in order to avoid the undesirable effect of aggregation, the precipitate was collected immediately after the addition of ligroin for the ensuing fractions. Fractions 5 and 6 were collected by evaporating the preceding supernatant to 570 and 100 ml., respectively, before the addition of ligroin. Fraction 7 is the residue remaining after evaporation of the supernatant.

More homogeneous fractions are obtained if the initial fractions are combined and reprecipitated (125, 129, 131, 132, 147, 150). Refractionation is more important for the higher molecular weight fractions which are more heterogeneous than the last fractions precipitated. The first two fractions (1a and 1b) were combined and refractionated into three fractions [I(1), I(2), and I(3)]. The next two fractions (2a and 2b) were combined and refractionated into two fractions [2(1) and 2(2)]. Fraction 3 was refractionated into two fractions [3(1) and 3(2)]. The original insoluble material was extracted again with pyridine and two more fractions collected [Insol. (1) and Insol. (2)] plus the amount that remained insoluble (Insol'.). All refractionations were carried out from a pyridine solution at approximately 0.5 g./100 ml. initial concentration. The precipitates were isolated by freeze drying from a pyridine water solution at

approximately a 1:3 ratio. This gave a light, fluffy product. Fraction 8-A was recovered in a yield of 91.56%. The results of the fractionation of 8-A are reported in Table XXIX.

Fraction 9-A is chemically identical to Fraction 8-A and is an acetylated glucomannan of lower molecular weight. Three grams of Fraction 9-A were also fractionated under the conditions used for 8-A. Fraction 9-A was recovered in a yield of 98.37%. These results are reported in Table XXX. The fractionation of the acetylated glucomannans is summarized in Fig. 12.

The color that was formed during the acetylation appears to be associated preferentially with the lower molecular weight fractions. In order to determine if any degradation had taken place in the pyridine solution during fractionation, infrared spectra were run for the original Fraction 8-A and Fractions 2(1) and 3(2). The proper concentration of each KBr pellet was adjusted by trial and error. Then, in an attempt to get rid of as much water as possible, the pellet was reground and dried overnight under vacuum at 110°C. The pellet was then remolded and the infrared spectrum obtained. The spectra were identical in every aspect and thus it appears that no degradation and in particular no deacetylation occurred in the pyridine solution.

TABLE XXIX

FRACTIONATION OF 8-A

First Fraction	Volume of Ligroin Added, ml.	Volume of Precipitate, ml.	Volume of Supernatant, ml.	Refractionated Fraction	Amount, g.	Per Cent Recovered	Color
Insol.	0	82	2,295[a]	Insol'.	2.6941	22.459	light with brown tint
				Insol. (1)	0.1013	0.844	white
				Insol. (2)	0.2351	1.959	light with brown tint
Ia	500	8.8	3,390	I (1)	0.0267	0.310[d]	white
				I (2)	0.2171	2.524[d]	light with brown tint
Ib	150	3.1	3,560	I (3)	0.1355	1.575[d]	light with brown tint
2a	150	2.6	3,670	2 (1)	1.4368	11.973	light brown
2b	150	4.6	3,750	2 (2)	0.3216	2.680	light with brown tint
3	1,500	> 3	5,160	3 (1)	2.2539	18.782	light brown
				3 (2)	2.7616	23.013	light brown
4	3,000	--[c]	7,110[e] → 570	4[b]	0.2686	2.239	light brown – brown
5	2,600	--[c]	3,160[e] → 100	5[b]	0.0467	0.389	brown
6	900	--[c]	1,000[e] → 0	6[b]	0.0373	0.310	brown
7	0	--[c]	0[f]	7[b]	0.2998	2.498	dark brown
					Total	91.559	

[a] Original solution = 2,400 ml.
[b] Not refractionated.
[c] Too small to measure.
[d] Takes into account an amount of material which was lost during fractionation.
[e] Concentrated by evaporation.
[f] Recovered by evaporation.

TABLE XXX

FRACTIONATION OF 9-A

Fraction	Volume of Ligroin Added, ml.	Volume of Precipitate, ml.	Volume of Supernatant, ml.	Amount, g.	Per Cent Recovered	Color
9-Insol.	0	8.3	585[a]	0.1687	5.623	white
9-1	270	4.0	800	0.7359	24.530	light brown
9-2	200	3.1	980	1.7861	59.536	light brown
9-3	800	--[b]	1,775[c] → 4	0.2432	8.106	light with brown tint
9-4	500	--[b]	500	0.172	0.573	brown
				Total	98.370	

[a]Original solution = 600 ml.

[b]Too small to measure.

[c]Evaporated to 4 ml.

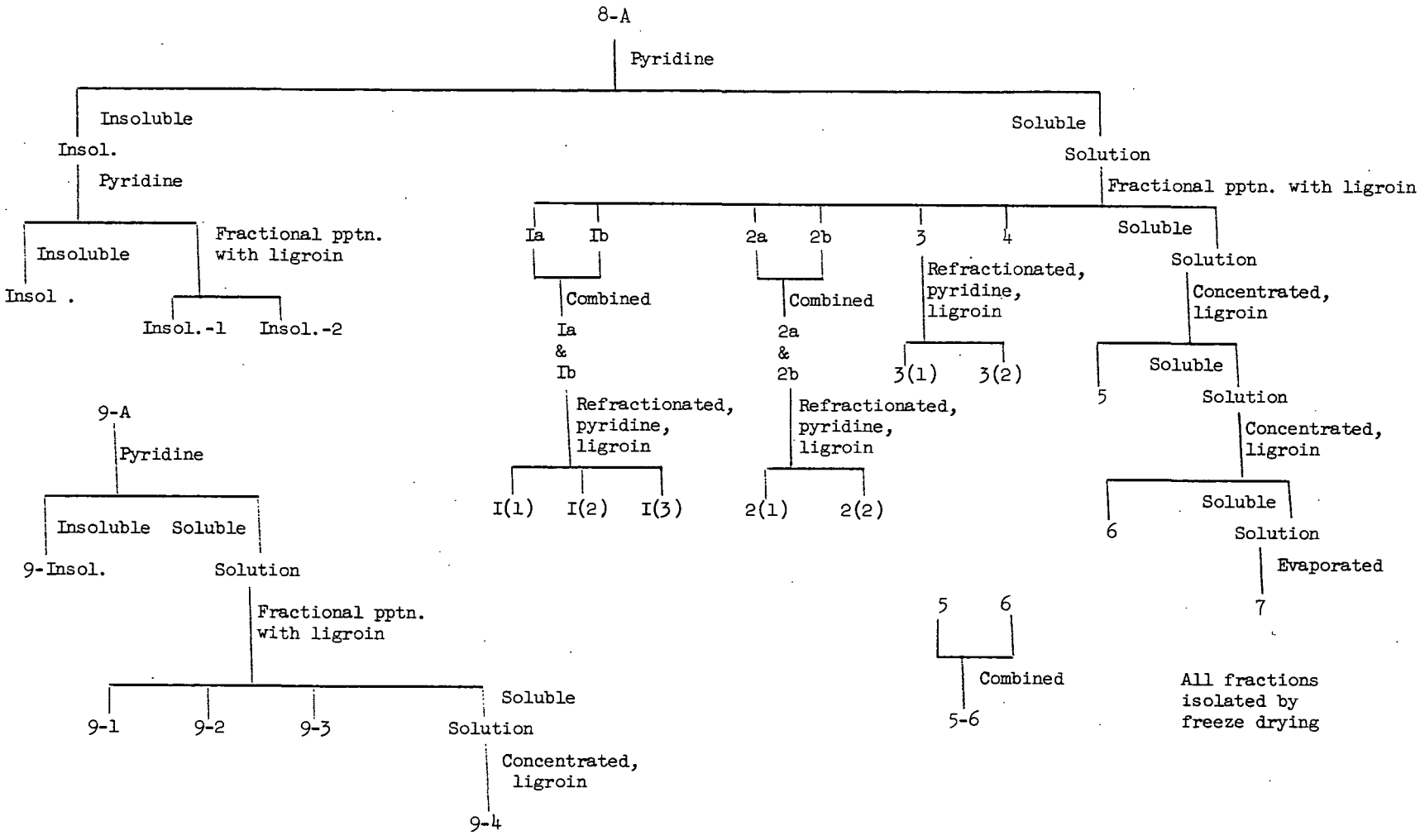

Figure 12. Fractional Precipitation of the Acetylated Glucomannan Fractions 8-A and 9-A

APPENDIX IX

QUALITATIVE SUGAR ANALYSIS OF THE ACETYLATED GLUCOMANNAN FRACTIONS OBTAINED BY FRACTIONAL PRECIPITATION

PROCEDURE AND RESULTS

Qualitative sugar analyses were carried out on the 13 fractions and the 5 fractions obtained from fractional precipitation of the acetylated glucomannan Fractions 8-A and 9-A, respectively. Thirty-milligram samples were dissolved in one milliliter of 72% sulfuric acid, diluted with fifteen milliliters of water, autoclaved at 120°C. for one hour, neutralized with barium carbonate, filtered, and evaporated to dryness. Four drops of water were added to dissolve the sugars and the samples were spotted on Whatman Number I chromatography paper. The papers were irrigated with 8:2:1 (ethyl acetate:pyridine:water) for twenty-four hours and developed with silver nitrate reagent.

The results are presented in Tables XXXI and XXXII. The qualitative sugars are presented in the order of decreasing amount as judged by the size and density of the spot. As a measure of the quantitative amount, the ratio of the spot areas are presented. Although these ratios are not directly proportional to the amounts, they should remain constant within about 20% for a given sugar content. It should be noted that, although the amount of xylose is less than the amount of galactose for most fractions, the spot area of xylose is consistently larger because it is less dense due to the greater distance traveled on the chromatogram. These spot area ratios are presented in order to illustrate when a given series of fractions are constant in their sugar ratios and to illustrate trends in the comparison of various fractions. The spot areas were determined with a planimeter.

TABLE XXXI

QUALITATIVE SUGAR ANALYSIS – FRACTIONS FROM 8-A

Fraction		Insol'.	Insol. -1	Insol. -2	I(1)	I(2)	I(3)	2(1)	2(2)	3(1)	3(2)	4	5-6	7
Qualitative sugar analysis		M. >[a] Gl. > Gal. > X.	M. > Gl. > Gal. > X.	M. > Gl. > Gal. > X.	M. > Gl. > Gal. > X.	M. > Gl. > Gal. > X.	M. > Gl. > Gal. > X.	M. > Gl. > Gal. > X.	M. > Gl. > Gal. > X.	M. > Gl. > Gal. > X.	M. > Gl. > Gal. > X.	M. > Gl. > Gal. > X.	M. > Gl. > Gal. > X.	No Spots
Spot area ratios	M:	3	3	3	3	3	3	3	3	3	3	3	3	--
	Gl:	1.7	1.8	1.6	2.0	1.6	1.6	1.8	1.8	1.7	1.7	1.8	2.0	--
	Gal:	0.9	0.9	1.1	1.0	1.0	1.0	1.1	1.1	0.9	1.1	1.1	1.5	--
	X:	1.2	P[b]	P[b]	1.2	1.3	1.1	1.3	1.1	1.0	1.2	1.8	P[b]	--
	A.	0	0	0	0	0	0	0	0	0	0	0	0	--
Spot area ratios	X: Gal.	1.3	--	--(1)	1.2	1.3	1.1	1.2	1.0	1.1	1.1	1.6	--	--

[a] M. = mannose, Gl. = glucose, Gal. = galactose, X. = xylose, A. = arabinose, > = greater than.

[b] P. = present.

(1) Columns in table are read vertically.

TABLE XXXII

QUALITATIVE SUGAR ANALYSIS — FRACTIONS FROM 9-A

Fraction		9-Insol.	9-1	9-2	9-3	9-4
Qualitative sugar analysis		M. >[a] Gl. > Gal. > X.	M. > Gl. > Gal. > X.	M. > Gl. > Gal. > X.	M. > Gl. > Gal. > X.	M. > Gl. > Gal.
Spot area ratios	M:	3	3	3	3	3
	Gl:	2.1	1.8	1.9	1.9	2.3
	Gal:	1.1	1.2	0.9	1.3	1.3
	X:	1.5	1.2	1.0	1.2	--
	A:	0	0	0	0	--
Spot area ratios	X: Gal.	1.3	1.0	1.2	1.0	--

[a]M. = mannose, Gl. = glucose, Gal. = galactose, X. = xylose, A. = arabinose, > greater than.
Columns in table are read vertically.

DISCUSSION

The fractions obtained from fractional precipitation of 8-A and 9-A are quite constant in their sugar ratios. No particular trend occurs in the sugar ratios except for a slight increase in the galactose content in the very low molecular weight range (Fractions 5-6, 9-3, and 9-4). The glucose content is also slightly higher for Fractions 5-6 and 9-4. With the exception of Fractions 9-Insol. and 4, the xylose content remains fairly constant. This implies either that the xylose is associated with the glucomannan molecule or that the fractional precipitation was a remarkably good one with respect to molecular size since the chemical nature of the xylose groups of a possible xylan contaminant had little apparent effect on the fractionation. Hydrolysis of Fraction 7 showed that no sugars were present in this fraction. It appears that this dark brown fraction is entirely composed of the colored impurity which was formed during acetylation.

During hydrolysis, it was noticed that all fractions contained a small amount of material insoluble in 72% sulfuric acid. This material had the appearance of Klason lignin and undoubtedly would show up in a Klason lignin analysis. This observation is in agreement with the previous result that the unacetylated Fractions 8 and 9 had a very small band in the infrared spectra which could only be attributed to lignin or an aromatic ring.

QUALITATIVE DETECTION OF URONIC ACIDS

The Fractions Insol'., 2(1), and 3(2) obtained from fractional precipitation of the acetylated glucomannan Fraction 8-A were analyzed qualitatively for the presence of glucuronic or galacturonic acid and 4-O-methylglucuronic acid. According to a procedure developed by Lambert (151), the qualitative hydrolyzates were spotted in the center of a double length sheet of chromatography paper. The sheet was then irrigated with 8:2:1 (ethyl acetate:pyridine:water) for 20 hours to separate the neutral sugars from the uronic acids. The half of the sheet containing the neutral sugars was then removed and irrigated with 9:2:2 (ethyl acetate: acetic acid:water). The uronic acids migrated from the initial line and were qualitatively analyzed by developing the sheet with silver nitrate reagent. Glucuronic acid, galacturonic acid, and 4-O-methylglucuronic acid were not detected in the fractions analyzed.

APPENDIX X

RESULTS OF THE ACETYLATION AND PURIFICATION OF VARIOUS GLUCOMANNANS AND GALACTOGLUCOMANNANS

The various glucomannans and galactoglucomannans isolated from the different extractions were acetylated by the procedure described in Appendix VI, p. 114. The yields and acetyl contents are presented in Table XXXIII. The acetate derivatives are designated by -A.

TABLE XXXIII

ACETYLATION OF VARIOUS GLUCOMANNANS AND GALACTOGLUCOMANNANS

Fraction	Yield of Acetate[a], g.	% of Theoretical Yield[a,b]	Ash, %	Acetyl, %[c]	DS[d]
6-7-A[e]	1.00	8.9[f]	2.78	42.80	2.79
13-A	2.20	62.0	2.85	43.97	2.93
14-A	2.30	62.0	11.76	42.85	2.79
16-A	1.00	40.1	59.39	39.15	2.40
17-A	2.80	63.0	20.95	44.11	2.93

[a] Ash content not taken into account.
[b] Based on the triacetate.
[c] Ash content taken into account.
[d] Degree of substitution.
[e] Acetylated a mixture of 5.5 g. of Fraction 7 and 0.8 g. of Fraction 6.
[f] Low yield due to purification procedure carried out.

PURIFICATION OF GALACTOGLUCOMANNAN ACETATE

The unacetylated Fractions 6 and 7 were possible galactoglucomannan fractions with considerable xylan impurities. An attempt was made to remove the xylan impurity by a method developed by Hamilton, Partlow, and Thompson (152) in which the galactoglucomannan acetate is extracted with acetone and the xylan acetate remains insoluble. Fractions 6 and 7 were combined, acetylated, extracted two

hours with 114 milliliters of acetone, the insoluble material removed by centrifugation and filtration, the supernatant concentrated to 15 milliliters and precipitated into 200 milliliters of diethyl ether, and the precipitate freeze dried from a water slurry. The yield of the purified and acetylated Fraction 6-7 is presented in Table XXXIII.

PURIFICATION OF THE VARIOUS ACETYLATED GLUCOMANNANS AND GALACTOGLUCOMANNANS

A portion of every acetylated glucomannan and galactoglucomannan fraction was insoluble in all the solvents investigated. Since physical measurements are to be made on these acetylated fractions, it was necessary to subject them to further purification in order to remove the insoluble material and the inorganic material that was present. The fractions in Table XXXIII and the main Fractions 8-A and 9-A were purified. A 2% solution of each fraction was made in pyridine and shaken from one to three days. The insoluble material was removed by centrifugation and the supernatant solution was filtered. Precipitation of the soluble material from the supernatant solution was attempted by addition of 95% ethanol. However, a large excess of 95% ethanol added to the supernatant of 8-A and 13-A resulted in the formation of only a very small amount of precipitate. Therefore, the ethanol was removed by evaporation and ligroin was employed as the precipitant. A volume of ligroin corresponding to five times the volume of pyridine was added to each supernatant solution. The precipitate was collected by centrifugation and designated as the soluble portion. All fractions were freeze dried from a pyridine-water solution and then dried overnight at 50°C. under vacuum.

The ash contents were determined on the soluble fractions by ashing for three hours at 575-600°C. All results are reported in Table XXXIV. In every instance the insoluble portion had a darker color than the soluble portion for a given

fraction and the ash contents have been reduced considerably for the soluble fractions. The soluble and insoluble acetylated fractions are designated by -S and -I, respectively.

TABLE XXXIV

PURIFICATION OF VARIOUS ACETYLATED GLUCOMANNANS AND GALACTOGLUCOMANNANS

Original Fraction	Previous Ash Content, %	Weight Purified, g.[a]	Volume of Pyridine, ml.	Volume of Ligroin Added,[b] ml.	Soluble & Insoluble Fractions[c]	Yield-Weight, g.[a]	Yield, %	Ash Content, %	Color
8-A	2.28	3.000	150	750	8-S	1.1879	39.60	0.14	light with brown tint
					8-I	1.1449	38.16	--	light brown - brown
9-A	2.53	1.400	100	500	9-S	0.9556	68.26	0	light with brown tint
					9-I	0.3590	25.64	--	light with brown tint
6-7-A	2.78	0.700	35	165	6-7-S	0.6253	89.33	0.42	light brown
					6-7-I	0	0	--	--
13-A	2.85	1.800	90	450	13-S	0.7248	40.27	0.20	light with brown tint
					13-I	0.9137	50.76	--	light brown
14-A	11.76	1.900	95	475	14-S	0.3943	20.75	0.65	light brown
					14-I	1.4008	73.73	--	light brown - brown
16-A	59.39	0.600	30	150	16-S	0.0601	16.67	1.4[d]	light with brown tint
					16-I	0.5180	86.33	--	light brown
17-A	20.95	2.000	100	500	17-S	0.8336	41.68	0.69	light with brown tint
					17-I	0.9060	45.30	--	light with brown tint

[a] Ovendry weight. [b] Five times the volume of pyridine.
[c] S = soluble and I = insoluble.
[d] Due to the very small amount of sample used in this determination, the error is greater than for the other samples.

APPENDIX XI

QUALITATIVE SUGAR CONTENTS OF THE VARIOUS ACETYLATED GLUCOMANNAN AND GALACTOGLUCOMANNAN FRACTIONS

The results of the qualitative sugar analyses and spot area ratio determinations (determination described in Appendix IX, p. 132) for the various acetylated glucomannan and galactoglucomannan fractions are presented in Table XXXV. Comparison of the qualitative chromatograms of the acetylated fractions, 8-A, 9-A, 6-7-A, 13-A, 14-A, 16-A, and 17-A, with their unacetylated counterparts showed that no significant change in their sugar ratios is caused by acetylation. Fractions deriving from 6-7-A, 14-A, and 16-A are galactose-rich glucomannans while fractions deriving from 8-A, 9-A, 13-A, and 17-A are more typical glucomannans with a lower galactose content. In most instances the sugar ratios of the soluble and the corresponding insoluble fractions are fairly constant. The galactose contents of the insoluble Fractions 13-1 and 17-1 are slightly higher than the soluble Fractions 13-S and 17-S, respectively. Again, xylose is found in every fraction. The xylose-to-galactose ratios are presented to see if there is a possible relationship between the xylose and galactose content. In most cases this ratio is in the range of 1.0 to 1.4 except where the fraction appears to be contaminated with a considerable amount of xylan.

Glucuronic acid, galacturonic acid, and 4-O-methylglucuronic acid were not detected (by the qualitative method of analysis described in Appendix IX, p. 132)in Fractions 8-A, 9-A, 6-7-A, 13-A, 14-A, 14-S, 14-I, 16-A, and 17-A.

TABLE XXXV

QUALITATIVE SUGAR CONTENTS OF THE VARIOUS ACETYLATED FRACTIONS

Fraction		8-A	8-S	8-I	9-A	9-S	9-I	6-7-A	6-7-S	13-A	13-S	13-I	14-A	14-S	14-I	16-A	16-I	17-A	17-S	17-I
Qualitative sugar analysis		M.>[a] Gl.> Gal.> X.	M.> Gl.> Gal.> X.	M.> Gl.> Gal.> X.	M.> Gl.> Gal.> X.	M.> Gl.> Gal.> X.	M.> Gl.> Gal.> X.	X.> M.~ Gal.> Gl.> A.	X.> M.~ Gal.> Gl.> A.	M.> Gl.> Gal.> X.	M.> Gl.> Gal.> X.	M.> Gl.> Gal.> X.	M.> Gl.> Gal.> X.> A.(T)	M.> Gl.> Gal.> X.> A.(T)	M.> Gl.> Gal.> X.> A.(T)	M.> Gl.~ Gal.> X.> A.(T)	M.> Gl.~ Gal.> X.> A.(T)	M.> Gl.> Gal.> X.	M.> Gl.> Gal.> X.	M.> Gl.> Gal.> X.> A.(T)
Spot area ratios	M:		3	3		3	3		3		3	3		3	3		3		3	3
	Gl:	[b]	1.9	2.0	[b]	1.8	1.7	[b]	1.9	[b]	1.8	1.8	[b]	1.8	1.8	[b]	2.2	[b]	1.9	2.2
	Gal:		1.1	1.1		1.1	1.0		2.1		0.9	1.3		1.4	1.4		2.0		1.3	1.5
	X:		P[c]	1.2		1.0	1.1		4.0		P[e]	1.3		2.0	2.0		2.0		1.0	1.7
	A:		0	0		0	0		1.7		0	0		T[d]	T		T		0	T
			--	1.1		1.0	1.1		2.0		[e]	1.0		1.5	1.4		1.0		0.8	1.2

[a] M. = mannose, Gl. = glucose, Gal. = galactose, X. = xylose, A. = arabinose, > = greater than, ~ = similar to, (T) = trace.

[b] Qualitatively similar to its soluble and insoluble counterpart.

[c] P = present.

[d] T = trace.

[e] Less xylose than 13-I and less xylose than 9-S.

Columns in tables are read vertically.

APPENDIX XII

INFRARED SPECTRA

The infrared spectra were run for the unacetylated Fractions 7, 8, 9, 13, 14, 16, and 17 and for the acetylated Fractions 6-7-A, 8-A, and 9-A*. The spectra were then analyzed with the goal of relating them to the structure of the polysaccharides in the fractions in order to determine the similarities and differences between the fractions. The spectra and the possible assignments of the bands are given in detail for Fraction 8 before acetylation and after acetylation (Fraction 8-A). All other spectra are compared to these spectra. Many sources (153-161) were used to interpret the spectra. The results are as follows, where vs = very strong, s = strong, m = medium, w = weak, and vw = very weak

FRACTION 8

Band, $cm.^{-1}$	Intensity	Possible Assignments
3950	w	O-H
3430	vs	O-H, H_2O
2890	s	C-H, $C^{-}H_2$
2330	vw	--
2070	vw	--
1725	m	C=O (of normal aldehyde or ketone, of xylan uronic acid, or carboxyl group)
1615	m-s	H_2O, COO^{-} (salt)
1515	w-m	lignin, phenyl C=C (of aromatic)
1410	(s) (broad area)	-OH (cellulose has this)
1380	(s) (broad area)	C-H (ivory nut mannan has this), -OH
1308	m-s (broad area)	CH_2
1240	m-s (broad area)	O-H of mannan, xylan (C-H, O-H, or C-O)
1143	m-s (broad area)	C-O, C-OH, C-O-C
1095-1010	vs (broad band)	C-O, C-C
935	m-s	β-1,4 mannan
890	m	β-1,4 mannan, characteristic of β-link, xylan
868	s	β-1,4 mannan ring stretching or C_1, configuration characteristic of glucomannan
807	s	β-1,4 mannan ring stretching, characteristic of glucomannan

*The spectra have been filed in the Analytical Department of The Institute of Paper Chemistry.

FRACTION 8 (Continued)

Band, cm.$^{-1}$	Intensity	Possible Assignments
775	m (shoulder to 807)	glucan β-linkage
753	w	glucose or galactose, α-1,4 linked ring breathing, methyl mannose has this
663	vw	cellulose has this

Discussion: (1) Fraction 8 has a considerable H_2O or COO^- band at 1615 cm.$^{-1}$. This is a little below the usual absorbed H_2O band at 1630 cm.$^{-1}$ to 1640 cm.$^{-1}$ and it is a little above the usual OOO^{-1} band at 1613 cm.$^{-1}$ to 1563 cm.$^{-1}$. It is probably due to a combination of these two bands. The COO^- band probably arises from the ash which might be $Ba(OAc)_2$. (2) The occurrence of a C=O band at 1725 cm.$^{-1}$ indicates the presence of a xylan, some oxidation to C=O or COOH, or the presence of HOAc or possibly acetyl groups. Unoxidized cellulose or ivory nut mannan do not have this band but it could be due to carboxyl groups introduced by oxidation with chlorite. (3) It appears that there may be a small amount of lignin present (1515 cm.$^{-1}$). (4) The characteristic bands for a β-1,4 linked mannan and glucomannan are present and distinct (935 cm.$^{-1}$, 890 cm.$^{-1}$, and 807 cm.$^{-1}$). (5) The spectrum of 8 is identical to a deacetylated glucomannan isolated from Paraña pine (18).

FRACTION 8-A

Band, cm.$^{-1}$	Intensity	Possible Assignments
3950	vw	O-H
3430	m	O-H, H_2O
2950	m	$C-H_3$, $^2C-H_2$, C-H
2130	vw	--
1750	vs	C=O (acetyl)
1635	w	H_2O
1507	w	lignin
1438	m	CH_3 (acetyl)
1373	s	CH_3 (acetyl)
1318	w	$C-H_2$, O-H
1230	vs	$\overset{O}{\overset{\|\|}{C}}-OR$ (acetyl)

FRACTION 8-A (Continued)

Band, cm.$^{-1}$	Intensity	Possible Assignments
1173	w-m	C-O, C-OH, C-O-C
1107	w	--
1067	s (broad area)	C-O, C-C
1038	s (broad area)	C-O, C-C
990	w	C-O
955	m	β-mannose acetate has this
900	m	mannose acetate has this, β-linkage xylan, acetate group
867	vw	β-mannose acetate has this
833	vw	α-mannose derivatives have this
775	m	β-glucans have this

Discussion: (1) The band at 2950 cm.$^{-1}$ in 8-A is probably due to CH_3 in contrast to the C-H band at 2890 cm.$^{-1}$ in 8. (2) The H_2O or COO^- band at 1615 cm.$^{-1}$ for 8 has been considerably reduced and shifted to 1635 cm.$^{-1}$ (H_2O) on acetylation. (3) The characteristic β-1,4 mannan bands at 935 cm.$^{-1}$, 868 cm.$^{-1}$, and 807 cm.$^{-1}$ for 8 are missing or greatly diminished after acetylation. (4) A distinct band at 775 cm.$^{-1}$ is present and is possibly characteristic of a β-linkage.

FRACTION 9 – COMPARED TO FRACTION 8

The spectrum is identical to the spectrum of 8.

FRACTION 9-A – COMPARED TO FRACTION 8-A

The spectrum is identical to the spectrum of 8-A.

FRACTION 7 – COMPARED TO FRACTION 8

(1) Has C=O (of normal aldehyde or ketone, of xylan uronic acid or carboxyl group) at 1735 cm.$^{-1}$ and larger than 8 (1725 cm.$^{-1}$).

(2) Has COO^{-1} or H_2O band at 1607 cm.$^{-1}$ instead of 1615 cm.$^{-1}$ for 8. The position of this band indicates it is probably COO^- rather than H_2O. Also this band is quite large.

(3) The possible lignin or aromatic band at 1510 cm.$^{-1}$ is larger and more pronounced for 7 than for 8 (1515 cm.$^{-1}$).

(4) Has O-H, CH_2, or lignin band at 1465 cm.$^{-1}$ which is blocked out or absent for 8.

(5) Has band at 1410 cm.$^{-1}$ which is blocked out or absent for 8.

(6) Possible C-H band at 1380 cm.$^{-1}$ (which also occurs in ivory nut mannan) not as strong as in 8.

(7) Possible CH_2 band at 1308 cm.$^{-1}$ is absent (is present in 8).

(8) Has distinct C-H (possibly C-H for β-1,3 linkage) or lignin band at 1265 cm.$^{-1}$ which is blocked out or absent in 8.

(9) Possible mannan or xylan band at 1240 cm.$^{-1}$ is absent (a small band or plateau is present in 8).

(10) Has possible O-H band at 1205 cm.$^{-1}$ which is blocked out or absent in 8.

(11) β-1,4 mannan band at 935 cm.$^{-1}$ is absent (is present in 8).

(12) β-1,4 mannan, β-linkage, or xylan band at 893 cm.$^{-1}$ more pronounced than in 8 (890 cm.$^{-1}$).

(13) β-1,4 mannan band at 868 cm.$^{-1}$ is absent (is large in 8).

(14) β-1,4 mannan band at 807 cm.$^{-1}$ is absent (is large in 8).

(15) Possible glucose or galactose or α-1,4 linkage band is absent (is present but small in 8).

Discussion: (1) The presence of possibly some xylan and some lignin is indicated. (2) Has a notable lack of mannan peaks at 935 cm.$^{-1}$, 868 cm.$^{-1}$, and 807 cm.$^{-1}$. (3) Some COO^- is present. (4) Fraction 7 also differs from 8 in the O-H and C-H regions.

FRACTION 6-7-A – COMPARED TO FRACTION 8-A

(1) Has a small COO^- or aromatic C=C band at 1595 cm.$^{-1}$ (is absent in 8-A).

(2) Has a more pronounced lignin or aromatic band at 1515 cm.$^{-1}$ than 8-A (1507 cm.$^{-1}$).

(3) Has a band at 962 cm.$^{-1}$ which is smaller than 955 cm.$^{-1}$ (same as in β-mannose acetate) band at 8-A.

(4) Has band at 893 cm.$^{-1}$ rather than 900 cm.$^{-1}$ as in 8-A. This is possibly attributed to xylan or α-galactose tetraacetyl group.

Discussion: (1) Possibly contains some lignin.

FRACTION 13 – COMPARED TO FRACTION 8

(1) Has COO^- or H_2O band at 1615 cm.$^{-1}$ as does 8.

(2) Has lignin band at 1515 cm.$^{-1}$ as does 8.

(3) Has small possible C-H band at 1413 cm.$^{-1}$ which is more pronounced than in 8.

(4) The O-H of mannan or C-H, O-H, or $\overset{O}{\overset{\|}{C}}$-O of xylan band at 1238 cm.$^{-1}$ is more pronounced than in 8 (1240 cm.$^{-1}$).

(5) β-1,4 mannan band at 935 cm.$^{-1}$ more pronounced than in 8.

(6) Mannan bands at 890 cm.$^{-1}$, 868 cm.$^{-1}$, and 805 cm.$^{-1}$ are identical to 8.

Discussion: (1) The spectrum is similar to the spectrum of 8.

FRACTION 14 – COMPARED TO FRACTION 8

(1) The COO^- or H_2O band is at 1605 cm.$^{-1}$ rather than 1615 cm.$^{-1}$ as in 8. The band is also considerably larger than in 8. The position of this band indicates it is probably mainly COO^-.

(2) Lignin or aromatic band at 1510 cm.$^{-1}$ more pronounced than 8 (1515 cm.$^{-1}$).

(3) Possible O-H band at 1462 cm.$^{-1}$ is present (similar to 7 which is blocked out or absent in 8).

(4) Has possible C-H band at 1405 cm.$^{-1}$ which is blocked out or absent in 8.

(5) Has distinct C-H (possibly C-H for β-1,3 linkage) or lignin band at 1265 cm.$^{-1}$ (same as in 7) which is blocked out or absent in 8.

(6) Possible mannan or xylan band at 1240 cm.$^{-1}$ is absent (a small band or plateau is present in 8).

(7) Mannan bands at 935 cm.$^{-1}$, 888 cm.$^{-1}$, 869 cm.$^{-1}$, and 805 cm.$^{-1}$ are identical to 8.

Discussion: (1) Fraction 14 is similar to 8 with respect to the mannan peaks at 935 cm.$^{-1}$, 888 cm.$^{-1}$, 869 cm.$^{-1}$, and 805 cm.$^{-1}$. (2) Fraction 14 is similar to 7 in the C-H and O-H regions. (3) COO^- is present.

FRACTION 16 – COMPARED TO FRACTION 8

(1) The COO^- or H_2O band is at 1605 $cm.^{-1}$ rather than at 1615 $cm.^{-1}$ as in 8. It is probably COO^{-1}. The intensity of this band for 16 is greater than for the other fractions (approaching the intensity of the O-H band at 3420 $cm.^{-1}$).

(2) The possible lignin or aromatic band at 1510 $cm.^{-1}$ is a little smaller than for 8 (1515 $cm.^{-1}$).

(3) Has O-H or C-H band at 1440 $cm.^{-1}$ which is blocked out or absent for 8.

(4) Has distinct band at 1398 $cm.^{-1}$ which is blocked out or absent for 8.

(5) The C-H band (which ivory nut mannan has) at 1380 $cm.^{-1}$ is absent or blocked (is present for 8).

(6) Has C-H (possibly C-H for β-1,3) or lignin band at 1267 $cm.^{-1}$ (same as in 7 and 14) which is blocked out or absent for 8.

(7) Has C-O, C-OH, or C-O-C band at 1175 $cm.^{-1}$ (14 has a shoulder there) which is blocked out or absent in 8.

(8) Has bands at 1020 $cm.^{-1}$, 982 $cm.^{-1}$, and 945 $cm.^{-1}$ which are blocked out or absent in 8.

(9) β-1,4 mannan band at 935 $cm.^{-1}$ is absent (is present in 8).

(10) β-1,4 mannan, β-linkage, or xylan band at 893 $cm.^{-1}$ is much smaller than in 8 (890 $cm.^{-1}$).

(11) Mannan bands at 872 $cm.^{-1}$ and 808 $cm.^{-1}$ are much smaller than for 8 (868 $cm.^{-1}$ and 807 $cm.^{-1}$).

Discussion: (1) The β-1,4-mannan bands have been greatly diminished or are absent. (2) Fraction 16 differs considerably from 8 in the C-H, C-O, O-H, and C-O-C regions. (3) The intensity of the COO^- is very great which corresponds with the high ash content of this fraction.

FRACTION 17 – COMPARED TO FRACTION 8

(1) Has COO^- or H_2O band at 1607-1615 $cm.^{-1}$ (about the same intensity as 1615 $cm.^{-1}$ band for 8).

(2) Has C-O, C-OH, or C-O-C band at 1177 $cm.^{-1}$ which is blocked out or absent for 8 (16 has this band and 14 has a shoulder at this point).

(3) β-1,4 mannan bands at 933 cm.$^{-1}$, 890 cm.$^{-1}$, 868 cm.$^{-1}$, and 807 cm.$^{-1}$ are identical to 8.

Discussion: (1) For all practical purposes the spectrum of Fraction 17 is similar to the spectrum of 8.

CONCLUSION

Fractions 8, 9, 13, and 17 are identical. Fraction 14 has the β-1,4-mannan bands but differs from Fraction 8 in the C-H and O-H regions. Fraction 16 has considerably diminished β-1,4-mannan bands and differs from Fraction 8 in the C-H, C-O, O-H, and C-O-C regions. Fraction 7 has a notable lack of β-1,4 mannan bands and differs from Fraction 8 in the C-H and O-H regions.

A band at 3430 cm.$^{-1}$ which is attributed to water or hydroxyl absorption appeared in all the acetylated samples. This band also appeared at approximately the same intensity in a sample of KBr which had been ground and dried. Therefore, it appears that this band is due to absorbed water rather than free hydroxyl groups in the acetylated samples.

APPENDIX XIII

COMPARISON OF THE GLUCOMANNAN AND GALACTOGLUCOMANNAN FRACTIONS ISOLATED IN THIS INVESTIGATION WITH THE FRACTIONS ISOLATED BY THOMPSON (2) IN A QUANTITATIVE MATERIAL BALANCE OF BLACK SPRUCE HOLOCELLULOSE

In this investigation and the investigation by Thompson (2), black spruce holocellulose fibers were prepared by the room temperature acid chlorite process at room temperature and the extractions were identical up to and including the 18% NaOH extraction. In this study this extraction was followed by an 18% NaOH containing 4% H_3BO_3 extraction and a final water extraction while Thompson froze the holocellulose first in 18% NaOH and then in 10% NaOH. A comparison of the holocelluloses and the extracted residues is given in Table XXXVI. From the results presented in Table XXXVI, it is seen that 7.1% more of the carbohydrates of the holocellulose were extracted in this investigation than in Thompson's investigation which is probably due to the final alkaline borate extraction step. Considerably more glucose and mannose, less galactose, and slightly less xylose and arabinose were extracted in this investigation.

A comparison is made between the glucomannan and galactoglucomannan fractions from both investigations. The methods of isolation and purification of the fractions differed considerably in the two investigations. Thompson isolated a galactoglucomannan with a galactose:glucose:mannose ratio of 1:1:3 from the 0.1N NaOH extract in a yield of 0.5% of the holocellulose. It was not possible to isolate this polymer from the 0.1N NaOH extract in this study but it was probably present in Fraction 1 which contained glucose and mannose along with a large amount of galactose and xylose. Some of this polymer may have been previously extracted by the acid chlorite liquors (162) and some of it was resistant to the 0.1N NaOH extraction and was subsequently extracted with the 10% NaOH solution (Fractions 6, 7, 10, and 11). Further purification of these fractions gave a

galactoglucomannan with a galactose:glucose:mannose ratio of 0.99:1.00:1.77 (Fraction 6-7-S) which contained 29.6% xylose and 4.4% arabinose.

TABLE XXXVI

COMPARISON OF HOLOCELLULOSES AND EXTRACTED RESIDUES

	Holocelluloses		Extracted Residues	
	Thompson's Study	This Study	Thompson's Study	This Study
Yield, %[a]	72	75.1	--	--
Klason lignin, %[b]	2	2.3	--	--
Galactose, %[c]	4.0	4.22	0.44	1.81
Glucose, %[c]	66.5	69.26	64.5	57.18
Mannose, %[c]	16.8	15.28	7.15	4.91
Arabinose, %[c]	2.9	1.65	trace	0.37
Xylose, %[c]	9.8	9.59	0.65	1.33
Total sugar, %[c]	100	100	72.74	65.60

[a]Based on wood.
[b]Based on holocellulose.
[c]Based on neutral sugar content of the holocellulose.

In Thompson's investigation glucomannan fractions were isolated from the 10% NaOH and 18% NaOH extracts and had ratios which varied from 0.03:1:3 to 0.04:1.3:3 to 0.3:1.1:3. In this investigation the glucomannan fractions isolated from the 10% NaOH extract (Fractions 4, 5, 8, 9, and all the fractions obtained from Fractions 8 and 9 by fractional precipitation of their acetate derivatives) had galactose:glucose:mannose ratios of 0.16-0.30:1.00:3.27-4.16 and the ratios for the glucomannan fractions isolated from the 18% NaOH extract (Fraction 13 and the soluble and insoluble portions of its acetate derivative) were 0.16-0.24:1.00:3.96-4.38. These fractions contained 2.1 to 4.0% xylose and many of Thompson's fractions also contained a small amount of xylose. The above

ratios remained constant within the above limits during careful fractional precipitation of the acetate derivatives of Fractions 8 and 9. In this study the bulk of the glucomannan was isolated from the 10% NaOH extract whereas in Thompson's extraction most of the glucomannan polymers were concentrated in the 18% NaOH extract although in other experiments Thompson also found the major portion of the glucomannan in the 10% NaOH extract. Thompson (2) points out that this extraction behavior is dependent on the lignin content and the severity of the drying procedure of the holocellulose.

From the freezing 18% NaOH and 10% NaOH extracts, Thompson isolated glucomannans (0.1:1.2-1.3:3) and galactoglucomannan polysaccharides (0.7:0.7:3, 1.4:2.2:3, and 3-3.3:1-1.4:3) containing 10.4 to 42.3% xylose and from a trace to 6.0% arabinose. In this investigation the resistant polysaccharides (Fraction 14 and the soluble and insoluble acetate derivatives of Fraction 14) were extracted with 18% NaOH containing 4% H_3BO_3 and had a galactose:glucose:mannose ratio of 0.62:1:3.42 (Fraction 14-S) and contained 9.1% xylose and 1.6% arabinose. It is possible that this fraction may have been a mixture of a galactose-rich galactoglucomannan (1-3:1:3-4) and a glucomannan (0.1-0.3:1:3-4) similar to those found by Thompson even though fractionation of the acetate derivative of this fraction into its soluble and insoluble components failed to reveal any variation in the sugar ratios. A final washing of the holocellulose with water resulted in the isolation of a resistant galactoglucomannan (1.01:1.00:3.07) containing 9.0% xylose and 2.1% arabinose (Fraction 16 and the fractions derived from its acetate derivative such as Fraction 16-S) and a resistant glucomannan (0.27-0.35:1.00:2.54-3.89) containing 3.9 to 6.7% xylose (Fraction 17 and the soluble and insoluble portions of its acetate derivative).

The greater amount of mannose in the glucomannan fractions in this study than in those from Thompson's investigation may be due to the different methods of sugar analysis employed. In this study the method of Saeman, et al. (23) was used and Thompson employed a spot area method.

APPENDIX XIV

PURIFICATION OF SOLVENTS

The acetophenone and 1,1,2-trichloroethane were purified by fractional distillation in a glass column which had a three-fourth inch inside diameter and was packed to a height of 31 inches with single-turn 1/4 by 1/32-inch glass helices. The middle fraction was collected and stored under nitrogen in the absence of light and the first and last fractions were discarded.

APPENDIX XV

OSMOMETRY

INTRODUCTION

Number average molecular weights and second virial coefficients were determined with a Mechrolab High Speed Membrane Osmometer, Model 501 (163). Flow through the membrane is detected with this instrument by means of an optical system in the solvent chamber and any net flow is prevented by means of an electromechanical servo system. Solvent flow is detected by a change in light scattering as a bubble in the capillary on the solvent side of the membrane moves into the light path. Since practically no flow of solvent is needed to establish equilibrium, an osmotic pressure measurement at a given concentration is obtained in about three to twenty minutes, and no dilution occurs on the solution side of the membrane. Diffusion of low molecular weight species is kept to a minimum in this short time interval and thus the determined molecular weight should be more accurate than that obtained with a conventional osmometer.

It has been shown that the osmotic pressure is lowered by the presence of a low molecular weight species which is capable of diffusing through the membrane, even when extrapolations to zero time are made (164-166). Tung (167) has demonstrated the importance of using a fast osmometer because measurements made close to zero time give values that deviate little from the true osmotic pressure.

The osmotic pressure-concentration relationship is expressed by Equations (8) and (9) (30, 31, 166).

$$\pi/c = RT\,[1/M_n + A_2c + A_3c^2 + \text{-----}] \qquad (8)$$

$$\pi/c = RT/M_n\,[1 + \Gamma_2 c + g\,\Gamma_2{}^2\,c^2 + \text{-----}] \qquad (9)$$

where

π is the osmotic pressure

$\underline{c}$ is the concentration

$\underline{M_n}$ is the number average molecular weight

$\underline{A_2}$ is the second virial coefficient

Γ_2 is also a parameter which depends on polymer-solvent interaction

In this investigation only the first two terms on the right-hand side of the equation were included in the extrapolation to zero concentration.

EXPERIMENTAL

Schleicher and Schuell number 07 membranes (Schleicher and Schuell Company, Keene, New Hampshire) with average pore diameters of five to ten millimicrons were employed. The membranes were conditioned by solvent exchanging. The solvent was purified 1,1,2-trichloroethane for the acetylated fractions (purification is described in Appendix XIV, p. 153). The bubble in the capillary of the osmometer slowly dissolved in this solvent. In order to replace the bubble it is necessary to change the membrane and this resulted in the use of nine different membranes in the determination of twenty number average molecular weights. Although the membranes varied in porosity, the determined molecular weight did not appear to be affected by the membrane.

Sufficient solution of each fraction was prepared to make duplicate osmotic molecular weight determinations, duplicate concentration determinations, and an intrinsic viscosity determination. As a precautionary measure against aggregation the solutions were shaken overnight, any insoluble material then removed by filtration, and finally the solutions shaken overnight again. The solutions were then filtered again before osmotic pressure or viscosity measurements were made.

All solutions were made up by weight and the concentrations determined by weight. Excellent precision was obtained for duplicate concentration determinations on the milliliter aliquots. Drying was carried out for two days under vacuum at 110°C. If appreciable insoluble material was present, the solution was first centrifuged before filtration. Ash contents of the material remaining after concentration determination were negligible.

The osmotic pressure measurements were made at 37°C. Duplicate osmotic pressure measurements were made at a given concentration before making a run at the next concentration. In this manner, any error due to polymer adsorption onto the membrane was minimized.

RESULTS

The extrapolation of $\pi/\underline{c}$ versus concentration was carried out by means of the method of least squares. Generally, the set of values of the duplicate analyses were chosen for extrapolation which gave the highest correlation coefficient. The results are presented in Table XXXVII and examples of the $\pi/\underline{c}$ versus $\underline{c}$ extrapolations are shown in Fig. 13. The precision of the osmotic pressure measurements is indicated by the results of separate determinations for Fraction 3(2) in acetophenone and trichloroethane. Measurements in acetophenone gave $\underline{M}_n$ = 17,700 and $\underline{A}_2 = 4.5 \times 10^{-4}$ cm.^{3} mole/g.^{2} and measurements in trichloroethane gave $\underline{M}_n$ = 17,500 and $\underline{A}_2 = 7.0 \times 10^{-4}$ cm.^{3} mole/g.^{2}. The number average molecular weights differ by only 1.4% thus confirming the reliability of the osmotic pressure measurements.

TABLE XXXVII

OSMOMETRY RESULTS

Series	Fraction	Molecular Weight (Number Average)	$\overline{DP}_n$ [a,b]	$A_2 \times 10^4$, cm.^{3} mole/g.^{2}	Γ_2, cm.^{3}/g.	Correlation Coefficient for A_2
Fractions	2(1)	75,200	261.0	4.26	32.0	0.965
derived from	Insol.-1	59,000	205.0	1.51	8.92	0.329
the main	I(2)[c]	47,600	165.0	--	--	--
acetylated	9-1	44,600	155.0	2.76	12.3	0.532
glucomannan	2(2)	35,400	123.0	6.42	22.7	0.995
Fractions	3(1)	29,500	103.0	6.95	0.5	0.998
8-A and 9-A	9-2	23,700	82.2	8.23	19.5	0.985
	3(2)	17,500	60.6	6.98	12.2	0.992
	9-3	10,500	36.3	3.52	3.68	0.916
	4	9,200	32.0	3.46	3.19	0.790
Various	8-S	23,400	81.1	4.41	10.3	0.977
acetylated	9-S	24,700	85.8	5.22	12.9	0.995
glucomannan	6-7-S	25,900	89.8	3.00	7.76	0.908
and galacto-	13-S	23,500	81.4	3.15	7.39	0.959
glucomannan	14-S	28,300	98.1	5.92	1.67	0.521
fractions	16-S	26,900	93.4	1.03	2.77	0.509
	17-S	25,500	88.5	6.89	17.6	0.997

[a] $\overline{DP}_n$ = number average degree of polymerization.

[b] Calculated using the value of 288 for the molecular weight of the triacetate monomer unit.

[c] Extrapolated by eye due to the peculiarity of this set of points.

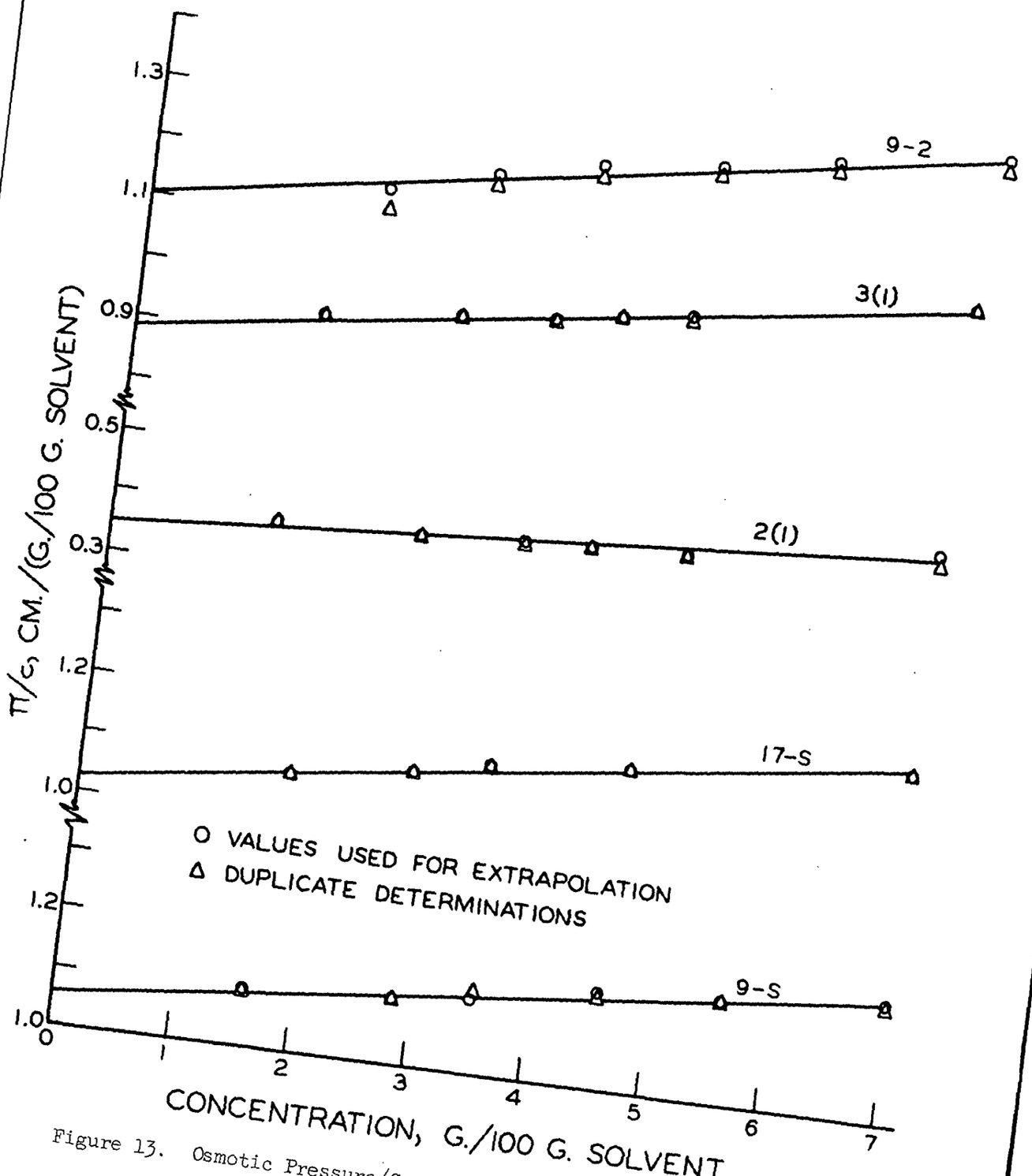

Figure 13. Osmotic Pressure/Concentration Versus Concentration

APPENDIX XVI

VISCOMETRY

PROCEDURE

The intrinsic viscosity of each fraction was determined on a one or two-milliliter aliquot taken from the solution prepared for osmometry. The solvent was 1,1,2-trichloroethane. Viscosity measurements were made with a number 50 Cannon Ubbelohde semimicro dilution viscometer. According to Cannon, et al. (168) the kinetic energy correction is negligible for this viscometer when a solvent is used with the kinematic viscosity of 1,1,2-trichloroethane. As a further check, an equation employed by Timell (169) was used to estimate kinetic energy correction of 0.5% which is certainly negligible for this system. No dependence of the intrinsic viscosity on shear rate occurs for polysaccharides with a degree of polymerization less than about 1,000 (169). Therefore, it was unnecessary to determine the intrinsic viscosity at various shear rates and extrapolate to zero shear rate. All dilutions were carried out with a micro-syringe fitted with a Chaney adaption. The measurements were made at 30 $\pm$ 0.005°C.

RESULTS

The intrinsic viscosity, $[\eta]$, is expressed in ml./g. rather than the customary 100 ml./g. The other viscosity expressions, defined according to the I.U.P.A.C. (170) recommendations, are η = solution viscosity, η_o = solvent viscosity, c = concentration in g./ml., $(\eta-\eta_o)/\eta_o c$ = viscosity number, and $[\ln(\eta/\eta_o)]/c$ = logarithmic viscosity number. The data were extrapolated in three ways to yield the intrinsic viscosity: (1) the viscosity number versus concentration, (2) the logarithmic viscosity number versus concentration, and (3) the logarithm of the viscosity number versus concentration. The method of least

squares was employed for extrapolation. The equations are (32)

$$(\eta-\eta_o)/\eta_o c = [\eta] + K_1 [\eta]^2 c \qquad (10)$$

$$[\ln(\eta/\eta_o)]/c = [\eta] - K_2 [\eta]^2 c \qquad (11)$$

$$\ln[(\eta - \eta_o)/\eta_o c] = \ln [\eta] + K_3 [\eta] c \qquad (12)$$

where K_1 is the Huggins constant and K_2 and K_3 are also constants.

The results are presented in Tables XXXVIII and XXXIX and examples of the extrapolations are shown in Fig. 14. The values for the intrinsic viscosity are consistently different for the three plots. The viscosity number plot yields the lowest value, the logarithm of the viscosity number plot yields an intermediate value, and the logarithmic viscosity number plot yields the highest value; however, the values differ only by the order of 1%. The values of the intrinsic viscosities determined from the viscosity number plot are employed in future analyses.

TABLE XXXVIII

VISCOSITY RESULTS – FRACTIONS FROM THE MAIN ACETYLATED GLUCOMANNANS 8-A AND 9-A

Fraction	Viscosity Number Plot				Logarithmic Viscosity Number Plot				Logarithm of the Viscosity Number Plot				
	$[\eta]$	K_1	Slope	C.C.[a]	$[\eta]$	K_2	Slope	C.C.[a]	$[\eta]$	K_3	Slope	C.C.[a]	$K_1 + K_2$
2(1)	53.6	0.749	2150	0.9997	54.9	-0.0450	135	0.797	54.6	0.591	32.3	0.998	0.704
Insol.-1	47.6	0.511	1160	0.984	47.7	0.0199	-45.2	-0.241	47.7	0.487	23.2	0.985	0.531
I(2)	45.7	--	--	--	45.7	--	--	--	--	--	--	--	--
9-1	44.0	0.659	1270	0.997	44.2	-0.0662	130	0.917	44.2	0.592	26.1	0.998	0.593
2(2)	44.6	0.667	1320	0.998	45.2	-0.0310	63.3	0.843	45.0	0.563	25.4	0.999	0.636
3(1)	35.7	0.383	489	0.919	35.8	0.136	-175	-0.686	35.8	0.351	12.6	0.915	0.519
9-2	29.7	0.496	438	0.999	29.9	0.0564	-50.3	-0.955	29.8	0.448	13.4	0.998	0.552
3(2)	23.4	0.398	219	0.946	23.4	0.112	-61.3	-0.679	23.4	0.378	8.87	0.943	0.510
9-3	14.2	0.664	134	0.832	14.2	-0.111	22.6	0.268	14.2	0.627	8.92	0.834	0.552
4	13.1	0.924	160	0.960	13.2	-0.359	62.4	0.803	13.2	0.879	11.6	0.957	0.565

[a]C.C. = correlation coefficient.

TABLE XXXIX

VISCOSITY RESULTS – VARIOUS ACETYLATED GLUCOMANNANS AND GALACTOGLUCOMANNANS

Fraction	Viscosity Number Plot				Logarithmic Viscosity Number Plot				Logarithm of the Viscosity Number Plot				$K_1 + K_2$
	$[\eta]$	K_1	Slope	C.C.[a]	$[\eta]$	K_2	Slope	C.C.[a]	$[\eta]$	K_3	Slope	C.C.[a]	
8-S	34.8	0.665	807	0.999	35.2	-0.0457	56.5	0.766	35.1	0.575	20.2	0.998	0.619
9-S	38.2	0.584	850	0.999	38.5	0.0096	-14.1	-0.538	38.4	0.509	19.6	0.999	0.594
6-7-S	32.5	0.944	998	0.999	32.7	-0.317	339	0.999	32.7	0.852	27.8	0.999	0.627
13-S	36.4	0.586	863	0.9997	38.7	0.0096	-14.3	-0.640	38.7	0.509	19.7	0.999	0.595
14-S	35.3	0.964	1200	0.9998	35.8	-0.218	283	0.990	35.8	0.783	28.1	0.999	0.746
16-S	34.9	0.692	843	0.991	35.0	-0.124	152	0.840	33.0	0.645	22.5	0.990	0.568
17-S	37.9	0.603	868	0.999	38.3	-0.0002	-0.317	-0.0193	38.2	0.522	19.9	0.999	0.604

[a]C.C. = correlation coefficient.

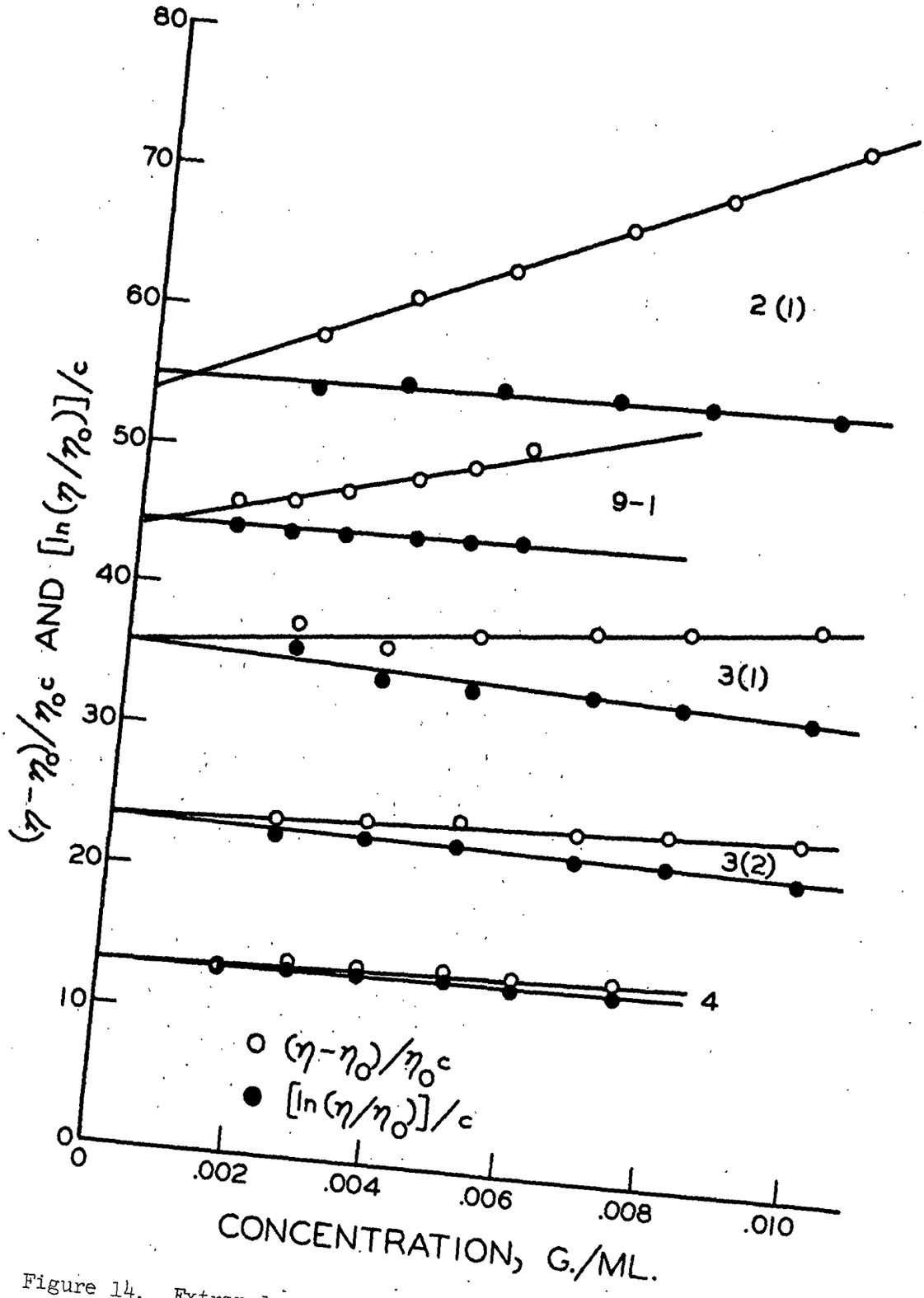

Figure 14. Extrapolation to Obtain Intrinsic Viscosity

APPENDIX XVII

LIGHT SCATTERING

Weight average molecular weights were determined from light scattering for the acetylated glucomannan Fraction 3(2) in acetophenone (purification of acetophenone is described in Appendix XIV, p. 153). The calculated molecular weights at wavelengths of 5461 A. and 4358 A. were 306,000 and 515,000, respectively, which are considerably higher than the number average value (17,400). The unreasonably high molecular weights from light scattering may be caused by the high fluorescence of the glucomannan triacetate solutions. Since the determined molecular weights and the fluorescence are both higher at the wavelength of 4358 A. than the wavelength of 5461 A., it appears that the corrections which have been applied do not adequately correct for the large amount of fluorescence involved. The molecular weights corrected for fluorescence were similar in magnitude to the molecular weights corrected for depolarization which indicates that most of the depolarization is due to fluorescence.

Another possible cause of the high light-scattering molecular weights is aggregation or the presence of a small amount of high molecular weight material. Aggregation was indicated by the extremely small second virial coefficients at the wavelength of 5461 A. and the negative second virial coefficients at the wavelength of 4358 A. Tanford (40) shows that when aggregation occurs a negative second virial coefficient is theoretically predicted. Other workers have attributed abnormally high molecular weights obtained by light scattering to the presence of small amounts of colloidal material or aggregation when working with various polysaccharides (37, 171-173) and in particular with hemicelluloses (174-176). The presence of lignin in the glucomannan triacetate fractions may be a contributing

factor in the aggregation or the lignin may be involved in a small amount of high molecular weight lignin-glucomannan complex.

The abnormally high molecular weights did not appear to be caused by the experimental technique since the data had very little scatter on extrapolation to zero concentration. Therefore, no further attempt was made to improve the light-scattering method.

APPENDIX XVIII

SEDIMENTATION EQUILIBRIUM

INTRODUCTION

The possibility of a small amount of aggregation affecting the light-scattering molecular weights was discussed previously (Appendix XVII, p. 164). In sedimentation equilibrium experiments with an ultracentrifuge, dust and large aggregates sediment to the bottom of the cell and have little effect on the determined molecular weight (25-27). The theoretical and practical aspects of ultracentrifugation have been discussed by many authors (25, 26, 40, 177-181). In this study weight average and z-average molecular weights were determined from sedimentation equilibrium experiments employing a short column (182). Molecular weights are determined from the equilibrium state in which the sedimentation of the molecules passing across a given surface in the sedimenting direction is exactly balanced by the centripetal transport due to diffusion (25). The data were analyzed according to the method of Lansing and Kraemer (183).

THE z-AVERAGE MOLECULAR WEIGHT

Lansing and Kraemer (183) have shown that for a heterogeneous polymer the z-average molecular weight at each point in the cell, M_{zx}, corresponding to the point $\bar{x} = (x_1 + x_2)/2$ at equilibrium is given by

$$M_{zx} = \frac{2RT \ln \left[\left(\frac{Z_2}{Z_1}\right)\left(\frac{x_1}{x_2}\right)\right]}{(1-\bar{v}\rho)\,\omega^2\,(x_2^2 - x_1^2)} \qquad (13)$$

where

Z = the ordinate of the photographic plate obtained with the schlieren optical system

x = the distance from the center of rotation

$\underline{T}$ = the absolute temperature

$\underline{R}$ = the gas constant

$\underline{\bar{v}}$ = the partial specific volume of the solute

ω = the angular velocity = (r.p.m.) $(2\pi)/60$

ρ = the density of the solution

The density, ρ, can be calculated from the solute concentration in grams per 100 grams of solution, $\underline{p}$, the partial specific volume, $\underline{\bar{v}}$, and the density of the solvent, ρ_o, from Equation (14).

$$\rho = \frac{\rho_o}{[1 + (\bar{v}\rho_o - 1)\, p/100]} \tag{14}$$

In this study, $\underline{M_{zx}}$ was calculated for 31 to 41 intervals across the cell. These molecular weights must then be integrated to give a z-average molecular weight for the entire solution, $\underline{M_z}$. Lansing and Kraemer (183) carry out the integration employing Equations (15), (16), and (17).

$$M_z = \frac{\int_a^b M_{zx}\, Z dx}{\int_a^b Z dx} \tag{15}$$

$$\int_a^b Z dx = \sum_a^b \int_{x_1}^{x_2} Z dx = \sum_a^b \frac{1}{2AM_{zx}} \left(\frac{Z_2}{x_2} - \frac{Z_1}{x_1} \right) \tag{16}$$

$$\int_a^b M_{zx}\, Z dx = \frac{1}{2A} \left(\frac{Z_b}{b} - \frac{Z_a}{a} \right) \tag{17}$$

where $\underline{A} = \dfrac{(1 - \bar{v}\rho)\, \omega^2}{2RT}$

$\underline{a}$ and $\underline{b}$ = the values of $\underline{x}$ at the solution-air meniscus and the solution-oil meniscus, respectively.

These calculations were carried out with the aid of an I.B.M. 1620 computer.

The above method of calculation was employed to calculate the values of $\underline{M}_{\underline{Z}}$ which were used throughout the rest of this investigation. However, initially a separate method of calculation devised by this investigator but employing the same basic equations of Lansing and Kraemer (183) was carried out. For a homogeneous polymer, a plot of log $(\underline{Z}/\underline{x})$ versus $\underline{x}^2$ should yield a straight line and the slope gives the molecular weight according to Equation (13) in which $\ln [(\underline{Z}_2/\underline{Z}_1)(\underline{x}_1/\underline{x}_2)]/(\underline{x}_2^2 - \underline{x}_1^2)$ is replaced by (2.303)(slope) (184). If the polymer is heterogeneous then an upward curvature will be obtained. It was found that this curve could be approximated by a series of linear segments and the slope of a particular segment (determined by the method of least squares) gave $\underline{M}_{\underline{Zx}}$ for the range of $\underline{x}$ in that segment according to Equation (13). Equation (15) was then used to integrate across the cell in the following manner.

$$M_z = \frac{\int_a^b M_{zx}\, Zdx}{\int_a^b Zdx} = \frac{\sum_{\text{segment } i=1}^{h} \left(M_{zx} \int_{x_1}^{x_2} Zdx \right)_{\text{segment } i}}{\int_a^b Zdx} \qquad (18)$$

Since the area under the $\underline{Z}$ versus $\underline{x}$ plot is equal to $\int_{\underline{x}_1}^{\underline{x}_2} \underline{Zdx}$ from $\underline{x}_1$ to $\underline{x}_2$ we get Equation (19).

$$M_z = \frac{\sum_{\text{segment } i=1}^{h} (M_{zx}\ \text{Area})_{\text{segment } i}}{\text{Total Area}} \qquad (19)$$

The areas under each segment were determined with the aid of a planimeter.

WEIGHT AVERAGE MOLECULAR WEIGHT

Lansing and Kraemer (183) have shown that the weight average molecular weight, M_{wx}, at each point in the cell corresponding to $\bar{x} = (x_1 + x_2)/2$ is given by Equation (20).

$$M_{wx} = \frac{1}{A} \frac{\ln \left(c_{x_1} / c_{x_2} \right)}{x_2^2 - x_1^2} \tag{20}$$

where

$$A = \frac{(1 - \bar{v}\rho)\omega^2}{2RT}$$

To use this equation for data obtained with the schlieren optical system, the value of Z which is proportional to the gradient of refractive index, dn/dx, at the point x must be converted to the concentration at point x, c_x. Van Holde and Baldwin (26, 182) give a good approximation for c_a which enables this conversion to be made.

$$c_a = \frac{\Delta c}{e^{\Delta c / c^o} - 1} \tag{21}$$

where

c_a = the solute concentration at $x = a$ at equilibrium

c^o = the initial concentration of the solution

$\Delta c = c_b - c_a$ at equilibrium

The value Δc is determined from Equation (22).

$$\Delta c = \frac{\tan \theta}{Lh\ (dn/dc)} \int_a^b Z dx \tag{22}$$

where

θ = the phase plate angle

L = the optical lever arm

h = the thickness of the solution in the centrifuge cell perpendicular to the plane of rotation

dn/dc = the refractive index gradient of the solute.

The value c_x is then calculated from Equation (23).

$$c_x = \frac{\tan\theta}{Lh(dn/dc)} \int_a^x Z dx + c_a \tag{23}$$

The values of $\int_a^b Z dx$ and $\int_a^x Z dx$ were previously calculated in the determination of the z-average molecular weight. The same intervals that were used for the z-average molecular weight were also used for the weight average molecular weight. The values of M_{wx} were integrated to give a weight average molecular weight for the entire solution, M_w, with the use of Equations (24), (25), and (26).

$$M_w = \frac{\int_a^b M_{wx} \times c_x \, dx}{\int_a^b x \, c_x \, dx} \tag{24}$$

$$\int_a^b x \, c_x \, dx = \sum_a^b \int_{x_1}^{x_2} x \, c_x \, dx = \sum_a^b \frac{1}{2AM_{wx}} (c_{x_2} - c_{x_1}) \tag{25}$$

$$\int_a^b M_{wx} \times c_x \, dx = \frac{1}{2A} (c_b - c_a) \tag{26}$$

These calculations were carried out with the aid of an I.B.M. 1620 computer.

EXPERIMENTAL

SEDIMENTATION EQUILIBRIUM MEASUREMENTS

Molecular weight determinations were made on the glucomannan triacetate Fractions 9-3, 3(2), 9-2, 3(1), 2(2), and 2(1) in acetophenone. Sedimentation equilibrium runs were made on the Spinco Model E Analytical Ultracentrifuge, using the schlieren optical system. This system gives a photographic record

of the refractive index gradient of the solute within the centrifuge cell. The abscissa of the photographic curve is the distance from the center of rotation, x, and the ordinate of the photographic curve, Z, is proportional to the gradient of refractive index, dn/dx, at the point x and is given by Equation (27).

$$Z = \frac{(dn/dx)\ Lh\ m_z}{\tan \theta} \qquad (27)$$

where m_z = magnification of the cylinder lens.

The acetophenone was purified as described in Appendix XIV, p. 153. Determinations were made at four concentrations for Fraction 3(2). For all other fractions determinations were made at a concentration of about 5×10^{-3} g./ml. The solutions were shaken overnight before being placed in the centrifuge cell.

Centrifugation was done in aluminum-filled Epon double sector cells. The sector shaped cell minimizes or eliminates convective flow (25). One sector is filled with solution and the other with solvent. The solvent base line is then recorded on the photographic plate along with the schlieren image for the solution. Runs were made with both one and two cells in the rotor. When two cells were run at once, a 1° positive wedged window was placed in one cell. The wedged window displaced the schlieren image, permitting the two samples and their respective base lines to be photographed simultaneously (177). The cells were filled, taking precautions to stagger the menisci of the solution and the solvent in order to obtain a sharp photographic image for each meniscus. The depth of the solution columns was approximately 0.2 cm. These short solution columns reduce the time required to reach equilibrium since this time depends directly on the square of the column depth (179, 182). In order to give a surface at the cell bottom with an arc of the center of rotation, a dense, inert liquid is placed on the cell bottom (25). Fluorochemical FC43(Spinco 6394) was immiscible with acetophenone and was used in this investigation.

The runs were made at 30.0 ± 0.1°C. and were considered to be at equilibrium when no measurable change occurred on the schlieren photograph. The runs were continued for a half a day to a day or more past the time of estimated equilibrium in order to be certain that equilibrium had been reached. The optimum speed of the rotor for each fraction was estimated as described in the Beckman manual (177). When two cells were run simultaneously it was necessary to choose a speed that was a compromise between the optimum speeds of the two fractions. The rotor speeds for the solutions were 19,160 r.p.m. for 3(2) ($\sim 1 \times 10^{-2*}$ g./ml.); 19,160 r.p.m. for 3(2) ($\sim 0.7 \times 10^{-2*}$ g./ml.); 19,160 r.p.m. for 3(2) ($\sim 0.5 \times 10^{-2*}$ g./ml.); 25,980 r.p.m. for 3(2) ($\sim 0.3 \times 10^{-2*}$ g./ml.); 25,980 r.p.m. for 9-3; 17,980 r.p.m. for 9-2; 17,980 r.p.m. for 3(1); 14,290 r.p.m. for 2(2); and 14,290 r.p.m. for 2(1).

The optical constants for the schlieren optical system were 2.1011 for m_x, the magnification factor for the camera in the radial or x direction; 3.7363 for m_z, the magnification factor for the cylinder lens; and 59.79 cm. for the optical lever arm. The optical lever arm was determined with the aid of a Spinco calibration cell (185) and the values for m_x and m_z had previously been determined by Carlson (186). The thickness of the solution in the centrifuge cell perpendicular to the plane of rotation, h, was determined to be 1.204 cm. by measuring the cell thickness with a micrometer. The phase plate angle, was 74.6°. The photographic plates were measured on a Wilder microprojector. Measurements were made at 0.0050-inch intervals in the x direction. Measurements were made in the Z direction from the solvent base line to the solution image. Measurements in the x direction were converted to distances from the center of rotation by using the position of the wire in the counterbalance as a reference when one cell was used and by using the

*Concentration of solution.

position of the inside edge of the rotor reference hole when two cells were run simultaneously.

REFRACTIVE INDEX GRADIENT

The refractive index gradients of Fractions 9-3, 3(2), 9-2, 3(1), 2(2), and 2(1) in solutions of approximately 1.5 x 10^{-2} g./ml. in acetophenone were determined from sedimentation velocity runs on the Spinco Model E Analytical Ultracentrifuge, using the Rayleigh optical system. The refractive index gradient, dn/dc, is calculated from Equation (28) (177).

$$dn/dc = \frac{J\lambda}{ch} \qquad (28)$$

where

J = the number of Rayleigh fringes

λ = the wavelength of light used = 5.461 x 10^{-5} cm.

h = the cell thickness = 1.204 cm.

c = the concentration in g./ml.

This equation is based on the fact that the refractive index of dilute solutions is a linear function of concentration for most polymers.

Five measurements were made on each Rayleigh photographic plate and the average value of the number of fringes, J, was employed in the calculation of the refractive index gradient. Centrifugation was carried out in aluminum-filled Epon capillary-type synthetic boundary double sector cells at 30.0 $\pm$ 0.1°C. and at rotor speeds of 7,000 to 8,000 r.p.m. The values for dn/dc are presented in Table XL. The values for Fractions 9-3 and 2(2) were a little lower than the values for the other fractions. An average refractive index gradient for Fractions 3(2), 9-2, 3(1), and 2(1) was determined to be -0.0277 ml./g. and this average value was employed in the calculation of the weight average molecular weights.

TABLE XL

REFRACTIVE INDEX GRADIENT

Fraction	Refractive Index Gradient, ml./g.
9-3	-0.0225
3(2)	-0.0284
9-2	-0.0263
3(1)	-0.0284
2(2)	-0.0255
2(1)	-0.0277

PARTIAL SPECIFIC VOLUME

Partial specific volumes were determined for Fractions 3(2) and 2(1) at concentrations of 0.6×10^{-2} to 0.7×10^{-2} g./ml. in acetophenone. Density measurements were made with a Lipkin pycnometer at 30.00 $\pm$ 0.005°C. on 4.5 to 5.0 ml. of solution. The pycnometer had previously been calibrated by other investigators (187, 188). Buoyancy corrections were made with Equation (29) (189).

$$W = W' + W' \, da \, (1/d_m - 1/d_w) \qquad (29)$$

where

W = true weights

W' = weights used

d_a = density of air

d_m = density of liquid in pycnometer

d_w = density of weights

The partial specific volume, $\bar{v}$, was calculated by making the assumption that it is equal to the apparent specific volume, ϕ_1. In actual practice ϕ_1 is only

slightly concentration-dependent and the above assumption is a very good one (178). The partial specific volume is then given by Equation (30) (189).

$$\bar{v} = \phi_1 = \frac{1}{\rho_o}\left[1 - \frac{100\,(\rho - \rho_o)}{p\,\rho}\right] \qquad (30)$$

where

ρ_o = density of solvent

ρ = density of solution

p = concentration of solute in grams per 100 grams of solution

The average of two determinations for Fraction 3(2) is $\bar{v} = 0.750 \pm 0.012$ ml./g. and the value from one determination for Fraction 2(1) is $\bar{v} = 0.754$ ml./g. The average density of acetophenone from duplicate determinations at 30.0°C. is 1.01949 ± 0.00008 g./ml. The partial specific volume of a polymer species in solution is practically independent of its molecular weight (178, 181). The nearly identical values for Fraction 3(2) with a $\overline{DP}_n = 60.6$ and Fraction 2(1) with a $\overline{DP}_n = 261$ substantiate this.

RESULTS AND DISCUSSION

MOLECULAR WEIGHTS AT A GIVEN CONCENTRATION

The z-average molecular weights were calculated employing the planimeter method of integration for three concentrations of Fraction 3(2). An example of the log (Z/x) versus x^2 plot is given in Fig. 15. The upward curvature of this plot is due to the heterogeneity of the fraction. The results are compared to the z-average molecular weights calculated by the method of Lansing and Kraemer in Table XLI. It is seen that the values of the molecular weights calculated by the two methods agree reasonably well. The method of Lansing and Kraemer is more accurate than the method in which the planimeter was used to carry out the

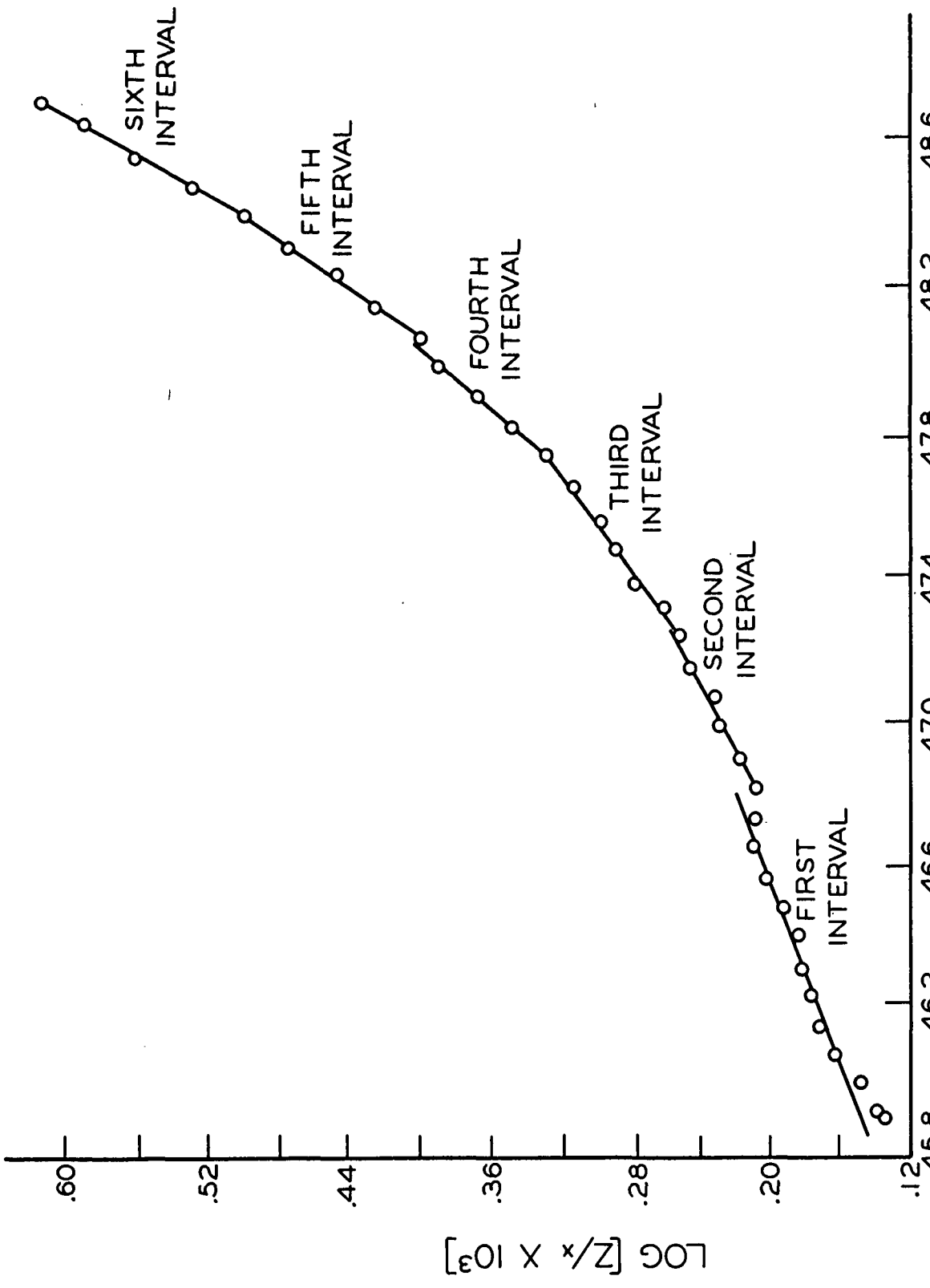

Figure 15. Log $\underline{Z}/x \times 10^3$ Versus x^2.
Fraction 3(2). Concentration = 0.5 x 10^{-2} g. ml.

integration and the z-average molecular weights of all the fractions were calculated by the former method.

TABLE XLI

COMPARISON OF Z-AVERAGE MOLECULAR WEIGHTS FROM THE "PLANIMETER" METHOD AND THE METHOD OF LANSING AND KRAEMER

Fraction	Concentration, g./ml.	$\underline{M}_z$ from "Planimeter" Method	$\underline{M}_z$ from L. & K. Method
3(2)	$\sim 1 \times 10^{-2}$	19,800	21,800[a]
3(2)	$\sim 0.7 \times 10^{-2}$	25,700	24,800
3(2)	$\sim 0.5 \times 10^{-2}$	25,400	24,300

[a]This plate was remeasured and $\underline{M}_z$ recalculated for future analysis.

The data were plotted as $\underline{Z}$ versus $\underline{x}$ on an expanded graph and smoothed before calculations were carried out. Due to optical effects, the values of $\underline{Z}$ from the schlieren photograph generally cannot be measured with high precision in the regions near the ends of the cell and must be obtained by extrapolation in these regions (179, 181). For Fractions 9-3 and 3(2) this extrapolation was relatively easy. However, for the other fractions this extrapolation was carried out with some arbitrariness due to the abrupt increase in the slope of $\underline{Z}$ versus $\underline{x}$ in the region near the solution-oil meniscus at the cell bottom. This abrupt increase in slope is due to the presence of a small amount of very high molecular weight material or a small amount of aggregation. In either case it is not representative of the molecular weight of the bulk of the polymer molecules in the fraction and was effectively ignored by making a "reasonable" extrapolation which did not consider the apparent abrupt increase in slope near the cell bottom. In this respect sedimentation equilibrium is superior to light scattering because it allows one to obtain a realistic molecular weight even when a small amount of high molecular weight impurities or aggregates are present.

The molecular weights calculated from the highest extrapolation and the "reasonable" extrapolation are presented in Table XLII. Also included in this table are values obtained from the lowest extrapolation which gives a minimum molecular weight. The molecular weights in Table XLII were calculated by the method of Lansing and Kraemer and are at a given concentration. The molecular weights obtained by the "reasonable" extrapolation were used in further analysis of the data. Two examples of the plots of $\underline{Z}$ versus $\underline{x}'$ and the extrapolations are shown in Fig. 16 and 17, where $\underline{x}'$ is the measured value of the abscissa before conversion to the distance from the center of rotation.

Examples of the $\underline{M}_{\underline{Zx}}$ versus $\bar{\underline{x}}$ plot and the $\underline{M}_{\underline{wx}}$ versus $\bar{\underline{x}}$ plot are shown in Fig. 18 and 19 and Fig. 20 and 21, respectively. The molecular weight should theoretically increase from $\underline{x} = \underline{a}$ to $\underline{x} = \underline{b}$. In the $\underline{M}_{\underline{Zx}}$ versus $\bar{\underline{x}}$ plot, Fraction 3(2) (Fig. 18) shows this increasing trend which is typical for all the other fractions except Fraction 2(1). Fraction 2(1) has a slight minimum although the general increasing trend is present (Fig. 19). The plots of $\underline{M}_{\underline{wx}}$ versus $\bar{\underline{x}}$ have a slight minimum for all fractions with the over-all trend in molecular weight increasing from $\underline{x} = \underline{a}$ to $\underline{x} = \underline{b}$. These slight minimums may be due to errors involved in measuring the schlieren photographs or may be due to the concentration dependence of the molecular weight. If the former reason is the cause, these errors would be minimized by the integration throughout the cell in which the abnormally high molecular weights ould be compensated by the abnormally low molecular weights. An attempt was also made to calculate the weight average molecular weights by the hinge point method of Van Holde and Baldwin (182) which employs a one point measurement of $\underline{Z}$ at the midpoint of the solution column from the center of rotation. The results obtained by this method were not satisfactory and the values of the molecular weights were generally too low. The low values of molecular weights obtained by this method can be attributed to the minimum that is observed in the $\underline{M}_{\underline{wx}}$ versus $\bar{\underline{x}}$ plots.

TABLE XLII

MOLECULAR WEIGHTS FROM SEDIMENTATION EQUILIBRIUM AT A GIVEN CONCENTRATION

Fraction	Concentration x 10^2, g./ml.	Extrapolation	$\underline{M}_w$	$\underline{M}_z$	$\underline{DP}_w$ [a]	$\underline{DP}_z$ [a]
9-3	~0.5	--	11,000	10,300	38.3	35.7
3(2)	~1.0 [b]	--	19,000	22,600	65.9	78.4
3(2)	~0.7	--	20,500	24,800	71.3	86.1
3(2)	~0.5	--	21,500	24,300	74.7	84.4
3(2)	~0.3	--	21,800	26,200	75.7	90.9
9-2	~0.5	highest	34,000	46,500	119.0	162.0
9-2	~0.5	"reasonable"	31,800	38,400	110.0	133.0
3(1)	~0.5	highest	42,700	93,100	148.0	323.0
3(1)	~0.5	"reasonable"	38,100	50,100	132.0	174.0
3(1)	~0.5	lowest	36,700	41,900	128.0	145.0
2(2)	~0.5	highest	62,300	163,000	216.0	564.0
2(2)	~0.5	"reasonable"	54,000	86,000	188.0	299.0
2(2)	~0.5	lowest	51,000	69,600	177.0	242.0
2(1)	~0.5	highest	93,300	138,000	324.0	478.0
2(1)	~0.5	"reasonable"	87,000	114,000	302.0	396.0
2(1)	~0.5	lowest	81,000	94,500	281.0	328.0

[a] Based on the value of 288 for the triacetate monomer unit.
[b] ~ Designates approximately.

EXTRAPOLATION OF MOLECULAR WEIGHTS TO ZERO CONCENTRATION

The molecular weights were determined at four concentrations for Fraction 3(2). The extrapolation to zero concentration is shown in Fig. 22. Fujita (181) has shown that for a polydisperse system the following equations hold.

$$1/M_{app} = 1/M_w + B_{SD}\, c^o \qquad (31)$$

$$1/M'_{app} = 1/M_z + B'_{SD}\, c^o \qquad (32)$$

The values $1/\underline{M}_{app}$ and $1/\underline{M}'_{app}$ are the weight average and z-average molecular weights, respectively, at an initial concentration equal to $\underline{c}^o$. The sedimentation equilibrium

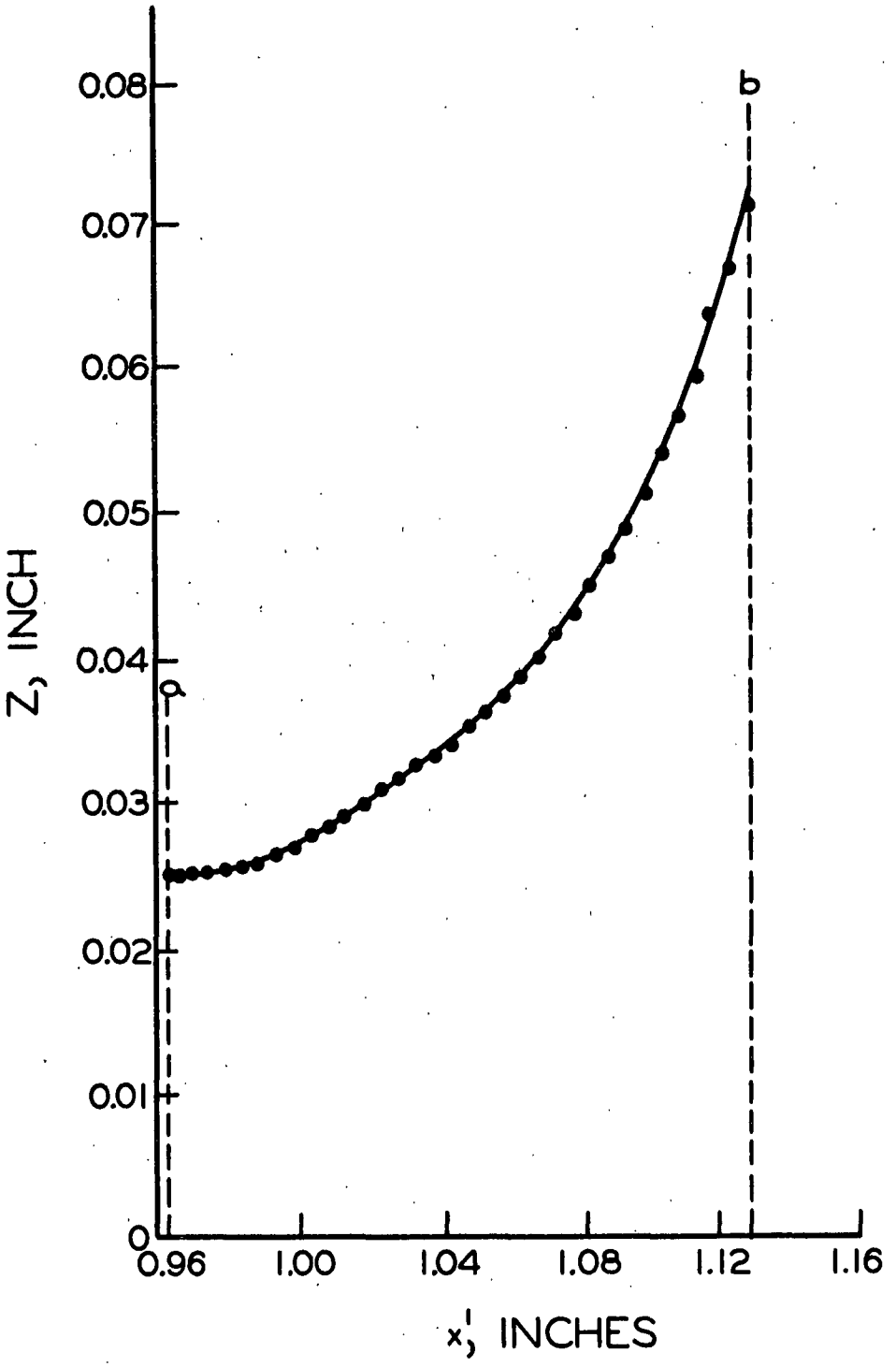

Figure 16. Z Versus x'.
Fraction 3(2). Concentration = 1 x 10^{-2} g./ml.

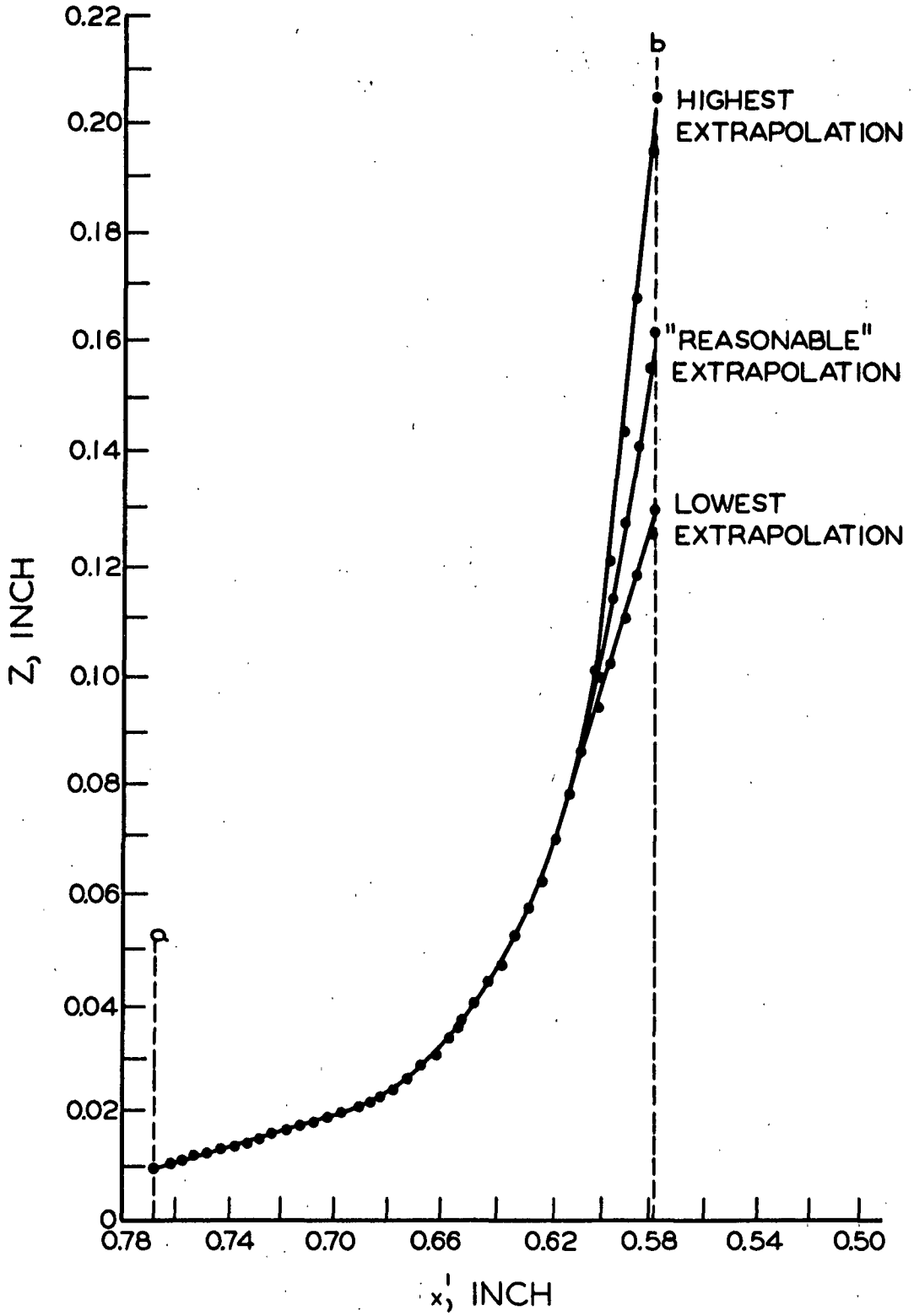

Figure 17. Z Versus x'.
Fraction 2(1). Concentration = 0.5×10^{-2} g./ml.

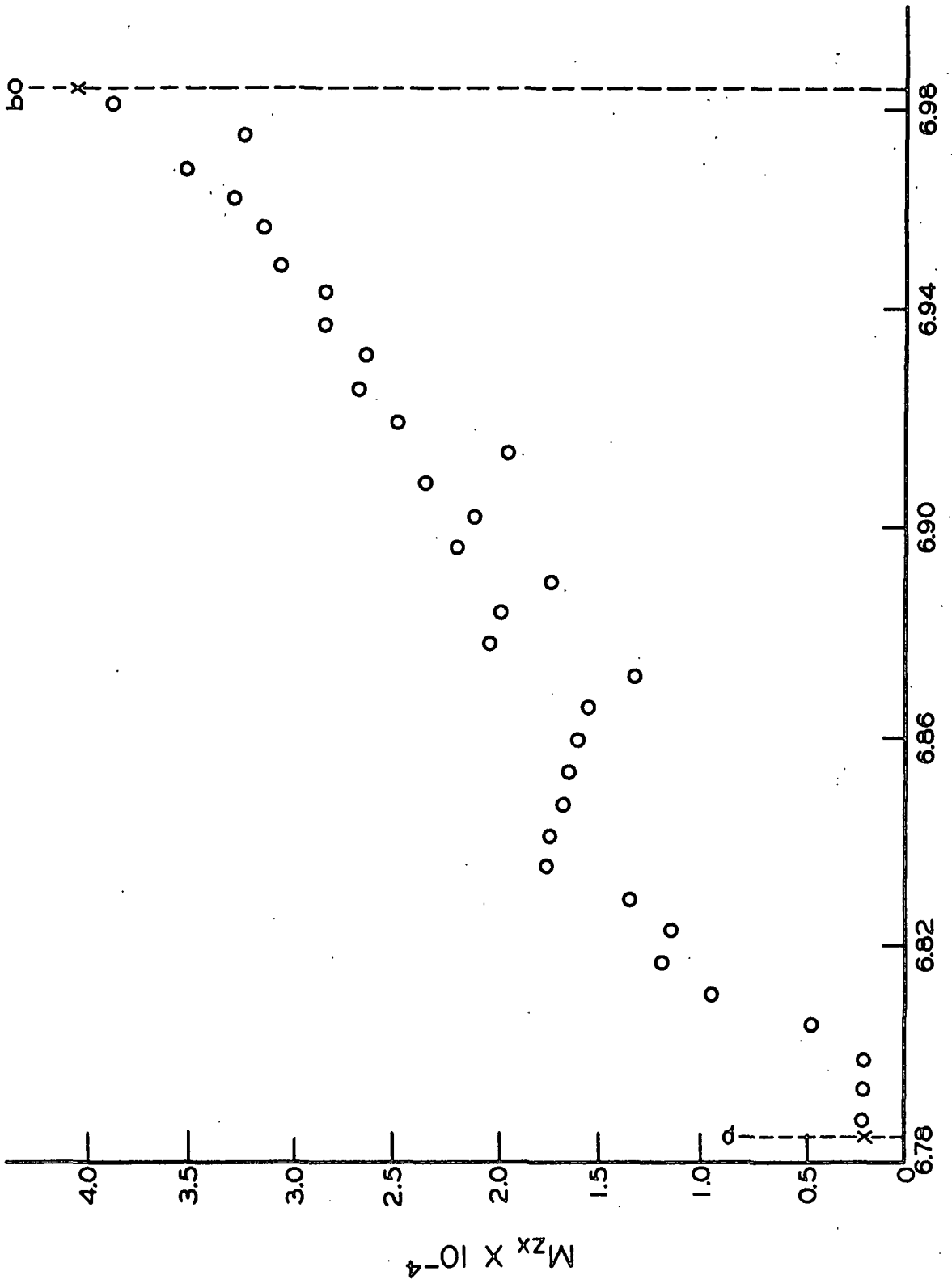

Figure 18. $\underline{M}_{zx}$ Versus $\underline{\bar{x}}$. Fraction 3(2). Concentration = 1 x 10^{-2} g./ml.

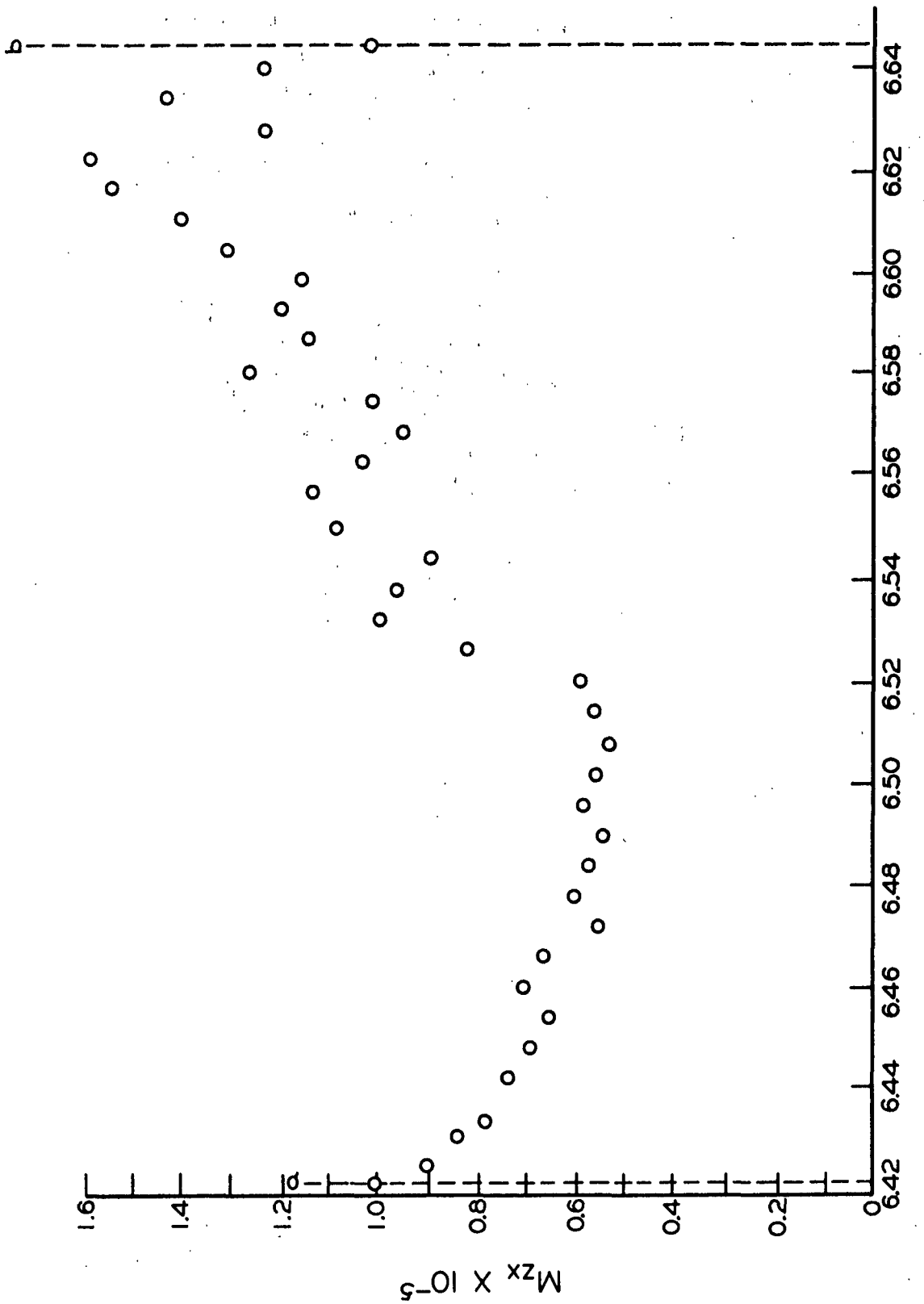

Figure 19. $\underline{M_{zx}}$ Versus $\bar{x}$

Fraction 2(1). Concentration = 0.5 x 10^{-2} g./ml. From "Reasonable" Extrapolation

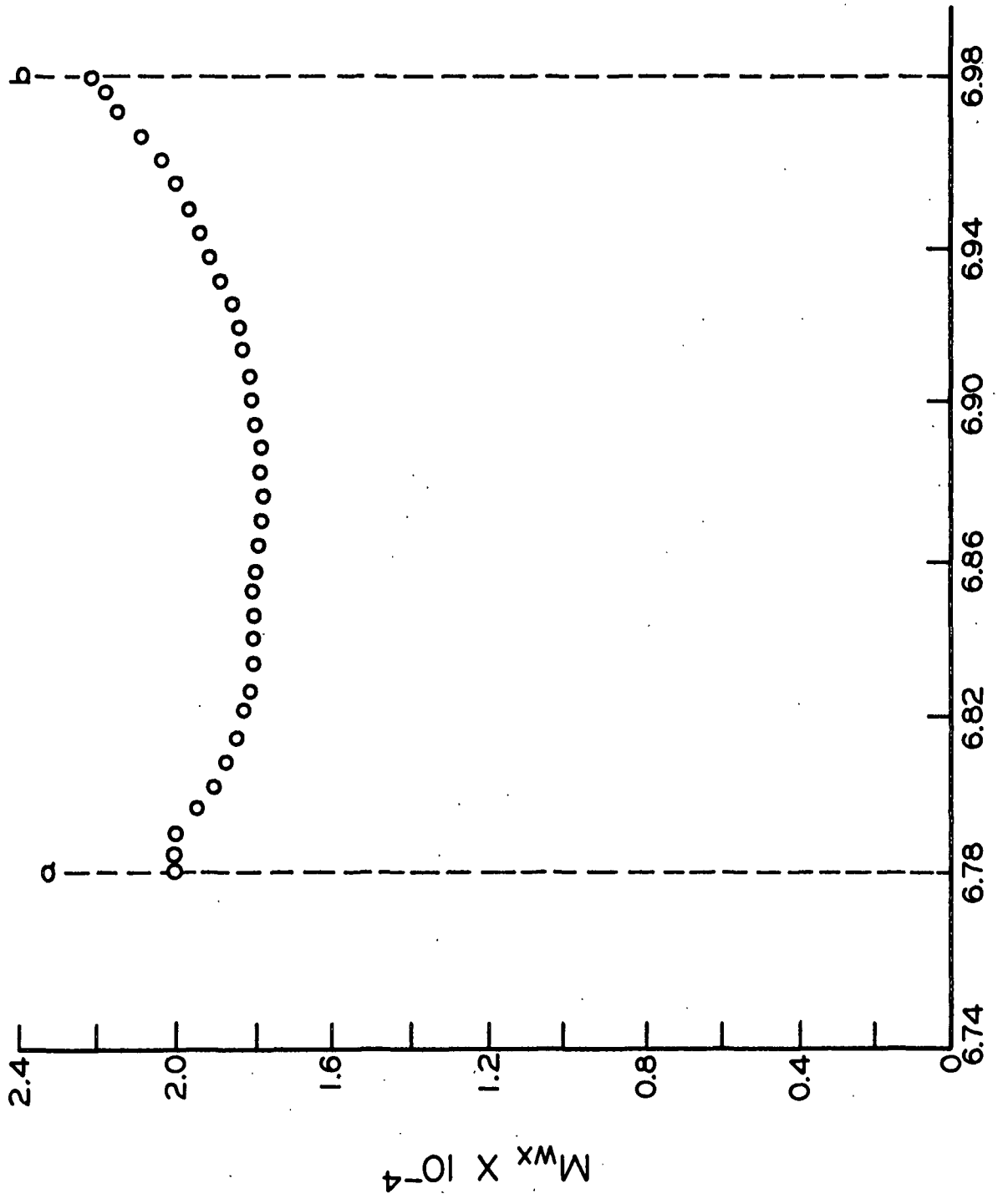

Figure 20. $\underline{M}_{wx}$ Versus $\bar{x}$. Fraction 3(2). Concentration = 1 x 10^{-2} g./ml.

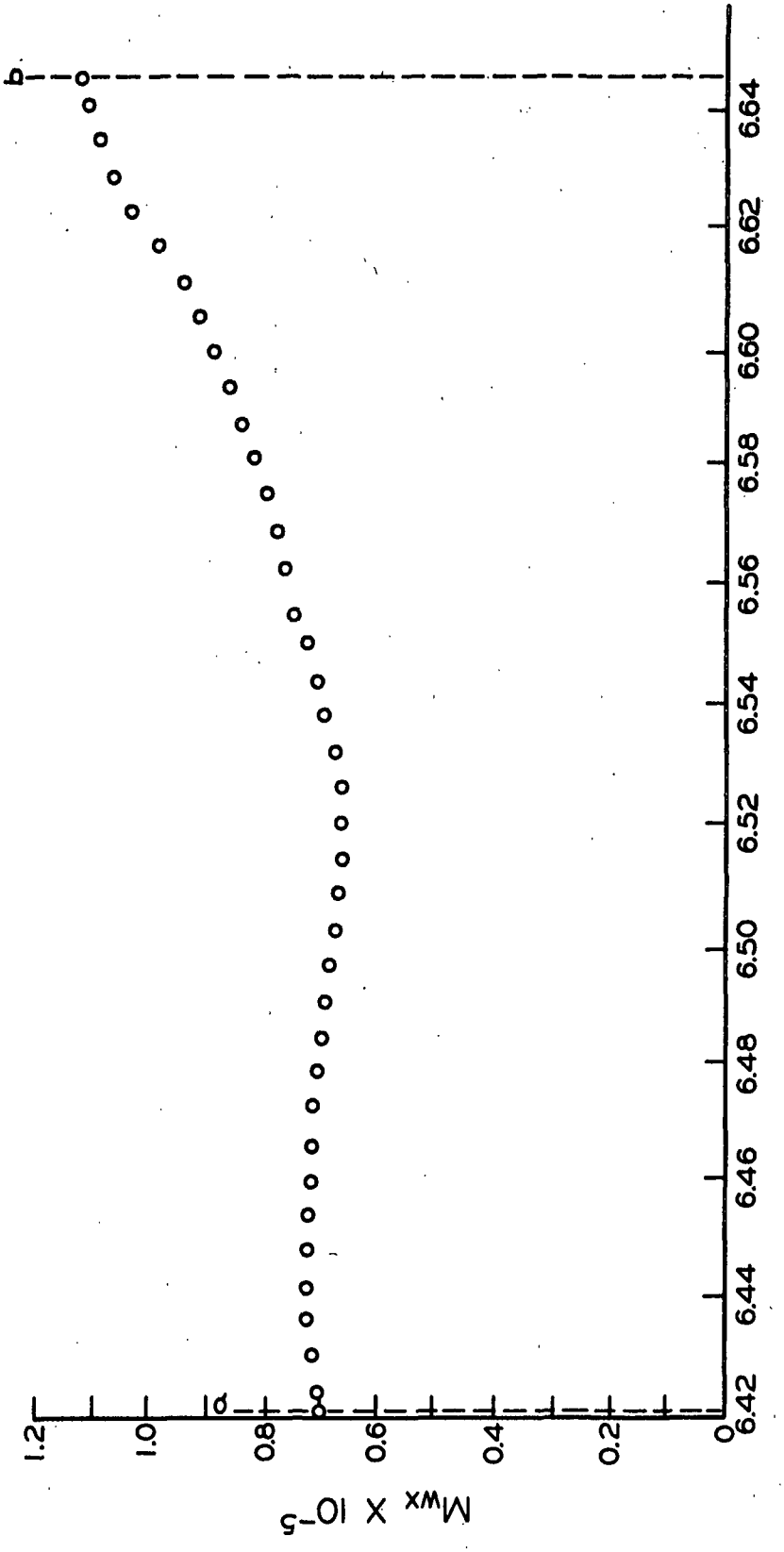

Figure 21. $\frac{M}{wx}$ Versus $\bar{x}$.

Fraction 2(1). Concentration = 0.5 x 10^{-2} g./ml. From "Reasonable" Extrapolation

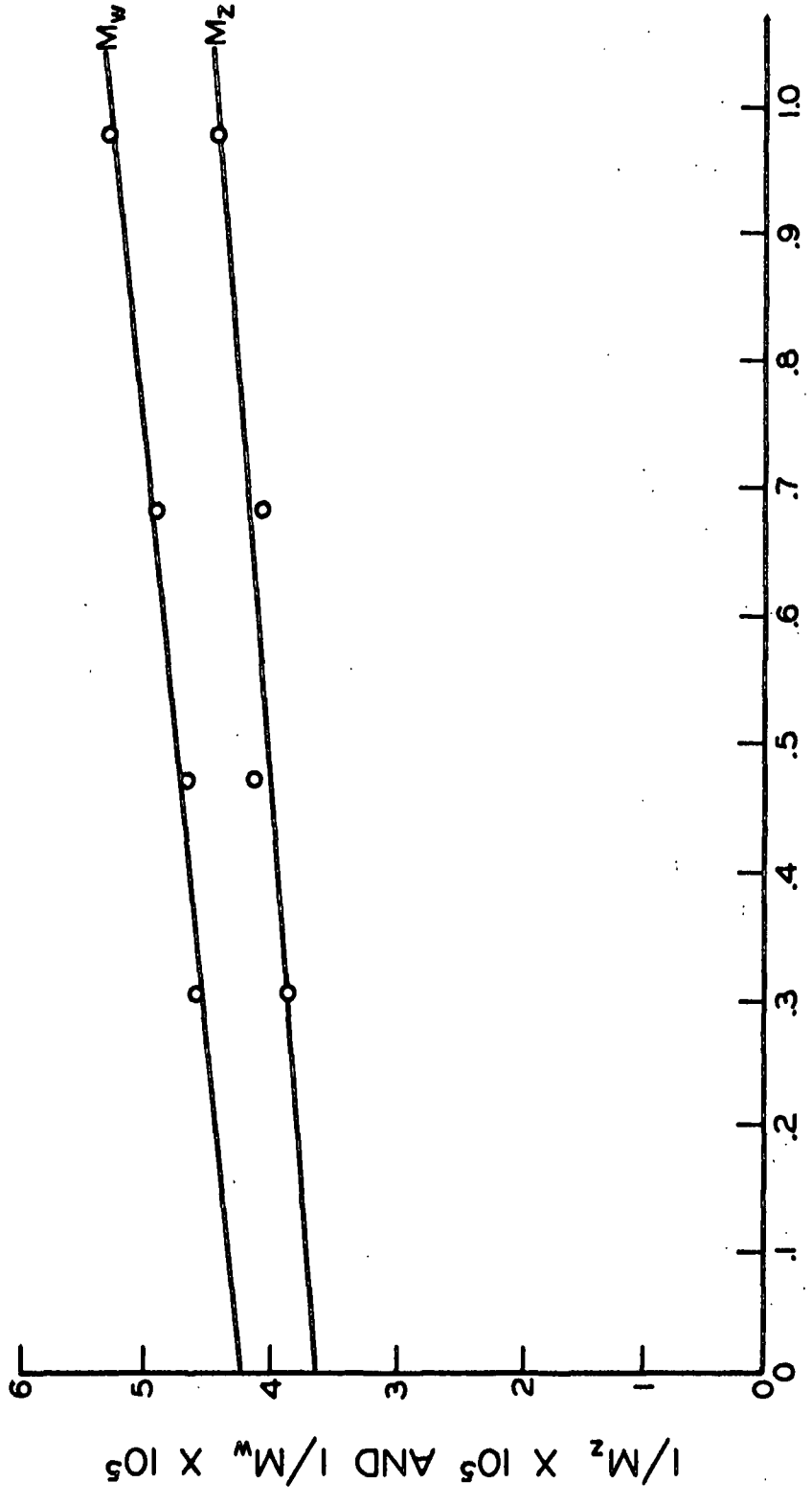

Figure 22. $1/\underline{M}_z$ and $1/\underline{M}_w$ Versus Concentration.. Fraction 3(2) in Acetophenone

second virial coefficients are designated by B_{SD} and B'_{SD} for the weight average and the z-average molecular weights, respectively. Fujita (181) also shows that Equation (33) applies when $M_z \approx 1$.

$$B_{LS} = \frac{B_{SD}}{1 + (1/12)\,(\lambda M_z)^2} \tag{33}$$

where B_{LS} = the light-scattering second virial coefficient,

$$\lambda = \frac{(1 - \bar{v}\,\rho_o)(b^2 - a^2)\,\omega^2}{2RT}$$

ρ_o = density of solvent

The assumption was made in this study that an equation of the same form applies to the second virial coefficients for the z-average molecular weights.

$$B'_{LS} = \frac{B'_{SD}}{1 + (1/12)(\lambda M_z)^2} \tag{34}$$

For a monodisperse system $B_{OS} = 1/2\ B_{LS}$ where B_{OS} is the osmotic pressure second virial coefficient (181). Although this relationship does not generally hold for a polydisperse system, the approximate values of B_{OS} and B'_{OS} were calculated on the assumption that the deviation from this relationship is not very great. The molecular weights at zero concentration and the second virial coefficients for Fraction 3(2) are presented in Table XLIII.

It is interesting that although the lowest concentration was run at a different rotor speed than the three higher concentrations, all the values fall on the same line for the extrapolation in Fig. 22. Thus, the variation in rotor speed had no appreciable effect on the values of molecular weight in this case. From Table XLIII, it is seen that the z-average second virial coefficients are lower than the weight average second virial coefficients. This behavior is

expected theoretically since the second virial coefficient theoretically decreases with increasing molecular weight (40). For this reason, the approximate osmotic pressure second virial coefficients given in Table XLII are lower than the actual values. The value of $\underline{B}_{\underline{OS}} = 4.30 \times 10^{-4}$ in acetophenone from Table XLIII is of the same order of magnitude as the measured value of 6.98×10^{-4} for Fraction 3(2) in trichloroethane.

TABLE XLIII

EXTRAPOLATION TO ZERO CONCENTRATION
FOR FRACTION 3(2)

Molecular Weight Average	Molecular Weight at $\underline{c} = 0$	Second Virial Coefficient, (cm.^{3} mole/g.^{2}) Sedimentation Equilibrium	Light Scattering	Osmotic Pressure
Weight av.	$\underline{M}_{\underline{w}} = 23{,}700$	$\underline{B}_{\underline{SD}} = 1.02\times10^{-3}$	$\underline{B}_{\underline{LS}} = 8.59\times10^{-4}$	$\underline{B}_{\underline{OS}} = 4.30\times10^{-4}$
z-Average	$\underline{M}_{\underline{w}} = 27{,}600$	$\underline{B}'_{\underline{SD}} = 7.70\times10^{-4}$	$\underline{B}'_{\underline{LS}} = 6.50\times10^{-4}$	$\underline{B}'_{\underline{OS}} = 3.25\times10^{-4}$

The molecular weights of all the other fractions were extrapolated to zero concentration with the use of Equations (31) and (32) and with the assumption that $\underline{B}_{\underline{SD}}$ and $\underline{B}'_{\underline{SD}}$ for all fractions were equal to the corresponding values for Fraction 3(2). This is a reasonable assumption as shown by the following analysis. First, the assumption is made that the light-scattering second virial coefficient in acetophenone, $\underline{B}_{\underline{LS}}$ or $\underline{B}'_{\underline{LS}}$, is proportional to the measured second virial coefficient, $\underline{A}_{2(\underline{OS})}$, in trichloroethane. Then from this assumption and Equations (33) and (34) we get the following equations from which $\underline{B}_{\underline{SD}}$ and $\underline{B}'_{\underline{SD}}$ for each fraction can be calculated.

$$\frac{B_{SD\text{-given fraction}}}{B_{SD\text{-Fraction 3(2)}}} = \frac{\left\{B_{LS}\left[1 + (1/12)(\lambda M_z)^2\right]\right\}_{\text{-given fraction}}}{\left\{B_{LS}\left[1 + (1/12)(\lambda M_z)^2\right]\right\}_{\text{-Fraction 3(2)}}}$$

$$= \frac{\left\{A_{2(OS)}\left[1 + (1/12)(\lambda M_z)^2\right]\right\}_{\text{-given fraction}}}{\left\{A_{2(OS)}\left[1 + (1/12)(\lambda M_z)^2\right]\right\}_{\text{-Fraction 3(2)}}} \qquad (35)$$

$$\frac{B'_{SD\text{-given fraction}}}{B'_{SD\text{-Fraction 3(2)}}} = \frac{\left\{B'_{LS}[1 + (1/12)(\lambda M_z)^2]\right\}_{\text{-given fraction}}}{\left\{B'_{LS}(1 + (1/12)(\lambda M_z)^2]\right\}_{\text{-Fraction 3(2)}}}$$

$$= \frac{\left\{A'_{2(OS)}\ [1 + (1/12)(\lambda M_z)^2]\right\}_{\text{-given fraction}}}{\left\{A'_{2(OS)}\ [1 + (1/12)(\lambda M_z)^2]\right\}_{\text{-Fraction 3(2)}}} \qquad (36)$$

The previously determined values of $A_{2(OS)}$ were used to calculate B_{SD} and B'_{SD} for each fraction. The molecular weights at zero concentration were then calculated with Equations (31) and (32) employing these calculated values of B_{SD} and B'_{SD}. These molecular weights are presented in Table XLIV along with the deviation from the molecular weights at zero concentration calculated by assuming a constant B_{SD} and B'_{SD} for all fractions.

TABLE XLIV

MOLECULAR WEIGHTS EXTRAPOLATED TO ZERO CONCENTRATION WITH THE USE OF $A_{2(OS)}$

Fraction	M_w	Deviation from M_w Calculated Assuming Constant B_{SD}, %	M_z	Deviation from M_z Calculated Assuming Constant B'_{SD}, %
9-3	11,300	-3.4	10,500	-2.4
3(2)	23,700[a]	0	27,600	0
9-2	39,300	+3.2	46,000	+1.7
3(1)	50,400	+6.1	66,100	+6.0
2(2)	79,600	+7.5	141,000	+8.4
2(1)	145,000	-9.8	189,000	-9.8

[a]Previously extrapolated value.

The molecular weights which were extrapolated to zero concentration with the assumption of constant B_{SD} and B'_{SD} for all the fractions agree within 10% with the molecular weights presented in Table XLIV. Thus, the assumption of constant B_{SD} and B'_{SD} is a good one and the molecular weights extrapolated to zero concentration with this assumption were used in the further analysis of the data. These molecular weights are presented in Table XLV.

TABLE XLV

MOLECULAR WEIGHTS EXTRAPOLATED TO ZERO CONCENTRATION ASSUMING CONSTANT B_{SD} AND B'_{SD}

Fraction	M_w	DP_w [a]	M_z	DP_z [a]
9-3	11,700	40.8	10,800	37.3
3(2)	23,700[b]	82.4	27,600	95.8
9-2	38,100	132.0	45,300	157.0
3(1)	47,500	165.0	62,300	216.0
2(2)	74,100	257.0	130,000	452.0
2(1)	161,000	557.0	210,000	729.0

[a] Based on the value of 288 for the triacetate monomer unit.
[b] Previously extrapolated value.

APPENDIX XIX

MOLECULAR WEIGHT HETEROGENEITY AND DISTRIBUTION

The number average, weight average, and z-average molecular weights are defined by Equations (37), (38), and (39), respectively (25, 30).

$$M_n = \frac{\Sigma n_i m_i}{\Sigma n_i} = \frac{\Sigma c_i}{\Sigma c_i / M_i} \tag{37}$$

$$M_w = \frac{\Sigma n_i M_i^2}{\Sigma n_i m_i} = \frac{\Sigma c_i M_i}{\Sigma c_i} \tag{38}$$

$$M_z = \frac{\Sigma n_i M_i^3}{\Sigma n_i M_i^2} = \frac{\Sigma c_i M_i^2}{\Sigma c_i M_i} \tag{39}$$

The variables n_i and c_i are the number of molecules and the weight concentration of molecules of molecular weight, M_i, respectively. The ratios of M_w/M_n and M_z/M_w are measures of the polydispersity of a polymer fraction. The measured values of M_w/M_n and M_z/M_w are presented in Table XLVI.

The most probable distribution or the Zimm-Schulz distribution is given by (181, 190, 191)

$$f(M) = \frac{p^{h+1}}{\Gamma(h+1)} M^h e^{-pM} \tag{40}$$

where

$f(M)$ = the normalized weight distribution of the molecular weight, M

h and p = adjustable positive parameters

Γ = the Gamma function.

The parameter, h, increases as the molecular weight distribution becomes sharper. Therefore, the deviation of $1/h$ from zero is a measure of the heterogeneity of the fraction. Based on the assumption that the Zimm-Schulz distribution

applies to glucomannan triacetate fractions, the following relationship was used to calculate three values of $\underline{h}$ by using the three possible combinations of $\underline{M}_n$, $\underline{M}_w$, and $\underline{M}_z$ for each fraction.

$$\frac{h}{M_n} = \frac{h+1}{M_w} = \frac{h+2}{M_z} \qquad (41)$$

The three values of $\underline{h}$ differed and it was assumed that this was due to errors in the molecular weight measurements rather than failure of the Zimm-Schulz distribution to apply. Therefore, an average value of $\underline{h}$ was determined for each fraction and the ratios of $\underline{M}_w/\underline{M}_n$ and $\underline{M}_z/\underline{M}_w$ were calculated from Equation (41). These "averaged" values of $\underline{M}_w/\underline{M}_n$ and $\underline{M}_z/\underline{M}_w$ are presented in Table XLVI.

TABLE XLVI

RATIO OF $\underline{M}_n:\underline{M}_w:\underline{M}_z$

Fraction	Measured		"Averaged"		Average
	$\underline{M}_w/\underline{M}_n$	$\underline{M}_z/\underline{M}_w$	$\underline{M}_w/\underline{M}_n$	$\underline{M}_z/\underline{M}_w$	$\underline{h}$
9-3	1.12	0.916	1.05	1.05	20.7
3(2)	1.36	1.16	1.26	1.21	3.79
9-2	1.61	1.19	1.37	1.27	2.70
3(1)	1.61	1.31	1.53	1.35	1.88
2(2)	2.09	1.76	2.51	1.61	0.663
2(1)	2.13	1.31	1.71	1.41	1.42

APPENDIX XX

DIFFUSION COEFFICIENTS

INTRODUCTION

If a concentration gradient exists in a solution, matter will flow from the region of higher concentration to the region of lower concentration, tending to equalize the concentration throughout the solution (40). For one-dimensional diffusion this process is described by Fick's first law of diffusion (40).

$$J = -D\left(\frac{\partial c}{\partial x}\right)_t \qquad (42)$$

where

J = the flow of particles per second, across unit area of a plane perpendicular to the direction x of the concentration gradient $(\partial c/\partial x)_t$

D = diffusion coefficient

c = concentration

When a polymer solution of initially uniform concentration is subjected to a centrifugal force in an ultracentrifuge cell, a concentration gradient is set up due to the sedimentation of the polymer molecules toward the bottom of the cell. In a sedimentation equilibrium experiment, equilibrium is attained, when the material migrating across a given surface in a centrifugal direction is exactly balanced by the transport centripetally due to diffusion (25).

Van Holde and Baldwin (182) have shown that the diffusion coefficient can be obtained from an analysis of the transient state (approach to equilibrium) in a sedimentation equilibrium experiment. They applied the equations of Mason and Weaver (192) for a rectangular cell to approximate the conditions in a sector-shaped cell. This is a very good approximation when the height of the solution column is less than 3 mm. The diffusion coefficient is obtained from

the following equation:

$$\log \epsilon = \log \left\{ \frac{4\left[1 + \cosh\left(\frac{1}{2\alpha}\right)\right]}{\pi^2 U^2(\alpha)} \right\} - \frac{D\pi^2 U(\alpha) t}{2.303(b-a)^2} \qquad (43)$$

where

$\underline{D}$ = diffusion coefficient

$\underline{t}$ = time

$\underline{b}-\underline{a}$ = length of solution column

$$\alpha = \frac{\underline{R}\underline{T}}{\underline{M}(1-\bar{\underline{v}}\rho)\,\omega^2\,\bar{\underline{r}}(\underline{b}-\underline{a})}$$

$\bar{\underline{r}}$ = $(\underline{b}+\underline{a})/2$ = the distance of the center of the solution column from the center of rotation

$\underline{U}(\alpha) = [1 + 1/(4\pi^2\alpha^2)]$

$$\epsilon = \frac{\Delta c_{eq.} - \Delta c_t}{\Delta c_{eq.}} = \text{a measure of the departure from equilibrium} \qquad (44)$$

$\Delta\underline{c}$ = $\underline{c}(\underline{b})-\underline{c}(\underline{a})$ = the concentration difference between the top and bottom of the solution column.

The parameter ϵ is measured as a function of time and the diffusion coefficient is determined from the slope of the plot of log ϵ *versus* time.

When the sample is heterogeneous the following average diffusion coefficient is obtained (182)

$$\bar{D}_\alpha = \sum_{i=1}^{q} \omega_i D_i U(\alpha_i)/U(\bar{\alpha})$$

where

$$\bar{\alpha} = \sum_{\underline{i}=1}^{\underline{q}} \underline{R_i}\ \underline{c_i^o} \Big/ \sum_{\underline{i}=1}^{\underline{q}} \underline{R_i}(\Delta \underline{c_i})_{eq.}$$

$$\underline{R_i} = \left(\frac{\partial \underline{n}}{\partial \underline{c_i}}\right)_{\underline{T},\underline{p},\underline{c_j}(\underline{J}\neq\underline{0})}$$ = the differential refractive increment evaluated at zero concentration of all solutes

$$\omega_{\underline{i}} = \frac{\underline{R_i}\ \underline{c_i^o}/\underline{\alpha_i}}{\sum_{\underline{i}=1}^{\underline{q}} (\underline{R_i}\ \underline{c_i^o}/\underline{\alpha_i})}$$

Unfortunately, this is an unusual average diffusion coefficient. Van Holde and Baldwin (182) point out that almost the same average is obtained by combining results of sedimentation velocity and sedimentation equilibrium experiments as long as no very high molecular weight species are present. The equation is

$$\bar{D}_\alpha \approx \frac{RT\bar{s}}{M_w(1 - \bar{v}\rho)} \qquad (45).$$

In a recent paper LaBar and Baldwin (193) reinvestigated the approximations made in deriving Equation (43). They concluded that the optimum conditions occur when ϵ is less than 0.5 and α is greater than 1.0.

EXPERIMENTAL

The transient state data were obtained from the approach to equilibrium in the sedimentation-equilibrium experiments. The experimental conditions are given in The Sedimentation Equilibrium Section, Appendix XVIII, p. 166.

The schlieren optical system was employed. Photographs were taken at intervals of time ranging from the time at top speed to the time when equilibrium was reached. Each photograph gives a record of the refractive index gradient of the solute versus radial distance within the centrifuge cell at a given instance of time.

The concentration difference between the top and the bottom of the solution column, Δc, is given by (177)

$$\Delta c = \int_a^b \frac{\partial c}{\partial x}\, dx = \frac{\tan\theta}{Lhm_Z m_x \Delta n} \int_a^b Z dx = K \int_a^b Z dx \qquad (46)$$

where

Z = the ordinate on the photographic plate

x = the abscissa on the photographic plate

The area, A, on the photographic plate is given by $A = \int_a^b Z dx$. Substituting this expression and Equation (46) into Equation (44), the following expression for ϵ is obtained

$$\epsilon = \frac{A_{eq.} - A_t}{A_{eq.}} \qquad (47).$$

The areas were determined by projecting the photographic image onto a ground-glass screen with a Wilder microprojector and tracing this image on onionskin paper. The area was then measured with a planimeter. This method of determining the area is much more rapid than the conventional method of measuring each plate on a microprojector and then integrating.

The time was corrected to take into account the lower angular velocities during acceleration with the following equation (182)

$$t_{cor.} = \int_o^t \omega^2(t)dt/\omega^2 \qquad (48)$$

where

t = the measured time to top speed

$t_{cor.}$ = the corrected time to top speed

$\omega(t)$ = the angular velocity

ω_f = the angular velocity at top speed

The height of the solution columns were about 2 mm. The concentrations of the solutions were approximately 5 x 10^{-3} g./ml. in acetophenone. The temperature was 30°C.

RESULTS

Equation (43) was employed in two ways to determine the diffusion coefficient. In Method 1, log (10^2 ϵ) was plotted versus time and the slope was determined by the method of least squares. When this was done, the intercept given by the method of least squares differed from the theoretical intercept given by Equation (43). Therefore, Method 2 was also employed in which the theoretical intercept was calculated from the known value of α. A line was then drawn through the theoretical intercept and the points which were consistent with this line. The slope was then determined from this line. The points employed in this method were generally below ϵ equal to 0.5.

The schlieren pattern was somewhat irregular near the solution-air meniscus in the transient photographs. This resulted in some ambiguity in the determination of the area. Due to this ambiguity the points employed in the two methods of calculation may differ slightly. However, a consistent interpretation of the area near the solution-air meniscus was employed in each method of calculation. Results were obtained for Fractions 9-3, 9-2, 3(1), 2(2), and 2(1). No attempt was made to extrapolate the diffusion coefficients to zero concentration. The results are presented in Table XLVII and examples of the ϵ versus time plots for Method 1 and Method 2 are shown in Fig. 23 and 24, respectively.

Since viscosity and osmometry was carried out in 1,1,2-trichloroethane it is desirable to know the diffusion coefficients in this solvent. The diffusion coefficients in 1,1,2-trichloroethane were calculated from the following relationship (40)

TABLE XLVII

DIFFUSION COEFFICIENTS – IN ACETOPHENONE

			Method 1		Method 2	
Fraction	$\underline{M}_w$ [a]	α	$\underline{D}_\alpha$ [a], $cm.^2/sec.$	Correlation Coefficient	$\underline{D}_\alpha$ [a], $cm.^2/sec.$	Intercept [b]
9-3	11,000	1.071	4.91×10^{-7}	-0.986	5.18×10^{-7}	-0.240
9-2	31,800	0.710	3.29×10^{-7}	-0.998	3.37×10^{-7}	-0.188
3(1)	38,100	0.567	2.43×10^{-7}	-0.992	2.61×10^{-7}	-0.157
2(2)	54,000	0.673	3.08×10^{-7}	-0.985	2.45×10^{-7}	-0.181
2(1)	87,000	0.419	2.46×10^{-7}	-0.991	2.10×10^{-7}	-0.112

[a] At concentration = 5×10^{-3} g./ml.
[b] Intercept from log ϵ versus time.

$$D_1 = D_2 \, \eta_2/\eta_1$$

where η = the viscosity of the solvent.

It should be emphasized that this is merely an algebraic procedure to correct for the change in frictional coefficient due to a change in solvent viscosity. It does not correct for a change in the frictional coefficient due to a change in the polymer configuration or solvation. The viscosities of 1,1,2-trichloroethane and acetophenone were determined by measuring the flow times of these two solvents and water in a Cannon number 50 viscometer. The flow times were converted to viscosities, using water as a standard with the following equation (168)

$$\eta_1 = \eta_2 \left(\frac{t_1 \, \rho_1}{t_2 \, \rho_2} \right)$$

where ρ = density.

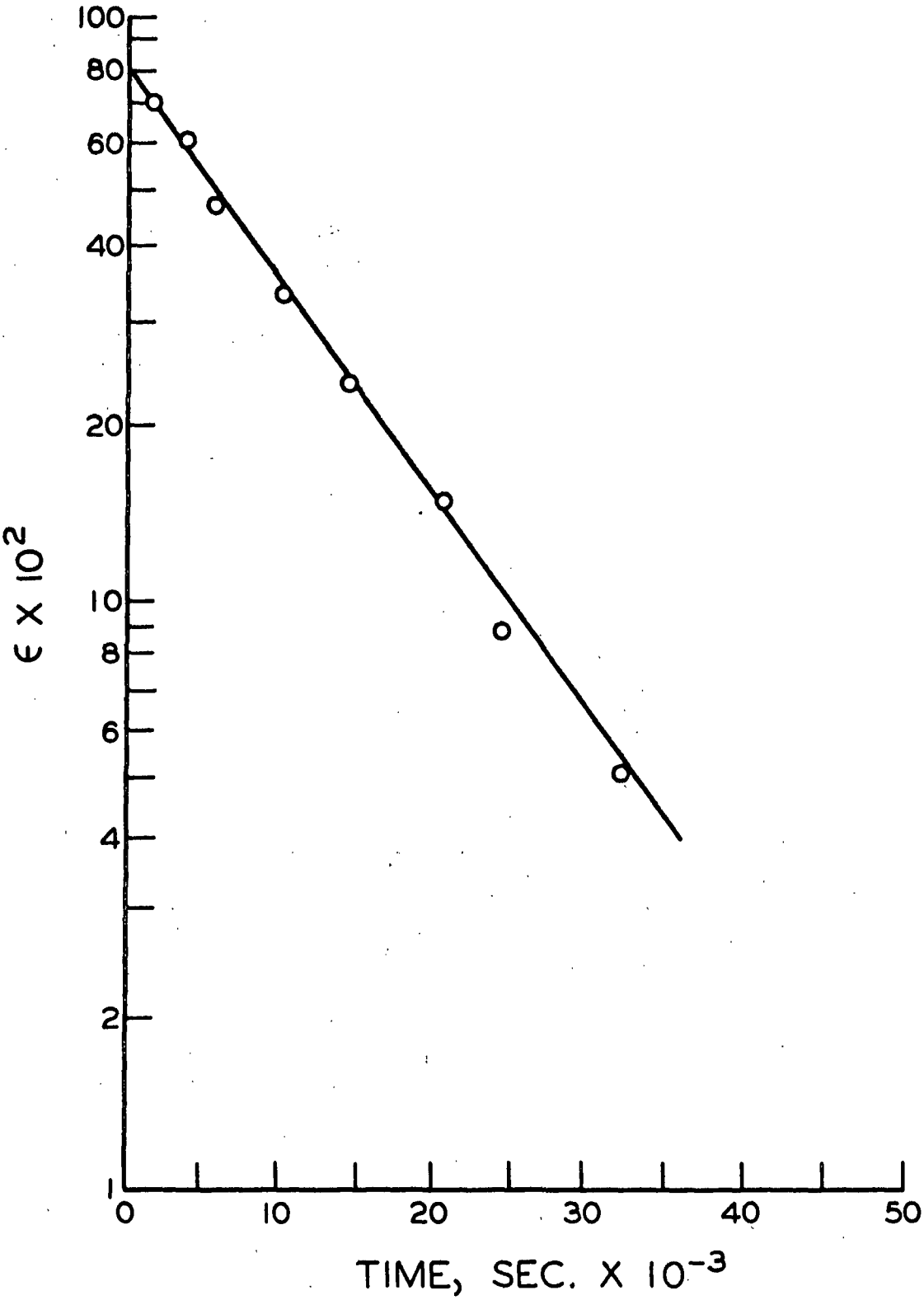

Figure 23. $\epsilon \times 10^2$ Versus Time
Method 1 (Least Squares Line). Fraction 9-2

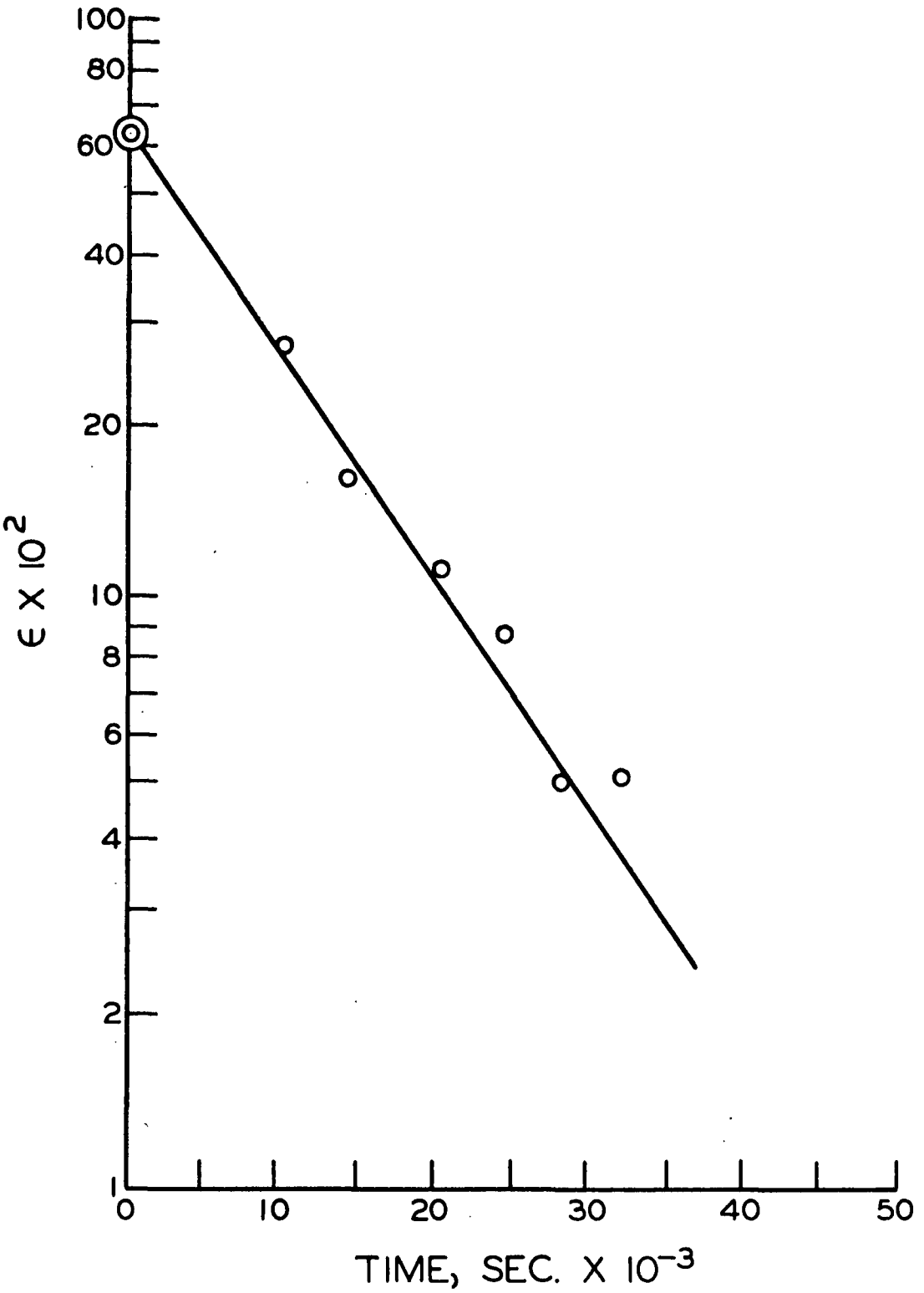

Figure 24. $\epsilon \times 10^2$ Versus Time
Method 2 (Line Determined by Intercept). Fraction 9-2

The viscosities at 30°C. are 1.516 c.p. for acetophenone and 1.024 c.p. for 1,1,2-trichloroethane. The diffusion coefficients in 1,1,2-trichloroethane are presented in Table XLVIII.

TABLE XLVIII

DIFFUSION COEFFICIENTS – IN 1,1,2-TRICHLOROETHANE

Fraction	$\underline{M}_w$ [a]	Method 1 $\underline{D}$, [a] cm.^{2}/sec.	Method 2 $\underline{D}$, [a] cm.^{2}/sec.
9-3	11,000	7.27×10^{-7}	7.66×10^{-7}
9-2	31,800	4.87×10^{-7}	4.98×10^{-7}
3(1)	38,100	3.61×10^{-7}	3.87×10^{-7}
2(2)	54,000	4.55×10^{-7}	3.63×10^{-7}
2(1)	87,000	3.64×10^{-7}	3.11×10^{-7}

[a] At concentration = 5×10^{-3} g./ml.

DISCUSSION

The diffusion coefficients calculated by Method 1 and by Method 2 differ from 2 to 7% for Fractions 9-3, 9-2, and 3(1) and differ about 20% for Fractions 2(2) and 2(1). The results from Method 2 are theoretically the most sound since they have been calculated from the slope of a line which has been forced to pass through a theoretical intercept at zero time. Furthermore, although Method 1 employs more points in the determination of the slope, the points used in Method 2 have more theoretical significance for the following reason. It was mentioned previously that LaBar and Baldwin (193) claim the optimum conditions occur when α is greater than 1 and ϵ is less than 0.5. In this series of experiments α ranged from 1 to 0.4 (Table XLVII). From curves presented by LaBar and Baldwin it can be seen that the error is negligible for $\alpha = 0.5$ when ϵ is less than 0.3.

In Method 2 the lower values of ϵ were employed; generally, these values were less than 0.3. For this reason the diffusion coefficients calculated by Method 2 are the most reliable and the future analyses is based on these values. The accuracy of this determination is controlled by the accuracy in the determination of the area under the schlieren pattern on the photographic plate.

LaBar and Baldwin (193) point out that the method has not been tested for systems that are heterogeneous or have appreciable concentration dependence. The diffusion coefficients were determined at a given concentration and therefore the concentration dependence is an unknown factor in this study. The effect of polydispersity was discussed previously.

APPENDIX XXI

SEDIMENTATION COEFFICIENTS

The sedimentation coefficient, s, is defined from the following relationship (40)

$$s = \frac{1}{r_H \omega^2} \frac{dr_H}{dt} \qquad (49)$$

where

r_H = the distance from the center of rotation to the boundary position

t = time.

The sedimentation coefficients were calculated from the following relationship (182)

$$s = \frac{D_\alpha M_w (1-\bar{v}\rho)}{RT} \qquad (50).$$

It was stated in Appendix XX, p. 193, that D_α approximates the average value that is obtained by combining results of sedimentation velocity and sedimentation equilibrium experiments. Thus, if the weight average value of molecular weight obtained from sedimentation equilibrium and D_α are employed in Equation (50) the value of s should be almost the same average that is obtained from sedimentation velocity experiments. Values of M_w and D_α at a concentration of 5×10^{-3} g./ml. were used to calculate s. The results are presented in Table XLIX. For the reasons given in Appendix XX, the results from Method 2 are employed in future analyses.

TABLE XLIX

SEDIMENTATION COEFFICIENTS — IN ACETOPHENONE

Fraction	$\underline{M}_w$ [a]	Method 1 [a,b] $\underline{s}$, sec.	Method 2 [a,b] $\underline{s}$, sec.
9-3	11,030	50.4×10^{-14}	5.31×10^{-14}
9-2	31,770	9.72×10^{-14}	9.95×10^{-14}
3(1)	38,080	8.62×10^{-14}	9.26×10^{-14}
2(2)	54,020	1.55×10^{-13}	1.23×10^{-13}
2(1)	87,010	1.96×10^{-13}	1.67×10^{-13}

[a] At concentration = 5×10^{-3} g./ml.
[b] Method 1 and Method 2 are defined in Appendix XX, p. 193.

APPENDIX XXII

COMPARISON OF HYDRODYNAMIC PROPERTIES OF VARIOUS POLYSACCHARIDES

TABLE L

EXPONENTS OF THE MARK-HOUWINK EQUATION FOR VARIOUS POLYSACCHARIDES

Polysaccharide	Solvent	Structure	Exponent	Reference
Cellulose	Cadoxen	Linear, β-1,4	0.77	(35)
Cellulose	Cadoxen	"	0.76	(194)
Cellulose	Cupriethylene-diamine	"	0.9	(195)
Cellulose	Cuprammonium	"	0.9	(195)
Cellulose	EWNN	"	1.01	(196)
Cellulose nitrate	Ethyl acetate	"	0.86	(197)
Cellulose nitrate	Acetone	"	1.00	(198)
Cellulose nitrate	Ethyl acetate	"	1.01	(199)
Cellulose nitrate	Acetone	"	1.0	(200)
Cellulose nitrate	Acetone	"	1.0	(201)
Methyl cellulose	Water	"	0.63	(202)
Ethyl cellulose	Methanol	"	0.65	(203)
Hydroxyethyl cellulose	Cadoxen	"	0.79	(204)
Hydroxyethyl cellulose	Water	"	0.87	(204)
Hydroxyethyl cellulose	Water	"	0.70	(205)

TABLE L (Continued)

EXPONENTS OF THE MARK-HOUWINK EQUATION FOR VARIOUS POLYSACCHARIDES

Polysaccharide	Solvent	Structure	Exponent	Reference
Sodium carboxymethyl cellulose	Cadoxen	Linear, β-1,4	0.73	(135)
Sodium carboxymethyl cellulose	Aqueous 0.1M NaCl	"	0.91	(37)
Sodium carboxymethyl cellulose	Aqueous 0.01M NaCl	"	1.20	(37)
Sodium carboxymethyl cellulose	Aqueous 0.001M NaCl	"	1.40	(37)
Sodium carboxymethyl cellulose	Aqueous 0.2M NaCl	"	0.74	(207)
Sodium carboxymethyl cellulose	Aqueous 0.005M NaCl	"	0.95	(207)
Guaran triacetate	Acetonitrile	"	0.87	(21)
Amylose	Ethylenediamine	Linear, α-1,4	0.70	(208)
Amylose	Aqueous N KOH	"	0.89	(208)
Amylose acetate	Chloroform	"	0.92	(209)
Amylose acetate	Nitromethane	"	0.87	(34)
Dextran	Water	Branched	0.50	(33)
Dextran	Water	Branched	0.42	(58)
Dextran	Water	Branched	0.32	(58)
Glucomannan triacetate	Trichloroethane	--	0.62	Present study

TABLE LI

EXPONENTS IN THE D VERSUS M RELATIONSHIP

Polysaccharide	Solvent	Structure	Exponent	Reference
Cellulose nitrate	Acetone	Linear, β-1,4	-0.685	(210)
Hydroxyethyl cellulose	Water	"	-0.54	(205)
Sodium cellulose xanthate	Aqueous NaOH	"	-0.521	(210)
Cellulose	Cuprammonium	"	-0.547	(210)
Cellulose	Cadoxen	"	-0.61	(35)
Carboxymethyl cellulose	Aqueous NaCl	"	-0.65	(37)
Methyl cellulose	Water	"	-0.56	(202)
Xylan	Dimethyl sulfoxide	"	-0.79	(174)
Glucomannan triacetate	Acetophenone	--	-0.451	Present study

TABLE LII

EXPONENTS IN THE S VERSUS M RELATIONSHIP

Polysaccharide	Solvent	Structure	Exponent	Reference
Cellulose nitrate	Ethyl acetate	Linear, β-1,4	0.29	(204)
Cellulose nitrate	--	"	0.30	(204)
Cellulose nitrate	Acetone	"	0.316	(210)
Sodium cellulose xanthate	Aqueous NaOH	"	0.483	(210)
Cellulose	Cuprammonium	"	0.452	(210)
Cellulose	Cadoxen	"	0.40	(35)
Hydroxyethyl cellulose	Water	"	0.46	(205)
Carboxymethyl cellulose	Aqueous 0.1M NaCl	"	0.35	(37)
Carboxymethyl cellulose	Aqueous 0.01M NaCl	"	0.23	(37)
Carboxymethyl cellulose	Aqueous 0.001M NaCl	"	0.11	(37)
Methyl cellulose	Water	"	0.45	(202)
Amylose acetate	Nitromethane	Linear, α-1,4	0.38	(34)
Dextran	Water	Branched	0.42	(58)
Dextran	Water	Branched	0.50	(58)
Dextran	Water	Branched	0.44	(33)
Glucomannan triacetate	Acetophenone	--	0.543	Present study

TABLE LIII

DIFFUSION COEFFICIENTS OF POLYSACCHARIDES

Glucomannan Triacetate (Present Study) $\underline{M}_w$ [a]	Glucomannan Triacetate (Present Study) $\underline{D}$, [a] $cm.^2/sec.$	Methyl Cellulose (202)	Cellulose Nitrate (198)	Xylan (174)	Carboxyl-methyl Cellulose (37)	Branched Dextran (58)
				8,400 2.67×10^{-7}		11,200 11×10^{-7}
11,030	9.80×10^{-7}					
		22,600 3.95×10^{-7} [b]	18,000 7.57×10^{-7}	20,300 2.25×10^{-7}		27,400 8.01×10^{-7}
31,770	6.37×10^{-7}					
		34,300 3.02×10^{-7}				35,200 6.35×10^{-7}
38,080	4.95×10^{-7}					
			40,000 4.38×10^{-7}		46,000 4.05×10^{-7}	52,000 5.48×10^{-7}
54,020	4.64×10^{-7}					
		70,600 1.92×10^{-7}	74,500 2.68×10^{-7}			67,800 4.72×10^{-7}
87,015	3.97×10^{-7}					
		151,000 1.19×10^{-7}	90,000 2.62×10^{-7}		90,060 2.35×10^{-7}	92,500 3.74×10^{-7}

All diffusion coefficients converted to the corresponding values in water at 30°C. with $\underline{D}_2 = \underline{D}_1 \underline{T}_2 \eta_1 / \underline{T}_1 \eta_2$.

[a] At concentration = 5×10^{-3} g./ml.

[b] {Molecular weight
{Diffusion coefficient.

APPENDIX XXIII

RELATIVE SHAPE AND SIZE OF THE GLUCOMANNAN TRIACETATE MOLECULE

The following technique is often used in the analysis of diffusion coefficients of proteins to obtain a measure of the relative shape of the polymer molecule in solution. The frictional coefficient, f, is given by (40)

$$f = \frac{kT}{D} = 6\pi\eta \frac{f}{f_o} \left[\frac{3M(\bar{v}_2 + \delta_1 v_1^o)}{4\pi\mu} \right]^{1/3} \qquad (51)$$

where

k = Boltzmann's constant

η = solvent viscosity

M = molecular weight

v_1^o = specific volume of pure solvent

v_2 = partial specific volume of polymer

μ = Avogadro's number

δ_1 = an empirical degree of solvation = number of grams of a solvent associated with 1.0 g. of unsolvated polymer

f_o = frictional coefficient of a hypothetical sphere which includes the solvent associated with the polymer (sphere volume = actual polymer volume plus associated solvent volume = $\bar{v}_2 + \delta\, v_1^o$)

R_o = radius of hypothetical solvated sphere

The factor f/f_o represents the deviation of the shape of the polymer hydrodynamic particle from a sphere. The minimum possible frictional coefficient, $f_{min.}$, for an unsolvated sphere is obtained by setting $f/f_o = 1$ and $\delta_1 = 0$.

$$f_{min.} = \frac{kT}{D_{max.}} = 6\pi\eta \left(\frac{3M\bar{v}_2}{4\pi\mu} \right)^{1/3} \qquad (52)$$

From Equation (51) and Equation (52), the useful ratio, $f/f_{min.}$ is obtained.

$$\frac{f}{f_{min.}} = \frac{D_{max}}{D} = \frac{f}{f_o} \cdot \left(\frac{\bar{v}_2 + \delta_1 v_1^o}{\bar{v}_2} \right)^{1/3} \qquad (53)$$

The ratio, $f/f_{min.}$ depends on two factors, solvation and asymmetry. Without further information it is impossible to separate the effects of these two variables. However, it is possible to determine the range of possible values which these variables might possess. At one extreme, we assume that the difference between the actual value of $f/f_{min.}$ and the ideal value of 1.0 for unsolvated spheres is due entirely to solvation. In this case, the assumption $f/f_o = 1$ is made and the maximum value of δ_1 is calculated from Equation (53). This is the value of δ_1 required to produce a sphere with the measured diffusion coefficient. The radius of this sphere, R_s, can be obtained from Stoke's equation, $f = 6\pi\eta R_s$. The extreme, in which the entire effect is assumed to be due to asymmetry, is determined by setting $\delta_1 = 0$. In this case $f/f_o = f/f_{min.}$. The magnitude of the asymmetry is expressed in terms of the axial ratio, a/b, of a prolate ellipsoid which would produce f/f_o. This maximum value of a/b is calculated by use of Equation (54)

$$\frac{f}{f_o} = \frac{(1 - b^2/a^2)^{1/2}}{(b/a)^{2/3} \ln \left[\frac{1 + (1 - b^2/a^2)^{1/2}}{b/a} \right]} \qquad (54)$$

Svedberg and Pedersen (178) have compiled tables of a/b versus f/f_o. The values of f, $f/f_{min.}$, maximum δ_1, R_s, and maximum a/b for the glucomannan triacetate in acetophenone are presented in Table LIV.

The values of $f/f_{min.}$ for the glucomannan triacetate molecule are in the range of 1.9 to 2.5. This is considerably lower than the values for this parameter which have been found for β-1,4 linked linear polysaccharides as seen in Table LV.

Thus, the glucomannan triacetate molecule in solution assumes a smaller sphere and/or a more symmetrical shape than typical linear β-1,4 linked polysaccharides. In fact, the values for $f/f_{min.}$ lead to the conclusion that the shape of the glucomannan triacetate molecule in solution more closely approximates that of a relatively compact branched dextran molecule than a linear β-1,4 linked polysaccharide.

TABLE LIV

SHAPE AND SIZE PARAMETERS FROM DIFFUSION COEFFICIENT

Fraction	M_w [a]	f [a], g./sec.	$f/f_{min.}$	Maximum Solvation δ_1, grams/gram	R_s (A)	Maximum Asymmetry a/b
9-3	11,030	8.09×10^{-8}	1.90	4.52	28.3	17.8
9-2	31,770	1.24×10^{-7}	2.06	5.91	43.5	21.7
3(1)	38,080	1.60×10^{-7}	2.50	11.11	56.0	34.3
2(2)	54,020	1.71×10^{-7}	2.37	9.40	59.8	30.4
2(1)	87,010	2.00×10^{-7}	2.36	9.29	69.8	30.0

[a] At concentration = 5×10^{-3} g./ml.

TABLE LV

THE PARAMETER $f/f_{min.}$ FOR POLYSACCHARIDES

Polysaccharide	Structure	Molecular Weight Range	$f/f_{min.}$	Reference
Hydroxyethyl cellulose	Linear, β-1,4	$125x10^3$ - $545x10^3$	3.96-5.29	(205)
Cellulose nitrate	"	$17.9x10^3$ - $386x10^3$	2.2 -6.1	(211)
Methyl cellulose	"	$14.1x10^3$-$38.1x10^3$	3.04-4.5	(212)
Cellulose	"	$44x10^3$-$5900x10^3$	4.6-13.1	(210)
Cellulose nitrate	"	$240x10^3$ - $780x10^3$	6.0-12.2	(210)
Sodium cellulose xanthate	"	$35x10^3$ - $126x10^3$	3.2 -4.3	(210)
Dextran	Branched	$21.6x10^3$ - $526x10^3$	2.03-3.22	(58)
Dextran	Branched	$39.8x10^3$ - $213x10^3$	2.07-2.98	(58)
Glucomannan triacetate	--	$11.0x10^3$-$87.0x10^3$	1.90-2.50	Present study

APPENDIX XXIV

THE EIZNER-PTITSYN THEORY

THEORETICAL

Eizner and Ptitsyn (41, 42) have derived equations for the intrinsic viscosity, diffusion coefficient, and sedimentation coefficient of semirigid macromolecules. The "wormlike" chain of Kratky and Porod (213) is used to evaluate $\overline{(1/r_{pt})}$*. In the case of the diffusion and sedimentation coefficients this value is substituted into a general expression for the translational frictional coefficient of macromolecules given by Kirkwood (214) to obtain the theoretical hydrodynamic equations. In order to derive the theoretical equations for intrinsic viscosity the expression for $\overline{(1/r_{pt})}$* is substituted into the intrinsic viscosity equation of Peterlin (215, 216). Eizner and Ptitsyn (42) show that the theory of Peterlin can be considered as general since it agrees with the most precise existing theories for the completely flexible Gaussian chain model, the flexible chain model in a good solvent which is impermeable to this solvent, and the rod-shaped molecule model.

The expression derived by Eizner and Ptitsyn (42) for the intrinsic viscosity of semirigid macromolecules is given in Equation (55).

$$[\eta] = \frac{2^{3/2}\,\Phi_o\,(b^3/M_o)\,N\,\chi\,(N/\lambda)}{\frac{45(2\pi/3)^{1/2}}{32(3-2^{1/2})}\frac{b}{\lambda r_o} + \frac{1}{\lambda^{3/2}}\,\phi(\lambda,N)N^{1/2}} \qquad (55)$$

*The variable r_{pt} is the distance between the p and t monomer units and the averaging is carried out for all chain configurations.

where $[\eta]$ is the intrinsic viscosity in ml./g., $\underline{N}$ is the degree of polymerization, Φ_o is the Flory coefficient whose limiting value is 2.86×10^{23} mole^{-1} at high molecular weight (42), $\underline{r}_o$ is the hydrodynamic radius of the monomer unit, $\underline{M}_o$ is the molecular weight of the monomer unit, $\underline{b}$ is the length of the monomer unit equal to 5.15×10^{-8} cm. for β-1,4 linked hexosans, and $\lambda = \underline{a}/\underline{b}$. The "stiffness" of the molecule is characterized by the persistence length of the Kratky-Porod wormlike chain, $\underline{a}$. The persistence length is defined as the integral of the average projections of chain elements of the infinitely long chain on its initial direction (31, 199, 213). The geometric function $\chi(\underline{N}/\lambda)$ and the hydrodynamic function $\phi(\lambda,\underline{N})$ are complex functions of λ and $\underline{N}$ and are given in Equations (56) and (57), respectively.

$$\chi(N/\lambda) = 1-[3/(N/\lambda)^3]\left\{(N/\lambda)^2 - 2\left[(N/\lambda) - 1 + e^{-(N/\lambda)}\right]\right\} \quad (56)$$

$$\phi(\lambda,N) = \frac{15(\pi/3)^{1/2}}{4(3 - 2^{1/2})} \frac{1}{\lambda^{1/2} N^{5/2}} \left\{ \sum_{k=1}^{n=1} \frac{(k^2+k-Nk-2N)\,\psi(k/\lambda)}{\left[k/\lambda-1+e^{-(k/\lambda)}\right]^{1/2}} + \sum_{k=1}^{(N/2)-1} \frac{[(N^2/2)- 2k^2 + N]\,\psi(k/\lambda)}{\left[k/\lambda -1+e^{-(k/\lambda)}\right]^{1/2}} \right\} \quad (57)$$

where

$$\psi(k/\lambda) = 0.427 + 0.573 \left\{ \frac{45(k/\lambda)^2 - 156k/\lambda + 214-54(4+k/\lambda)e^{-(k/\lambda)}+ 2e^{-(3k/\lambda)}}{27\left[k/\lambda - 1 + e^{-(k/\lambda)}\right]^2} \right. \quad (58)$$

The expressions derived by Eizner and Ptitsyn (41) for the diffusion coefficient, $\underline{D}$, and the sedimentation coefficient, $\underline{s}$, are given in Equations (59) and (60), respectively.

$$D = \frac{kTA}{6\pi \eta_o N} \tag{59}$$

$$s = \frac{M_o (1 - \bar{v}\rho) A}{6\pi \eta_o N_A} \tag{60}$$

where T is the absolute temperature, η_o is the viscosity of the solvent, $\bar{v}$ is the partial specific volume of the solute, ρ is the density of the solvent, N_A is Avogadro's number, and A is defined by Equations (61) and (62).

$$A = \frac{1}{r_o} + \frac{8f(\lambda,N)}{\sqrt{3\pi}} \frac{N^{1/2}}{b\sqrt{\lambda}} \tag{61}$$

$$f(\lambda,N) = \frac{\sqrt{6\pi}}{8} \frac{1}{\sqrt{\lambda}\ N^{3/2}} \sum_{k=1}^{N-1} \frac{(N-k)\ \psi\ (k/\lambda)}{\sqrt{k/\lambda - 1 + e^{-k/\lambda}}} \tag{62}$$

where $\psi(k/\lambda)$ is defined by Equation (58).

The Flory coefficient, Φ, is defined by (217, 218)

$$\Phi = \frac{[\eta]\ M_n}{6(\overline{s_n^2})^{3/2}} \tag{63}$$

where $\overline{s_n^2}$ is the number average mean square radius of gyration. The theoretical value of the Flory coefficient from the Eizner-Ptitsyn theory is given by

$$\Phi = \frac{\Phi_o}{\left[\phi(\lambda,N) + \frac{45(2\pi/3)^{1/2}}{32(3 - 2^{1/2})} \frac{b}{r_o} \left(\frac{\lambda}{N}\right)^{1/2}\right] \chi^{1/2}(N/\lambda)} \tag{64}$$

RESULTS AND DISCUSSION

TREATMENT OF THE EXPERIMENTAL DATA TO OBTAIN THE PERSISTENCE LENGTH

In order to treat the intrinsic viscosity data, Eizner and Ptitsyn rearrange Equation (55) to yield:

$$2^{3/2}\,\Phi_o\,\frac{b^3}{M_o}\,\frac{N}{[\eta]}\,\chi(N/\lambda) = \left(\frac{2\pi}{3}\right)^{1/2}\frac{45}{32(3-2^{1/2})}\,\frac{b}{\lambda r_o} + \frac{1}{\lambda^{3/2}}\,\phi(\lambda,N)\,N^{1/2} \qquad (65)$$

which is of the form, $\underline{Y} = \underline{A} + \underline{B}\underline{X}$. When the appropriate value of λ is used, a plot of $\underline{Y} = 2^{3/2}\Phi_o(\underline{b}^3/\underline{M}_o)(\underline{N}/[\eta])\chi(\underline{N}/\lambda)$ versus $\chi = \phi(\lambda,\underline{N})\underline{N}^{1/2}$ should be a straight line. The appropriate value of λ was determined by trial and error. Initial values of $\lambda_{\underline{i}}$ were assumed and from a least squares treatment of the data according to Equation (65) a final value of $\lambda_{\underline{f}}$ was calculated. This procedure was repeated several times and a correct value of λ was determined from the intersection of the curve relating $\lambda_{\underline{i}}$ to $\lambda_{\underline{f}}$ with the straight line, $\lambda_{\underline{i}} = \lambda_{\underline{f}}$. Equations (56) and (57) were used to calculate $\chi(\underline{N}/\lambda)$ and $\phi(\lambda,\underline{N})$. Calculations were carried out with the aid of an IBM 1620 computer.

Examples of the $\underline{Y}$ versus $\underline{X}$ plots are shown in Fig. 25 and 26. Intrinsic viscosity correlations with respect to the number average molecular weights, the weight average molecular weights, and the z-average molecular weights were treated. In the Intrinsic Viscosity-Molecular Weight Section it was shown that there was a definite break in the $\log[\eta]$ versus $\log \underline{M}$ plot in the high molecular weight region. Therefore, treatment according to the Eizner-Ptitsyn theory was applied to the data points which determine the initial linear portion of the

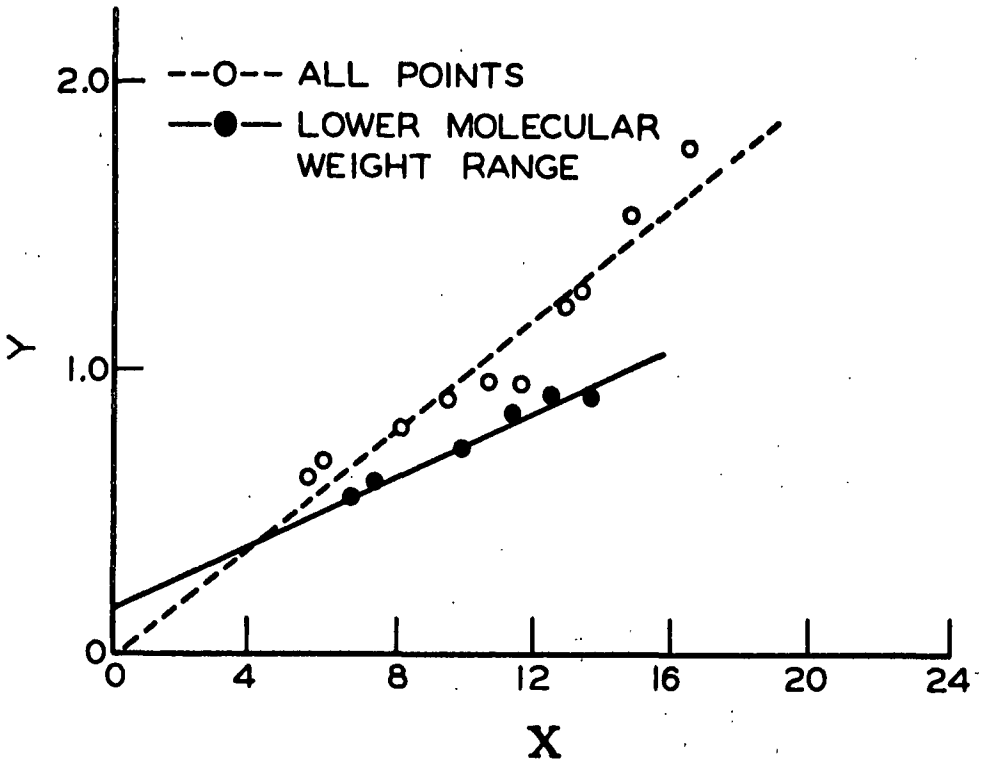

Figure 25. Y Versus X For M_n

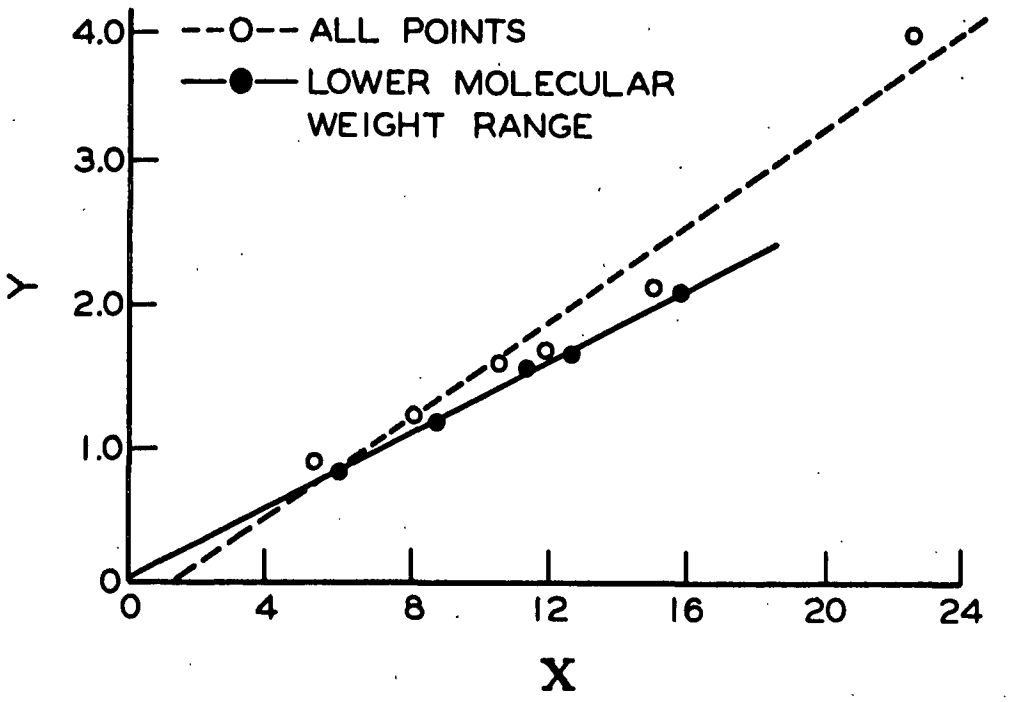

Figure 26. Y Versus X For M_w

$\log [\eta]$ versus log $\underline{M}$ plot (the lower molecular weight range) as well as the data over the entire molecular weight range. From Fig. 25 and 26 it is seen that the theory applies better to the lower molecular weight data than to the data over the entire molecular weight range. For this reason, the future conclusions and discussion will be based on data from the lower molecular weight range. The values of λ and the persistence length, $\underline{a}$, are presented in Table LVI.

TABLE LVI

RESULTS FROM EIZNER-PTITSYN THEORY

Molecular Weight Average Employed	Data Points Employed	λ	Persistence Length, A.
$\underline{M}_n$	Lower M.W.[a] range	6.78	34.9
$\underline{M}_n$	All points	4.70	24.2
$\underline{M}_w$	Lower M.W. range	3.92	20.2
$\underline{M}_w$	All points	3.19	16.4
$\underline{M}_z$	Lower M.W. range	3.34	17.2
$\underline{M}_z$	All points	2.82	14.5

[a] M.W. = molecular weight.

The Eizner-Ptitsyn theory describes the experimental data of the semirigid linear β-1,4-linked polysaccharides more adequately than any of the other existing polymer theories (41-45). Swenson (45) has tabulated the results of an Eizner-Ptitsyn treatment of the experimental data for various linear β-1,4-linked polysaccharides. These results are presented in Table LVII along with the results for the glucomannan triacetate from this study and the results for a branched dextran. From Table LVII, it is seen that the persistence length of linear β-1,4-linked polysaccharides is generally in the range of 50 to 70 A. The one exception to this rule is cellulose nitrate which has a persistence length of 132 A. Thus,

TABLE LVII

RESULTS FROM EIZNER-PTITSYN THEORY
FOR VARIOUS POLYSACCHARIDES

Polysaccharide	Structure	λ	a, A.	Reference
Cellulose trinitrate	Linear, β-1,4	25.5	132	(198)[b]
Cellulose in FeTNa	"	13.8	71.9	(45)[b]
Cellulose in cadoxene	"	13.8	70.8	(35)[b]
Cellulose acetate	"	11.5	59.3	(240)[b]
Galactomannan triacetate	"	11.2	57.8	(21)
Cellulose acetate	"	11.0	55.6	(45)[b]
Glucomannan triacetate	"	10.7	55.3	(43)
Diethylacetamide cellulose xanthate	"	10.5	54.0	(241)[b]
Cellulose caproate	"	9.3	47.7	(219)[b]
Dextran	Branched	1.60	8.23	(33)[b]
Glucomannan triacetate	--	3.92[a]	20.2[a]	Present study

[a]Results obtained by using the data from the lower molecular weight range for M_w.
[b]Eizner-Ptitsyn treatment by Swenson (45).

the generalization can be made that if a polysaccharide has a linear β-1,4-linked structure then it has a persistence length of approximately 50 A. or greater. Since the glucomannan triacetate from this study has a persistence length of 20.2 A., it by necessity is not a linear β-1,4-linked polysaccharide. Considerable evidence exists in the literature which shows that coniferous glucomannans are composed primarily of β-1,4 links (3). Therefore, one arrives at the conclusion that the glucomannan from this study is branched. It was previously mentioned that the persistence length is a measure of chain stiffness. Low values of the persistence length for branched polymers are due to the compact molecular structure resulting from branching.

CALCULATION OF THEORETICAL INTRINSIC VISCOSITY, MEAN SQUARE RADIUS OF GYRATION, AND FLORY COEFFICIENT

Equation (55) was used to calculate the theoretical values of the intrinsic viscosity. Examples of the theoretical curve and the experimental data are shown in Fig. 27 and 28. It is seen that the theoretical curves fit the data considerably better in the lower molecular weight range than over the entire molecular weight range. Thus, the previous decision to base the conclusions on results obtained from data in the lower molecular weight range is given support. The failure of the theory to adequately describe the data over the entire molecular weight range is undoubtedly due to the branching in the glucomannan molecule.

Equation (64) was used to calculate the theoretical value of the Flory coefficient, $\Phi_{theor.}$. An "experimental" value of the Flory coefficient, $\Phi_{exp.}$, was calculated with Equation (66)

$$\Phi = \frac{q_o [\eta] M_w}{6(\overline{s_z^2})^{3/2}} \qquad (66)$$

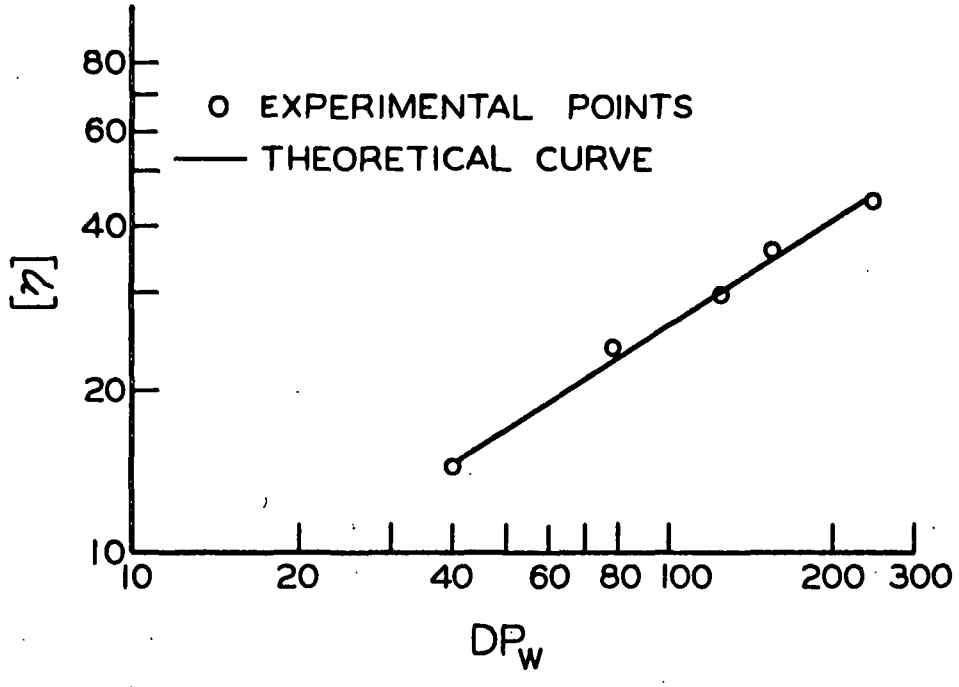

Figure 27. [η] Versus $\underline{\underline{DP}}_{\underline{w}}$ For Lower Molecular Weight Range

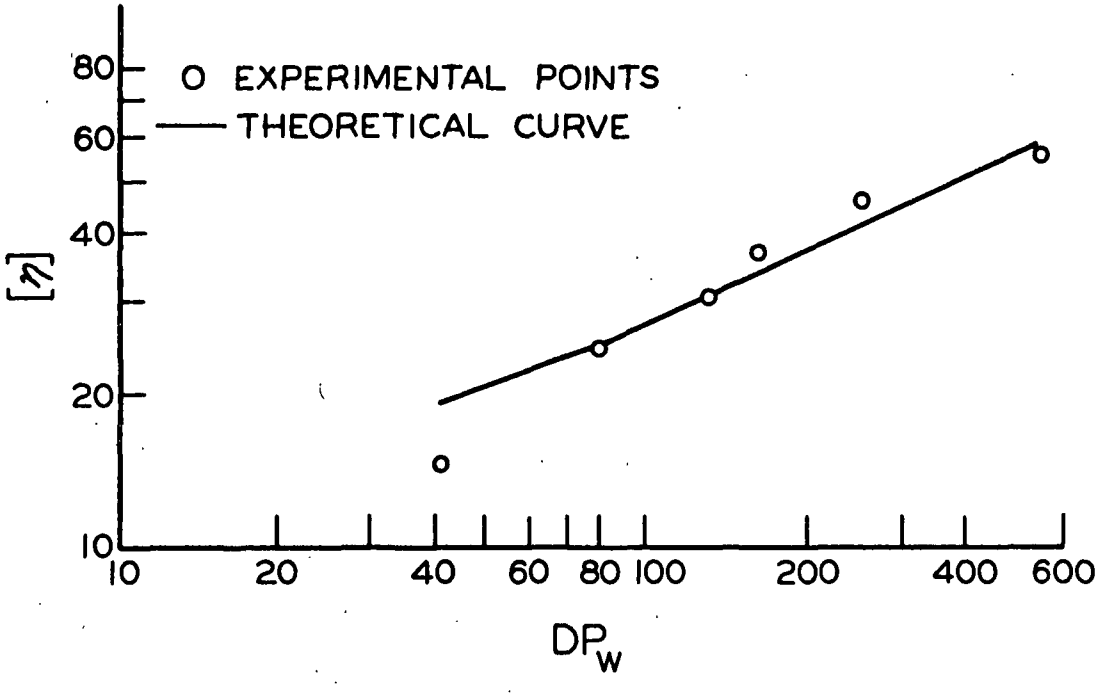

Figure 28. [η] Versus $\underline{\underline{DP}}_{\underline{w}}$ For All Points

where $\overline{s_z^2}$ is the z-average mean square radius of gyration and q_o is a factor to correct for sample heterogeneity. A Zimm-Schulz distribution (181, 190, 191) was assumed and q_o was calculated with Equation (67) (219, 220)

$$q_o = \frac{(h+2)^{3/2}\,\Gamma(h+2)}{(h+1)^2\,\Gamma(h+1.5)} \qquad (67)$$

where h is the Zimm-Schulz parameter, and Γ is the gamma function. The z-average mean square radius of gyration, $\overline{s_z^2}$, was calculated with Equation (68) which was derived from the Kratky-Porod "wormlike" chain model (199, 221).

$$(\overline{s_z^2}) = a^2 \left\{ (N_z\, b/3a - 1 + (2a/N_w b)[1 - (a/N_n b)] \right\} \qquad (68)$$

The values of $\overline{s_z^2}$, q_o, $\Phi_{exp.}$, and $\Phi_{theor.}$ for the lower molecular data from M_w are given in Table LVIII. The limiting value of the Flory coefficient is 2.86×10^{23}. The results are plotted in Fig. 29. A reasonable correlation is obtained between the theoretical and "experimental" values of Φ. Since the "experimental" value was calculated using λ and a from the Eizner-Ptitsyn theory, agreement between $\Phi_{theor.}$ and $\Phi_{exp.}$ is not proof of the validity of the theory but merely an indication that the theory and the experimental data are internally consistent. The agreement between $\Phi_{theor.}$ and $\Phi_{exp.}$ for the data from M_n and M_z was not nearly as good as for the data from M_w. For linear polymers the Flory coefficient increases up to its limiting value as the molecular weight increases and the molecule becomes more tightly coiled. The values of the Flory coefficient higher than the limiting value is undoubtedly due to the compact structure of the glucomannan molecule caused by branching.

CALCULATION OF THE THEORETICAL DIFFUSION COEFFICIENT AND SEDIMENTATION COEFFICIENT

A true test of the applicability of the Eizner-Ptitsyn equations is to use intrinsic viscosity *versus* molecular weight data to calculate r_o and λ and then

TABLE LVIII

FLORY COEFFICIENTS

Fraction	$\underline{M}_w$	$\overline{\underline{s}_z^2}$, cm.^{2}	$\underline{q}_o$	$\Phi_{exp.} \times 10^{-23}$	$\Phi_{theor.} \times 10^{-23}$
9-3	11,700	9.44×10^{-14}	1.08	4.22	3.29
3(2)	23,700	2.95×10^{-13}	1.37	3.22	2.97
9-2	38,100	5.05×10^{-13}	1.49	3.19	2.91
3(1)	47,500	7.09×10^{-13}	1.63	3.16	2.90
2(2)	74,100	1.53×10^{-12}	2.16	2.58	2.89

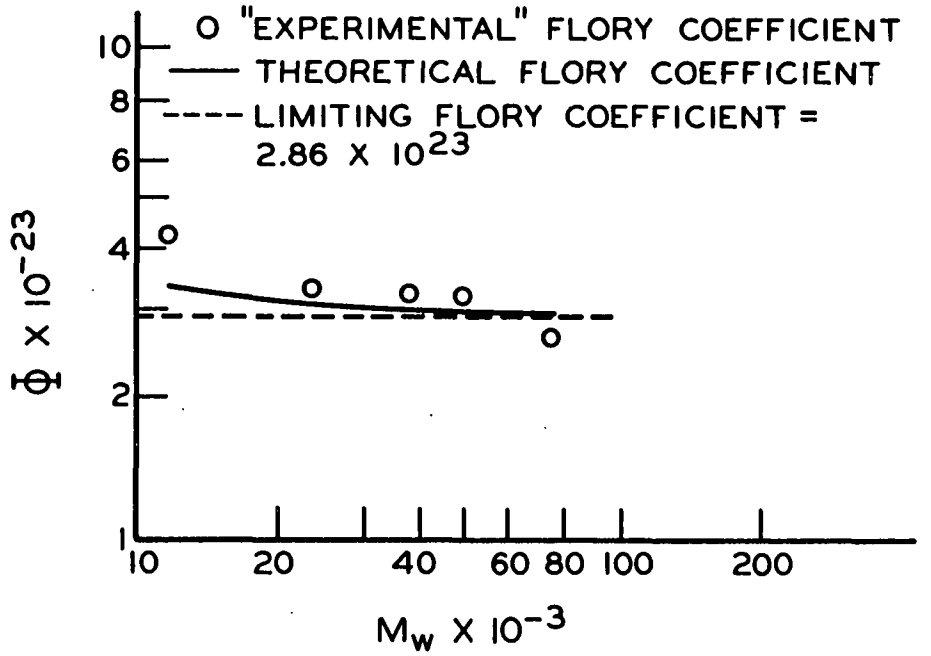

Figure 29. Φ Versus $\underline{M}_w$

use these values to calculate a theoretical diffusion coefficient, $\underline{D}_{theor.}$, or a theoretical sedimentation coefficient, $\underline{s}_{theor.}$. If these theoretical values then compare favorably to the experimental values, $\underline{D}_{exp.}$ and $\underline{s}_{exp.}$, one can then say that the theory is valid for this particular set of data. The theoretical values of $\underline{D}$ and $\underline{s}$ were calculated using Equations (59), (60), (61), and (62). Since the experimental diffusion and sedimentation coefficients were calculated at concentrations of approximately 5×10^{-3} g./ml., the data from the weight average molecular weights corresponding to these concentrations were used to calculate the theoretical values. These results are presented in Table LIX and Fig. 30 and 31. Also shown in Fig. 30 and 31 are the theoretical curves obtained by using the data from the weight average molecular weights which have been extrapolated to zero concentration. The similarity of the two theoretical curves indicates that the previous use of a diffusion coefficient versus molecular weight correlation and a sedimentation coefficient versus molecular weight correlation at a concentration of approximately 5×10^{-3} g./ml. rather than at zero concentration did not introduce any large error.

TABLE LIX

THE THEORETICAL DIFFUSION AND SEDIMENTATION COEFFICIENTS

Fraction	$\underline{M}_w$ [a]	$\underline{D}_{exp.} \times 10^{7}$, [a] cm.^{2}/sec.	$\underline{D}_{theor.} \times 10^{7}$, [a] cm.^{2}/sec.	$\underline{s}_{exp.} \times 10^{14}$, [a] sec.	$\underline{s}_{theor.} \times 10^{14}$, [a] sec.
9-3	11,000	5.18	6.30	5.31	6.49
3(2)	21,500	--	4.34	--	8.73
9-2	31,800	3.37	3.49	9.95	1.04
3(1)	38,100	2.61	3.18	9.26	1.13
2(2)	54,000	2.45	2.65	1.23	1.34
2(1)	87,000	2.10	--	1.67	--

[a] At a concentration of approximately 5×10^{-3} g./ml.

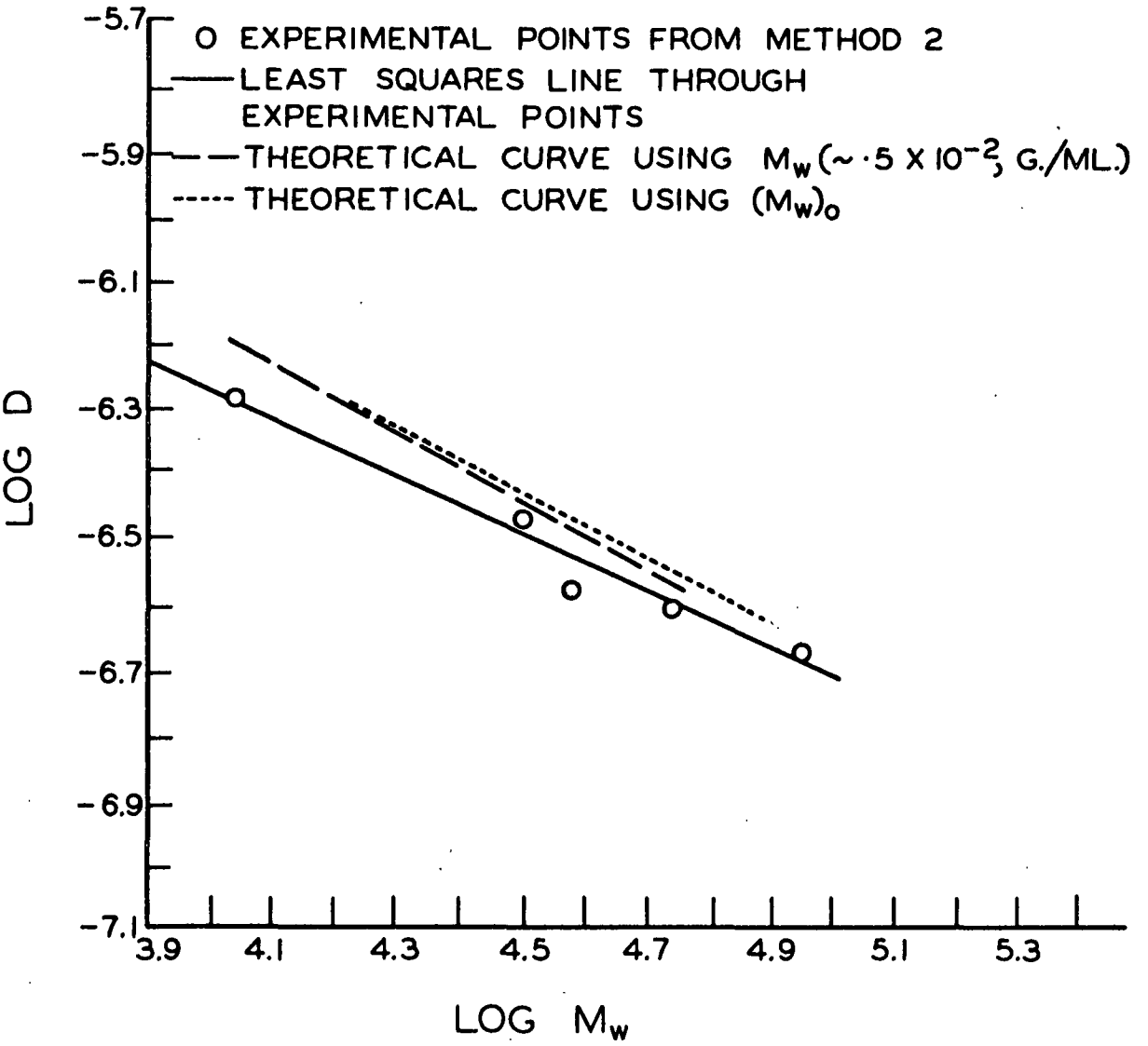

Figure 30. Log D Versus Log M_w

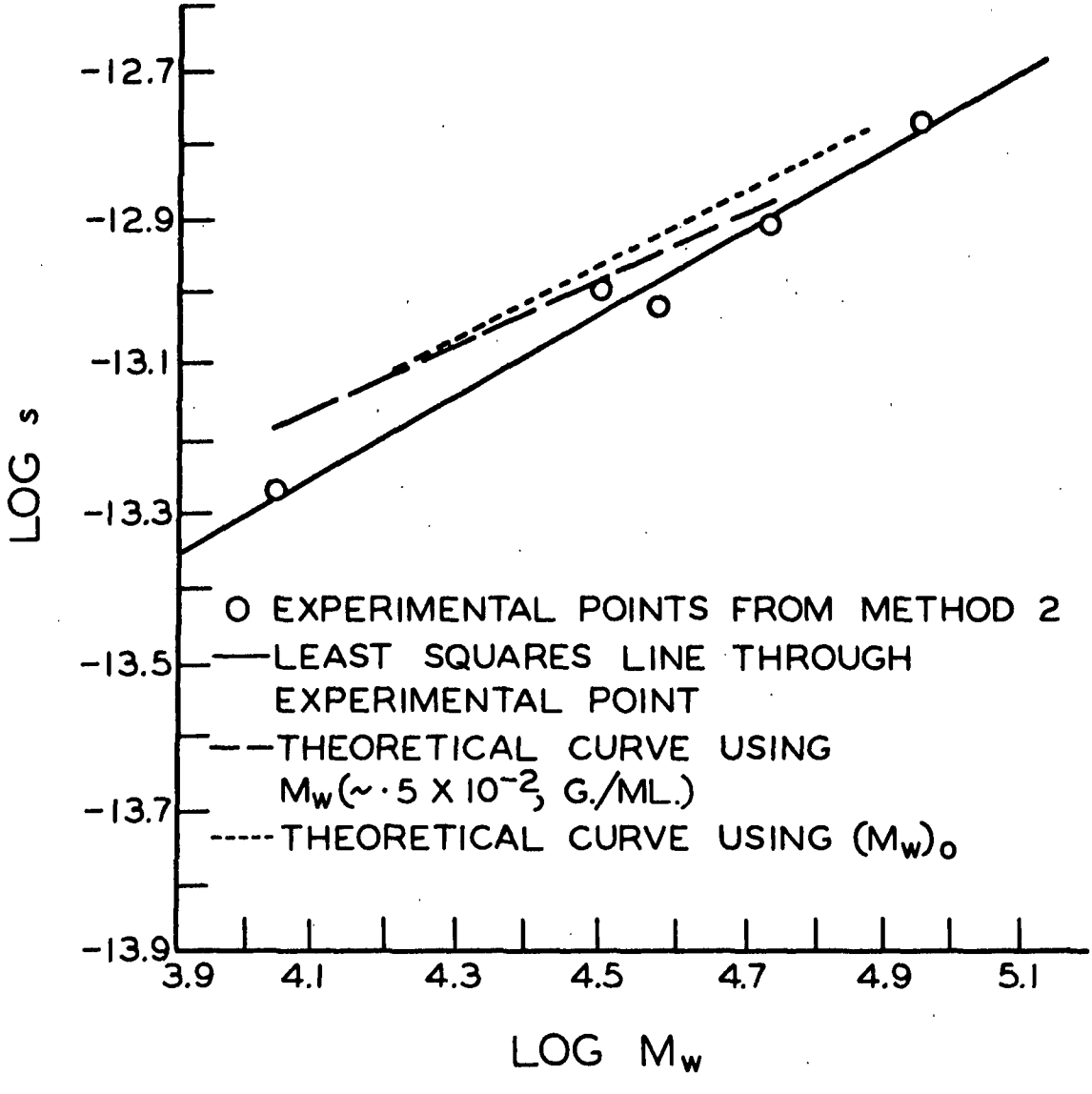

Figure 31. Log s Versus Log M_w

The experimental values of the diffusion and sedimentation coefficients deviate from the theoretical values by 3 to 18% in the range investigated. The agreement between theory and experiment is best in the high molecular weight range. In light of the unknown effect of polydispersity and the error involved in the determination of the experimental diffusion coefficients it is felt that the 3 to 18% agreement is reasonable. Since the equations of Eizner and Ptitsyn are based on a linear polymer chain model it is remarkable that theory and experiment agree within 20% for the branched glucomannan triacetate fractions. Thus, it appears that the gross behavior of the molecule in solution is adequately described by the theory regardless of the detailed structure of the molecule. Thus, a low value of the persistence length obtained from the theory indicates that the molecule has a relatively compact configuration in solution and it is not important whether this compact configuration results from a flexible linear molecule or a branched molecule made up of semirigid chains.

APPENDIX XXV

SECOND VIRIAL COEFFICIENT FROM OSMOMETRY

The values of A_2 and Γ_2 are presented in Appendix XV, p. 154. The log-log plots of A_2 versus $\underline{DP}_n$ and Γ_2 versus $\underline{DP}_n$ are shown in Fig. 32 and 33, respectively. Only the most reliable second virial coefficients as indicated by the highest correlation coefficients are plotted. The second virial coefficient, A_2, depends on three factors: (1) the molecular weight, (2) the thermodynamic interaction parameters which characterize the segment-solvent interaction, and (3) the configuration, or size of the molecules in solution (30). The latter factor is important in the interpretation of the results in Fig. 32. For rodlike molecules or extended chains, A_2 should be independent of molecular weight; however, as the molecules become less extended and more compact due to coiling or branching, A_2 decreases and becomes dependent on the molecular weight (30, 40, 222). At the limit of extreme compactness for solid spherical molecules, A_2 is very small and theoretically varies inversely as the molecular weight (40, 222). Disregarding for the moment the low DP Fractions 4 and 9-3, it is seen from Fig. 32 that the highest molecular weight Fraction 2(1) has a significantly lower A_2 than the other fractions. This low value is undoubtedly due to the greater compactness caused by a greater degree of branching of this fraction than the other fractions. The low values of A_2 for Fractions 4 and 9-3 are probably due to a relatively low segment-solvent interaction but the reason for this phenomenon is unknown. From Fig. 33, it is seen that all the fractions lie on the smooth curve of log Γ_2 versus log $\underline{DP}_n$.

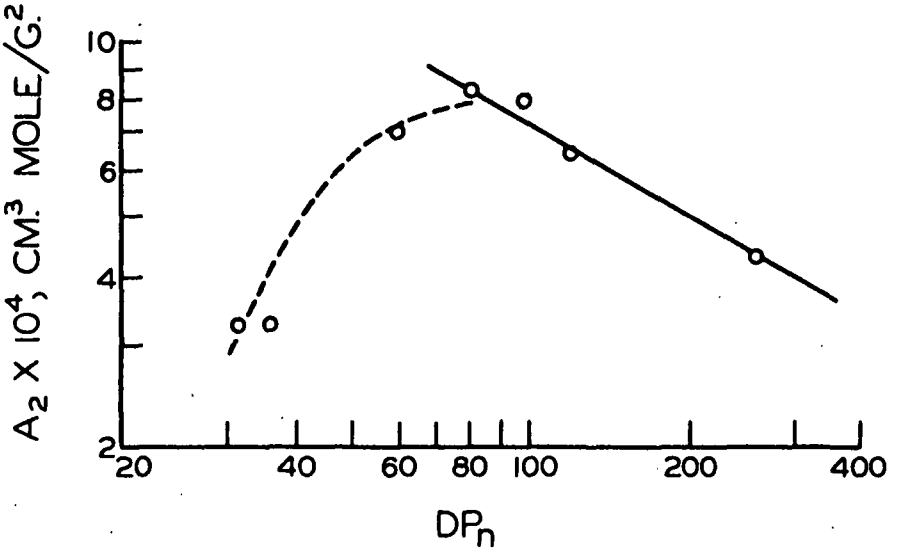

Figure 32. A_2 Versus DP_n

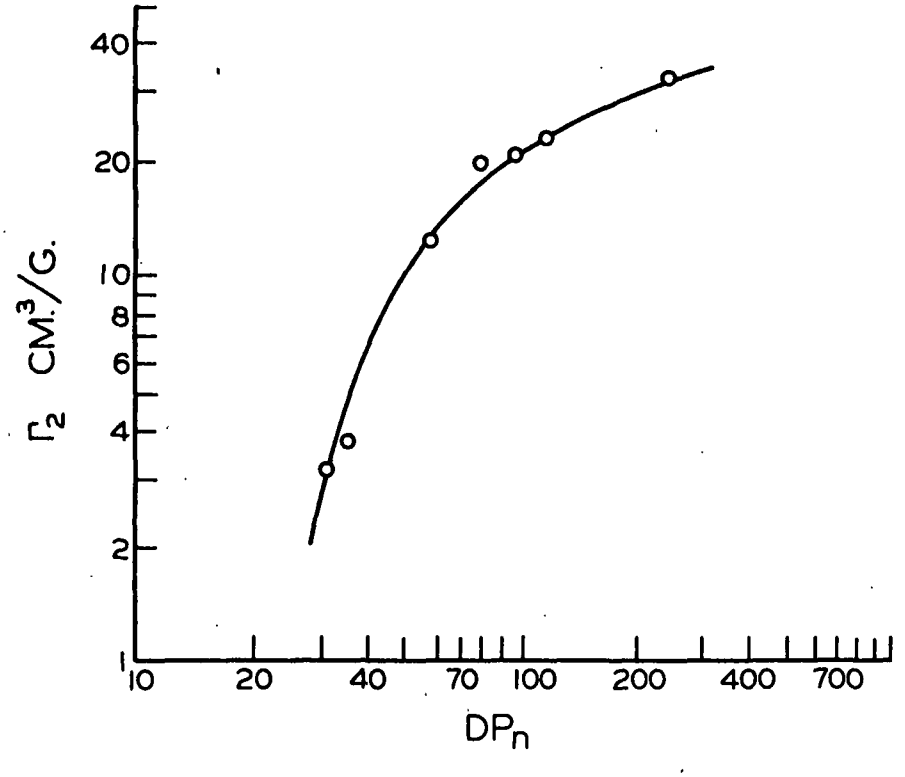

Figure 33. Γ_2 Versus DP_n

APPENDIX XXVI

VISCOSITY EXTRAPOLATION CONSTANTS

The most important variable besides molecular weight which influences viscosity is the concentration of the solute. In general, the viscosity of a dilute polymer solution increases more rapidly than the concentration (32). This behavior is due to increasing disturbances of the flow caused by a greater probability of interaction between molecules as the concentration increases.

The values of the viscosity extrapolation constants are presented in Appendix XVI, p. 159. The plot of K_1 versus $[\eta]$ is shown in Fig. 34. Only the most reliable extrapolation constants as indicated by the highest correlation coefficients are plotted. For all fractions except the two lowest molecular weight fractions an increasing trend in K_1 with increasing $[\eta]$ is evident. This behavior is not typical of a pure polymer which is homogeneous with respect to molecular weight and structure and has a constant configuration. Under these conditions a constant value of K_1 is obtained which is generally in the range of 0.30 to 0.40 for flexible polymers (30, 32, 40). Only Fraction 3(2) with $[\eta]$ = 23.4 ml./g. has a value of K_1 in this range (K_1 = 0.398) and the values of K_1 for the other fractions is between 0.50 to 0.92. Although polydispersity increases K_1 the effect is quite small (31, 32, 223) and does not account for the increases in K_1 observed in this study.

Branching or cross-linking results in a higher K_1 for these molecules than for linear molecules because the relatively dense and compact branched molecules do not affect the solution viscosity as much as linear molecules at very low concentrations but the denser branched molecules have a greater opportunity to interact as the concentration is increased and thus the solution viscosity increases faster with concentration (224). The increase in K_1 with branching has

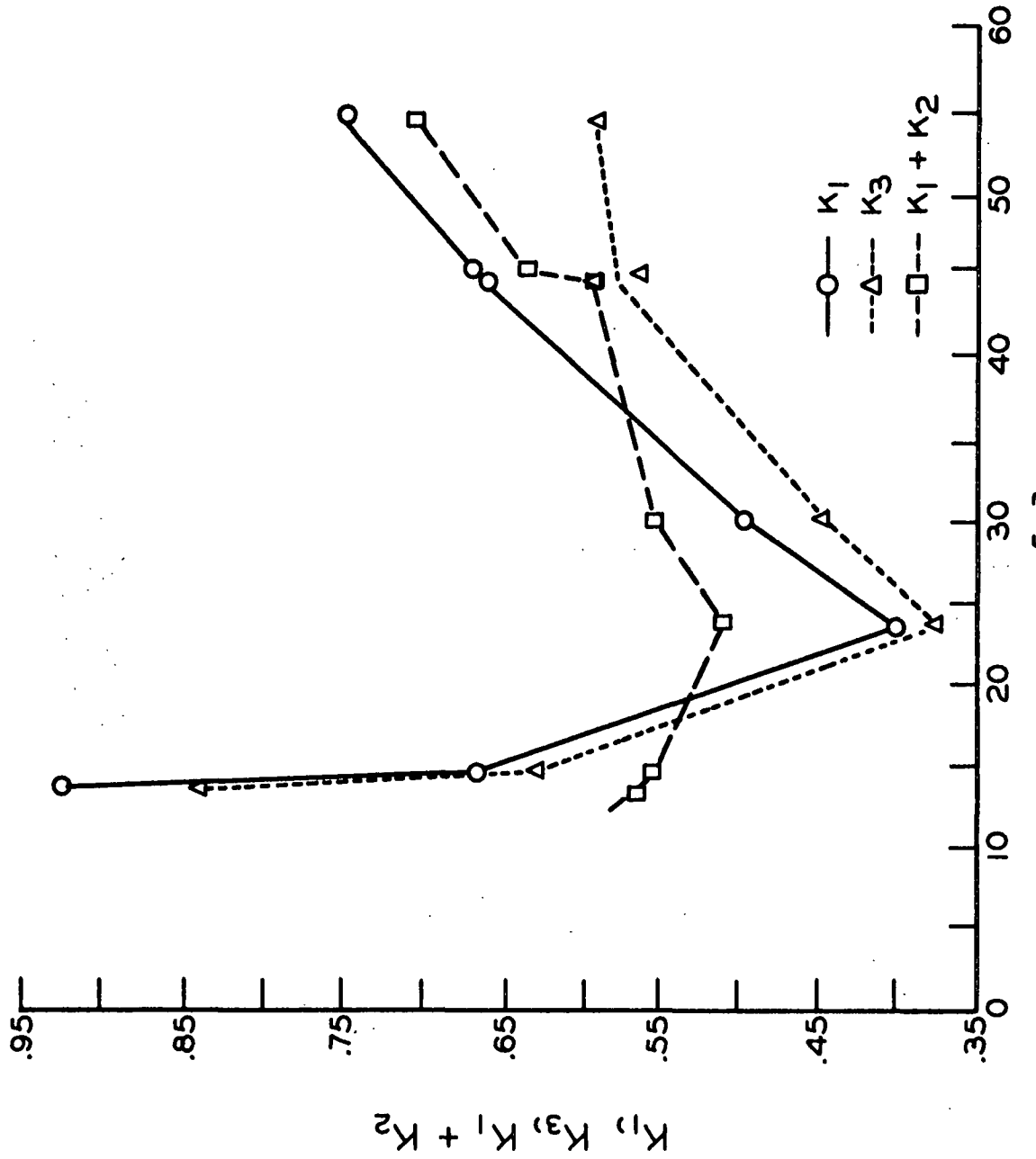

Figure 34. Viscosity Extrapolation Constants Versus [η]

been found for synthetic polymers (224, 225), amylopectin (226), and branched dextrans (33, 58). The high values of K_1 in Fig. 34 and the increasing trend in K_1 with increasing molecular weight in the high molecular weight region is probably due to branching in these fractions. When the two low molecular weight fractions are considered, a minimum occurs in K_1 with respect to molecular weight. Senti and co-workers (33) also found a minimum in K_1 for a branched dextran but were unable to explain this minimum. In a poor solvent, K_1 is higher (even though the slope, $K_1[\eta]^2$ is lower) than in a good solvent (32, 224, 227, 228). The high values of K_1 for the low molecular weight fractions in this study may be due to a lower polymer-solvent interaction for these fractions. The relatively low second virial coefficients of these fractions (see Appendix XV, p. 154) support this explanation but the cause of the low polymer-solvent interaction is unknown. Another possible explanation for the high values of K_1 for the low molecular weight fractions is based on the fact that an ellipsoid has a larger K_1 than a sphere (227). If the assumption is made that the low molecular weight fractions (below a DP of 40) have an ellipsoidal shape which approaches a spherical shape as the molecular weight is increased, the high values of K_1 for the low molecular weight fractions is accounted for and a satisfactory explanation is arrived at for the minimum in K_1 for branched molecules.

The curve of K_3 versus $[\eta]$ is similar to the curve of K_1 versus $[\eta]$ and is shown in Fig. 34. Also shown in Fig. 34 is the plot of $K_1 + K_2$ versus $[\eta]$. The sum $K_1 + K_2$ should theoretically equal 0.5 (31, 32, 229) and is in the range of 0.51 to 0.70 in this study. It was found empirically that all the data fall on a straight line if a log-log plot is made of the slope for K_1, $K_1[\eta]^2$, minus the slope for K_2, $-K_2[\eta]^2$, versus $[\eta]$ (Fig. 35). This value $K_1[\eta]^2 + K_2[\eta]^2$ is a measure of the separation of the two straight lines in the double extrapolation plot.

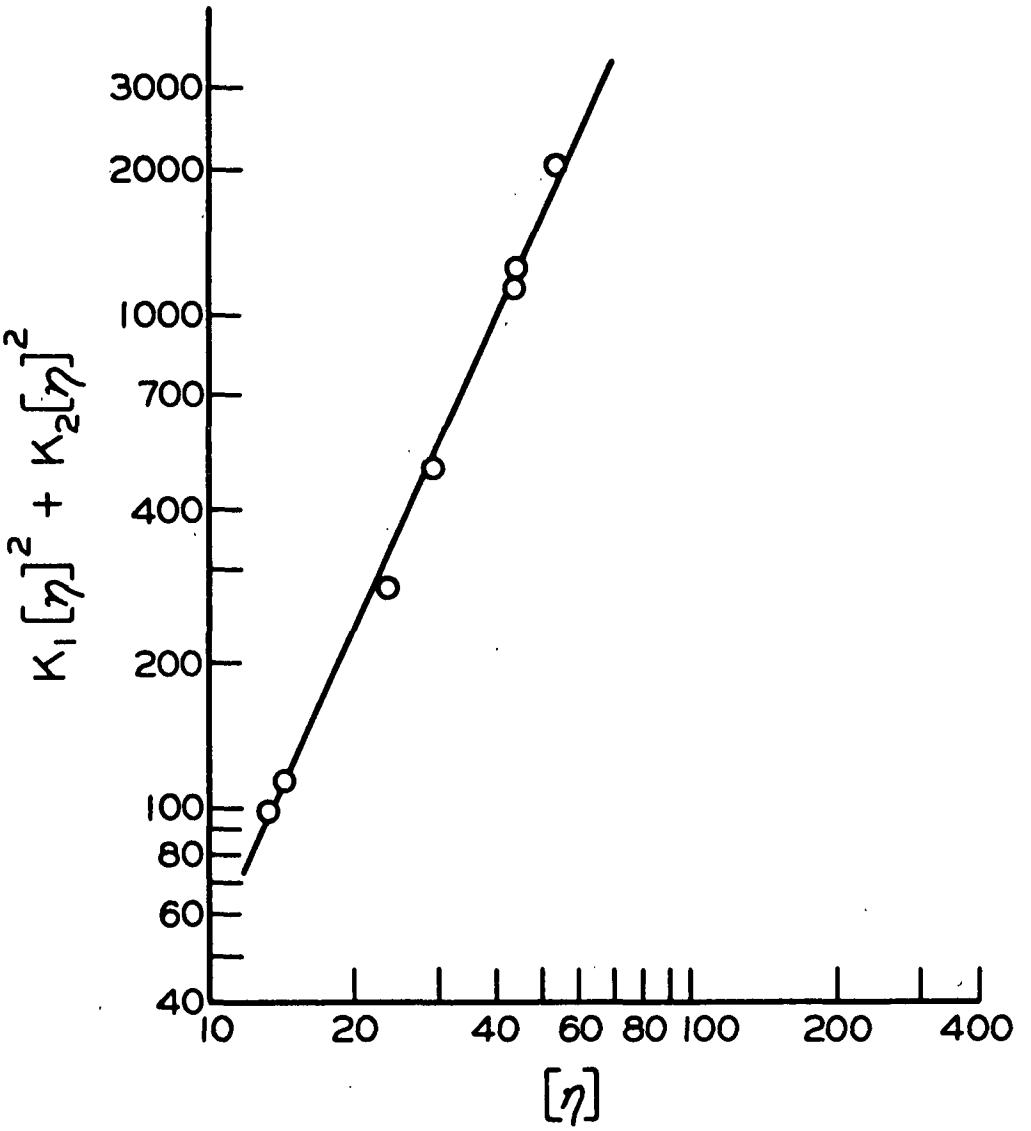

Figure 35. $(\underline{K}_1\ [\eta]^2 + \underline{K}_2\ [\eta]^2)$ Versus $[\eta]$

From the above discussion of the variables which effect $\underline{K}_1$ and from the previous discussion of the variables which affect $\underline{A}_2$ (Appendix XXV, p. 229) it is apparent that the same variables are important in both cases and that there should be an inverse relationship between $\underline{A}_2$ and $\underline{K}_1$. From the log-log plot of $\underline{K}_1$ versus $\underline{A}_2$ in Fig. 36, it is seen that a correlation does exist between the Huggins constant and the second virial coefficient with $\underline{K}_1$ decreasing as $\underline{A}_2$ increases.

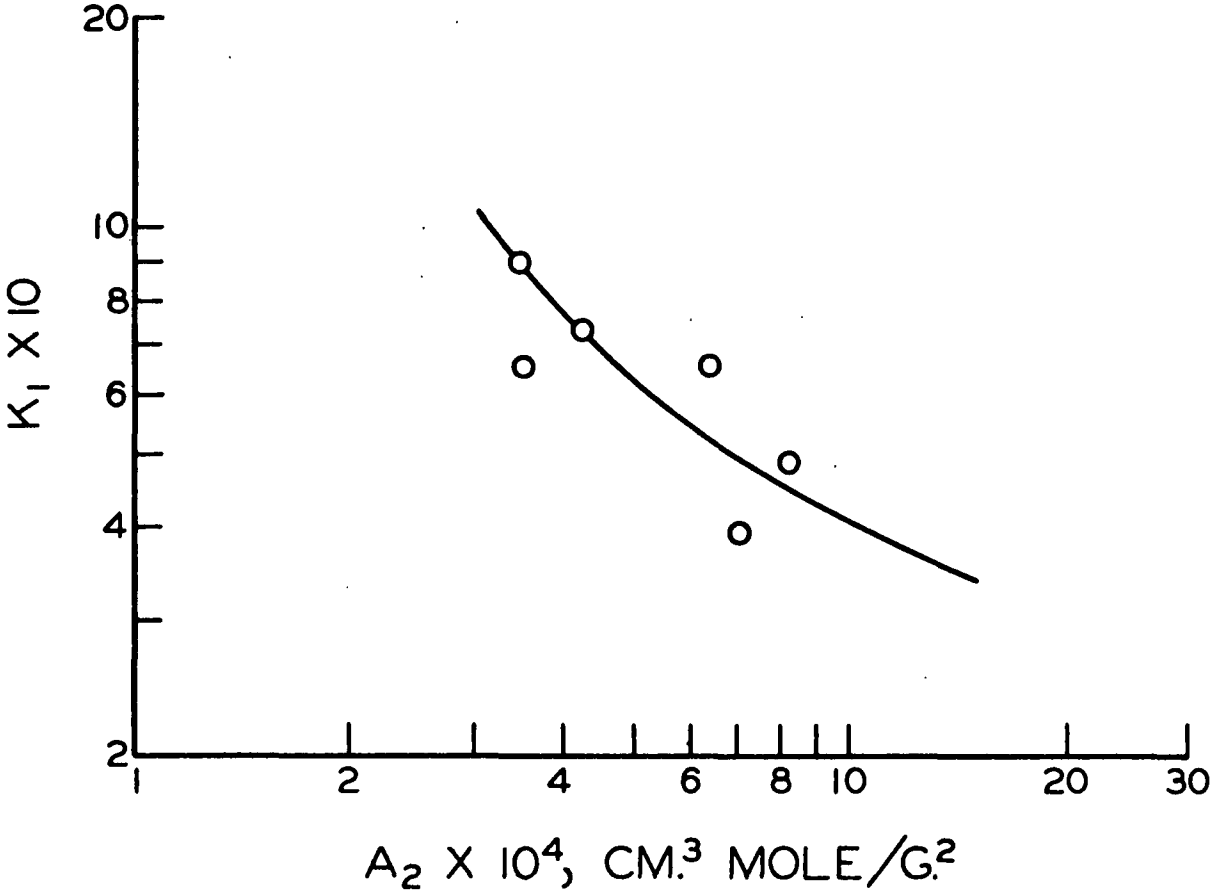

Figure 36. $\underline{K}_1$ Versus $\underline{A}_2$

APPENDIX XXVII

VISCOSITIES IN CUPRIETHYLENEDIAMINE

Viscosity measurements were made in 0.5M cupriethylenediamine (cuene) with a Cannon-Ubbelohde semimicro dilution number 100 viscometer at 30 ± 0.005°C. One per cent solutions were made up by first dispersing the glucomannan in water, adding sufficient 1.0M cuene to make the solution 0.5M, shaking under nitrogen, and finally centrifuging prior to the viscosity determination. The viscosity measurements were made in the presence of nitrogen over a period of an hour to minimize degradation and the glucomannan was in contact with the cuene for 1-1/2 to 2 hours prior to the viscosity determination. Viscosity measurements were made on the acetylated main glucomannan Fractions 3(2), 3(1), and 2(1) and on the unacetylated glucomannan Fractions 8 and 13, and the unacetylated galacto-glucomannan Fraction 14. The ash contents were determined on Fractions 8, 13, and 14 by ashing at 575 ± 25°C. for three hours and the viscosities were corrected with these values. Fraction 14 had some insoluble material which was collected, the ash content determined, and the viscosity subsequently corrected for the amount of insoluble organic material. Examples of the extrapolations to give the intrinsic viscosities are shown in Fig. 37. The $(\eta-\eta_o)/\eta_o c$ versus c plots all have correlation coefficients greater than 0.97 and no degradation trend is noticeable. Therefore, it can be concluded that degradation is not an important factor over the period of time required for the viscosity determination.

The number average, weight average, and z-average degrees of polymerization have been determined previously on the acetylated main glucomannan Fractions 3(2), 3(1), and 2(1) (Appendices XV, p. 154, and XVIII, p. 166). These degrees of polymerization and the intrinsic viscosities in cuene are given in the log-log

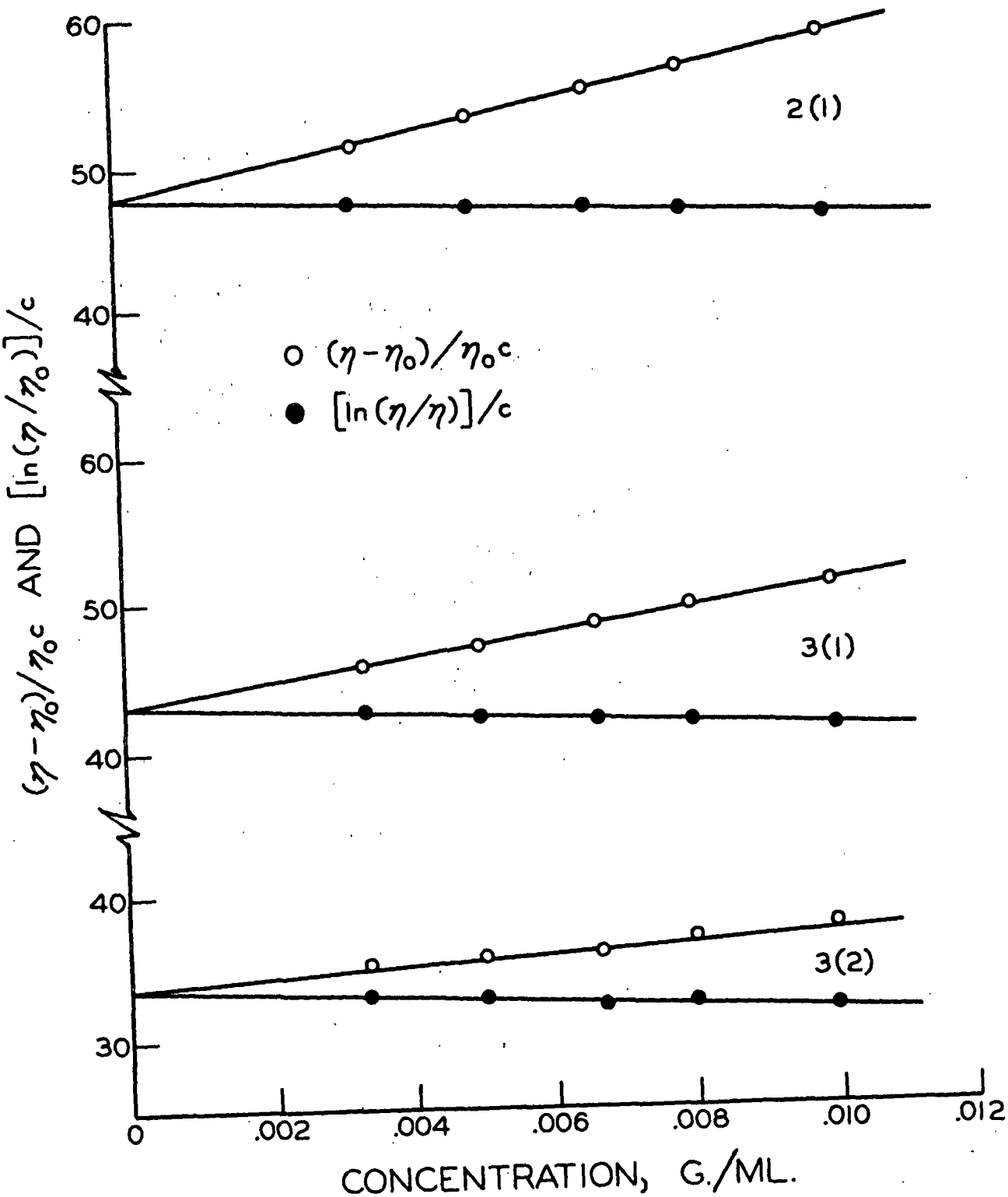

Figure 37. Extrapolation to Obtain Intrinsic Viscosity in Cupriethylenediamine

plot in Fig. 38 and presented in Table LX. In the cuene solutions complete deacetylation takes place and the viscosities are therefore determined on the unacetylated glucomannan (47, 48).

TABLE LX

CUENE VISCOSITIES AND DEGREES OF POLYMERIZATION OF ACETYLATED FRACTIONS

Fraction	$[\eta]$, ml./g.	$\underline{DP}_w$	$\underline{DP}_n$	$\underline{DP}_z$
3(2)	33.62	82.4	60.6	95.8
3(1)	43.01	165	102.5	216
2(1)	47.67	557	261	729

The intrinsic viscosities of the unacetylated Fractions 8, 13, and 14 in cuene are reported in Table LXI. The curves presented in Fig. 38 were used to determine the degree of polymerization from the limiting viscosity number in cuene. The viscosity average degree of polymerization is closer to the weight average degree of polymerization than other degrees of polymerization (30-32). Therefore, the value determined in the above manner is less affected by the polydispersity of the fractions and consequently more reliable than the values of $\underline{DP}_n$ and $\underline{DP}_z$. These latter two values were determined merely to give an estimation of their range if the unacetylated Fractions 8, 13, and 14 had distributions similar to the acetylated glucomannan Fractions 3(2), 3(1), and 2(1) and all conclusions will be based on $\underline{DP}_w$.

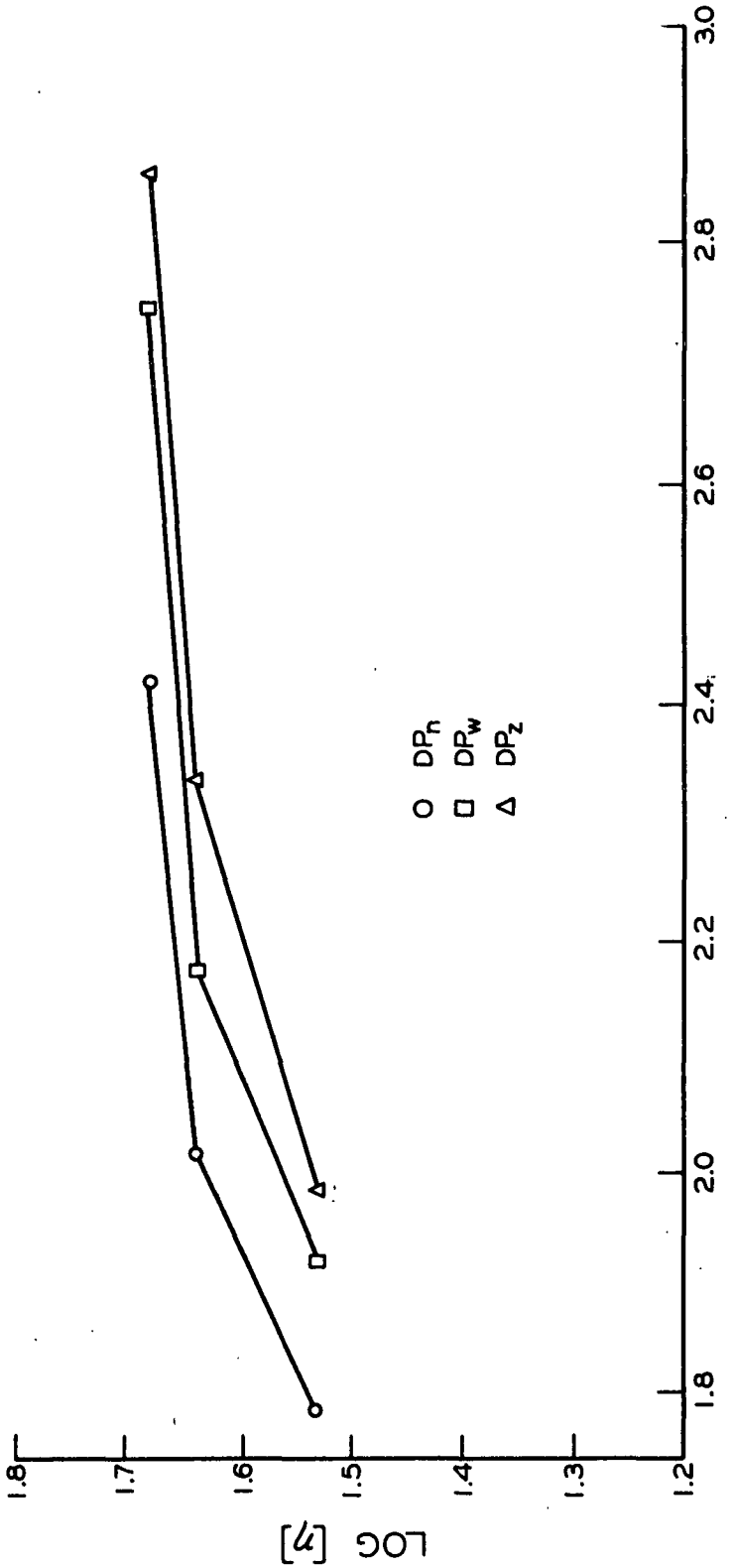

Figure 38. Log $[\eta]$ Versus Log DP For Cuprietheylenediamine

TABLE LXI

CUENE VISCOSITIES AND DEGREES OF POLYMERIZATION OF UNACETYLATED FRACTIONS

Fraction	Solution Used to Extract from Holocellulose	[η], ml./g.	Determined from Figure $\overline{DP}_w$	$\overline{DP}_n$	$\overline{DP}_z$
8	10% NaOH	37.96	111	79.1	144
13	18% NaOH	40.52	130	90.8	178
14	18% NaOH – 4% H_3BO_3	46.20	374[a]	197[a]	516[a]

[a]The large increase in $\overline{DP}$ with respect to the relatively small increase in [η] is due to the progressively decreasing slope of the log [η] versus log $\overline{DP}$ plot shown in Fig. 38. This type of behavior is typical of branched molecules.

APPENDIX XXVIII

ESTIMATION OF LIGNIN CONTENTS IN THE UNACETYLATED FRACTIONS

The estimated lignin contents in the unacetylated Fractions 8, 13, and 14 are presented in Table LXII. The estimated lignin content in the acetylated Fraction 8-A was calculated by assuming that the lignin contents in the acetylated fractions derived from 8-A, Fractions Insol'., 2(1), and 3(2) are representative of the total lignin in Fraction 8-A. This is a fairly good assumption since the fractions are widely separated and account for 57.4% of the original acetylated Fraction 8-A. The lignin content in the unacetylated Fraction 8 was then calculated by correcting for the presence of acetyl groups. The same type of analysis was carried out for the soluble and insoluble acetylated fractions, 13-S and 13-I, which account for 91.0% of the acetylated Fraction 13-A and for the soluble and insoluble acetylated Fractions 14-S and 14-I, which account for 94.5% of the acetylated Fraction 14-A. The reliability of the estimation is indicated by the value of 8.5% for the estimated lignin content of the unacetylated Fraction 14 compared to the measured value of 7.2%.

TABLE LXII

LIGNIN CONTENT

Fraction	Estimated Lignin Content, (based on unacetylated glucomannan), %
8	4.23
13	4.53
14	7.17

APPENDIX XXIX

POSSIBLE APPLICATIONS OF THE CROSS-LINKED LIGNIN-CARBOHYDRATE MATRIX CONCEPT

The concept that lignin is chemically linked to the glucomannan and perhaps other polysaccharides within the fiber, resulting in a cross-linked lignin-carbohydrate matrix is applicable to various areas of wood chemistry. The existence of this type of linkage may be significant in interpreting the function of the glucomannan in the fiber. A branched lignin-glucomannan complex with a relatively high degree of polymerization would be expected to play a quite different role in its contribution to the strength properties of the fiber than smaller and essentially linear glucomannan chains. The effect of the lignin-glucomannan linkage on the resistance to extraction of the glucomannan from the holocellulose has been discussed in the text and this type of linkage may also relate to other chemical reactions of the glucomannan in the fiber. It is mentioned in the text that this linkage may be important in interpreting the degree of polymerization, degree of branching, and sugar content of isolated glucomannans.

Along more practical lines, a detailed knowledge of the lignin-carbohydrate linkage would be valuable in developing pulping methods in which this type of linkage is cleaved without the simultaneous degradation of the polysaccharides. One possible application is in the interpretation of the pretreatment of coniferous woods to obtain increased yields of the glucomannan during pulping. Increased yields by alkaline pretreatment have been explained by a deacetylation of the glucomannan and subsequent adsorption and/or crystallization onto the fiber surface (230). However, it is also possible to obtain increased yields of the glucomannan by pretreatment with acid sulfite solutions (231) under conditions where no deacetylation should occur. A possible explanation of this phenomenon is that

during the acid sulfite pretreatment, lignin-glucomannan linkages may be cleaved, releasing relatively short and essentially linear glucomannan chains which are then adsorbed or crystallized onto the cellulose surface. These "absorbed" glucomannans should be more resistant to chemical degradation than the glucomannans in the original cross-linked matrix.

Cellulose acetates prepared from dissolving pulps of coniferous woods often exhibit haze and anomalous viscosities (232-236). These phenomena are probably closely related to the insolubility of a portion of the acetylated glucomannan observed in this investigation and in turn may be due to a lignin-glucomannan complex. Glucomannans have important effects on pulp and paper properties (101, 106, 237-239) and the factors contributing to their effect such as diffusion and adsorption properties, adhesive characteristics, and degradation during pulping are undoubtedly influenced by the extent of the glucomannan's combination with lignin.